The evolution of diversity and life history traits in annual killifish (*Austrolebias*) and other Cyprinodontiformes

Andrew J. Helmstetter

A thesis submitted for the degree of Doctor of Philosophy at Imperial College London,

Department of Life Sciences

Thesis Abstract

Members of the annual killifish genus *Austrolebias* live in temporary ponds across South America and possess a remarkable life cycle. These fish live in small ponds that dry out completely; killing the adults but not before they have laid eggs in the substrate of their pond. The desiccation-resistant eggs develop during the dry season, going through multiple stages of diapause until the next wet season rains trigger hatching and the cycle is repeated. There is considerable variation in size in *Austrolebias*, the largest species can reach up to 150mm in length while the typical size is just 40mm. Phylogenetic trees and species distribution models were built and used together to identify the factors that influence patterns of co-occurrence within this genus. Differences in growth and morphology among *Austrolebias* species were examined to quantify how differences in growth pattern can lead to the large variation in size and shape seen within the genus. Genomic data was generated for hybrid offspring of two species of *Austrolebias* using double-digest RAD sequencing. These data were then used to build linkage maps that were in turn used to identify any regions associated with sex determination and potential chromosomal rearrangements. At a broader scale, a generic-level tree for the order Cyprinodontiformes was constructed. *Austrolebias* is a member of this order, as well as many model fish genera such as *Fundulus*, *Nothobranchius* and *Poecilia*. Two extraordinary reproductive life-history adaptations have evolved in this order; viviparity and annualism. The new tree was used to determine whether the evolution of viviparity or annualism lead to increased rates of diversification. Finally this generic-level tree was used to examine patterns of positive selection in the low-light vision gene, rhodopsin and whether sites under selection were linked to functional changes.

Declarations

I confirm that the research presented in this document is my own work. The co-authors of manuscripts that have been prepared for submission as well as those who have provided assistance during my thesis have been acknowledged on page 4.

Chapter 2

This chapter has been adapted from a manuscript being prepared for submission to *Evolution* under the authorship of Andrew J Helmstetter, Alexander ST Papadopulos, Javier Igea, Tom JM Van Dooren, Armand M Leroi, and Vincent Savolainen

Chapter 3

This chapter has been adapted from a manuscript being prepared for submission to the *Journal of Evolutionary Biology* under the authorship of Andrew J Helmstetter, Alexander ST Papadopulos, Tom JM Van Dooren, Armand M Leroi, and Vincent Savolainen

Chapter 4

This chapter has been adapted from a manuscript being prepared for submission to *BMC Genomics* under the authorship of Andrew J Helmstetter, Alexander ST Papadopulos, Tom JM Van Dooren, Armand M Leroi, and Vincent Savolainen

Chapter 5

This chapter adapted from a manuscript that is in review at *Nature Communications* under the authorship of Andrew J Helmstetter, Alexander ST Papadopulos, Javier Igea, Tom JM Van Dooren, Armand M Leroi, and Vincent Savolainen

Chapter 6

This chapter has adapted from a manuscript being prepared for submission to the *Journal of Molecular Evolution* under the authorship of Andrew J Helmstetter, Luke T Dunning, Tom JM Van Dooren, Armand M Leroi, and Vincent Savolainen

Acknowledgements

First and foremost, thank you to my supervisors at Imperial College London, Vincent Savolainen and Armand Leroi for the opportunity to undertake this PhD and the guidance you have given me throughout.

Thank you to Tom Van Dooren for the tireless effort you have put in. For teaching me how to take care of these dastardly fish, the long Skype calls discussing problems, the solutions to these problems and perhaps most of all, the opportunity to go to Foljuif, which changed my life and my PhD.

Thank you to Tim Barraclough (Dad) and Mike Tristem for acting as my panel and helping to get me to this stage.

Thank you to Henri Thomassen for providing samples and advice on various aspects of my thesis.

Thanks to Foxy Trev and Big C of the British Killifish Association for letting me write an article for your journal and helping me establish connections in the association.

Thank you to Heber & Marie Salvia for your hospitality and your guidance in Uruguay. Especially to thank you to Cocoa for teaching me so much about my study system despite a considerable language barrier and providing me with what I needed to start my PhD. Thank you also to Javier Sarasola for getting me through my collection trip and giving me a great deal of memories beyond what I expected.

Thank you to everyone from William Penney – particularly Holly, Helen, Hannah, Alistair, Will, Jonny, Daisy and Alex. You made my first year at Silwood and I've missed your presence here ever since.

Thank you to all of the Amphibians in the Kitchen, I've never had so much fun playing music as I did with all of you.

To Robbie I'Anson-Price for being a great friend and a voice of reason and advice. So staronguh. Plaguuu.

Merci a toutes les personnes que j'ai rencontré a Foljuif. En particulier - Thibault, Amandine, Helene, Jean-Francois, Beatriz, Sam, Sarah and Alex.

Thank you to the Slodgers Joe, Laura, Eric, Gio, Adriana, Adam, James, Clare, Ollie and Claire, Fred and Carol. Sorry about all of the noise.

Thank you to those in the lab who got me through the first years; Martyn Powell – who prevented the disaster only few will ever know, Lynsey Bunnefeld - I will treasure your cricket shirt forever, Rob Dyer - your happiness was contagious, Richard Fautley – your words of advice have stayed with me throughout my PhD, Adam Britton – you taught me I could in fact, down it and Helen Hipperson for putting up with my office antics.

Thank you to Maria Kaye for those trips to get ice creams and unheard duets. To Alan Walker for touching me inappropriately.

To Luis Valente for convincing me to go to my first conference and discussing the pros and cons of baby oil with me.

To Emily Humble for never really getting me into Gilles but sharing JB with me.

Thanks to Dom Swift for letting me know how much of a nerd I am.

Thank you to all of the rest who have passed through the Savolainen lab – Alba, Jun, CT, Claire, Xueping and others, for making my time there more enjoyable.

To Marco Castiello for being you and someone who kept me in line when I needed it. To Richard Dearden for sharing so many of the things I like. To Adam Ciezarek for preventing me from sliding down the razor blade of life. To all of the Western Blocks for shakin' them legs with me.

Thank you to the writers of the I newspaper and to everyone who ever came and contributed to the morning crossword.

To James Taggart for teaching me who I do not want to be.

To Elyas Farstrider (and Orion), Gelb, Pox Lamblaster, Fray Perico and Ragnar Ringsplitter. Blood for the blood god.

Thank you to Tom Smith for dealing with all of the tedious things I made you do with not so much as a word of complaint.

To Luke Dunning for sharing your opinions on Morrissey and your love of Columbo.

To Javier Igea for teaching me how to tame the BEAST and providing me with enough pots to fill an entire kitchen. May your snail forever skid.

To Alex Papadopulos for being an inspiration and a teacher, for being there for me every step of the way, but most of all thank you for being a great friend.

Thank you to Marie-Claire Danner for being the loving, caring, kind and wonderful person that you are. Je t'aime.

And thank you to my family, to Mom, Dad and Liana. For your constant, unquestioning support, love and guidance throughout my life.

Table of Contents

List of Tables

List of Figures

Chapter 1

Thesis Introduction

1.1 The evolution of diversity and the phylogenetic tree

The distribution of species richness is uneven through time, among clades and in different geographic regions. Understanding how this diversity in species, and their phenotypes, arises is a fundamental goal and one of the major challenges in evolutionary biology. There are many different approaches to studying the evolution of diversity, but first it must be quantified. This may be assessing the variation in a particular character trait or determining the rate of diversification of a particular clade compared to others. Once this information has been obtained one can move on to attempt to discover why this diversity has evolved – are certain traits correlated with others that have enabled the occupation of a new niche? Perhaps competition between species pushed the values of a trait to their opposite extremes to facilitate coexistence? Was there a sudden explosion of species after their common ancestor dispersed to a new geographic region or acquired a character trait? Evolution can also be examined at the molecular level by asking, for example, if the molecular variation we detect among species in a gene is due to random drift or if it is adaptive. Furthermore, the rapidly advancing field of genomics has allowed one to determine the size, location and number of genomic regions that underlie a variable trait. This thesis examines the process of evolution and the origins of diversity at multiple levels in order to answer these types of questions and this introduction will give background and context to the approaches used.

Perhaps the most important component when investigating the evolution of diversity is the phylogeny, the branching tree of evolutionary relationships among taxa. Phylogenies can be reconstructed based on differences in morphological characters or molecular sequence data, typically using parsimony, Bayesian (Ronquist & Huelsenbeck 2003; A. J. Drummond & Rambaut 2007) or maximum likelihood (Stamatakis 2006) frameworks. Trees can be time-

calibrated (A. J. Drummond & Rambaut 2007; Yang 2007) using fossils or time calibrations from other phylogenetic trees. Calibrating a tree will produce branch lengths that give historical evolutionary context to divergence events and enable more complex analyses that take into account shared ancestry. The reduction in sequencing costs and the advent of high-throughput sequencing has allowed for more accurate inference with more sequence data. The availability of very large phylogenetic trees (Jetz et al. 2012; R. A. Pyron et al. 2013; Hinchliff et al. 2015) and the introduction of methods to account for incomplete sampling (FitzJohn et al. 2009; Rabosky, Donnellan, et al. 2014) have facilitated the study of diversity in previously untouched, non-model groups. The information provided by a reconstructed phylogenetic tree can allow one to examine evolutionary processes that have occurred over the course of thousands or millions of years. To study the evolution of diversity it is important to first understand how species originate.

1.2 Speciation

Speciation is the evolutionary process through which new species arise and, along with extinction, shapes the branching evolutionary relationships of the phylogenetic tree. The process of speciation is typically explained using instances of adaptation radiation (Schluter 2000), which can produce incredible phenotypic variation in adaptive traits, such as the plethora of beak shapes in Darwin's Finches, which allow different species to specialise in feeding on specific prey (P. R. Grant 1999). The *Anolis* lizards of the Greater Antilles (Roughgarden et al. 1983; Losos 2009) are another celebrated example; they vary in body size and limb length among ecomorphs so that they may better suit their microhabitat niche. The family Cichlidae is the most species-rich family of vertebrates and much of this diversity is the result of repeated adaptive radiations (Brawand et al. 2015). The most famous of these

radiations is in the Great Lakes of East Africa where almost 2,000 species have arisen over a short evolutionary timescale of approximately 10 million years (Kocher 2004), which is on average one species per 5000 years! Speciation research has been a major topic in evolutionary biology in recent years (Coyne & Orr 2004; Nosil 2012) but despite this investment, many major questions still remain unanswered and additional research is needed (The Marie Curie SPECIATION Network 2012). At the scale of species diversity these include understanding the tempo and mode of speciation i.e. what causes variation in speciation rate? Are patterns in diversity related to mechanisms of speciation? Other questions relate to the relative importance of hybridisation and natural versus sexual selection in generating reproductive isolation. At a finer scale more work is needed to understand the nature of "speciation genes" and how reproductive isolation is manifested in the genome (The Marie Curie SPECIATION Network 2012).

1.2.1 Speciation and geography

The principal way of classifying speciation is by its geography. Geographic context is an integral part of the speciation process; it affects the sources of divergent selection as well as the level of gene flow during speciation. Gene flow will cease between geographically isolated populations, allowing genetic drift and mutation to occur, which will eventually lead to pre or post-zygotic isolating barriers among groups (Coyne & Orr 2004). If gene flow is present between two groups it will act against the development of genetic incompatibilities, so other biological mechanisms are required for speciation to take place (Tregenza & Butlin 1999; Coyne & Orr 2004). This interaction between the homogenising effect of gene flow and divergent selection shapes how speciation unfolds. The geographic classification of speciation exists as a continuum (Mallet et al. 2009) and modes are defined as in Table 1.

Table 1.1 Verbal definitions of geographic modes of speciation from (Mallet et al. 2009)

Geographic mode	Definition
Allopatric	"Where groups of populations are separated by uninhabited space across which dispersal and gene flow occurs at very low frequency."
Parapatric	"Where groups of populations occupy separate but adjoining geographic regions, such that only a small fraction of individuals in each encounters the other. Typically, populations in the abutment zone between two forms will be considered sympatric."
Sympatric	"Where individuals are physically capable of encountering one another with moderately high frequency. Populations may be sympatric if they are ecologically segregated, as long as a fairly high proportion of each population encounters the other along ecotones; and they may be sympatric, yet breed at different seasons."

At one end is allopatric speciation, where a barrier of uninhabitable space separates populations and migration and gene flow occurs very rarely. After extensive complete geographic isolation, the accumulation of genetic incompatibilities will lead to pre or post-zygotic isolation between isolated populations (Coyne & Orr 2004). Allopatric speciation is considered by many to be the dominant mode of speciation (Mayr 1982; Coyne & Orr 2004). At the other end of the continuum is sympatric speciation, where individuals from different populations physically encounter each other often (Mallet et al. 2009). In between the two extremes are parapatry and peripatry. Parapatric speciation occurs when two populations are present in separate but adjacent geographic regions, meaning that only a small proportion of individuals will encounter individuals from the adjoining population (Futuyma & Mayer 1980; Mallet et al. 2009). Peripatric speciation is a rare mode that is very similar to allopatric

speciation and occurs when a new species is formed in an isolated, smaller periphery population (Coyne & Orr 2004). When populations are in contact with one another, the extent of divergence is controlled by the relative power of selection and gene flow. The capability of selection to overcome gene flow has been heavily debated in the past (Felsenstein 1981; Via 2001) but a number of convincing examples of sympatric speciation in the face of gene flow have emerged. There are two *Howea* palm trees, *H. belmoreana* and *H. forsteriana*, endemic to the remote island of Lord Howe. These two species were shown to have diverged from one another after Lord Howe Island formed 6.9 million years ago, which indicates that speciation was in sympatry on the island (Savolainen et al. 2006). Divergence was likely related to differences in flowering time and soil preference among *H. belmoreana* and *H. forsteriana* (Savolainen et al. 2006). An additional 11 potential instances of divergence with gene flow have been documented in various other species on Lord Howe Island (Papadopulos et al. 2011). In the Midas cichlid species complex (*Amphilophus* sp.) a single high-bodied benthic species, *A. citrinellus*, colonised Crater Lake Apoyo (Barluenga et al. 2006). From this species evolved *A. zaliosus*, an elongated limnetic species, no more than 10,000 years ago. The two species within the lake are reproductively isolated and eco-morphologically distinct. Still, sympatric speciation remains a controversial subject and even these well-regarded examples are not without their detractors (Stuessy 2006; Schliewen et al. 2006; Bolnick & Fitzpatrick 2007) and new approaches are revealing previously hidden complexities in classic examples of sympatric speciation (Martin et al. 2015).

Where in the previous examples geographic contact may constrain divergence through gene flow, there are some cases in which contact between populations can promote divergence (Nosil 2012). In the frog genus *Litoria*, reinforcement (Dobzhansky 1937; Butlin 1987) is shown to have caused speciation by altering mate preferences (Hoskin et al. 2005). This

change also caused divergence in mate preferences for different populations within one species (Hoskin et al. 2005). Chromosomal rearrangements, such as inversions can also spread through a population to fixation with the aid of gene flow. If genes important in ecological divergence lie on an inversion, its fixation may lead to speciation (Nosil 2012). If locally adapted alleles at more than one locus are found on the inversion it will increase fitness of those individuals that possess the inversion, as it keeps the favoured loci together, and selection will therefore cause the inversion to spread within the population (Kirkpatrick 2006). An example of chromosomal rearrangements leading to divergence in nature is in the monkeyflower, *Mimulus guttatus,* where genes influencing reproductive isolation lie on a chromosomal inversion that is under divergent selection (Lowry & Willis 2010). This process, where divergent selection on a locus reduces the migration rate of closely linked gene regions and thereby increases divergence, is known as divergence hitchhiking (Feder et al. 2012). Hybridisation can also provide novel genetic variation that can be used in order to adapt to new environments (for review see (Seehausen 2004)). Hybridisation can help to maintain the standing genetic variation within a species, therefore providing more opportunities for adaptation to occur. Transgressive segregation can also be a product of hybridisation, where traits of hybrid taxa are either novel or more extreme than their parental taxa (Rieseberg, Archer, et al. 1999). The new variation created may allow hybrids to exploit environments that their parents could not. The *Helianthus* sunflowers are a typical example of transgressive segregation. *Helianthus paradoxus* is a hybrid of two parental species; *H. annuus* and *H. petiolaris*. *Helianthus paradoxus* possesses a number of traits that are extreme in comparison so the parental traits, including leaf area, days until budding and mineral uptake (Rieseberg et al. 2003).

1.3 Factors that shape patterns of species co-occurrence

Speciation has the ability to affect the geographic distribution of diversity and species assemblages by influencing how species co-occur; if speciation is allopatric, closely related species will not co-occur and if it is sympatric their ranges will overlap immediately after speciation. After this, ecological or stochastic processes will determine the distribution of species. The role of the geography of speciation has been comparatively underrepresented in field of community phylogenetics relative to the subsequent ecological processes (C. O. Webb et al. 2002; Warren et al. 2014; Mittelbach & Schemske 2015). Community phylogenetics aims to examine the phylogenetic structure of communities, the niches occupied by species in these communities and the processes that drive trait evolution and biogeography to produce the species assemblages we observe in nature (C. O. Webb et al. 2002). The primary focus of this field has historically been put upon ecological processes that shape distributions post-speciation, which are typically divided into three groups. First, interspecific interactions such as competition, which can prevent species occupying a similar niche from co-occurring (W. L. Brown & E. O. Wilson 1956). Second, environmental filtering (P. R. Grant 1972), where co-occurring species are more similar as they are adapted to the same environment. Third, stochastic processes such as random dispersal may also play a role when selection is not acting (Hubbell 2001).

The importance of species interactions in limiting ranges is debated (Sexton et al. 2009; Wiens 2011) and the extent to which competition shapes distributions remains unknown. Competition is a source of disruptive selection, a type of divergent selection where important phenotypic traits are pushed towards opposite extremes by selection acting in one population or between closely related species. Competition is present in two major processes that affect

co-occurrence; competitive exclusion (Hardin 1960) and character displacement (W. L. Brown & E. O. Wilson 1956). If a species cannot occupy a region because another species is present, it is known as competitive exclusion (Hardin 1960). A classic example of the competitive exclusion principle occurring in nature can be seen in two species of barnacle found in Western Europe. When these species are found together, *Chthamalus stellatus* is found on the upper zone of the shore and *Balanus balanoides* is found in the lower zone. Two mechanism govern the distribution of the two species along the shore. *B. balanoides* cannot survive the dessication and temperature extremes that affect individuals at the highest part of the shore. However, *B. balanoides* grows at a much faster rate than *C. stellatus* and can smother the smaller species or prise it from the surface of the rocks preventing it from invading the lower shores. If *B. balanoides* is removed from a lower area, *C. stellatus* is able to colonise up to the low tide line, suggesting that it is direct competition between these two species that is limiting the range of *C. stellatus* (Connell 1961).

Character displacement (W. L. Brown & E. O. Wilson 1956; P. R. Grant 1972) is the evolutionary divergence of traits caused by competition between coexisting species or populations. Divergence may be ecological, behavioural, morphological or physiological (P. R. Grant 1972) in nature. Ecological character displacement has received a considerable amount of focus recently but its role in the generation of biodiversity is unknown (Stuart & Losos 2013). One of the strongest cases for character displacement is from a long-term study on the Darwin's finches of the Galapagos Islands. The beak size of the medium ground finch, *Geospiza fortis*, was found to have diverged from the large ground finch, *G. magnirostris,* 22 years after the latter arrived on the island (P. R. Grant & B. R. Grant 2006). This divergence was in response to depleted food supply caused by the co-occurrence of these two species. Another example is character displacement of tadpole trophic phenotype, which has been

demonstrated to have indirectly contributed to reproductive isolation between populations of the spadefoot toad (*Spea multiplicata*). When *S. multiplicata* is in allopatry with the congeneric species *S. bombifrons*, these two species produce both a carnivorous and omnivorous tadpole morph but when in sympatry, *S. multiplicata* tadpoles are almost exclusively omnivores and *S. bombifrons* carnivores. Additionally, sympatric populations of *S. multiplicata* have changed their mate call preferences, seemingly to avoid interspecific hybridization with the faster calling *S. bombifrons* (Pfennig & Simovich 2002). Using mitochondrial and nuclear sequence data, a reduction in gene flow was found between these two selective environments, suggesting that character displacement may contribute to reproductive isolation and ultimately speciation. Fish systems also provide examples of character displacement. The three-spined stickleback inhabits small lakes in British Columbia. In lakes where two species are present, one species possesses benthic morphology and habitat and the other limnetic. When only one species is present in a lake, it takes an intermediate form that exploits both habitats depending on its morphology, indicating that divergent selection pressures are present (Schluter & McPhail 1992). Competition for food is found to be the likely driver of the species' divergence and may have played a role in the formation of the two species.

It is undoubtedly a combination of geography of speciation, ecological and stochastic processes that shape the patterns of co-occurrence we see in nature but determining the relative importance of each is difficult, especially when attempting to infer causal mechanisms from current species distributions. Two recent reviews (Warren et al. 2014; Mittelbach & Schemske 2015) have suggested that patterns of co-occurrence produced by the geographic mode of speciation and colonisation dynamics can be misinterpreted as the result of ecological processes. This issue is exemplified by the use of two similar approaches to

infer entirely different historical processes from patterns of distribution and phylogeny. The community phylogenetic metrics of net relatedness index (NRI) and nearest taxon index (NTI) are used to determine whether communities are more clustered or overdispersed (C. O. Webb et al. 2002). A positive relationship between phylogenetic distance and level of co-occurrence is produced by competition, while environmental filtering causes a negative relationship. The age-range correlation (ARC) (Barraclough & Vogler 2000) is instead typically used to determine the primary mode of speciation within a group by investigating the relationship between node age and range overlap. High levels of co-occurrence between closely related, recently diverged species likely indicates speciation was in sympatry while low levels of co-occurrence typically signals allopatric speciation. The fact that these two very similar methods can be used to reveal different mechanisms highlights one of the primary challenges in understanding patterns of co-occurrence.

1.4 Macroevolutionary trends in diversification

One of the main goals in evolutionary biology is to understand what causes the uneven distribution of species across the tree of life. The balance of speciation and extinction dictates the rate of diversification of a clade. Two closely related clades of the same age may contain vastly different numbers of species; there are more than 850,000 species of insects compared to just 7,500 species in their sister group, Entognatha (Mayhew 2002). In plants, the family Amborellaceae is monotypic while the Orchidaceae consists of approximately 25,000 species. Determining the factors that drive differences in species diversity is a fundamental goal of evolutionary biology (Ricklefs 2007). Stochastic processes will generate some disparity among clades (Raup et al. 1973) but variation in species richness exists that cannot be explained by random chance (Mooers & Heard 1997). A change in speciation or extinction

rate can be caused by a range of factors including population size, generation time, gamete dispersal and sexual selection (Barraclough et al. 1998). Other processes and events such as dispersing to a new environment, the extinction of a competitor or the evolution of a trait that acts as a key innovation (Hunter 1998) can generate ecological opportunity which may stimulate diversification (Yoder et al. 2010).

As larger phylogenetic trees become available studies of diversification over large timescales and geographic regions have become more common. Speciation and extinction taking place over long timescales and can be difficult to estimate, especially with incomplete taxonomic coverage (Rabosky 2009; Stadler & Bokma 2013) or a sparse fossil record (Morlon 2014). In the past ten years a larger range of methods have appeared aiming to quantify diversification rates, especially using phylogenetic trees consisting of only extant species (Alfaro, Santini, et al. 2009; Stadler 2011; G. H. Thomas & Freckleton 2011; Rabosky 2014). These have been to used identify diversification rate shifts in a variety of different groups. For example, diversification in mammals was most rapid between 30-33 mya, driven by explosive speciation in Rodentia, Cetartiodactyla and Marsupialia (Stadler 2011). The most recent methodological advances have been aimed at accommodating heterogeneous mixtures of diversification rates acting upon a phylogenetic tree (Rabosky 2014) and have been used to identify diversification rates shifts in clades of lizards (Rabosky, Donnellan, et al. 2014), birds (McGuire et al. 2014) and plants (M. G. Weber & Agrawal 2014).

1.4.1 Trait-dependent diversification

The presence of a convergent trait with multiple evolutionary origins is often considered as evidence that these traits have evolved by natural selection (Harvey & Pagel 1991). Traits that have evolved independently, many times, in a large number of lineages provide excellent opportunities to study their roles in shaping the tree of life. Replication is necessary to conclusively show that a trait drives diversification but this is often lacking in many studies proclaiming a key innovation (C. S. Drummond et al. 2012; Maddison & FitzJohn 2015). Even with replication, clearly and irrefutably showing that the evolution of a novel trait promotes diversification is difficult – the repeated modification of pharyngeal jaws in Labrid fishes was classed as a key innovation until new data emerged which revealed a lag between the evolution of pharyngeal jaw modifications and diversification rate shifts (Alfaro, Brock, et al. 2009). While a trait may appear to stimulate diversification, that evolution of the focal trait may be correlated with the evolution of other traits that could be more important. The mammalian hypocone (Hunter & Jernvall 1995) and floral nectar spurs (Hodges & Arnold 1995; Ree 2005) are considered to be well supported examples as they have evolved multiple times and are associated with increased diversification in more than one instance.

Determining whether diversification rates are trait dependent has been another focus in recent years following the development of a model able to estimate the effect of a binary character on speciation and extinction rates (Maddison et al. 2007). Previous efforts focused on sister clade comparisons (S. M. Vamosi & J. C. Vamosi 2005), which are not able to disentangle the effects of differential speciation and different extinction (Barraclough et al. 1998) or deal with complex patterns of character evolution involving more than one state (Maddison et al. 2007). The binary state speciation and extinction (BiSSE) model can be used to detect

differential speciation, extinction and transition rates based on a character trait but also to reconstruct character states taking into account these rate asymmetries (Maddison 2006). This spurred the development of new and more complex methods in maximum likelihood or Bayesian frameworks, with the goal of determining whether speciation and extinction rates are correlated with the evolution of a particular discrete or quantitative character trait (FitzJohn et al. 2009; FitzJohn 2010; Goldberg et al. 2011; Rabosky 2014; Rabosky & Huang 2015; Beaulieu & O'Meara 2015). These methods have been used effectively to show that colour polymorphism is associated with accelerated speciation rate in birds (Hugall & Stuart-Fox 2013) and that speciation rate and morphological evolution are correlated across ray-finned fishes (Rabosky et al. 2013). Complications can arise when investigating large phylogenetic trees with complex evolutionary histories and dynamics (Beaulieu & O'Meara 2015). Viviparity has evolved over 100 times in reptiles and ancestral state reconstructions using BiSSE revealed an unexpected early origin of viviparity (R. A. Pyron & Burbrink 2014) accompanied by increased speciation and extinction rates in viviparous groups. These conclusions were disputed by several follow-up papers that used alternative methods or phylogenetic trees to yield different results (B. King & Lee 2015; Wright et al. 2015) or assessed the plausibility of the original paper by suggesting that the inclusion of the biological requirements of frequent reversal to oviparity must be included to understand the evolution of reproductive modes (Blackburn 2015). Attempting to identify the causal mechanisms behind bursts of diversification is notoriously difficult. The challenges of false positives (Davis et al. 2013; Rabosky & Goldberg 2015), identifying a study system with enough replication to form reliable conclusions (Maddison & FitzJohn 2015) and disentangling causation from correlation at evolutionary timescales all provide challenges for which the rapidly developing field strives to find solutions.

1.5 Correlated trait evolution, convergence and the phylogenetic comparative method

All species are related by common descent (Darwin 1859). Closely related species are typically more similar than distantly related species, a phenomenon that must be overcome when conducting comparative analyses of trait evolution (Harvey & Pagel 1991). The phylogenetic comparative method (PCM) was invented for this purpose and is defined by Paradis (Paradis 2014; Garamszegi 2014) as "*the analytical study of species, populations, and individuals in a historical framework with the aim to elucidate the mechanisms at the origin of the diversity of life*." The PCM acts to distinguish traits that are common among species because of shared ancestry and those traits that have evolved independently in different lineages. One of the main goals of the PCM is to explore the correlated evolution of character traits in a phylogenetic context. The key initial advancement of the modern PCM was Felsenstein's Phylogenetic Independent Contrast (PIC) (Felsenstein 1985) which takes into account species relationships when assessing correlated evolution between two characters. Another method, phylogenetic least squares regression (PGLS) (Grafen 1989), soon followed which enabled the use of more complex models of correlation between character traits with multiple factors. Additional methods for examining correlated trait evolution include the phylogenetic mixed model (Housworth et al. 2004) and Monte Carlo Markov Chain (MCMC) based methods (Pagel & Meade 2006). These methods have been used to reveal the relationship between range size and body mass in mammals (Garland et al. 1992) and fish (M. Pyron 1999) as well as many other correlations (Freckleton et al. 2002). The two most commonly models of trait evolution in PCMs are Brownian motion (BM) and Ornstein-Uhlenbeck (OU). The BM model is a random walk process while the OU model of trait evolution can account for stabilizing selection for trait optima and thus more biologically realistic scenarios (Hansen 1997). It is important to note that under a Brownian motion model of evolution, PIC and PGLS are equivalent (Blomberg et al. 2012). The models themselves

have been used to investigate the tempo and mode of trait evolution that leads to the variation we see in nature (O'Meara et al. 2006; Eastman et al. 2011; Revell et al. 2012), notably in mammals where a 10-52 fold increase in the rate of evolution was found in some lineages (Venditti et al. 2011). The OU model has been harnessed to examine different rates of evolution along different branches of a tree and investigate clade-wide convergence (Butler & A. A. King 2004; Beaulieu et al. 2012; Ingram & Mahler 2013). Other models of trait evolution used less frequently are the early-burst model (Harmon et al. 2010) and Pagel's transformations (Pagel 1997; Pagel 1999).

The PCM is commonly used to infer adaptation or causal mechanisms driving the evolution of a particular trait although this is often criticised, as it is difficult to conclusively demonstrate adaptation (Leroi et al. 1994; E P Martins 2000; Grandcolas et al. 2011) and distinguish causality from correlation (Garamszegi 2014). For example, in *Anolis* lizards, similar phenotypes have arisen in different lineages (Losos 2011), which is typically considered evidence for adaptation (Harvey & Pagel 1991). However in this case convergence is not complete, in that changes towards herbivory do not override differences between lineages, so standard PCMs are not able to pick up on these patterns of convergence as they are masked by other interspecific differences (Losos 2011). Newer developments of the PCM have allowed traits to evolve in response to each other and towards fixed or randomly evolving predictor variables to demonstrate adaptation (Bartoszek et al. 2012) or using path analysis to attribute causality (Hardenberg & Gonzalez Voyer 2013). Regardless of the challenges faced, the modern phylogenetic comparative method is of critical importance when trying to disentangle the mechanisms that lead to the evolution of diversity.

1.6 Molecular signatures of natural selection and their functional consequences

In order to fully understand how natural selection has shaped interspecific differences among species it is necessary to examine the genetic differences among species and identify which changes are adaptive. Positive selection is the fixation of advantageous mutations caused by natural selection (Yang 2005) and observing this is considered evidence that adaptive evolution has taken place. Tests for positive selection revolve around calculating the ratio of non-synonymous to synonymous substitution in protein-coding DNA sequences. A non-synonymous substitution is one that changes the amino acid sequence of a protein, while a synonymous substitution does not. If the dN/dS ratio of a particular region is greater than one it indicates that positive selection is acting, if it equals one it signifies the change is neutral and if the change is deleterious it will prevent fixation producing a dN/dS ratio less than one. In the Australian Lancerocercata stick insects, positive selection in genes related to glycolysis were linked to adaptation to new stressful lifestyles (Dunning et al. 2013). Linking signatures of positive selection to the phenotypes they change is key to understanding how detected adaptive evolution shapes diversity. In the cichlids of East Africa, positive selection has been found in various rod (Sugawara et al. 2002) and cone (Spady et al. 2005) visual pigments in a number of lakes across which parallel evolution in visual pigments was detected (Sugawara et al. 2005; Seehausen et al. 2008). Further work revealed that divergent natural selection at different depths coupled with sexual selection based on different colour preferences in different photic environments has been shown to lead to speciation in cichlids (Seehausen et al. 2008). Studying the process of adaptation at a molecular level is an important step in uncovering how selection can cause changes that have a functional effect and given rise to the diversity that may ultimately play a role in speciation.

1.7 The genomic basis of trait diversity

1.7.1 The advent of high-throughput sequencing and its applications

A rapidly growing field that is contributing more and more to our understanding the origins of diversity is genomics. Rather than looking at the function of specific genes at the outset, evolutionary genomics aims to determine the location, size and number of regions of the genome, or loci, that govern a trait important to the process of evolution. Recently developed high-throughput, reduced-representation sequencing techniques have enabled the study of almost any organism a reasonable quality DNA sample can be obtained from, without needing any prior information (Stapley et al. 2010).

The Human Genome Project cost almost three billion dollars and took 13 years to complete. Today, a genome can be sequenced in less than 24 hours for $1000 or less (Grada & Weinbrecht 2013) using massively parallel, "next generation sequencing" (NGS). The development of high-throughput reduced representation sequencing has led to the production of large amounts of low-cost genomic data ideal for understanding the genomic basis of traits. Where previously, genomic studies have been conducted on model organisms (e.g. species that are simple to culture with short life-cycles), NGS methods have opened up avenues to the study of non-model organisms and thus a huge array of evolutionary scenarios that can increase the breadth of knowledge relating to adaptive evolution (Stapley et al. 2010). There are two schools of approaches that can be used to identify the genes governing a particular trait. The first is the bottom-up approach, where the investigation begins with a set of candidate gene or genes and usually involves expression analyses of these genes in relation to the relevant phenotype. Prior work to identify candidate genes is required, meaning that the bottom-up approach is usually restricted to well-studied organisms. When working with a

non-model organism it is preferable to use the top-down approach as no prior genomic data or information regarding adaptive traits is needed. The top-down methodology determines phenotype-environment correlations and subsequently the genomic architecture of those phenotypes, but it can be difficult to establish correlations between genome and reality. Regardless, this unrestricted approach allows the investigation of species with unique and interesting ecology. In organisms where the ecology is well understood the genetic underpinning of phenotypic traits is often not known. Likewise, in study organisms where genetic studies are the focus, an assessment of the ecological significance of any underlying genetic architecture is usually lacking. NGS methodology has allowed investigators to 'genomicise' ecologically well-understood species thereby bringing together two fields. The wealth of genomic resources produced by studies using NGS and the initial observations made about the genomic basis of adaptive evolution provides an excellent backbone for further study. The increasing ability to apply NGS techniques to non-model organisms has facilitated the study of species that possess unique and interesting traits and opened up many different avenues to study genomic processes.

1.7.2 Identifying genomic regions underlying phenotypic traits

A variety of techniques can be used to identify genomic regions governing a trait. Quantitative trait locus (QTL) mapping determines the location of genomic regions that explain the variation in trait using a mapping cross (Stapley et al. 2010). Performing a QTL analysis requires one to build a linkage map, which involves assessing patterns of the frequency of recombination in a mapping cross in order to determine the relative positions of sequenced loci; the higher the frequency of recombination between a pair of markers the further away they are from each other. QTL mapping has been used to identify regions that

control adaptive morphology in sticklebacks (Colosimo et al. 2004; Shapiro et al. 2004; Chan et al. 2010) and burrowing behaviour in mice (J. N. Weber et al. 2014). Linkage mapping can also identify putative chromosomal rearrangements that can play an important part in divergence by allowing rearranged regions to differentiate more than collinear regions. This could allow incompatibilities to arise and prevent introgression, which may ultimately lead to speciation (Rieseberg 2001; Faria & Navarro 2010).

Genome-wide association studies (GWAS) expand upon this by using unrelated individuals and a strong association between QTL and marker to locate regions controlling traits. A GWAS was used to identify the genetic basis of a horn type and horn size in the Soay sheep, *Ovis aries*, highlighting the ability of this technique to determine genomic regions underpinning both discrete and quantitative traits (Johnston et al. 2011).

Genomic approaches have also been used to investigate the basis of sex determination. Linkage mapping was used to identify markers tightly linked to the principal sex-determining locus in the Nile Tilapia, *Oreochromis niloticus* (Palaiokostas et al. 2015) and has revealed a putative sex chromosome in the zebrafish, *Danio rerio* (Anderson et al. 2012). Understanding the genomic basis of sex determination can shed light on the diversity produced by sex-linked traits and how this sexual dimorphism arises (Adkins-Regan & Reeve 2014) or the formation of sex determining regions (Charlesworth et al. 2005). Candidate gene or genome enrichment (Stapley et al. 2010) approaches, where a specific region known to be relevant to the trait of interest, require a considerable amount of prior genomic information and are therefore not applicable to groups where this information is not available. To improve our understanding of

the origins of diversity and identify general patterns and trends in diversity we must continue to investigate evolution in new groups with interesting and unique characteristics.

1.8 Study groups

1.8.1 The genus *Austrolebias*

The genus *Austrolebias* (order: Cyprinodontiformes) consists of over 40 species of annual killifish found in seasonal ponds distributed across the grasslands, wetlands and savannah of eastern South America (Costa 2006; García et al. 2014). These fish are found in Uruguay, Argentina and Southern Brazil with a small number of species in Bolivia and Paraguay. The small bodies of water Austrolebias inhabit are usually anywhere between 8 – 60cm in depth and dry out completely during the warm summer months, from December to March (Miller 1978). Individuals must grow to maturity, mate and lay eggs during the wet season that typically lasts 6-8 months. During mating, males and females dive into the substrate at the bottom of their pond, simultaneously depositing their gametes so that the fertilized eggs remain buried in in the soil. Once laid, these desiccation-resistant eggs survive an extended period of drought by going through multiple stages of diapause until hatching is triggered by the first autumn rains (Wourms 1972) (see Figure 1). *Austrolebias* occur primarily in four areas; the La Plata delta, Western Paraguay, the Patos-Merin lagoon system and Rio Negro tributary of the Rio Uruguay (Costa 2010). Periodic flooding can lead to dispersal between ponds but dispersal between river basins appears very unlikely, though it may have been feasible in the past during marine transgressions (Costa 2010). If we are to understand how the current distributions of *Austrolebias* species came about and the evolutionary processes that shaped them, it is important to understand the evolutionary history of the group.

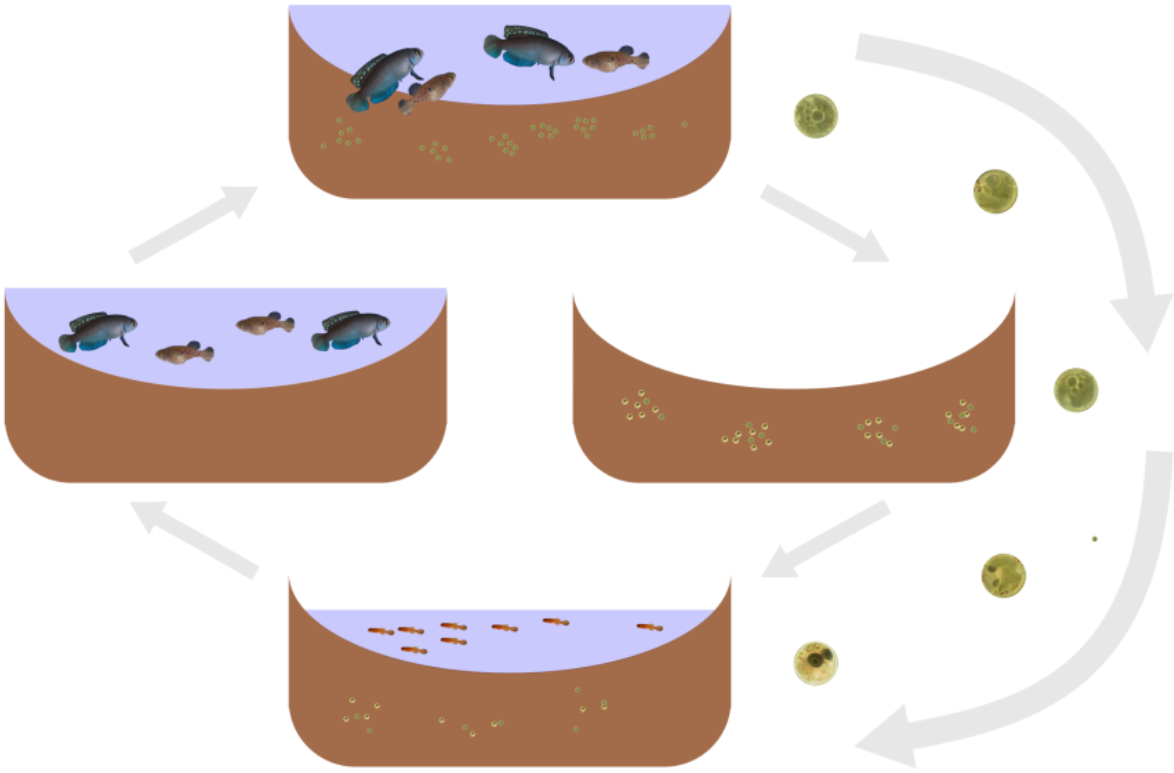

Figure 1.1 A diagram representing the life cycle of *Austrolebias*. Moving clockwise from the top pane; eggs are laid within the soil substrate of the pond. The pond then dries out and adult fish die. During this dry period eggs go through multiple stages of diapause. Rains then trigger the hatching of fry, which grow rapidly to maturity. The process then repeats.

Current members of *Austrolebias* previously belonged to the genus *Cynolebias*, before it was split into three genera (*Cynloebias, Austrolebias* and *Megalebias*) (Costa 1998). Then, in 2006, Costa redefined *Austrolebias* based on morphological characters to include those species in *Megalebias* (Costa 2006). *Austrolebias* is a rapidly growing genus - 65% of *Austrolebias* species have been described since 1985 (Loureiro et al. 2011) and new species

have been described very recently (Costa 2014). As of yet the phylogenetic relationships within the genus are unresolved as genetic and morphological trees show somewhat contradictory results (Costa 2006; García et al. 2014). The most recent published molecular-based phylogenetic tree is based on a single mitochondrial gene, cytochrome B (García et al. 2014). Using only mitochondrial sequence data can present issues because of changes in effective population size and mutation rate in the single locus mitochondrial DNA represents (Ballard & Whitlock 2004). Therefore, a more robust phylogenetic tree based on multiple nuclear DNA loci is needed to understand relationships among *Austrolebias*.

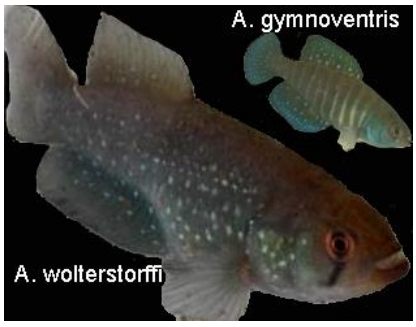

Figure 1.2 The co-occurring *A. wolterstorffi* and *A. gymnoventris* (males), to scale.

Austrolebias are have a relatively short life cycle, are easy to culture in the lab and possess a large amount of variation in various aspects of their biology including genome size & structure (García et al. 2014), morphology and body size (Costa 2006). These factors make the genus an excellent model for the study of the origins of diversity. *Austrolebias* species are typically 40-50mm in standard length (Costa 2006). The smallest species can reach maturity at only 23mm and some species such as *A. elongatus* or *A. monstrosus* can grow to be more than 150mm in standard length (Costa 2006). These size differences have largely been attributed to divergence in diet, for example, *A. wolterstorffi* eats molluscs shares its range

with *A. gymnoventris*, a crustivore (Fig. 1.2) (Costa 2009). *Austrolebias cheradophilus,* a large species, has been shown to have a more variable diet than smaller conspecifics found in the same pond (Laufer et al. 2009). Body shape has also diverged alongside size; larger species are typically more elongated, with a wider gape and larger teeth (Costa 2006). Size differentiated fish are repeatedly found in sympatry, both in their range and in the same temporary ponds (Costa 2006; Laufer et al. 2009) which indicates that different *Austrolebias* likely occupy different niches in these temporary ponds. Therefore, *Austrolebias* provides an excellent opportunity to study how growth, size and shape differences arise in their small, ephemeral pond system.

Males of each species of *Austrolebias* have unique colouring and patterning (Fig. 1.2, for example), indicating that these traits may be important in mate choice and assortative mating may occur when species are found in sympatry. Despite this, prezygotic barriers to reproduction are not absolute and interspecific hybridisation has been successfully achieved by hobbyists and in closely related genera (Oviedo Alcoba 2009). Methods such as linkage mapping and Quantitative Trait Locus (QTL) analysis require crosses with a known pedigree to identify loci underlying phenotypic traits. When investigating a trait that varies between species, the ability to hybridize is critical, making *Austrolebias* an ideal study species for investigating the genetic underpinning of character traits. Sex determination has previously been a research focus in these fish, but no clear conclusions on the mechanism have been reached (Arezo et al. 2014). The genomes of *Austrolebias* species are unusually large, with an average DNA content of 5.95 picograms (pg) per diploid cell (García et al. 2014), which is larger than the genomes of almost all other diploid actinopterygian fishes that have been measured. The closely related *Cynolebias melanotaenia* has a genome size of just 2.72pg indicating that *Austrolebias* has experienced one or more rapid increases in genome size

which have been suggested to be associated with bursts of speciation in the genus (García et al. 2014). Furthermore, there is extensive variation in karyotype among *Austrolebias* species. 2n ranges from 34 in *A. luteoflammulatus* to 48 in a number of species including *A. gymnonventris* (García et al. 1993). *Austrolebias* provide an interesting opportunity to study genome structure and chromosomal rearrangements while attempting to determine the factors most important in sex determination in these fishes. The recent development of NGS approaches provides a cheap and effective means to conduct genomic analyses in non-model taxa such as *Austrolebias*. Finally, conservation concerns have already been raised for *A. cherdaophilus*, *A. cyaneus*, *A. wolterstorffi* and *A. juanlangi*, which are endangered in some or all of their ranges (Lanés & Maltchik 2010; Volcan et al. 2011; Lanés et al. 2014). Consequently, it is important that we understand the biology of these species to better inform their conservation efforts.

1.8.2 The order Cyprinodontiformes

The Cyprinodontiformes are an order of approximately 1,200 ray-finned fish species found primarily in Africa and the Americas but also in Asia and Europe (Parenti 1981). Many of these species are popular in the aquarium trade including guppies, mollies and killifish. Living in a wide range of habitats, they have also evolved different and peculiar reproductive life history strategies. Members of the Poeciliidae, Goodeidae and Anablepidae give birth to live young and are viviparous or ovoviviparous (Meyer & Lydeard 1993). There are also many genera in the suborder Aplocheiloidei that are annual including the aforementioned *Austrolebias* as well as *Nothobranchius*, *Austrofundulus* among others (Furness et al. 2015). One of the most well-known members of the order is the mangrove killifish, *Kryptolebias marmoratus*, a self-fertilizing hermaphrodite that can exist for up to one month out of water

(Abel et al. 1987). Two remarkable reproductive life history traits have evolved in Cyprinodontiformes. Viviparity (the ability to give birth to live young) has evolved at least three times, in the Anablepidae, Poeciliidae and Goodeidae (Meyer & Lydeard 1993). Annualism, as explained in section 1.8.1, has also evolved several times independently (Furness et al. 2015) in Africa and South America (Costa 2011; Costa 2013). It may be that these traits have played an important role in generating diversity in the Cyprinodontiformes. Considerable morphological diversity exists in Cyprinodontiformes, from the miniaturized livebearing *Fluviphylax* that do not grow larger than 26mm when adult (Weitzman & Vari 1988) to the comparatively gargantuan *Anableps* genus where some species grow up to 350mm . *Anableps anableps* is particularly remarkable, possessing eyes that are split to allow it to see above and below the water's surface simultaneously (Sivak 1976; Owens et al. 2012). There is also a large amount of variation in generic level diversity within Cyprinodontiformes, for example the genus *Oxyzygonectes* is monotypic while *Aphyosemion* contains almost 100 species (FishBase (Froese & Pauly 2015), accessed 15/04/2015).

Cyprinodontiformes contains a number of model organisms important to a range of biological fields. The *Nothobranchius* African annual killifish are the shortest lived vertebrates (Blažek et al. 2013) and a model for the study of aging (Genade et al. 2005). Members of the *Fundulus* genus are used for the assessment of pollution (Eisler 1971). Guppies (Poeciliidae) are have frequently been used in studies on natural and sexual selection (Endler 1984; Reznick et al. 1990; Schlüter et al. 1998; Pollux et al. 2015). *Xiphophorus maculatus*, the Southern Platyfish, was one of the first fish species to have its whole genome sequenced (Schartl et al. 2013), and several other draft genomes are available including *Cyprinodon nevadensis* (GenBank accession no. JSUU00000000) and *Poecilia reticulata* (GenBank accession no. AZHG00000000). While detailed phylogenetic trees of genera (Dorn et al.

2011; Jones et al. 2013), families (Hrbek & Larson 1999; Pollux et al. 2015) and suborders (Furness et al. 2015) are available there is no DNA-based phylogenetic tree covering all major groups of Cyprinodontiformes. As Cyprinodontiformes are popular with researchers and hobbyists there is also a large amount of location and phenotype data stored in online databases (e.g. FishBase, (Froese & Pauly 2015)). Collating the wealth of genetic information available for Cyprinodontiformes would enable the construction of a phylogenetic tree suitable for the study of macroevolutionary dynamics and the mechanisms behind them. The variation in species richness among clades as well as variety of habitats, geographic regions and ecological niches these fishes occupy (Parenti 1981) make them an excellent study from for investigating patterns of genetic and phenotypic diversity at a broad scale.

1.9 Aims and Objectives

1. To reconstruct the evolutionary history of *Austrolebias* and to use this information to disentangle factors influencing patterns of co-occurrence in the genus
2. To understand and quantify the development and evolutionary history of growth, morphology and body size variation in the *Austrolebias* genus.
3. To create a high-resolution linkage map of *Austrolebias*
4. To identify diversification rate shifts in Cyprinodontiformes and understand the factors that drive them.
5. To determine the extent to which positive selection acts on the low-light vision pigment rhodopsin in the Cyprinodontiformes and its functional significance.

1.10 Thesis Outline

Chapter 2 uncovers the evolutionary relationships among species of the annual killifish genus *Austrolebias* by inferring phylogenetic trees. These trees are used to reveal extensive mito-nuclear discordance, the biogeographic history of *Austrolebias* and to show how body size determines patterns of co-occurrence among *Austrolebias* species.

Chapter 3 assesses the growth and development of 18 species of *Austrolebias* by measuring length and body shape over a 49-day period. Hatching size is found to be an important factor driving interspecific differences in size and shape and was influenced by maternal effects in hybrids. Phylogenetic comparative methods reveal convergent evolution towards a large, streamlined body in two groups of *Austrolebias*.

Chapter 4 uses cutting edge, high-throughput sequencing techniques to construct maternal and paternal linkage maps of an interspecific cross between two *Austrolebias* species. There are many areas of low recombination, particularly in the paternal map. Little evidence for a genetic sex determination system is found.

Chapter 5 investigates patterns of diversification in the Cyprinodontiformes. A new generic-level phylogenetic tree of this order was constructed and multiple rate shifts are identified. Viviparity is found to trigger two of these rate shifts and is associated with a higher rate of diversification.

Chapter 6 investigates how selection acts on the low-light visual pigment rhodopsin in Cyprinodontiformes. Signatures of selection are found at 12 sites across rhodopsin, some of which have previously been shown to affect retinal release rate and dimerisation. Selection is found to be acting across all major Cyprinodontiform lineages.

Chapter 2

Body Size Divergence Facilitates Co-occurrence in Annual Killifish (*Austrolebias*)

2.1 Abstract

Patterns of species co-occurrence are driven by the geography of speciation and subsequent range shifts. I this chapter I investigate the extent to which ecological and evolutionary processes shape patterns of range overlap among species from the *Austrolebias* annual killifish genus. I present new nuclear DNA (nDNA) and mitochondrial DNA-based (mtDNA) phylogenetic trees of *Austrolebias,* constructed from multiple loci, and reveal differences from previous phylogenetic hypotheses. I use the nDNA tree to infer the biogeographic history of the genus, showing that *Austrolebias* likely originated in the Patos Lagoon region of eastern Uruguay and southern Brazil. Furthermore, I assemble over 500 site locations to model the distribution of these species and quantified levels of range overlap among closely related species. I found that body size was the most important factor explaining patterns of overlap - those species pairs that differ more in body size have higher levels of range overlap. This effect was pervasive regardless of the mode of speciation at each node. I suggest that patterns of co-occurrence were driven by competition, with size differences evolving in sympatry or facilitating co-existence.

2.2 Introduction

Understanding what factors influence the patterns of co-occurrence among species we see in nature is a major goal in evolutionary and ecological research. A combination of current distributions, ecological trait data and phylogenetic relationships can often give insight into the processes that created these patterns (C. O. Webb et al. 2002). These processes can be ecological, evolutionary or stochastic in nature, though the relative importance of each of these factors is widely debated (Wiens 2011; Chase & Myers 2011; Mittelbach & Schemske 2015). Initially, the geography of speciation will affect the patterns of co-occurrence among closely related species. If speciation is allopatric, incipient species are initially isolated and thus ranges will not overlap. Sympatric speciation will lead to the co-occurrence of species during and after divergence. After speciation, species ranges can alter due to a change in dispersal ability, ecological processes or purely neutral processes (Hubbell 2001) (e.g. random dispersal).

There are two main ecological processes than can affect patterns of co-occurrence post-speciation: competition and environmental filtering. Competitive exclusion prevents the coexistence of species that are competing for the same resources (Hardin 1960). This process has been shown to dictate the distribution of tropical stream fishes (Zaret & Rand 1971), desert mammals (Bowers & J. H. Brown 1982) and passerine birds (Pigot & Tobias 2012). Secondly, competition can drive ecological character displacement (ECD), whereby co-occurring species diverge in resource use and phenotype in order to reduce competition, thereby facilitating coexistence (W. L. Brown & E. O. Wilson 1956). Evidence for ECD exists in a number of groups including Darwin's finches (Schluter et al. 1985), anoles (Losos 1990b) and sticklebacks (Schluter & McPhail 1992), although its importance in the generation of species diversity is debated (Stuart & Losos 2013). Environmental filtering

causes species to co-occur based on shared environmental requirements and produces a distribution pattern opposite to competitive exclusion. Environmental filtering is important in the assembly of lagoon fish (Mouillot et al. 2007) and tropical rainforest communities (Lebrija-Trejos et al. 2010). However, a recent review by Warren et al. (Warren et al. 2014) suggested that seemingly non-random patterns produced by geographic mode of speciation and colonisation dynamics can be misinterpreted to be the result of ecological interactions between species or environmental filtering. Mittelbach & Schemske (Mittelbach & Schemske 2015) put forward a similar opinion, suggesting that a stronger focus should be put on the effects of the geography of speciation and secondary contact after allopatric speciation. Here, I aim to determine the relative importance of ecological and evolutionary processes influencing patterns of co-occurrence in a genus of annual killifish, *Austrolebias*.

The South American annual killifish genus *Austrolebias* (Costa 1998; Costa 2006) contains over 40 species found in seasonal, freshwater pools and wetlands on the South American grasslands, savannahs and forests. These fish possess a peculiar life history. During the reproductive season, a mating pair will dive into the muddy substrate of the pond, oviposit and fertilize their eggs. As the dry season commences water evaporates from the ponds and the adult fish die. Eggs persist within the soil, going through several stages of diapause until hatching is triggered by the earliest wet season rains (Wourms 1972). Once hatched, fish grow rapidly to adulthood and the reproductive cycle is repeated. *Austrolebias* are found in seasonal ponds distributed throughout the basins of the La Plata, Paraguay and Uruguay Rivers as well as the Patos-Merin lagoon drainage system (Costa 2010). Van Dooren et al. (Van Dooren et al. In review) observed that a number of such events occurred between major basins but that within-basin speciation events are not uncommon. Major historical dispersal events in *Austrolebias* are thought to have been caused by tectonic plate movements and

marine transgressions allowing them to spread throughout these areas (Costa 2010). Previously published phylogenetic trees for *Austrolebias* have been based on either morphology (Costa 2006) or single locus mitochondrial DNA (mtDNA) sequences (García et al. 2014) or several mitochondrial DNA markers combined with a single nuclear locus (Van Dooren et al. In review). Using only mtDNA has been cautioned against on a number of occasions (Shaw 2002; Rubinoff & Holland 2005) in phylogeographic studies in particular, due to changes in recombination, effective population size and mutation rate in the single mitochondrial locus (Ballard & Whitlock 2004). Here, I reconstruct the phylogeny of *Austrolebias* using multiple nuclear DNA (nDNA) markers from 25 species of *Austrolebias*. I also expand upon the most recent phylogenetic trees by adding new nuclear loci, allowing me to examine discordance between mtDNA and nDNA trees. I then use the nDNA tree to determine the geographic origins of *Austrolebias* and subsequent patterns of dispersal based on the primary regions of endemism defined by Costa (Costa 2010).

Species in *Austrolebias* vary substantially in adult body size with the largest species reaching up to 150mm in length and the smallest species only 2.3cm when mature (Costa 2006). Multiple *Austrolebias* species are often found in the same pond and it is common to find small and large species in sympatry. Body size influences resource use in freshwater systems (Woodward & Hildrew 2002) and stronger competition is expected between those species with similar body sizes (MacArthur & Levins 1967; May & MacArthur 1972) as they vie for the same resources. Diet richness has already been shown to be linked body size in *Austrolebias* (Laufer et al. 2009) indicating that it may play a role in resource use in this system and evidence within a single pond indicates that community structure is also based on body size (Canavero et al. 2013). Therefore, I predict that body size influences patterns of co-occurrence across *Austrolebias* through competition between similarly sized species.

Assessing the patterns of range overlap requires estimates of current species ranges. To accurately define the current distribution of *Austrolebias* species I collated a new and extensive database of occurrence locations. In order to estimate levels of range overlap among species, these occurrences were used to build species distribution models (SDMs). Data on body size and mode of speciation as well as node ages obtained from the phylogenetic tree were then used to identify how these factors can explain the patterns of range overlap in *Austrolebias.* I also then attempt to go beyond current methods to determine whether geographic mode of speciation can be classified and whether this classification has an effect on the relationship between range overlap and size.

2.3 Materials and methods

2.3.1 DNA sequencing

Genomic DNA was extracted from 56 individuals using the Qiagen DNeasy Blood & Tissue kit. A total of 15mg of tissue was used for each extraction, usually from fin tissue except for especially small fish where I complemented the fin with muscle tissue to make up 15mg. DNA extraction steps were performed as in the Qiagen DNeasy Blood & Tissue kit protocol. All individuals were sequenced for fragments of ectoderm-neural cortex protein 1 gene (ENC1), recombination activating gene 1 (RAG1), SH3 And PX domain containing 3 (SH3PX3), rhodopsin (RH1), three fragments of 28S ribosomal DNA (28S rDNA). Three mitochondrial genes were also sequenced; 12S ribosomal DNA (12S rDNA), 16S ribosomal DNA (16S rDNA) and cytochrome b (cytB). Primers for the amplification and sequencing of three fragments of 28S rDNA and the mitochondrial genes 12S rDNA, 16S rDNA and cytB were taken from Van Dooren et al. ENC1 was amplified and sequenced using primers from (C. Li et al. 2007). I also designed new primers to amplify and sequence SH3PX3, RAG1 and

RH1. All primers used were designed using Primer3 (Untergasser et al. 2012) and can be found in Table S2.1. Sequences for *Pterolebias longipinnis* (GenBank accession EF455709, KC702007, KC702072) and *Hypsolebias magnificus* (KC701989, KC702056, KC702122) were downloaded from GenBank to be used as outgroups with divergence time estimates from a new tree of Cyprinodontiformes (Chapter 5).

PCRs were carried out in 25 µl volume reactions containing primers at 0.2 µM final concentration. Reactions were carried out using the following parameters: An initial 4 minutes at 94ºC; 36 cycles of 30-60 seconds at 94ºC, 30-60 seconds at 45-61ºC (depending on primer pair) and 60-90 seconds at 72ºC; and 6 minutes at 72ºC. PCR products were cleaned using ExoSAP-IT (Affymetrix) and sequenced using both forward and reverse primers and Big Dye terminator v3.1 on an ABI 3130xL Genetic Analyzer.

In addition to those sequences generated in this study, my dataset for tree inference was supplemented with sequence data from a recent paper by Van Dooren et al. (Van Dooren et al. In review). If sequences from different sources were combined to improve the coverage for an individual, the missing sequence was taken from a conspecific of the same breeding source population from Van Dooren et al. (Van Dooren et al. In review) to ensure a minimal amount of noise (see Table S2.2).

Sequences were aligned in Geneious (v6.1, Biomatters) using the MAFFT alignment plugin (MAFFT v7.017, (Katoh et al. 2002)) and low quality ends were trimmed. The combined nuclear matrix is composed of 66 individuals across 27 (25 *Austrolebias* & 2 outgroups) species and 2,835 aligned characters (ENC1: 653, RAG1: 640, SH3PX3: 450, 28S rDNA: 691, RH1: 501). The combined mitochondrial matrix comprised of 65 individuals from 27

species totaling 1561 aligned characters (cytB: 718, 12S rDNA: 345, 16S rDNA: 498). All sequences will be uploaded to GenBank. This represents the most extensive molecular phylogenetic analysis of *Austrolebias* to date.

2.3.2 Phylogenetic inference

Sequences representing 64 *Austrolebias* individuals and two outgroups were used to build a nDNA tree. Five independent loci were used; SH3PX3, ENC1, RAG1, RH1 and a concatenation of three fragments of 28S rDNA. I used PartitionFinder v1.1.1 (Lanfear et al. 2012) to assess which substitution models and codon-partitioning schemes were most suited to my data. I used Akaike Information Criterion (AIC) score to select my models with branch lengths unlinked and a greedy search algorithm. I ran analyses on each of the genes individually except the three 28S fragments that were run as a concatenated alignment. This ultimately produced 10 partitions that were used in the construction of the nDNA tree (Table S2.3).

I then used BEAST v 1.7.5 (A. J. Drummond et al. 2012) to construct my phylogenetic tree. I linked the trees of five loci, separated into partitions with substitution models as specified by PartitionFinder. A relaxed lognormal molecular clock model was used for all genes, allowing substitution rates to vary between branches. The tree was calibrated using divergence times of *Austrolebias* with two outgroups and normal priors; *Pterolebias longpinnis* (mean = 47.8914; s.d. = 4.835) and *Hypsolebias magnificus* (mean = 16.9724; s.d.= 3.29), both secondary calibrations from the Cyprinodontiform tree in chapter 5, where the mean heights and 95% highest posterior density were used as the mean and the standard deviation values for the prior. I also constrained clades containing *Austrolebias* and *Hypsolebias* and only *Austrolebias* to be monophyletic to match the topology in the tree of Cyprinodontiformes

(chapter 5). BEAST was run for 100 x 10^6 generations and trees were sampled every 10,000 generations. Tracer v1.6 (A. J. Drummond & Rambaut 2007) was used to identify at which point stationarity had been reached (Effective Sample Size > 200 for all important characters) and the relevant percentage of trees were discarded as burn-in. I ran BEAST multiple times in order to ensure that independent runs converge. TreeAnnotator v1.7.5 (A. J. Drummond et al. 2012) was then used to generate the tree with the highest sum of posterior probabilities for all clades. Sequences representing 63 *Austrolebias* individuals and two outgroups were used to build the mtDNA tree. Three mitochondrial genes were used; 12S rDNA, 16S rDNA and cytB, which were assigned to a total of four partitions to construct the mtDNA tree (Table 2.3). The same methodology as explained above was used when constructing the mtDNA tree including the same outgroups and priors for calibration.

2.3.3 Ancestral range reconstruction

Ancestral ranges of all species within the tree of *Austrolebias* were reconstructed using two methods; Bayesian Binary MCMC (BBM) and statistical dispersal-extinction-cladogenesis (S-DEC) mode, both in the program RASP (v3.1, (Yu et al. 2015)). The BBM approach uses a full hierarchical Bayesian approach derived from MrBayes (Ronquist & Huelsenbeck 2003) that takes a single consensus tree and does not fix the relative rates of change among character states under models of range evolution. The S-DEC approach allows for the implementation of the DEC (or Lagrange) model (Ree & Smith 2008) on a distribution of trees to account for phylogenetic uncertainty. The model is applied to each tree in the posterior distribution, leading to the calculation of a probability of each area for each node on a summary tree.

For the BBM analysis, the nDNA tree was converted to a single representative per species using the GLASS algorithm implemented speciesTree function (Liu et al. 2009) in the R package ape (Paradis et al. 2004) . The ranges of species were separated into four different areas as in Costa (Costa 2010) (Fig. 2.1); the western region of the Paraguay River basin (W), the lower La Plata River basin and the middle-lower Rio Uruguay basin (L), the Rio Negro drainage of the Rio Uruguay basin and the upper/middle parts of the Jacuí, Santa Maria, Jaguarão and Quaraí river drainages (N) and the Patos-Merin lagoon system including the southern coastal plains (P). *Austrolebias* species are typically found in just one of these four defined regions (Costa 2010). I restricted the maximum number of areas in reconstructed ancestral ranges to two, as this encompassed all present ranges and was the minimum allowed by the program,. BBM analyses were run for 5 million generations with 4 chains and a temperature of 0.05. As number of species per area varied, state frequencies were estimated using the F81 model and rates were allowed to vary among areas of endemism. The chain was sampled every 500 steps and the first 10% of samples were discarded. The analysis was run twice and parallel and then combined to produce the final result.

For the S-DEC method, I randomly sampled 1,000 nDNA trees from the posterior distribution produced by BEAST, producing trees different to the GLASS species tree. These trees were pruned to contain a single representative from each species. The maximum number of areas was restricted to two and ranges with two areas not geographically adjacent to each other were excluded from the analysis. I constrained dispersal between non-adjacent regions to 0.1 while dispersal between adjacent regions remained at 1.0.

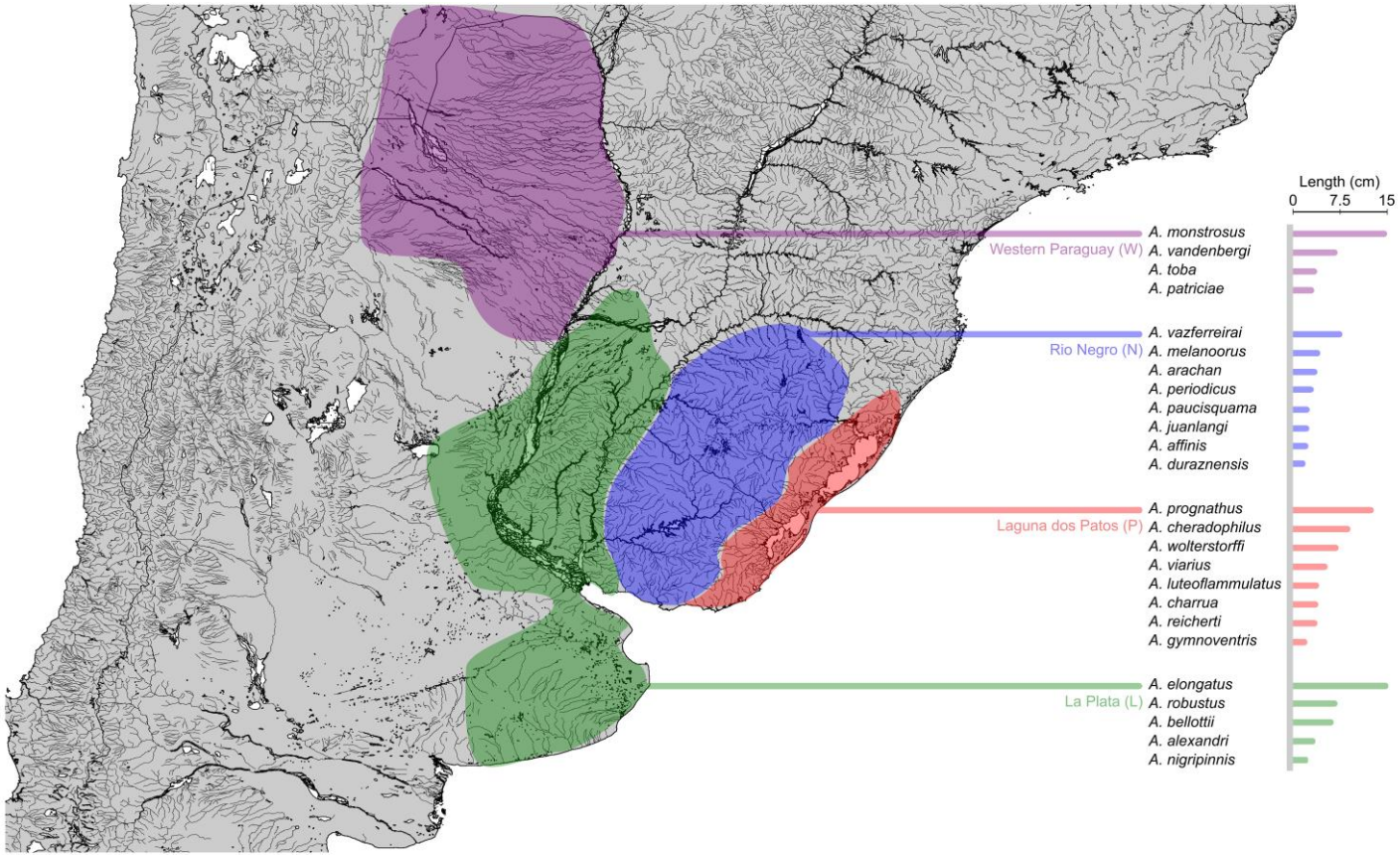

Figure 2.1 A map depicting the four main regions in which *Austrolebias* are found. The most northern region, in purple, is the area west of the Paraguay River. Below this is the basin of the La Plata river and its delta, in blue. To the east is the drainage of the Rio Negro, part of the Rio Uruguay basin, represented in green. Further to the east still is the Patos-Merin Lagoon region highlighted in red. To the right of the figure the species used in this study are placed in their primary regions, alongside body size measurements for each species

2.3.4 Location data

I aggregated coordinates of ponds where species occurrences of *Austrolebias* have been observed from personal collection trips, primary publication data (for example (Costa et al. 2004; Costa 2006; Volcan et al. 2010)), GBIF, amateur egg trading websites and data shared by hobbyist collectors. Sometimes only location names were available. Using Google Earth and Streetview, I obtained coordinates for these locations, resolved synonyms and verified pond locations when images were available. This resulted in a validated location table per species (Table S2.4).

2.3.5 Species distribution models

Often a limited number of sites are known and comprehensive sampling has not taken place in many regions, I also built species distribution models (SDMs) using the validated location data and MaxEnt (version 3.3.3k;(Phillips et al. 2006; Phillips & Dudík 2008)) in an attempt to more accurately determine species ranges than just by region membership. MaxEnt was chosen due to its ability to provide accurate species distributions (Elith et al. 2006), successful implementation with small sample sizes (Pearson et al. 2006) and its capacity to work with presence-only data. MaxEnt is a general-purpose method for making predictions using incomplete information. It minimises the relative entropy between probability densities estimated from presence data and the landscape, which are defined in covariate space (Elith et al. 2011). In the case of species distribution modeling with presence-only data, the cells of the chosen study area are where the MaxEnt probability distribution is defined. Cells where species are known to occur act as sample points with features that can include; climatic variables, land use, elevation and other environmental variables. I used current global climate data layers of 19 bioclimatic variables and altitude were taken from WorldClim

(http://www.worldclim.org) at a spatial resolution of 30 arcseconds (approximately 1km^2). Species occurrences were collated as specified above.

The geographic scale of the model for each species encompassed the distribution of all species. The logistic output of MaxEnt produces a grid where each cell is given a value from 0 to 1 indicating the relative habitat suitability of that cell for the chosen species. Ranges were calculated by applying the 10 percentile logistic threshold produced by the MaxEnt run; if a cell possessed a habitat suitability score of above this threshold, the species was counted as present in that cell. Once the ranges for all species were calculated they were added together to produce a mask that covered all cells where at least one species was predicted to occur. The range of each species was then added to this mask, producing a binary map showing presence and absence of that species in all cells of the mask, allowing for range overlap comparisons among species. I calculated range overlaps between species and groups of species as fractional overlap of smallest range size following Barraclough & Vogler (Barraclough & Vogler 2000).

2.3.6 Body size data

Body size data were obtained by taking the largest known field measurements of adult standard length (SL) for each species from the literature and personal field records (see Table S2.5). Phylogenetic independent contrasts (Felsenstein 1985) were based on a pruned GLASS tree and log transformed SL and were calculated using the pic() function in the R package ape (Paradis et al. 2004) and contrasts were scaled with their expected variances. The body size measure was log transformed to bring together large species and better match the expectation that body size is linked to niche (Costa 2009) in the annual pond system.

2.3.7 Overlap comparisons

I used the approach of Barraclough and Vogler (Barraclough & Vogler 2000) to perform an age-range correlation (ARC) as well as to assess the relationship between body size differences and range overlap. I included node age taken from the GLASS species tree and PICs for size explanatory variables (detailed above) to detect patterns caused by competitive species interactions based on size. This approach analyses range overlap between the two sets of descendants at each node in the phylogeny in dependence on explanatory variables calculated at each node. Arcsine transformations have previously been applied to range overlap data in this type of analysis (Barraclough & Vogler 2000; Davies et al. 2007) but the transformation has since been shown to produce nonsensical predictions and is thus undesirable (Warton & Hui 2011). As a result I analysed untransformed overlaps and the suggested logit transformed overlaps (Warton & Hui 2011). I also performed ARCs and size/range overlap analyses for 1000 trees sampled from the posterior distribution obtained from my BEAST analysis, where I recalculated node ages, overlaps and contrasts for each tree. I also fitted stable distributions as the model for trait evolution (Elliot & Mooers 2014), this transformed the tree branch lengths so that the contrasts produced were according to a stable traits model of evolution. The resulting tree and contrasts were almost identical to those assuming Brownian motion (BM), so I used the original GLASS tree and BM for all analyses.

2.3.7 Mixture models and overlap comparisons

I then expanded upon this approach by using mixture models to try to discern how the geography of speciation affects the size/overlap relationships observed. I modeled multiple regressions for range overlap on explanatory variables to try to classify nodes into allopatric or sympatric speciation and examine how the relationship between size and range overlap

varies with different geographic modes of speciation. If a speciation event is allopatric, I expect that the overlap value at zero node age is equal to zero and that it may increase with node age. If competition based on body size is shaping the distribution of *Austrolebias* there should be a positive relationship between size divergence and overlap for non-zero node ages as secondary contact is facilitated by size divergence. For sympatric speciation, I expect a non-zero intercept at node age zero and a positive effect of size divergence at this node age (i.e. in order to coexist species must be of different size).

Range overlap patterns are thus expected to differ between nodes where speciation is either sympatric or allopatric, so I fitted mixture regression models to the data using the flexmix R package (Grün & Leisch 2008) to attempt to classify nodes into either sympatric or allopatric speciation. I then compared one-component and two-component models by inspecting BIC and ICL. I first fitted 'maximum' mixture regression models with node age, SL contrast and age × contrast effects. After, I selected the best fitting regression model by comparing AIC and ICL. When I analysed untransformed range overlap data, I also fitted mixture models where the intercept of one component was constrained to be zero, and the other at value one as this fit the expectations of completely allopatric and completely sympatric speciation. In the selected models, I inspected signs and magnitudes of coefficients using *z*-tests.

2.4 Results

2.4.1 Phylogenetic inference

The topologies of nDNA (Fig. 2.2) and mtDNA (Fig. 2.3) trees were well supported (PP > 0.9) for most nodes. I identified three major groups within *Austrolebias* that were recovered in both the mitochondrial and nuclear analyses. The first group (Fig. 2.2a, 2.3a) contained *A. affinis, A. alexandri, A. duraznensis, A. juanlangi*, *A. periodicus* and *A. toba*. In the nDNA

tree *A. nigripinnis* and *A. paucisquama* are also part of a clade containing these groups but this was not reconstructed in the mtDNA where the position of these two species relative to group one was unclear (Fig. 2.3). Group two contained the largest species in the genus; *A. cheradophilus, A. elongatus, A. monstrosus* and *A. prognathus* (Fig. 2.2b, 2.3b). The third group contained *A. apaii, A. arachan, A. bellotii, A. charrua, A. cinereus, A. melanoorus, A. reicherti, A. robustus, A. vazferreirai* and *A. viarius* (Fig. 2.2c, 2.3c). The remaining three species; *A. luteoflammulatus*, *A. gymnoventris* and *A. wolterstorffi* were grouped together with low support (PP = 0.57) in the mtDNA. However, in the nDNA tree *A. wolterstorffi* and *A. gymnoventris* were the earliest diverging *Austrolebias* (PP = 0.89). *Austrolebias luteoflammulatus* was placed as at the base of the clade containing the largest species with strong support (PP = 1).

I found several strong incongruences among the mtDNA and nDNA gene trees (i.e. incompatible sets of relationships supported by nodes with a PP > 0.9 in both mtDNA and nDNA trees). For example, *Austrolebias toba* was shown to diverge before *A. paucisquama* in the mtDNA tree (Fig. 2.3d) while the opposite occurs in the nDNA tree. *Austrolebias cheradophilus* (Fig. 2.3e) was sister to *A. elongatus* in the mtDNA tree while in the nDNA tree *A. elongatus*, *A. prognathus* and *A. monstrosus* form a clade to which *A. cheradophilus* is basal. The clade containing *A. robustus* (Fig. 2.3f) was found to be sister to the clade containing *A. charrua* in the nDNA tree but sister to the *A. bellottii* clade in the mtDNA tree. Due to the previously stated drawbacks, number of incongruences and generally lower level of support in the mtDNA tree, I used the topology shown in the nDNA tree for my downstream analyses.

The time to the most recent common ancestor (tMRCA) of all *Austrolebias* used in this study was calculated to be 13.85 (95% highest posterior density = 9.57, 18.10) million years ago (Ma) in the nDNA tree. This value was found to be slightly older in the mtDNA tree at 16.99 (95% highest posterior density = 12.80, 21.51).

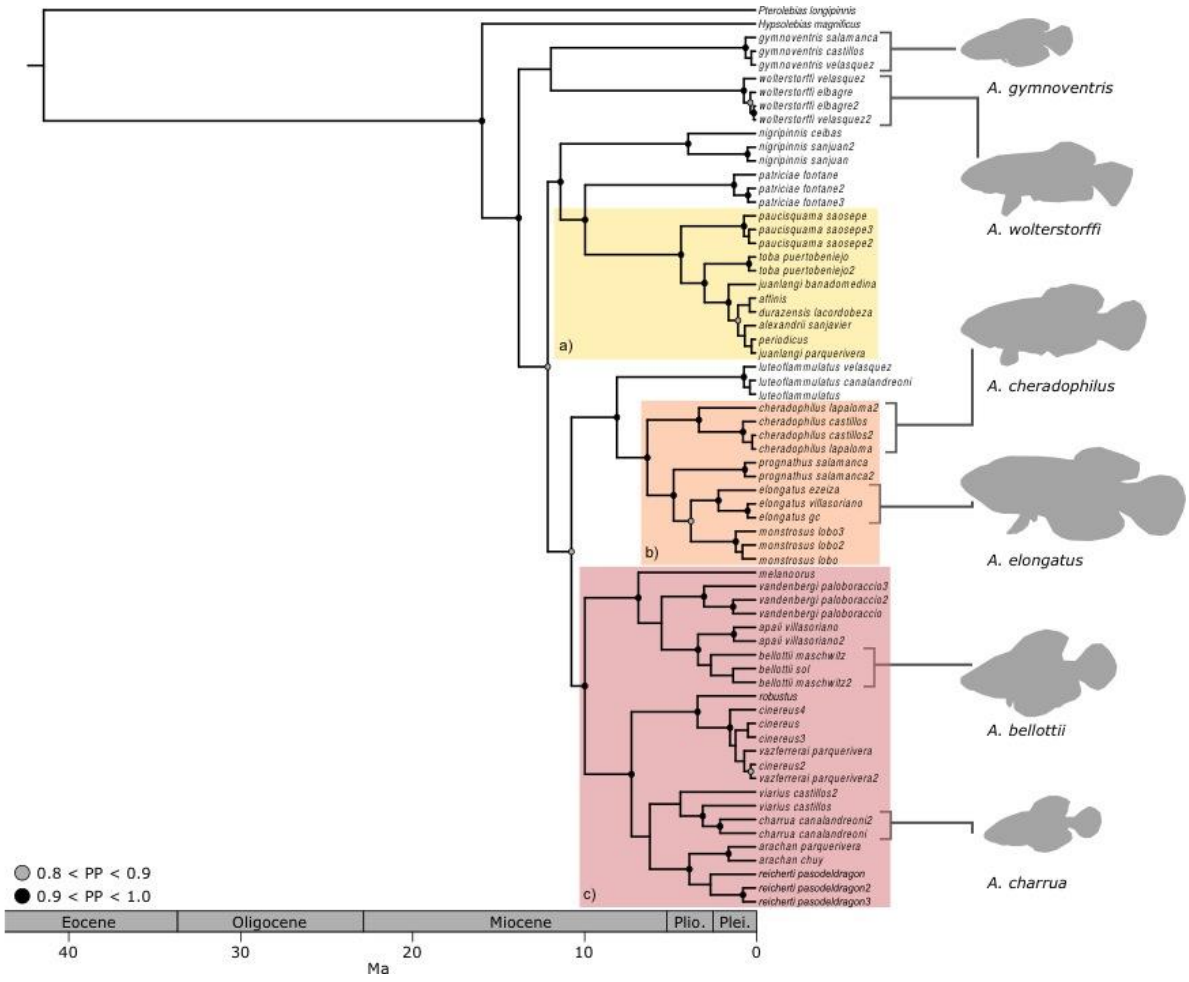

Figure 2.2 A maximum clade credibility tree for 64 *Austrolebias* taxa and two outgroups from a Bayesian analysis of nDNA. Black circles indicate a posterior probability (PP) from 0.9 – 1.0 and grey circles indicate a PP from 0.8 to 0.9. Images represent the range of sizes and shapes found in the *Austrolebias* genus, species names are shown below each photo. Highlighted regions (a), (b) and (c) represent three major clades that are recovered in both mtDNA and nDNA trees, though relationships within are different.

Figure 2.3 A maximum clade credibility tree for 63 *Austrolebias* taxa and two outgroups from a Bayesian analysis of mtDNA. Black circles indicate a posterior probability (PP) from 0.9 – 1.0 and grey circle indicate a PP from 0.8 to 0.9. Highlighted regions (a), (b) and (c) represent three major clades that are recovered in both mtDNA and nDNA trees. Boxes (d), (e) and (f) show regions of the tree that contain hard mito-nuclear incongruence.

The nDNA tree (Fig. 2.2) revealed several instances where species were not monophyletic. Two individuals from different *A. juanlangi* populations did not group together neither in the mtDNA tree nor in the nDNA-based trees, revealing strong support for non-monophyly of this species. *A. viarius* did not form a monophyletic group, instead one individual formed a clade with *A. charrua* and the other was an ancestor of this clade with poor support (PP = 0.6933). However *A. viarius* was found to be monophyletic with strong support (PP = 1) in the mtDNA tree. A clade containing *A. vazferreirai* and *A. cinereus* was well supported but relationships within this clade were not. A node in the nDNA tree groups individuals of *A. vazferreirai* and *A. cinereus* (PP = 0.81), which may indicate that these two species are not monophyletic. These two species are almost identical morphologically (Costa 2006) and *A. cinereus* is known from only a single population. Due to these three reasons I decided to merge *A. vazferreirai* and *A. cinereus* for the comparative analyses in this paper. Monophyly of *A. bellottii* had weak support (PP = 0.70) in the nDNA tree while the mtDNA tree had strong support for non-monophyly with some *A. bellottii* individuals more closely related to *A. apaii*. Hence *A. bellottii* and *A. apaii* were merged due to evidence in this study with further support from (García et al. 2012) who proposed that *A. apaii* was a junior synonym of *A. bellottii*. The mtDNA tree also showed that *A. prognathus* was not monophyletic although this was not well supported (PP = 0.74) and monophyly of this species had a PP of 1.00 in the nDNA tree.

2.4.2 Current species distributions

Species distributions estimated with MaxEnt possessed test and training area under curve (AUC) values of greater than 0.93 for all species, with the majority greater than 0.98. This indicated that these models were significantly better than random predictions (Phillips et al. 2006). The 10 percentile presence logistic threshold varied among species from 0.16 to 0.63.

A list of these outputs can be found Table S2.6. I applied the 10 percentile presence threshold and created a binary table of species occurrences. Examples of predicted maps can be found in Figure S2.4.

2.4.3 Historical biogeography

BBM reconstruction methods revealed a complex biogeographic history of *Austrolebias* with 13 instances of dispersal and 12 divergence events within the same basin (Fig. 2.4). My results indicated that the ancestor of all *Austrolebias* originated in the Patos Lagoon area (P). There was an early dispersal event to the La Plata region (L), this clade then spread further north into the Western Paraguay region (W) before moving back south to the Rio Negro (N) area. Dispersal from this region to La Plata and Western Paraguay then occurred. The ancestors of the remainder of *Austrolebias* remained within the Patos region before some species spread east and north. For example, the ancestors of the large species appear to have first speciated within the Patos region before *A. elongatus* and *A. monstrosus* dispersed to the La Plata and Western Paraguay regions respectively.

S-DEC results (Fig. S2.5) showed a pattern where the historical biogeography of *Austrolebias* that was more focused on the River Negro region. Examining most likely states in S-DEC reveals agreement with BBM, placing the origin of *Austrolebias* in the Patos region but also including the Rio Negro region. Only four nodes did not involve River Negro as part of their range, these were splits within the Patos and La Plata regions. From the Patos & Rio Negro regions, the ancestor of *A. gymnoventris* and *A. wolterstorffi* became restricted to the Patos region while the rest of *Austrolebias* remained in the River Negro drainage. This was until a bout of dispersal between 10-7 Ma where lineages began moving east into the Patos Lagoon and west to the La Plata river basin.

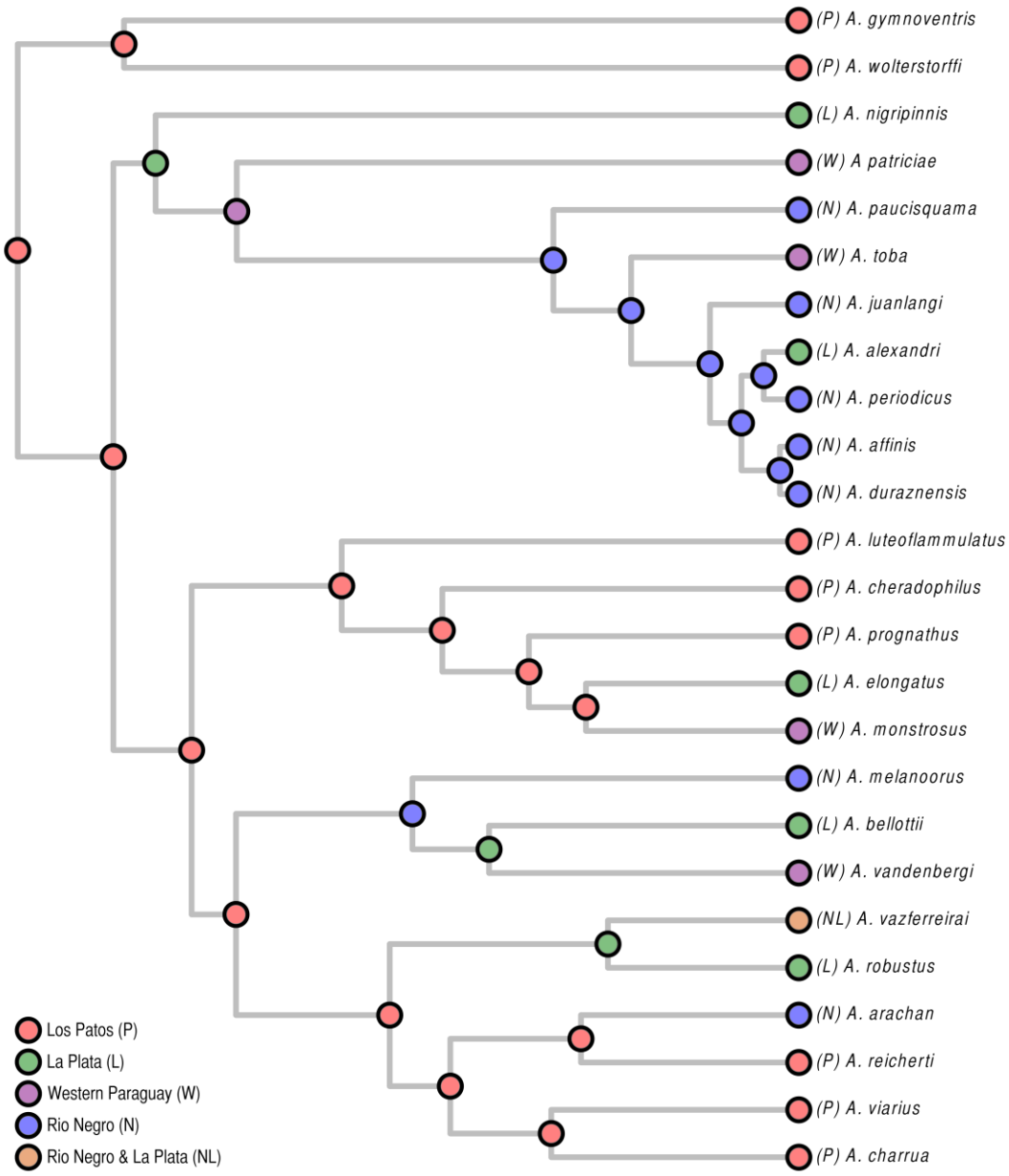

Figure 2.4 A biogeographic reconstruction of ancestral ranges using Bayesian Binary MCMC (BBM) using the GLASS constructed species tree. Most likely states from BBM analyses are shown on each node of a trimmed MCC tree with one representative per species. Colours correspond to regions as in Figure 2.1 and are shown in the legend.

2.4.4 Body size

The largest species was *A. monstrosus,* at 152mm in standard length (SL), the smallest species was *A. affinis* at 32.3mm. The largest value size contrast value was on the node where *A. luteoflammulatus* diverged from the large species clade containing *A. cheradophilus, A. prognathus, A. elongatus* and *A. monstrosus*. Other large contrasts values were found at the node of the divergence between *A. wolterstorffi* and *A. gymnoventris* and at the ancestral node of all other species except this pair.

2.4.5 Overlap comparisons

There was a significant relationship between body size contrast and range overlap ($t = 3.654$, $R^2 = 0.400$, $P = 0.002$), showing that with increased levels of overlap species differed more in SL (Fig. 2.5a). The regression between node age and range overlap, referred to as the age range correlation (ARC) (Barraclough & Vogler 2000), was also significant ($t = 2.253$, $R^2 = 0.202$, $P = 0.036$) and the fitted line of this regression intercept was not significantly different from 0 ($t = 1.282$, $P = 0.214$) (Fig. 2.5b). This ARC indicates that recent speciation has been primarily allopatric in *Austrolebias* (Barraclough & Vogler 2000). Running univariate regressions between SL/node age and range overlap on the posterior distribution of trees yielded a distribution of P-values where more than 80% were less than 0.05 for SL contrast vs. overlap and 55% for node age vs. overlap (Fig. S2.1) indicating that even with phylogenetic uncertainty accounted for, size is still consistently a good predictor, while node age is less so. Values of range overlap and body size contrasts for each node can be found in Figs S2.2 and S2.3 respectively. When using logit transformed overlaps the size overlap contrasts remains significant ($t=3.056$, $R^2 = 0.3183$, $P = 0.006$) while the ARC does not ($t = 1.724$, $R^2 = 0.1294$, $P = 0.100$).

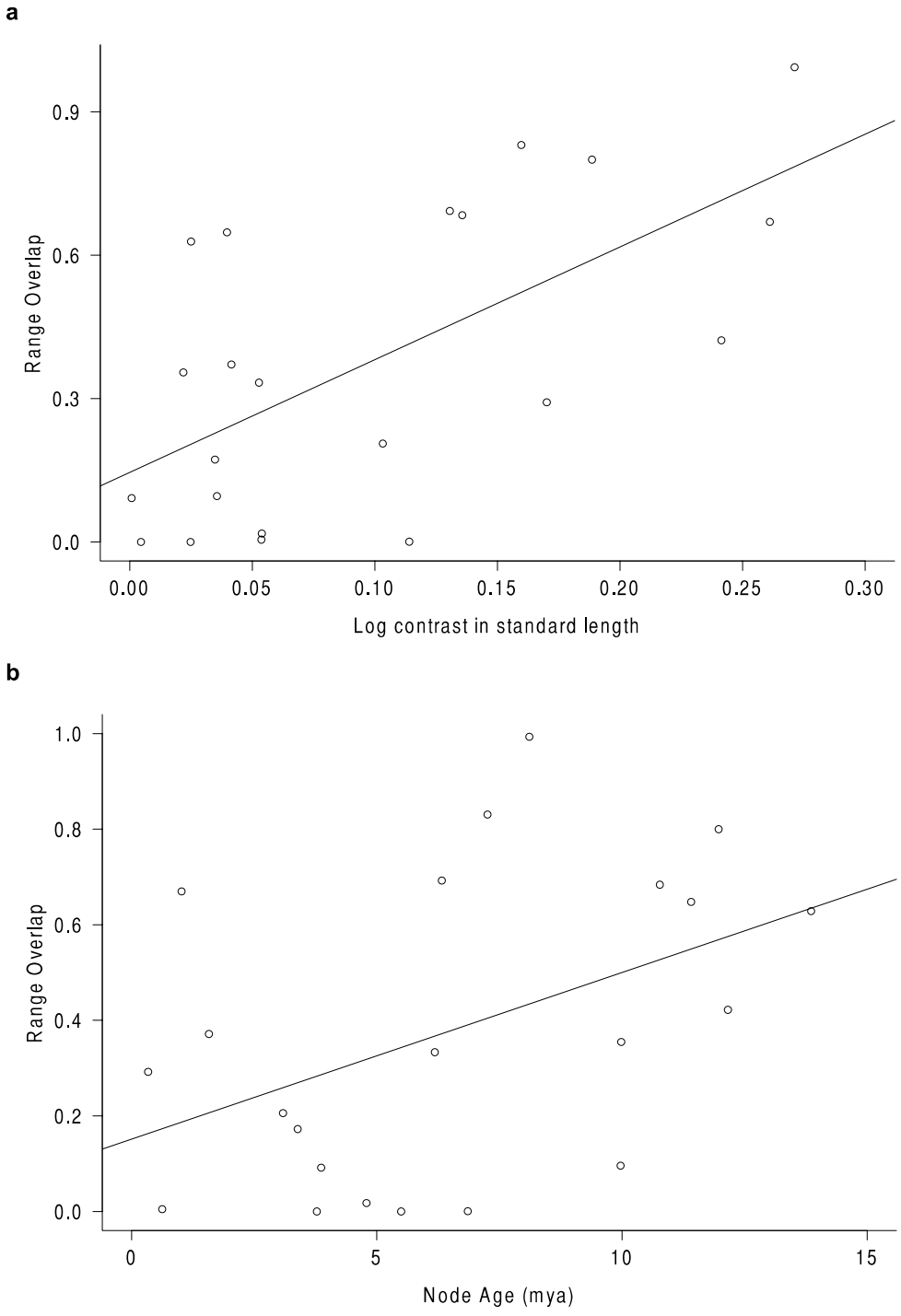

Figure 2.5 Scatterplots of range overlap against (a) log contrast standard length ($t = 3.654$, $R^2 = 0.400$, $P = 0.002$) and (b) node age ($t = 2.253$, $R^2 = 0.202$, $P = 0.036$). Fitted lines represent those produced by univariate regression models. The age-range correlation (ARC) (b) fitted line crosses the y-axis close to 0, indicating that recent speciation in *Austrolebias* was mostly allopatric.

2.4.6 Mixture models and overlap comparisons

When I fitted mixture models to the overlap data, it became clear that transformed overlap values often led to models with unusual assignment of nodes to mixture components that did not reveal anything about the mode of speciation. The analysis seemed to be more informative using untransformed data so that is used hereafter. Fitting mixture models to the overlap data from species distribution models revealed that the selected model contained only a single mixture component, which had the overall lowest BIC and ICL. The selected regression model had a zero intercept, a positive effect of node age (estimate = 0.028, s.e. = 0.008, $z = 3.533$, $P < 0.001$) and an effect of size contrast (estimate = 2.120, s.e. = 0.462, $z = 4.588$, $P < 0.001$). The data patterns in Figures 2.6a & 2.6b indicate that predictions are not completely according expectations when all speciation events would have been allopatric. For very small node ages and contrary to predictions from purely allopatric scenarios, the model predicts non-zero overlap values due to the positive size contrast effect. This regression model seems to find a positive effect of size contrast irrespective of what the speciation modes at the nodes have been and accommodates both in a single regression. Therefore, to classify events at nodes as allopatric or sympatric, a simpler model is required. When I fit a mixture model to the data with only node age as an explanatory variable and intercepts fixed at either zero or one, a single node is assigned with over 0.95 probability to the cluster that represents sympatric speciation. This node has a relatively large overlap for its node age and size contrast and represents the divergence of *A. luteoflammulatus* from the clade containing *A. cheradophilus, A. prognathus, A. monstrosus* and *A. elongatus*. Comparing BIC and ICL revealed that a mixture model containing only size contrasts fit better to the data than the model containing only node age.

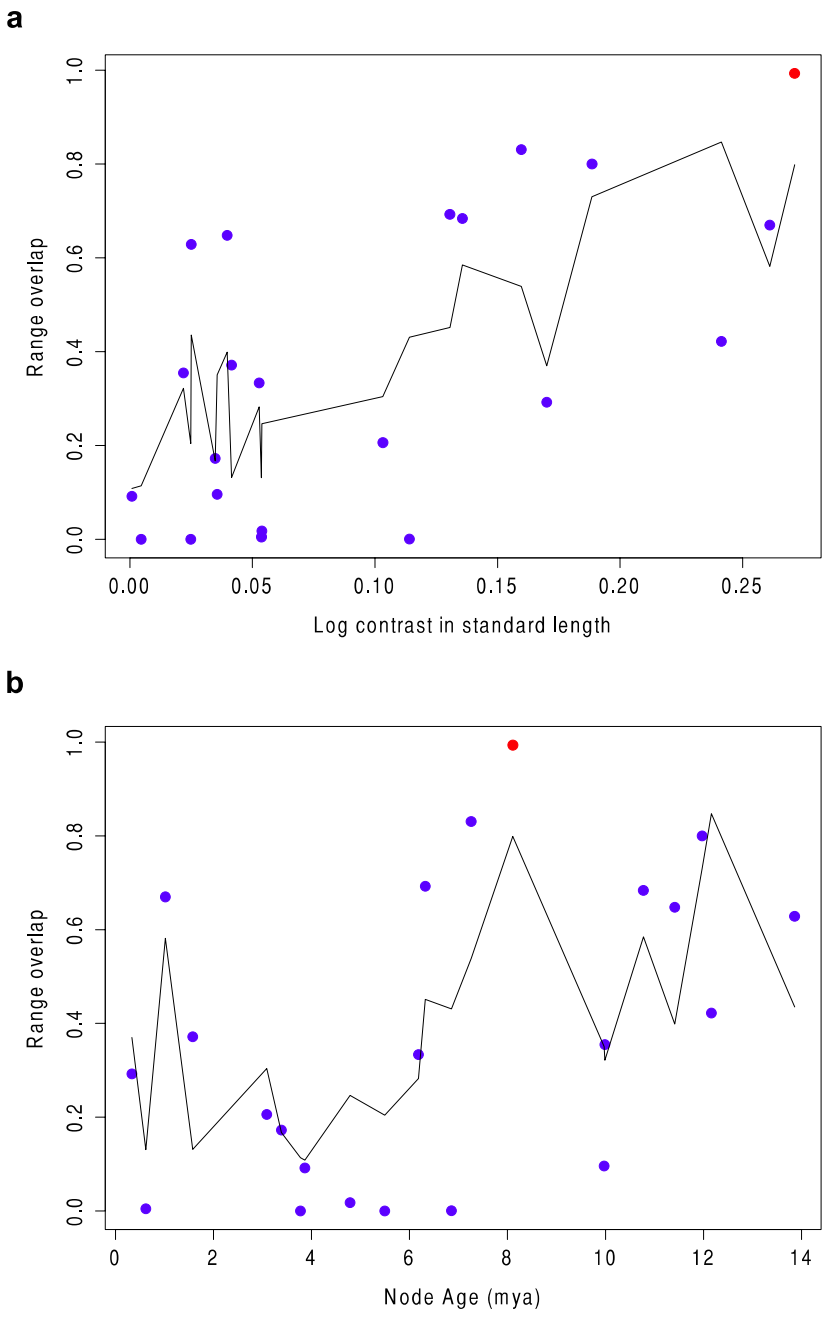

Figure 2.6 Scatterplots of range overlap against (a) SL contrast and (b) node age. The lines are selected model predictions and are jagged because they are not partial regressions on a single covariate. Colours indicate whether the point has been classified as sympatric or allopatric speciation by the model containing only node age information, with red indicating sympatric speciation and blue allopatric.

2.5 Discussion

2.5.1 Phylogenetic trees

Here I present two new phylogenetic trees of *Austrolebias*, made from multiple loci of mtDNA and nDNA. When comparing my topologies to the most recently published cytB tree (García et al. 2014), I find that they are largely similar, but there are a few key differences. *Austrolebias gymnoventris* was grouped with *A. luteoflammulatus* with strong support in the tree of Garcia et al., I found similar results with poor support (PP < 0.5) in my mtDNA tree, while the nDNA tree indicated that *A. luteoflammulatus* was part of the clade containing the largest species (e.g. *A. elongatus* and *A. monstrosus*). *Austrolebias melanoorus* was more closely related to the clade *A. vazferreirai* in Garcia et al. (García et al. 2014) rather than *A. bellottii* as in my mitochondrial and nuclear trees. Garcia et al. also found that *A. wolterstorffi* was the earliest diverging *Austrolebias* as in my nDNA tree, but support was not strong in either case. The cytB tree produced in Garcia et al. (García et al. 2014) indicated a more recent tMRCA of approximately 8 Ma. This may be due to a difference in approaches to dating: Garcia et al. (García et al. 2014) used a conventional mutation rate of 0.02 mutations per site per million years while I used secondary calibrations that produced a mutation rate of cytB of approximately 0.01 per site per million years. The tree used in Van Dooren et al. (Van Dooren et al. In review) was based on the same three mitochondrial genes same 28S rDNA fragments used in this study, but lacked the extra four nuclear loci from this study. Like the Garcia et al. tree and my mtDNA tree (Fig. 2.3), the Van Dooren et al. reconstruction groups *A. luteoflammulatus* with *A. gymnoventris* as well as swapping the positions of *Austrolebias cheradophilus* and *A. monstrosus*. *Austrolebias nigripinnis* was placed as the earliest diverging species in the genus (Van Dooren et al. In review). *Austrolebias wolterstorffi* and *A. gymnoventris* have been placed in different places in the tree in each attempt to reconstruct the *Austrolebias* phylogeny (Costa 2006; García et al. 2014;

Van Dooren et al. In review). I suggest that more sequence data is needed to determine whether this poorly supported (PP = 0.49) and difficult to resolve sister-pair relationship is real. The two previously published trees (García et al. 2014; Van Dooren et al. In review) are similar to my mtDNA tree, which was expected as they are based either entirely or in the most part, on mtDNA. Some of the differences I find between my mtDNA and nDNA trees may be representative of a different evolutionary history of mtDNA and nDNA in *Austrolebias*.

2.5.2 Mito-nuclear discordance

Determining the root cause of discordance between mtDNA and nDNA-based trees can often be difficult as different processes can produce similar patterns. The mitochondrial genome is haploid and typically inherited through the mother, which can often lead to different evolutionary histories than those inferred from nuclear genes. While mtDNA will complete lineage sorting quicker than nDNA, it may not represent the true relationships among species and thus produce discordance. Incomplete lineage sorting occurs when multiple speciation events happen over a short time period and divergence of alleles does not reflect the true relationships among taxa. The discordance between *A. toba* and *A. paucisquama* may be result of incomplete lineage sorting in the nDNA. Furthermore, the use of multiple nDNA markers can allow for a much more accurate view into phylogeographic patterns than the single mtDNA locus. If selection acts on particular mtDNA variants based on geographic region, this may lead to discordance between mtDNA and nDNA topologies (Ballard & Whitlock 2004). The *A. robustus* group and *A. bellottii* group are in the same regions so selection or previous introgression may have lead to these groups being more closely related in the mtDNA. Discordance related to biogeography can also be caused by hybridisation after secondary contact that can lead to mitochondrial capture – where the mtDNA of a species is

completely replaced by that of another. A number of *Austrolebias* species are known to hybridise in laboratory conditions (chapter 4; (Oviedo Alcoba 2009)) but it is unclear how common hybridisation is in the wild. The trees indicate that there may have been past history of introgression between *A. cheradophilus* and *A. elongatus,* causing them to be closer in the mtDNA than the nDNA tree. Many other cases of discordance can be explained by low PP in one or both phylogenetic trees. This is especially evident in the clade containing *A. duraznensis, A. alexandri, A. periodicus*, *A. affinis* and *A. juanlangi*. Relationships among these species appear difficult to resolve in both mitochondrial and nuclear datasets, perhaps due to relatively recent divergence times and incomplete lineage sorting. All of these species except *A. alexandri* are found in the Rio Negro region, therefore introgression among these species is another possibly explanation for their unclear and recent divergence. I stress that there are multiple explanations for each of the instances of hard incongruence between mtDNA and nDNA trees. Only further work with a greater number of independent molecular markers and species tree estimation techniques will shed light on the processes that lead to these hard incongruences and validate those that are current poorly-supported.

The extensive mito-nuclear discordance I found in my data made using programs for resolving species trees such as *BEAST (Heled & A. J. Drummond 2010) difficult. In addition, attempting to estimate species trees based on multiple loci like the dataset used in this study may lead to inaccuracies when using coalescence-based approaches (Gatesy & Springer 2014; Roch & Warnow 2015), though relative suitability of each method depends on the dataset and criticisms of the coalescence-based method are debated (Wu et al. 2013).

2.5.3 Historical biogeography of *Austrolebias*

My BBM biogeographic analyses revealed the origin of *Austrolebias* was in the Patos Lagoon region, and this was followed by multiple dispersal episodes. In no case did a lineage that left the Patos Lagoon region return, which indicates that this region may be saturated. There were several cases of dispersal between two regions that are not geographically adjacent such as the movement of *A. elongatus* lineage from the Patos region to the La Plata region. This could be explained by the extinction of an ancestral species within an intermediate region or simply a dispersal event strong enough to allow a region to be bypassed. S-DEC analyses however, reveal a higher prevalence of the River Negro region. Patterns are generally similar to the BBM but with the addition of River Negro to the La Plata and Patos regions. This may be due to a bias introduced by limiting dispersal between non-adjacent areas. Exchanges between La Plata and Patos are fairly frequent and must travel through the River Negro area, which may be inflating the importance of these ranges.

The biogeographic analysis contrasts with Costa (Costa 2010), who finds that the ancestral range of *Austrolebias* consisted of three areas (La Plata, River Negro and Patos Lagoon) instead of my findings of just Patos or Patos and Rio Negro. *Austrolebias* are rarely found in more than one region in the wild, so I feel it is unlikely their ancestors inhabited three regions. However, Costa (Costa 2010) suggests that marine transgressions during the middle to late Miocene (11-15 Ma) may have connected the River Paraguay, River Negro and Patos areas allowing for dispersal and isolation, which may have allowed ancestral ranges consisting of more than one region.

2.5.4 Factors shaping patterns of co-occurrence

My results show that body size is a good predictor of range overlap in *Austrolebias,* satisfying my initial expectation. I found a positive effect of node age on range overlap, indicating that recent speciation was mostly allopatric. The effect of divergence in body size exists across different speciation modes and therefore the pattern of range overlap observed is likely to be the result of divergence due to competition and size differences facilitating co-existence. I also found that a model containing only size contrast information better explained patterns in the data than a model that contained only node age data. This suggests that size divergence, rather than node age, is the more important factor in determining patterns of co-occurrence in *Austrolebias*.

The dispersal of the largest piscivores - *A. elongatus* to the La Plata region and *A. monstrosus* to the Western Paraguay region has lead to several closely related but non-overlapping very large species that likely contributed heavily to this pattern. These species were the product of a single event of large body size evolution that appears to have occurred in sympatry. After the divergence of *A. luteoflammulatus* there was a dramatic increase in size, leading to *A. cheradophilus*. This generalist, is almost twice the size of *A. luteoflammulatus* and is known to eat both small fish and crustaceans (Laufer et al. 2009). This trend continued with the origin of *A. prognathus*, an even larger piscivore (Costa 2006; Costa 2009). The biogeographic reconstructions (Fig. 2.4) revealed that these splits occurred in the Patos Lagoon area, where *A. luteoflammulatus* and *A. cheradophilus* are currently known to occur in the same ponds (Pers. Obs.; (Laufer et al. 2009)). The node representing the divergence between these two species was the only node to be classified as sympatric in the mixture model analysis and also had the highest value of size contrast (Fig. S2.3). I therefore suggest that large body size evolved in the Patos Lagoon region, perhaps while these species were in

contact, as a result of character displacement where diet gradually changed from crustivory (*A. luteoflammulatus*) to a generalist (*A. cheradophilus)* to piscivory (*A. proganthus, A. monstrosus* & *A. elongatus*) (Laufer et al. 2009; Costa 2009). The nDNA phylogenetic tree did indicate that *A. proganthus* diverged before *A. elongatus* and *A. monstrosus,* although the support was not extremely high (PP = 0.81) and more sequence data could be used to confirm this.

The sister pair *A. wolterstorffi* and *A. gymnoventris* are found in sympatry in the wild (Pers. Obs; Table S2.4) but were not classified as an instance of sympatric speciation in my analysis. Van Dooren et al. (Van Dooren et al. In review) found high support for speciation in sympatry for this species pair, and attribute it to speciation by cannibalism. This process involves selection that favours larger individuals that are able to consume their smaller conspecifics and thus grow faster. This leads to size and shape divergence that ultimately contributes towards speciation. This could also be a driving mechanism in the previously discussed instance of potential sympatric speciation involving *A. luteoflammulatus, A. cheradophilus* and *A. prognathus*. The inconsistency between this study and Van Dooren et al. (Van Dooren et al. In review) may also highlight a weakness in the power of the methodology used here, as the *A. wolterstorffi* & *A. gymnoventris* sister pair has high levels of range overlap (0.8) and one of the largest differences in body size. The node where sympatry was classified in this study had an overlap of 0.99 and the largest size contrast, indicating that only the most extreme example of potential sympatric speciation could be detected with these methods.

It is clear that the age-range correlation (ARC) approach cannot detect sympatric speciation well, especially when it is not frequent (Barraclough & Vogler 2000). As older nodes are

compared, the pools of species compared grow larger, which is likely to mask any observable pattern caused by allopatric and sympatric speciation. It is thus difficult to disentangle the relative importance of different ecological processes and the geography of speciation with this method. Developing upon this approach by classifying nodes as either entirely sympatric or allopatric is certainly crude, as speciation exists as a continuum (Mallet et al. 2009). Nevertheless, it is useful to try to identify which nodes are likely to be representative of particular modes of speciation to understand how ecological processes and geographic mode of speciation interact.

The scale of this study was at that of a binary map of predicted range across large regions. Whether and how often these fish exist in the same ponds is a critical avenue of future research if we are to truly understand patterns of co-occurrence among these annual killifish. Work has been done in *Austrolebias* showing how across 52 ponds in Uruguay, ecological mechanisms related to size likely structured communities, rather than species identities (Canavero et al. 2013). Such studies should be expanded and could use the size divergent species pairs with high levels of range overlap identified in this study, such as *A. luteoflammulatus* & *A. cheradophilus* or *A. wolterstorffi* & *A. gymnoventris*.

In this study I used sequence data and geographic information of 25 *Austrolebias* species, while more than 40 have been classified (Costa 2006; García et al. 2014). Many of the species I have not included were discovered recently or have few known sites of occurrence e.g. (Loureiro et al. 2011; Ferrer et al. 2007). I have also merged some species for analysis due to their genetic and morphological similarities (Costa 2006; García et al. 2012). For others I had sequence data but limited location information and thus species distribution models could not be built or vice versa, and thus they could not be included in the analysis.

Further effort to find more sites and DNA samples from these species would benefit future work by adding more range overlap and size comparisons to increase the power of the analysis. However, due to multiple instances of non-monophyly and potential introgression in this study and others (García et al. 2012), I suggest that the most pertinent avenue of research lies in understanding the gene flow among *Austrolebias* species, especially those that have few known sites of occurrence or signs of introgression.

2.6 Conclusion

A new nDNA-based phylogenetic tree has revealed phylogenetic relationships that differ from the previous hypotheses based on mostly mtDNA. I have assembled a set of over 500 occurrence data points and use these to construct species distribution models. I have used these models and the new nDNA tree to reveal the importance of body size in determining the co-occurrence patterns in *Austrolebias*. The principle mode of speciation appears in *Austrolebias* to be allopatric speciation but I have highlighted a potential example sympatric speciation. I have attempted to develop upon established models to determine whether the geographic mode of speciation affects the relationship between size and range overlap and found little evidence. With current methods it remains difficult to disentangle relative importance of the geography of speciation and ecological processes such as competition, despite numerous calls to address this interaction (Warren et al. 2014; Mittelbach & Schemske 2015). Considering both speciation and ecology when attempting to understand how species assemblages are formed is of critical importance going forward.

Chapter 3

The Development and Evolution of Size and Shape Variation in Annual Killifish (*Austrolebias*)

3.1 Abstract

The size and shape of an organism are intrinsically linked to its habitat and ecological niche. By studying groups with large variation in size and shape we can begin to understand the evolutionary and developmental processes that have lead to this variation. Annual fishes of the genus *Austrolebias* live in small, seasonal ponds across South America. Despite this restrictive environment there are still large differences in size and shape among *Austrolebias* species, for example, the largest species can reach over 150mm in length and the smallest just 23mm when mature. Here, I examine the evolutionary and developmental processes that have lead to variation in size and shape among 18 species of *Austrolebias*. I collect growth and shape data from over 300 individuals to quantify variation over a 49-day period in the lab and compare this with size and shape data from field caught individuals. I uncovered extensive interspecific variation in growth, size and shape, all of which were strongly linked to size at hatching. I then used the most recent phylogenetic tree of *Austrolebias* (chapter 2) to identify convergent evolution in both increased size and streamlined shape in two clades of *Austrolebias.* I also assessed initial size variation in hybrid offspring and found that F_1 hybrids are typically intermediate. However, when a two of species with large differences in initial hatching size are crossed, hybrid initial sizes resemble those of the maternal species, indicating maternal effects may be taking place. This chapter sheds light on how phenotypic diversity has arisen in the killifishes of the South American ephemeral ponds

3.2 Introduction

Understanding how and why variation in size and morphology arises is a major goal in evolutionary biology. These complex traits are shaped by processes such as sexual selection (Price 1984; Blanckenhorn 2000), local adaptation (Mousseau & Roff 1989; Nagel & Schluter 1998) and by interactions within and between species. For example, the Neotropical Crater Lake cichlids are morphologically specialised and ecomorphs within lakes include elongated, limnetic predator species, species with large jaws -used to crush snails- and species with small mouths used to scrape algae from the surface of rocks (Fan et al. 2012; Fan et al. 2011). Anolis lizards vary extensively in body size and shape (Losos 1990a) and the distribution of these species in the Lesser Antilles is driven by competition among similar ecomorphs (Losos 1990b). Variation in size and shape among closely related species is not uncommon. Divergence in size and shape among closely related, sympatric species of sticklebacks has been shown to drive speciation and adaptive radiation in sticklebacks (Schluter & McPhail 1992; Schluter 1993).

To understand how differences in growth, size and shape have evolved, an appropriate study group should be chosen where interspecific size and shape differences occur, where these can be related to local conditions and ecological interactions and where a phylogenetic tree is available such that comparative methods can be used. Preferably, size and shape variation should be assessed in controlled conditions to separate environmental effects from constitutive species differences.

To date, the vertebrate with the shortest lifespan belongs to the killifish genus *Nothobranchius* (Blažek et al. 2013). These killifish are in the order Cyprinodontiformes and the fastest developing species have a peculiar and remarkable annual life cycle. Annual killifish are found in grasslands, wetlands and forests in Africa and South America where they inhabit small bodies of water that dry out completely during the yearly drought. Individuals must grow to maturity, mate and lay eggs during the wet season, usually a period of 2-7 months (Cellerino et al. 2015). During mating, males and females simultaneously deposit their gametes in the substrate at the bottom of the ponds so that the fertilized eggs remain buried in the soil. Once laid, the desiccation-resistant eggs survive an extended period of drought by going through multiple stages of diapause until hatching is triggered by the wet season rains (Wourms 1972). From hatching to maturity and reproduction can take as little as 17 days in African *Nothobranchius* species (Blažek et al. 2013). The *Austrolebias* of South America are another genus of annual killifish with similar life history. Despite living in temporary ponds *Austrolebias* species show a five-fold difference in body size (Costa 2006). The typical *Austrolebias* species is usually 30-50mm in length; however a number of species such as *A. elongatus* or *A. monstrosus* can grow over 150mm (Costa 2006; Osinaga 2006). These differences have largely been attributed to divergence in diet; for example, *A.cheradophilus* has a more diverse diet than its sympatric congenerics *A. viarius* or *A. luteoflammulatus* (Laufer et al. 2009). Van Dooren et al. (Van Dooren et al. In review) have found that for two clades of *Austrolebias* species, large species might have evolved from small in a sympatric process where cannibalism has produced disruptive selection on size. Coupled with variation in size is variation in shape - large species expected to be piscivores have longer, more streamlined bodies with longer jaws. Smaller fish tend to possess taller bodies and a narrower gape (Costa 2006). *Austrolebias* provide a unique opportunity to investigate how differences in body size and shape are achieved during growth in the

seasonal pond system. Furthermore, I am able to investigate the evolutionary history of size and shape using a new phylogenetic tree (Chapter 2).

In this study, I document the growth and morphology of 18 species of *Austrolebias* over a period of 49 days from hatching to quantify how and when these traits vary between species and sexes. I hypothesise that large *Austrolebias* species will reach a larger size by growing at a faster rate than their smaller congenerics. My expectation is that this is favoured by time limitations imposed by seasonal ponds on maintaining size differences and by the multiplicative effects of faster growth rates. I use phylogenetic comparative methods to determine whether species differences in shape and size have been caused by changes in selection regimes and whether these selection regimes tend towards the same optima and are thus evidence for convergent evolution. I also use phylogenetic comparative methods to determine whether differences in shape can be explained as mainly driven by changes in size. I have collated field data on size (chapter 2) and shape of adult fish to explore evolutionary patterns of size and shape when individuals are fully grown and to compare the results with my lab measures. I also examined size at hatching of hybrid individuals from three different species crosses for which I expected traits to be intermediate between the traits of their parents. This will determine whether such crosses could be used in the future to elucidate patterns and determinants of size and shape in *Austrolebias* further.

3.3 Materials and methods

3.3.1 Animals and husbandry

202 individuals across 18 species were raised for this experiment. Hatching was triggered by immersing brown peat containing eggs in water at 15°C. Once hatched, fish from each species were isolated individually in separate 0.25L plastic raising tanks. As an individual grew it was moved into progressively larger volume tanks (5L; 15L). Water parameters for juvenile and adult fish were controlled to conform to the following values; <12°dGH, <10 mg/L NO_3^-, <0.1 mg/L NO_2^-, <0.25 mg/L NH_3, pH = 7.0-8.0 and temperature = 22±0.5 °C. The photoperiod fish experienced was set to 14L:10D throughout the duration of the experiment. Hatched fry were fed *Artemia salina* nauplii daily for two weeks after which they were fed a combination of *Artemia salina*, Chironomid larvae, *Tubifex* and *Daphnia* to satiation. Tanks contained a mixture of the plants *Vesicularia dubyana* and *Egeria densa* as well as 5g of boiled brown peat to aggregate waste and maintain water parameters.

3.3.2 Photography

202 *Austrolebias* individuals were photographed at day 1 and surviving individuals again at days 4, 8, 11, 15, 22, 29, 35, 42 and 49. In order to standardize this process, individuals were place into a small, narrow container with two chambers. The fish was first photographed from the lateral perspective in a container with 20mm water depth (Fig. 3.1a). It was then transferred to the second chamber with a water depth just higher than that of the fish and photo was taken from the dorsal perspective (Fig. 3.1b). A millimetre scale was positioned below the container as a reference for measuring body length. After 15 days, most individuals were too large for the method above so they were instead placed in a wet petri dish with a

millimetre scale beneath (Fig. 3.1c). Photos were taken solely from the lateral perspective when the fish was lying flat and still. All photographs were taken using a CONRAD digital microscope 2.0 USB camera.

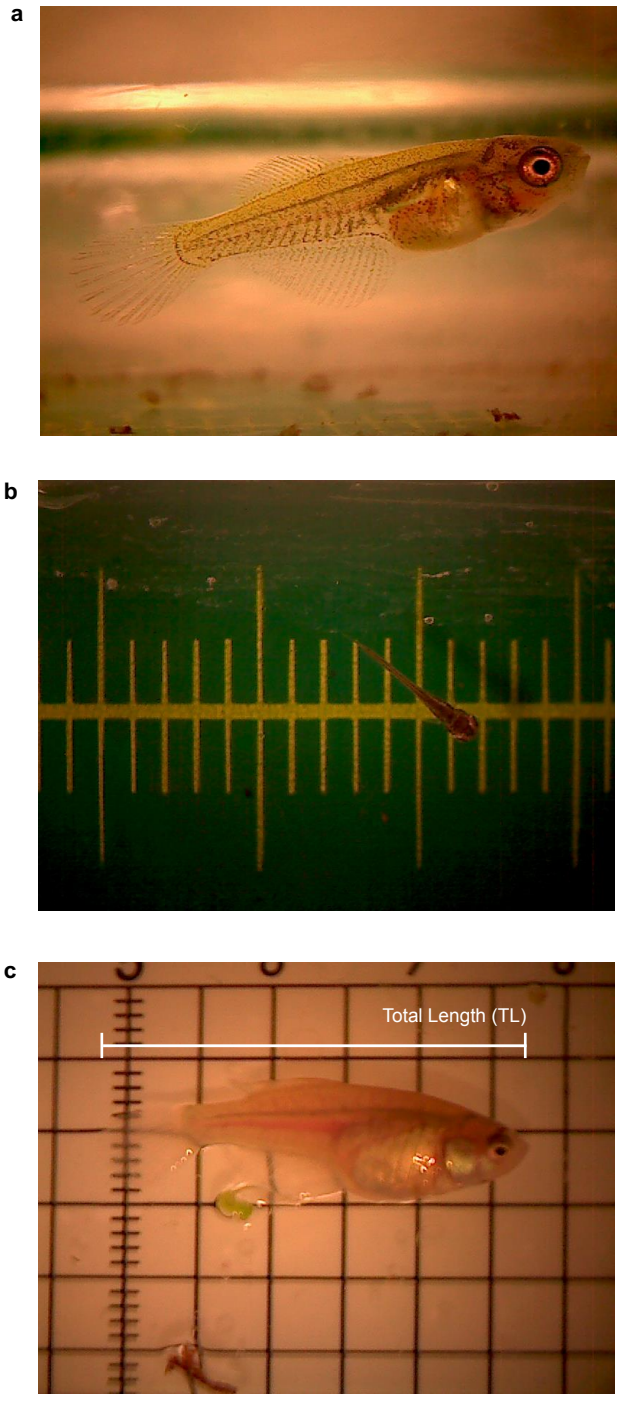

Figure 3.1 Photos of the measurement process. A series of example photos used for size and shape measurements: (a) lateral perspective when small, (b) dorsal perspective when small and (c) lateral perspective when large with total length labelled.

3.3.3 Body size and growth rate

The measure used when calculating growth rate and body size was total length (TL), the distance from anterior tip of the maxilla to the posterior tip of the caudal fin (Fig 3.1c). The software ImageJ (http://imagej.nih.gov/ij/) was used to take length measurements and was calibrated using a millimetre scale in each photo. Growth rate is calculated as relative change in TL per day using the formula:

$$\text{Relative growth} = (y / x) \text{ ^ } (1/ z)$$

where x is the current size of the individual, y is the size of the individual at the next time point and z is the number of days between observation time points.

Using the lme4 library in R (Bates et al. 2015) I investigated variation in size at hatching using mixed linear models with random species effects. I then assessed time patterns in relative growth rates using smooth functions fitted with the sme library v0.8 (Berk 2015) in R. I also used mixed models to assess and test for species differences in relative growth rate patterns on time intervals 8-11 days (early growth) and 30-40 days (late growth) as these contained the most variation in growth and shape variables that was not non-linear. In all these models, the maximal model I fitted to the data included random regressions on age for species effects and individual random effects (no random regressions). I include fixed effects of individual sex (determined at day 49 by visual inspection) and whether the individual at day 49 showed visible evidence of stunting or hampered growth (bent spine - extreme lack of growth) and interactions of these effects with age. I tried to simplify the maximal model by

comparing nested models with likelihood ratio tests, where the null distribution was simulated if possible (Scheipl et al. 2008). Random effects were simplified first, followed by the interactions of fixed effects. The sex and stunting effects were not removed from the models.

3.3.4 Morphometrics

Outline-based morphometrics were used to analyse shape differences between *Austrolebias* species across all time points when measurements were taken. This was chosen in preference to the typical landmark based methods as it allows areas between landmarks to be assessed also, where important shape differences may lie. Outline and landmark capture was done using Image Pro Plus (Media Cybernetics, 2006). The outlines were exported as a set of Cartesian x,y coordinates via a sample outline macro. Lateral perspective images of individuals were used in the geometric morphometric comparisons. Body shape was analysed using standard eigenshape methdology (MacLeod 1999). A set of semi-landmarks were generated along the outline by interpolation in order to remove an effect of size (Lohmann 1983; MacLeod 1999). This allows cartesian coordinates that describe the outline to be converted to the φ form of the (Zahn & Roskies 1972) shape function. Singular value decomposition (SVD) was then used to create axes representing eigenshape vectors that explain the shape variation among *Austrolebias* species.

I again inspected time patterns in the main shape components using smooth functions (R package sme, (Berk 2015) and I used mixed models with the same structure as for relative growth to assess and test for species differences in shape patterns. Linear mixed models were

fitted to values for shape components either above or below age twenty, or to the value at hatching for one shape component. I again avoided fitting mixed models to age segments with non-linear patterns or little species variation.

3.3.5 Phylogenetic comparative analyses of size and shape

For descriptive purposes, I first carried out a cluster analysis based on fitting mixture models using the mclust R package (Fraley et al. 2012) on all size and shape variables together. I used automated Bayesian Information Criterion (BIC) and Integrated Completed Likelihood criterion (ICL) model selection procedures, with identical results and report the preferred models only. I then used a new nuclear DNA-based phylogenetic tree of *Austrolebias* (chapter 2), pruning it so that it only represented the species used in this chapter, to determine whether there is convergence in the investigated variables. Among the shape and size measures for which I estimated species effects, I selected initial size and the early growth rate plus all shape variables estimated at ages above twenty days for comparative analysis. Using the species random effects for all these traits, I investigated whether changes in selection regime along the tree had occurred using the SURFACE R package (Ingram & Mahler 2013), running a forward followed by a backward procedure and performing bootstrap with 200 resamples and model fits in order to calculate confidence intervals. I repeated this procedure for the variables that derived from the total length measures only and for initial size separately.

I assessed whether body size was a good predictor of shape variation among species using regression models. I used phylogenetic generalizesd least squares regression (PGLS) to

determine whether variance in shape can be explained by body size (initial size) when taking phylogenetic non-independence into account. I first carried out the multivariate randomisation test proposed by Adams (Adams 2014), which assumes that the residuals of the regressions of species shape variables on size evolve according Brownian motion. The multivariate analysis were followed by univariate PGLS regression of each variable, to better assess the effects of size. In each model, I included optimization of parameters changing the covariances between species with phylogenetic distance, which improves inference (Revell 2010). These analyses were conducted using the pgls() function in the R package caper (Orme 2013), which allows branch lengths to be adjusted to account for the strength and type of phylogenetic signal in the data. I allowed ML optimisation of all three parameters for branch length, i.e. kappa, lambda and delta. I also carried out PGLS regressions using the corMartins() function in package ape to fit between species covariances (E P Martins & Hansen 1997; Paradis et al. 2004).

3.3.6 Comparison with field size and shape data

I collated maximum field male body size measures from different sources, the same as those used in chapter 2 (Table S2.4). I also conducted standard eigenshape analysis on outline shapes, as above, on the photographs of male individuals from Costa (Costa 2006). These size and shape measures were analysed as with the experimental data except that the mixed model structure was much more simple from the start due to the absence of several explanatory variables. I then compared results from these analyses to those on experimental data to see how well they matched.

3.3.7 Alevin sizes of hybrid crosses

I measured the day 1 size of hybrid offspring in order to assess the variation produced when crossing species of different sizes. I performed three crosses; *A. vazferreirai* male × *A. bellottii* female, *A. nigripinnis* male × *A. affinis* female and *A. charrua* male × *A. juanlangi* female. I then ran pairwise comparisons to determine whether hybrid offspring were significantly different in size from either of their parental species on day 1. Per cross, I used simultaneous p-values and confidence intervals (Bretz et al. 2010).

3.4 Results

3.4.1 Interspecific differences in growth and body size

I measured sizes and shapes of 202 individuals. Of these, 153 became older than 20 days and 126 older than 40 days. Figure 3.2 plots the individual growth curves per species. Differences in initial sizes were observed on day one (Fig. 3.3), the day after adding water to eggs, and the largest fish reached almost 70 mm total length after 49 days (Fig. 3.2). In several species, some individuals started lagging in size with respect to the majority of individuals of their species. I inspected all photos of individuals older than 30 days to assign sexes to them, which was possible for 107 individuals. The remaining individuals were scored as "sex unknown". When I saw individuals with bent spines, or fish still looking like alevins after one month of age, the individual was scored as "stunted". There are 27 such individuals in the dataset.

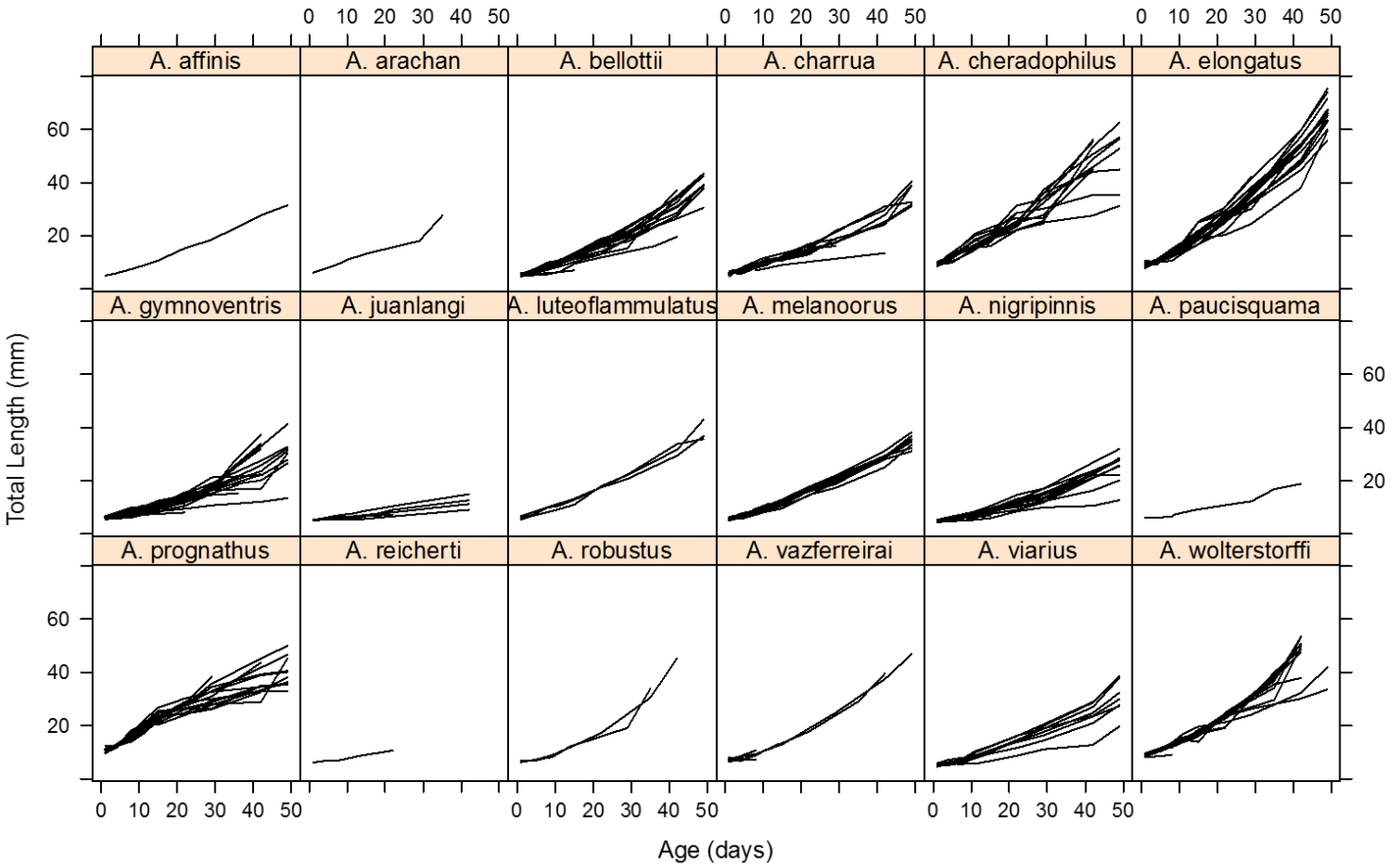

Figure 3.2 Change in total length of 18 *Austrolebias* species over a 49-day period. TL measures per individual are connected by a line. Measurements were taken on days 1, 4, 8, 11, 15, 22, 29, 35, 42 and 49.

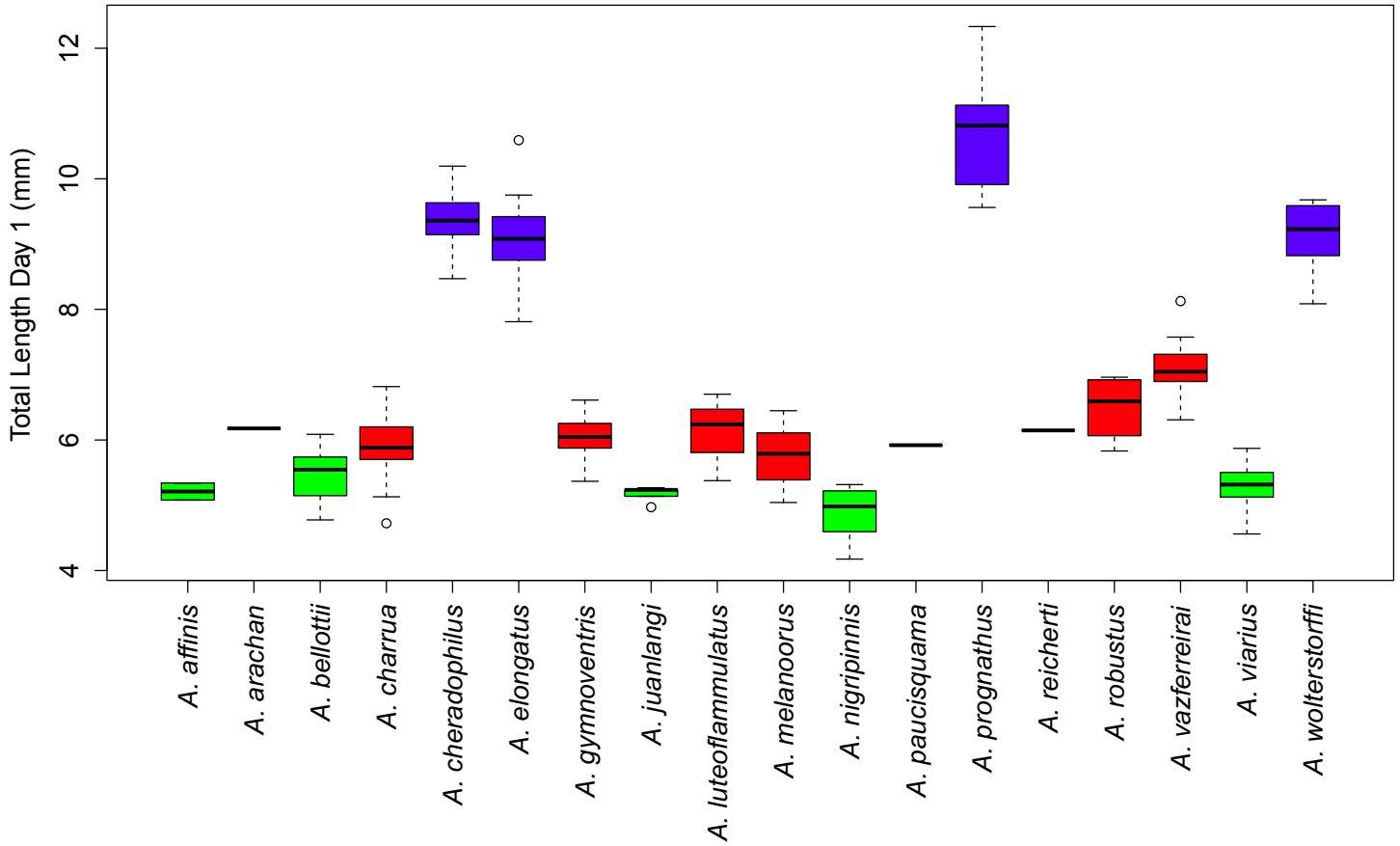

Figure 3.3 Boxplots of initial sizes for 18 *Austrolebias* species. Colours indicate the cluster each species belongs to according to the best fitting multivariate normal mixture model including all shape and size variables.

Table 3.1 Parameters of the mixed models fitted to size and shape data. The name of each trait is reported as well as profile likelihood confidence intervals for all parameters in the selected models. Model selection was performed on the random effects, and the fixed effects involving age, not on sex and stunting effects, were kept in the model in order not to excessively bias any species effects. P-values of significant tests are indicated by symbols: *: $p < 0.05$, **: $p < 0.01$, ***: $p < 0.001$. When a test involved several parameters, i.e. all parameters reported in a cell, P-values are indicated in front of the effect, otherwise after. A confidence interval could not be obtained for species variation in ES2 at young ages.

Trait	Species St. Dev.	Individual St. Dev	Error St. Dev.	Intercept	Age Slope	Sex Effect	Stunting
initial size	[1.25,2.44]***		[0.40,0.49]	[5.88, 7.55]		***[0.02, 0.37] (males) [-0.31, 0.05] (unknown)	[-0.64, -0.06]*
growth rate days 8 to 11	[0.005,0.017]***	NS	[0.026,0.030]	[1.048,1.064]	NS	[-0.009,0.007] (males) [-0.012,0.005](unknown)	[-0.018,0.006]
growth rate days 30 to 40	[NA,0.009]*	NS	[0.014,0.016]	[1.039,1.079]	[-0.001,-0.000]**	[-0.002,0.007](males) [-0.010,0.003](unknown)	[-0.016,-0.000]*
ES1 Age < 20	***[0.003,0.008] (Int.) [0.036,0.083] (Age slope)	NS	[0.082,0.090]	[-0.182,-0.118]	[0.011,0.017]***	**[-0.037,-0.005] (males) [-0.046,-0.011] (unknown)	[-0.034,0.017]
ES1 Age>20	[0.035,0.077]***	[,0.008,0.033]*	[0.063,0.073]	[-0.021-,0.051]	[0.001,0.002]***	*[-0.003,0.032] (males) [0.005,0.052] (unknown)	[-0.064,-0.006]**
ES2 Age<20	NA*	NS	NA	[-0.060,-0.027]	[0.000,0.003]*	[-0.00,0.011] (males) [-0.014,0.006] (unknown)	[-0.004,0.033]*
ES2 Age>20	***[0.023,0.067] (Int.) [0.001,0.002] (Age slope)	[0.007,0.023]*	[0.041,0.049]	[-0.035,0.022]	[0.001,0.003]***	***[-0.031,-0.008] (males) [-0.052,-0.020] (unknown)	[-0.007,0.032]
ES3, Age = 1	[0.014,0.037]***		[0.034,0.041]	[0.032,0.065]		[-0.021,0.008] (males) [-0.016,0.014] (unknown)	[-0.040,0.004]
ES3 Age> 20	**[0.007,0.035] (Int.) [0.000,0.001] (Age slope)	[0.014,0.024]***	[0.032,0.037]	[-0.081,-0.044]	[0.001,0.002]	[-0.016,0.005] (males) [-0.012,0.016] (unknown)	**[-0.004,0.069] (Int.) [-0.002,-0.000] (Age slope)

I found considerable interspecific variation in relative growth rate among *Austrolebias* species (Fig. 3.4a). The species variability in growth rates is largest between days 7 and 12, and between days 30 and 40. I therefore analysed the growth rates in these intervals using mixed models, to estimate amounts of species variation and other effects. If I re-calculate the relative growth rates of *N. furzeri* as observed by Blažek et al. (Blažek et al. 2013) as rates per day, then the values reported there become 1.15 (NF222), 1.12 (NK430, NF121), and 1.13 (NK91). I have nine observations with relative growth rates above 1.12 and three larger than 1.15. The individuals that grew fastest were of *A. viarius*, *A. charrua* and *A. cheradophilus*.

3.4.2 Shape variation during growth

I initially ran standard eigenshape analyses on all species for all days to compare how body shape developed for all species over the 49-day period. Scores along the first three eigenshape vector directions explained 50.64% variation in body shape, with ES1 explaining 36.37% (Fig. 3.4b), score ES2 9.36% (Fig. 3.4c) and score ES3 4.91% (Fig. 3.4d). I then examined how shape changed during growth by plotting scores for the first three eigenshape vectors against age for all species (Fig. 3.4b,c,d). ES1 showed a non-linear relationship that has an initial burst of shape change alone ES1 before the curve levels out. ES2 increases steadily throughout the 49-day growth period. Finally ES3 decreases after hatching and then at most gradually increases during growth (Fig. 3.4d). For the mixed model analysis, I analysed the observations before and after 20 days separately for ES1 and ES2, and I looked at initial values for ES3 and the observations after 20 days. The results are summarized in Table 3.1.

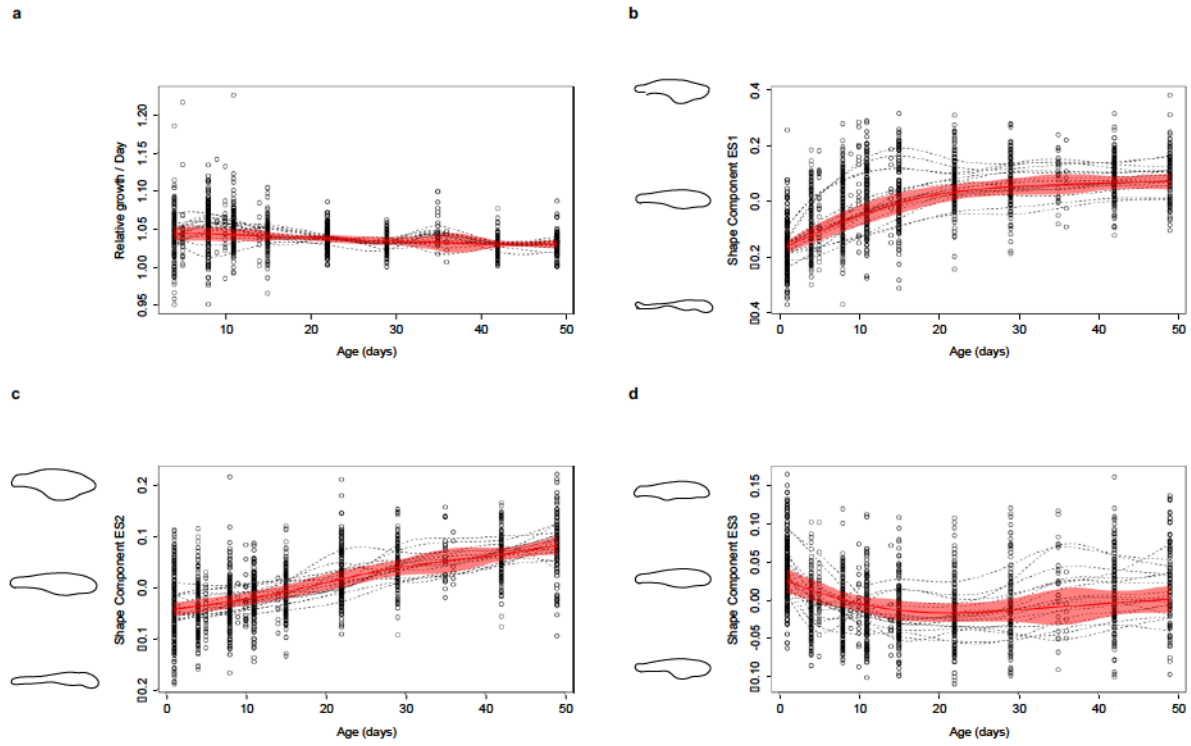

Figure 3.4 Visualisations of smoothing-splines mixed-effects models of (a) relative growth, and scores for shape components (b) ES1, (c) ES2 and (d) ES3. The red line on each plot represents the fitted mean curve around which the 95% confidence intervals are shown. Other lines are smoothing curves fitted per species. Along y-axes in (b), (c) and (d) are the minimum, median and maximum models for the respective eigenshape vector taken from the standard eigenshape test on experimental data.

3.4.3 Species random effects

Significant variation was found between species for all size and shape measures investigated using mixed models (Table 3.1). Individual within-species variation is found for late (age > 20 days) shape components only. With the exception of relative growth after day 30, day slopes are positive, meaning that shape scores increase with age and the per-day relative

growth rate for ages above 30 decreases with age. For the third shape component, the increase is less for stunted individuals (significant age × stunting interaction, Table 3.1). Sex and stunting have effects on some variables, but not all. Notably, individuals later scored as males had significantly larger initial sizes and a smaller early age score for shape component ES1 scored than females.

3.4.4 Mixture Analyses

When I fitted normal mixture models with different numbers of components, BIC or ICL model selection preferred a model with three clusters, when all variables were analysed together (Fig. S3.1). Initial size seems to separate clusters of species most clearly among all variables (Fig. S3.2). *Austrolebias prognathus*, *wolterstorffi*, *elongatus* and *cheradophilus* belong to the cluster with largest initial sizes. *Austrolebias arachan*, *charrua*, *gymnoventris*, *luteoflammulatus, melanoorus, paucisquama, robustus* and *vazferreirai* to a second with smaller initial sizes, and *A. affinis, bellottii, juanlangi, nigripinnis* and *viarius* to a third group with the smallest initial sizes (Fig. 3.3). None of the uncertainties in classification were larger than 2%. *Austrolebias reicherti* is not included in the complete clustering analysis, as it lacks an estimate for growth during the later period. When shape variables are clustered separately, *reicherti* is placed in the middle cluster for initial size.

3.4.5 Convergent evolution

As a result of running the SURFACE method, where OU models with different combinations of selective optima along the branches are fitted, I found that a scenario with two changes in selection regime is most supported, where each change is towards the same new optimum

(Fig. 3.5, Table 3.2). When the analysis is repeated with just with initial size, I recover in the same results. When I used all experimental size data the regime change was only recovered on the branch towards *A. elongatus, prognathus* and *cheradophilus*.

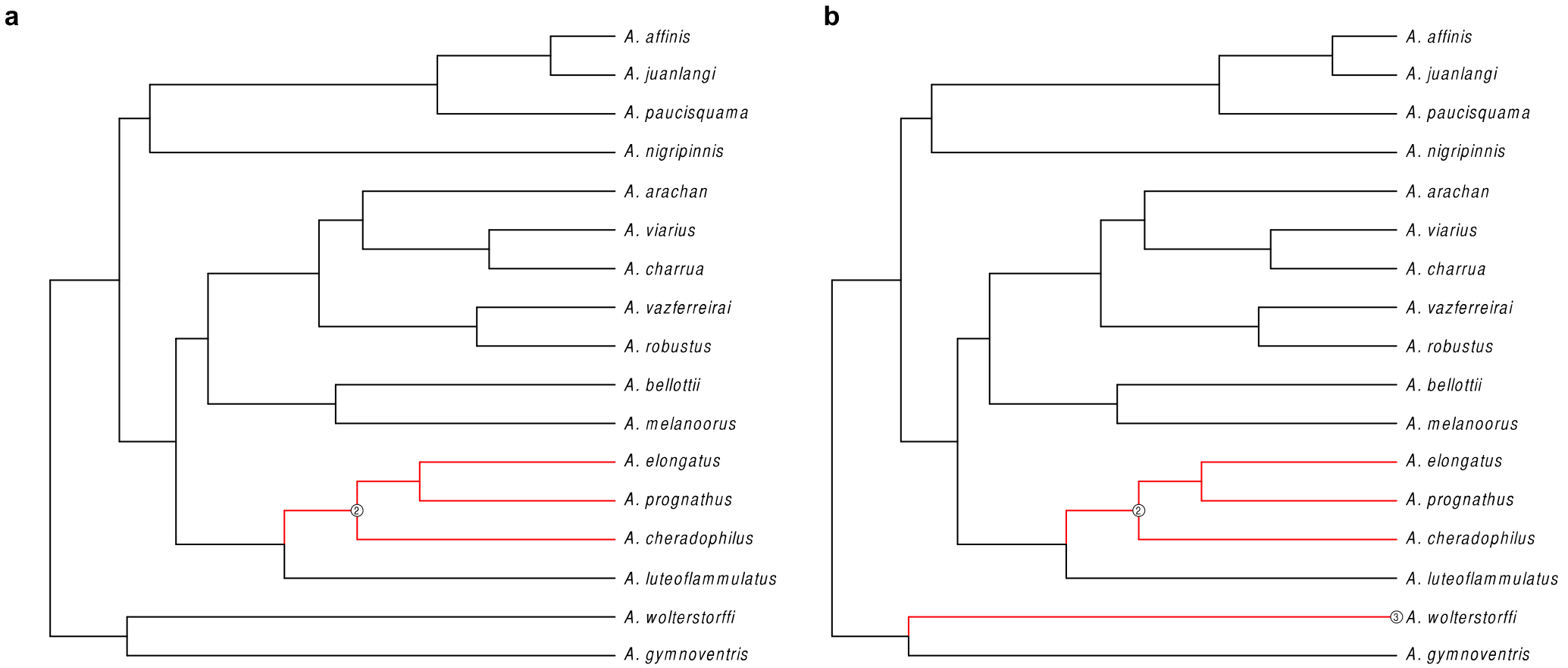

Figure 3.5 Phylogenetic trees of *Austrolebias* showing regime shifts in size and shape identified using the program SURFACE. Panel (a) shows the single regime shift identified using size data alone from this growth experiment. Panel (b) shows the two regime shifts returned by the analysis on initial size data and the analysis on all size and shape data from this growth experiment. Forward and backward approaches (Ingram & Mahler 2013) yielded were combined. Regimes 2 and 3 in panel b share the same parameters.

Table 3.2 Bootstrapped confidence intervals of selection optima for the model selected by SURFACE. There are two different selection regimes as 2 and 3 have the same optima. For clarity, the intercepts of the mixed models from which species effect were used (Table 3.1) are added in an extra column.

Model	Selection Optimum CI regime 1	Selection Optimum CI regimes 2 and 3	Intercept
initial size (TL)	[-1.18,-0.47]	[2.30,4.33]	[5.88, 7.55]
growth early	[-0.0056,0.0010]	[0.0018,0.0141]	[1.048,1.064]
ES1	[-0.033,0.002]	[0.025,0.094]	[-0.021-,0.051]
ES2 Intercept	[-0.034,-0.004]	[0.038,0.099]	[-0.035,0.022]
ES2 Age Slope	[0.000097,0.000949]	[-0.002706,-0.00120]	[0.001,0.003]
ES3 Intercept	[-0.00029,0.00001]	[0.00020,0.00103]	[0.001,0.003]
ES3 Age slope	[-0.010,0.000]	[0.012,0.043]	[0.001,0.003]

3.4.6 Evolutionary relationships between size and shape

When I fit a multivariate phylogenetic regression model of shape variables on initial size and test for the effect of initial size on the shape variables during late growth using a randomization test proposed by Adams (Adams 2014), I find that initial size has a significant effect on the shape variables ($P = 0.022$). It is thus reasonable to see size and initial size here as variables structuring the shape variation observed. When PGLS models are fitted to each shape trait separately and branch length parameters are optimized, I find significant effects of initial size on each of the shape parameters (Table 3.3). Inspecting the parameter estimates of branch length transformations that affect species covariances, λ is frequently estimated at zero, or α is large, which both decrease species correlations and indicate that ES1 and ES2 shape scores have no real phylogenetic pattern when shape is corrected for the pattern explained by size variation. Only shape score ES3 seems to have phylogenetic signal independent of initial size.

Table 3.3 Results from phylogenetic regressions of size on shape parameters. In each model fit, tree branch transformation parameters were jointly adapted with the size slope to maximize the model likelihood.

Trait	Model	Slope (s.e.)	t-test, P[>t]	Tree parameters
ES1	transformation λ, κ, δ	0.017 (0.005)	0.002	λ□□□□, κ□□□□, δ□□□□□□□
ES1	OU	0.018 (0.005)	0.003	α□□□□□□□
ES2 intercept	transformation λ, κ, δ	0.016 (0.002)	<0.001	λ□□□□, κ□□□□, δ□□□□
ES2, intercept	OU	0.021 (0.005)	<0.001	α□□□□□□□
ES2 age slope	transformation λ, κ, δ	-0.00043 (0.00007)	<0.001	λ□□□□, κ□□□□, δ□□□□
ES2 age slope	OU	-0.00057 (0.00014)	<0.001	α□□□□□□□
ES3 intercept	transformation λ, κ, δ	0.00014 (0.00004)	0.004	λ□□□□, κ□□□□□□□, δ□□□□
ES3 intercept	OU	0.00014 (0.00005	0.0115	α□□□□□□□
ES3 age slope	transformation λ, κ, δ	0.0062 (0.0015)	0.001	λ□□□□□□□, κ□□□□□□□, δ□□□□
ES3 age slope	OU	0.0062 (0.0015)	0.001	α□□□□□□□

3.4.7 Hybrid offspring hatching size

The alevins of the *A. vazferreirai* × *A. bellotti* cross are significantly smaller then alevins of *A. vazferreirai* (estimate difference = -1.68, s.e. = 0.12, $P < 0.001$). There are no other significant differences between hybrids and offspring from either parental species. Figure 3.6 shows that hybrids are generally intermediate in size between parental species, but that they can resemble one parental species more in size.

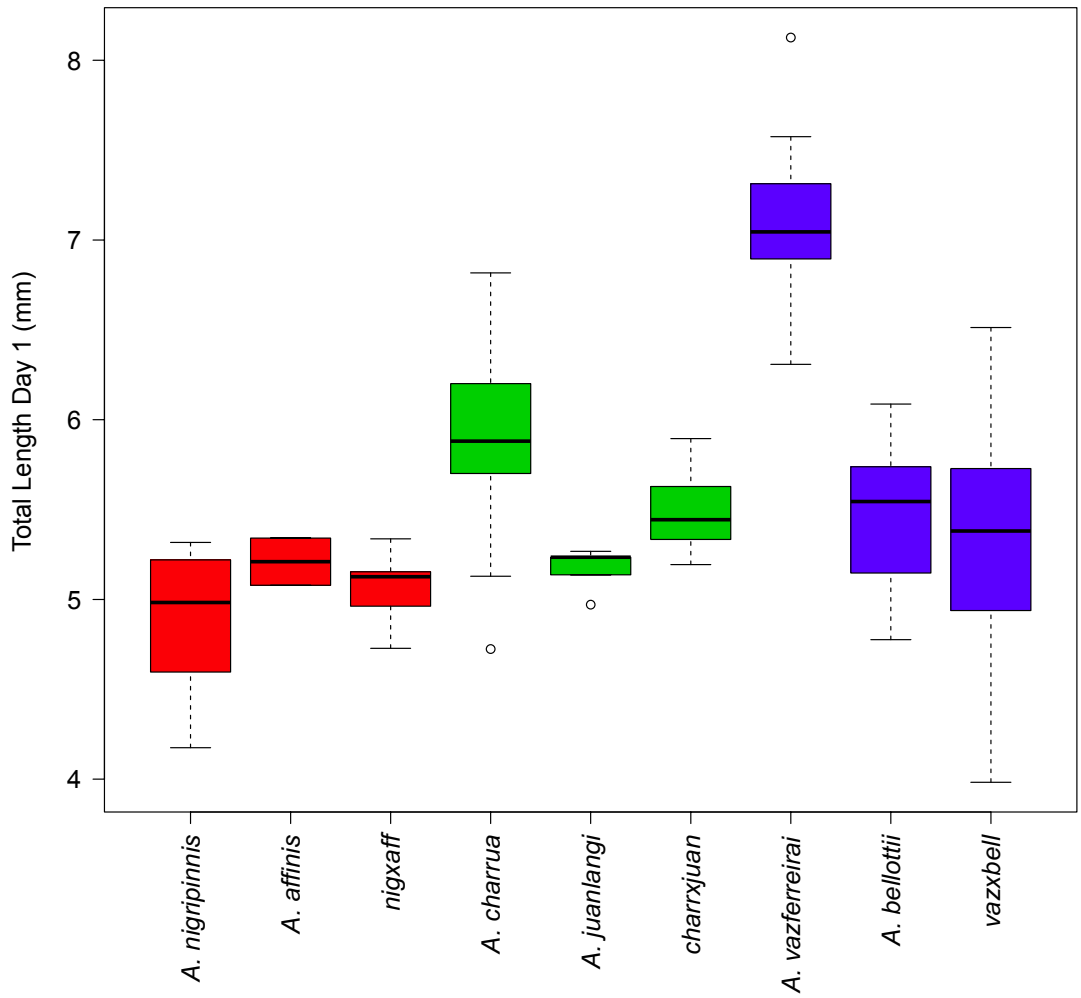

Figure 3.6 Boxplots of day 1 total length for parental species and hybrid F_1 individuals. Parents and offspring of each cross are adjacent and grouped by colour; F_1 individuals are denoted by an abbreviation of paternal species x maternal species. Boxes show the median value, upper and lower quartiles.

3.4.8 Analysis of field data

Data on size (SL) indicated the largest species in the genus were *A. elongatus* and *A. monstrosus* at 152 and 150 mm respectively. There is no replication in the data per species, so raw values were used as species traits. I found a significant correlation between experimental initial size and field data maximum size (PMCC, $t = 5.352$, $df = 13$, $P < 0.001$)

as well as all size variables and field data maximum size (PMCC, t = 7.9217, df = 10, P < 0.001). The first three eigenshape vectors taken explained 48.6% of the variation in shape (Fig. S3.3). These largely explained variation where the outline became more streamlined – a taller, short body versus a longer, narrower shape. While ES1, ES2 and ES3 are labelled the same as the shape axes of the growth experiment, they do not represent the same shape axes or variation. When the automatic model selection algorithm of Ingram and Mahler (Ingram & Mahler 2013) is run, results are similar to those from the growth experiment (Fig. S3.4, Table 3.4). When shapes and sizes are analysed together or sizes alone, only one shift in selection regime is found. This is for the clade including *A. cheradophilus, monstrosus, elongatus* and *prognathus* (size and shape) or the same clade without *A. cheradophilus* (size alone). The regime shift towards *A. wolterstorffi* is not recovered from these field data.

Table 3.4 Bootstrapped confidence intervals of selection optima for the model selected by SURFACE on field data. Adult male size and male shape data are taken from Costa (2006). There are two different selection regimes.

Model	Selection optimum regime 1	Selection optimum regime 2
Size (SL)	[36,67,64.92]	[110.98,276.97]
ES1	[-0.100,0.036]	[0.081,0.531]
ES2	[-0.056,-0.031]	[0.012,0.088]
ES3	[-0.033,0.001]	[-0.113,-0.025]

When a multivariate PGLS is fitted to the data, size has a significant effect on shape (P = 0.002). Inspection of PGLS models for individual shape components (Table 3.5) reveals that maximum size per species has significant effects on ES1 and ES2, and that the residual for score ES1 has a significant phylogenetic signal next after regression on size.

Table 3.5 Results from PGLS regressions applied to field data. In each model fit, tree branch transformation parameters were jointly adapted with the size slope to maximize the model likelihood. The OU model for ES1 did not fit.

Trait	Model	Slope	t-test,P[>t]	Tree Parameters
ES1	transformation λ, κ, δ	0.0016 (0.0007)	p = 0.024	$\lambda = 1, \kappa = 0.84, \delta = 1.55$
ES1	OU	NA	NA	NA
ES2	transformation λ, κ, δ	0.00080 (0.00014)	p < 0.001	$\lambda = 0, \kappa = 1.10, \delta = 3$
ES2	OU	0.0007 (0.0002)	p < 0.001	$\alpha = 0.17$
ES3	transformation λ, κ, δ	-0.0003 (0.0003)	p = 0.30	$\lambda = 1, \kappa = 0.26, \delta = 2.16$
ES3	OU	-0.0004 (0.0003)	p = 0.13	$\alpha = 0.22$

3.5 Discussion

3.5.1 Variation in growth, size and shape

I found considerable interspecific variation in relative growth rate, initial size and shape among *Austrolebias* species. I revealed that *Austrolebias* can grow at a similar rate, and faster in some instances, than the African annual *Nothobranchius* (Blažek et al. 2013). The African and South American seasonal pond systems likely apply similar selection pressures for rapid growth in these annual fish genera, resulting in their comparable growth rates. The large adult species hatched larger, had a slightly higher early relative growth rates but these differences soon disappeared. Shape analysis on fish from the growth experiment documented general patterns of shape change during growth in all *Austrolebias* species and revealed both linear and non-linear patterns of shape development across three axes explaining over 50% of shape variation. Part of the shape variation identified in the experiment is related to age-dependent

changes from an alevin to adult shape, but this still could represent ecologically relevant variation. Shape axes of adult, field caught fish largely explained shape variation between streamlined, elongated species such as *A. elongatus* or *A. prognathus* and smaller, taller-bodied species such as *A. bellotii* or *A. charrua*. Similar shape variation has been found in cichlids where large jawed, elongated species are limnetic and predatory and small-jawed species typically eat crustaceans (Fan et al. 2012). I suspect that the size and shape variation seen in *Austrolebias* are similarly related to diet, as differences have been documented where large elongated species are piscivores and smaller species prey upon invertebrates (Costa 2009). In the experiment, ES3 especially seems to represent such variation.

3.5.2 Convergent evolution in *Austrolebias*

In conjunction with the most recent molecular phylogeny of *Austrolebias* (chapter 2), I reveal convergence in initial size and body shape between the clade containing *A. elongatus* and the species *A. wolterstorffi,* where selection regime shifts tend towards a similar optimum of larger size and more streamlined shape. This convergence was not recovered using the field data, where a selection regime shift was only found in the *A. elongatus* clade. This may be because there was only a single sample per species in the field data, which has not captured the appropriate size and shape variation to construct the additional regime shift. My results are largely concurrent with those from Van Dooren et al. (Van Dooren et al. In review), which identified selection regime changes for field data of standard length and lower jaw length in *A. wolterstorffi* and the *A. elongatus* clade. Like Van Dooren et al. (Van Dooren et al. In review), I found that the *A. elongatus* clade had the highest evolutionary rates across the phylogeny in both experimental and field data. However, I did find some discrepancies when different traits were investigated for selection regime shifts.

The species *A. cheradophilus* and *A. wolterstorffi* are not recovered in all selection regime shift analyses, which may indicate that they occupy intermediate niches between the typical generalist aquatic invertebrate feeders and the piscivores (Costa 2009). Selection pressures on these intermediate species appear to have caused convergent in evolution in some, but not all, of the size and shape traits found in the more extreme *A. elongatus, prognathus* and *monstrosus.* Competition may have acted as selection pressure to produce this pattern, for example, *Austrolebias wolterstorffi* co-occurs with *A. prognathus* (chapter 2, Table S2.4), and competitive interactions such as character displacement (W. L. Brown & E. O. Wilson 1956) between these species may cause *A. wolterstorffi* to occupy a more intermediate niche, leading to a comparatively slower growth pattern than other larger species but a similar shape. There is also evidence that mulloscivory, rather than piscivory is the primary food for *A. wolterstorffi*, which possesses modified teeth ideal for crushing mollusc shells (Costa 2009). Specialisation for this diet may have required similar adaptations as piscivory and lead to the convergence I detect. *Austrolebias cheradophilus* was found to eat a larger variety of prey compared to smaller congenerics (Laufer et al. 2009) and is thought to be less specialised than *A. elongatus* or *A. prognathus* (Costa 2009), which also matches the pattern I observe.

Phylogenetic analysis of trait-correlated evolution revealed that shape axis ES3, which seems to represent variation going from tall-bodied to streamlined, keeps phylogenetic signal after correcting for species size differences. This indicates that selective regimes on shape might operate somewhat independent of size. There are a number of possible reasons as to why large, streamlined species have repeatedly evolved in *Austrolebias*, and why shape

differences might be associated to different selective pressures for being large. Large *Austrolebias* almost certainly occupy a different niche than smaller fish in seasonal ponds. These large species can catch a wider variety of prey (Laufer et al. 2009) and are likely the top predators in the annual pond system, eating other fish including congenerics (Costa 2009). The ability to consume a wider range of food may be a selective advantage in the resource-limited ephemeral ponds *Austrolebias* inhabit. Van Dooren et al. (Van Dooren et al. In review) proposed that speciation by cannibalism as a process to explain the evolution of large-bodied *Austrolebias.* Species that more readily cannibalise their conspecifics may have an advantage as they can grow faster. This would cause selection to favour larger individuals with a more streamlined, predatory body shape that is well suited to cannibalism. This process would eventually lead to sympatric speciation, thus if it were to have happened I would expect to find species either side of a regime shift to be in the same geographic region. This is true for both identified regime shifts where *A. wolterstorffi* and *A. gymnoventris* and *A. luteoflammulatus*, *A. cheradophilus* and *A. prognathus* are known to coexist are all found in the Patos Lagoon region of South Western Uruguay and Southern Brazil (chapter 2). I therefore believe my results add to the growing support that speciation in sympatry by cannibalism (Van Dooren et al. In review) or diet-related character displacement (chapter 2) has occurred in *Austrolebias* and repeated instances may have caused the convergent evolution detected in this study.

3.5.3 Initial hatching size and hybrid offspring

One surprising result from my analysis was the importance of initial size in the evolution and development of size and shape variation in *Austrolebias.* I found a significant evolutionary relationship between initial size and all tested aspects of body shape and I found convergent

evolution in initial size between two *Austrolebias* groups. Furthermore, I identified a significant correlation between species initial size and maximum size in the field. Initial size is linked to all investigated aspects of *Austrolebias* morphology, and thus I suggest it is a key component facilitating size, growth and shape variation in *Austrolebias*. I investigated this further by determining how interspecific hybridisation could affect initial sizes of hybrid offspring. Hybrid crosses and their average sizes might provide opportunities to check the validity of PGLS regression models, because they allow experimental manipulation of size, the explanatory variable of the regression, instead of using a regression to investigate simply a correlative pattern as is commonly done now (Garamszegi 2014).

In two of three tested cases, my prediction that hybrid offspring would hatch at sizes intermediate between maternal and paternal species was met. For these two crosses, average initial size was not significantly different from either parent. In the third cross, between *A. vazferreirai* and *A. bellotii* I found that offspring hatched with a size similar to the maternal species. A mother's size is known to affect egg size in species (Kamler 2005; Chambers & Leggett 1996), but so far evidence of maternal effects related to body size was absent in *Austrolebias* (Moshgani & Dooren 2011). Egg size is likely to be important in dictating hatching size as it is in many species (Duarte & Alcaraz 1989) and if females produce smaller eggs this may limit hatching size of hybrids from fathers of large species. This has implications for processes such as reinforcement (Dobzhansky 1937; Butlin 1987), where hybrid offspring of larger fathers that mate with smaller mothers may be less fit and thus act as a prezygotic isolating mechanism between diverging populations.

Now that I have established growth patterns of many *Austrolebias* species, assessing not only initial size but also adult size, shape and growth of hybrids could provide further insights into how size and shape variation in *Austrolebias* evolves across species and develops at the individual level. Crossing different combinations of large and small maternal and paternal species would not only improve our understanding of the dependence of shape on size. It would also allow us to better understand the importance of maternal effects, assess the potential viability of hybrids in the wild and characterize general patterns of hybrid development and survival.

3.6 Conclusion

Body size and shape and their development play an important role in the ecology of an organism. Understanding how size and shape evolve can give insight into the adaptation and speciation process in groups where variation is found. I have revealed extensive variation in growth, size and shape among species of *Austrolebias*. Variation in size was observed from hatching, and was also a strong predictor of interspecific shape variation. I have found evidence for convergent evolution for both size and shape, where species derived from multiple independent origins tend towards a larger body size and a more elongated shape. Analysis of hybrid offspring showed evidence for potential maternal effects on initial size, opening further avenues of research into understanding how variation in size and shape evolved and is maintained in annual killifish.

Chapter 4

High-density linkage mapping in *Austrolebias*

4.1 Abstract

The construction of a linkage map is an important first step towards determining the genomic basis of character traits. Genetic mapping is especially useful in non-model organisms where genomic resources are not available. Here, I present the first linkage map of a South American annual killifish, and specifically the genus *Austrolebias*. The mapping family consisted of 81 F_1 individuals of an interspecific cross between *A. bellottii* and *A. vazferreirai* sequenced using double-digest restriction-site associated DNA (ddRAD) sequencing. The paternal map was constructed using 1974 markers and the total length of the map was 841.1 cM over 22 linkage groups. The maternal map was constructed using 2652 markers and consisted of 24 linkage groups spanning 1202.2 cM. I found many areas of low recombination, which can be evidence for recombination suppression. These were more common in the male map where the densest area contained over 120 makers in a 10cM region. Areas such as this may represent chromosomal rearrangements such as inversions. A single locus weakly associated with sex was found on maternal linkage group 17, with no other evidence for sex associated loci. I suggest that maternal effects, environmental variables or differences in expression may be more important in sex determination in *Austrolebias* than genetic differences. The linkage map constructed in this study can be used as a tool for future genomic analysis in *Austrolebias*.

4.2 Introduction

Understanding the architecture of the genome and the genomic regions underlying phenotypic traits are major goals evolutionary biology. With the advent of high-throughput reduced representation sequencing, the study of the genomics of non-model organisms has become more feasible (Stapley et al. 2010). These methods can be used to create high-density linkage maps in biologically interesting groups without the need for extensive prior genomic information. Linkage mapping allows one to determine the position of genetic markers relative to one another using recombination frequency among markers. Measures of map distance are not true physical distance but are instead measured in centimorgans (cM), where one cM typically represents 1% recombination frequency. Once a linkage map has been built it can be used to determine the size, position and number of loci that underlie character traits (e.g. (Colosimo et al. 2005; J. N. Weber et al. 2014)) or compare the structure of genomes and chromosomes among individuals from different species or populations to detect rearrangements (e.g. (Kai et al. 2014; Van't Hof et al. 2012)). In this study I construct the first linkage map of a South American annual killifish, from the genus *Austrolebias*, in order to identify putative chromosomal rearrangements and regions of the genome associated with sex determination.

The study of chromosomal rearrangements can develop our understanding of their importance as isolating mechanisms among species and populations (M. King 1995; Rieseberg 2001; Kirkpatrick 2006). When two individuals with different karyotypes interbreed the resulting heterokaryotypic offspring are often infertile because of unbalanced gametes or segregation problems. This hybrid sterility can be a barrier to gene flow between populations that have fixed karyoptypic differences (Rieseberg 2001). Lower recombination

between chromosomes that have different chromosomal rearrangements may also play a role in speciation (Ortíz-Barrientos et al. 2002). Chromosomal rearrangements (CRs) such as inversions and translocations can suppress recombination and thus allow these regions differentiate more than others (Faria & Navarro 2010). In *Helianthus* sunflowers, low levels of introgression were found on chromosomes with rearrangements and it was suggested that approximately 50% of the barrier to introgression is a result of rearrangements (Rieseberg, Whitton, et al. 1999). In the sister species *Drosophila pseudoobscura* and *D. persimilis* divergence was high within inversions and neighboring regions with suppressed recombination and lower in the regions far from inversions on the same chromosome (McGaugh & Noor 2012). However, the relative importance of chromosomal rearrangements in speciation is a divisive topic and more data is needed to fully understand how CRs can shape evolution (Rieseberg 2001; Navarro & Barton 2003; Faria & Navarro 2010).

Recombination suppression is also thought to be an important step in the formation of sex determining regions and sex chromosomes (Charlesworth et al. 2005). In the medaka, *Oryzias latipes*, male recombination was suppressed around the sex determining gene while female recombination was supressed around telomeric regions (Kondo et al. 2001). As recombination suppression can be caused by chromosomal rearrangements, identifying putative CRs is also critical for understanding the evolution of genetic sex determination (Charlesworth et al. 2005; M. A. Wilson & Makova 2009). The mechanisms of sex determination in fish are highly variable and can be influenced by genetics and/or the environment (Devlin & Nagahama 2002). Genetic elements of sex determination may consist of a single gene such as DMY in *Oryzias latipes,* (Matsuda et al. 2002) or distinct sex chromosomes as found in approximately 10% of fish species assessed (Devlin & Nagahama 2002). Alternatively, environmental variables such as temperature or pH may be the major

driver of sex determination, as demonstrated in cichlids (Römer & Beisenherz 1996). Sex chromosomes in fishes are thought to be relatively young (Charlesworth et al. 2005) and may not be entirely heteromorphic, so more powerful methods may be needed to identify the sex determining regions. High-throughput sequencing and trait mapping was used in the zebrafish, *Danio rerio*, to reveal multiple sex-associated regions and a putative sex chromosome (Anderson et al. 2012). A similar approach was used to map a major sex-determining region in the nile tilapia, *Oreochromis niloticus* (Palaiokostas et al. 2015). Fish are especially useful for studying the evolution of sex as species have different sexes but typically no sex chromosomes (Devlin & Nagahama 2002). Therefore, if a genetic sex determination mechanism is found, it can be used as a window to look into the early processes involved in the evolution of sex (Charlesworth et al. 2005).

The study group, *Austrolebias,* are a genus of annual killifish that live in seasonal ponds found across the forests, wetlands and grasslands of South America (Costa 2006). Adults will deposit their gametes in the substrate at the bottom of ponds. These ponds then dry out completely, killing all individuals while the desiccation-resistant eggs go through multiple stages of diapause (Wourms 1972). The next wet season rains then trigger the eggs to hatch, after which individuals grow rapidly and the process repeats. The African annual killifish *Nothobranchius furzeri* lives in a similar habitat to *Austrolebias.* (Valenzano et al. 2009) found strong evidence for a genetic sex determination system in *N. furzeri*, which indicates that a major component of the *Austrolebias* sex determination system may be genetic.

There is a large amount of karyotypic variation among species of *Austrolebias* (García et al. 1993; García et al. 1995; García et al. 2001; García et al. 2014) where chromosome number

ranges from 2n = 34 in *A. luteoflammulatus* to 2n = 48 in many species including *A. nigripinnis* (García et al. 1993). Four different cytotypes have been detected in a single species, *A. charrua,* with many potential examples of chromosomal rearrangements highlighted (Garcia 2006). The extensive karyotypic variation among *Austrolebias* species makes the genus ideal for the study of chromosomal rearrangements and their consequences. After examination of the physical chromosomes, sex chromosomes were not identified in *A. charrua* (Garcia 2006), so if a genetic sex determination mechanism is present it is likely to be one or more genomic regions rather than heteromorphic chromosomes. A recent study by Arezo et al. (Arezo et al. 2014) used a candidate gene approach to isolate a cDNA sequence closely related to the *dsx* gene in *Drosophila melanogaster* that showed a differential expression pattern among sexes, indicating the differences in expression may play a role. *Austrolebias* present an opportunity to use recently developed high-throughput sequencing approaches and linkage mapping to determine if genetic determinants of sex are present and where they are located in the genome.

In this study, I use double-digest restriction-site associated DNA (ddRAD) sequencing to build a high-density linkage map from a hybrid outcross family of *Austrolebias bellottii* and *A. vazferreirai*. I describe the differences between maternal and paternal maps and identify potential chromosomal rearrangements. Chromosomal rearrangements have been observed previously (García et al. 1993; García et al. 1995; García et al. 2001; Garcia 2006) so I expect to find evidence for putative rearrangements. I also perform a preliminary genome scan to detect loci that influence sex determination. I expect to find one or more trait loci, as a genetic sex determination mechanism has been found in other annual killifish (Valenzano et al. 2009). The development of a linkage map will be beneficial to the study of genetics and

genomics in this genus, as they have been in other genera in Cyprinodontiformes (Valenzano et al. 2009; Walter et al. 2004; Tripathi et al. 2009).

4.3 Methods

4.3.1 Mapping family

Pure line individuals of *A. vazferreirai* and *A. bellottii* were raised in the following common garden conditions until adult. Hatching was triggered by immersing eggs in water at 15°C. Once hatched, fish from each species were isolated individually in separate 0.25L plastic raising tanks. As an individual grew it was moved into progressively larger volume tanks (5L; 15L). Water parameters for juvenile and adult fish were controlled to conform to the following values; <12°dGH, <10 mg/L NO3−, <0.1 mg/L NO2−, <0.25 mg/L NH3, pH = 7.0 -8.0 and temperature = 22±0.5 °C. The photoperiod fish experienced was set to 14L:10D. When the fish reached adulthood they were transferred to a large breeding tank. Eggs were harvested from multiple breeding pairs and stored at 22°C for 4 months. The process was then repeated for the F_1 hybrid offspring and a single family with high yield was chosen. F_1 individuals were sexed by examining pigmentation patterns and stored in 100% alcohol upon death. 94 F_1 full-sibling individuals from a male *A. vazferreirai* and female *A. bellottii* cross were selected for sequencing along with their parents.

4.3.2 Library preparation and sequencing

DNA was extracted from fin tissue using the Qiagen DNeasy Blood & Tissue kit. A total of 15mg of tissue was used for each extraction, usually from fin tissue except for especially small fish where I complemented the fin with muscle tissue to make up 15mg. DNA

extraction steps were performed as in the Qiagen DNeasy (C) Blood & Tissue kit protocol. After extraction the amount of DNA from each individual was quantified using spectrophotometry in the Nanodrop (Thermo Scientific).

Library preparation generally followed Peterson et al. (Peterson et al. 2012) but is briefly summarised here. DNA was quantified using the Qubit 2.0 fluorometer (Life Technologies) and diluted with H_2O to make a 40µl solution containing 1µg of genomic DNA. The DNA was then digested using two enzymes, EcoRI and MspI, incubated at 37°C for 1 hour with EcoRI and a further two hours at 37°C after adding MspI. The double digested DNA was then cleaned using AMPure XP beads (Beckman Coulter). 48 unique barcoded P1 adapters were assigned ligated to individuals of two sets of 48. Two different P2 adapters were also ligated to differentiate the two sets of 48. Samples with unique P1 barcodes were then pooled into four sets of 12 and cleaned using AMPure XP beads. DNA was size selected for fragments between 276-324 base pairs using a Pippin Prep (Sage Science). Polymerase chain reaction (PCR) amplification using the Phusion polymerase kit (NEB) was then conducted on size selected pools. 12 cycles of 98°C for 12 seconds, 65°C for 30s, 72°C for 30 seconds were run. Six separate PCRs were done for each set of 12 individuals and these six were combined after amplification in order to avoid PCR bias. Finally, amplified DNA was cleaned and quantified. Four sets of 12 were pooled based on their P2 barcode adapter to produce two libraries of 48 individuals. Libraries were sequenced on an Illumina HiSeq 2500 at the Genomics Laboratory of the Clinical Sciences Centre at Imperial College London. Each library was run on a separate lane of a flow cell with 100 base, paired-end reads.

4.3.3 Genotyping

Illumina reads were processed using Stacks v. 1.10 (Catchen et al. 2011). Sequences were sorted into individuals using the unique P1 and P2 barcode combinations. Tags with poor quality were removed and as well as those with ambiguous barcodes. Paired end reads were joined together to create 200bp tags, which were then formed into stacks. To assemble stacks, the minimum number of identical raw reads required was three, the minimum number of mismatches allowed between loci was six and the number of mismatches allowed when building the catalog was six. Highly repetitive RAD-tags were removed or broken up and the maximum number of stacks at a single de novo locus was set to four.

4.3.4 Linkage mapping

A linkage map was constructed using Joinmap 4.1 (Van Ooijen 2006) as a cross-pollinating (CP) type population suited for an outbreeding cross. Loci were pruned so that only those present in at least 50% of the F_1 individuals remained. Markers were loaded into the program, checked for errors and then split into maternal and paternal populations. Those individuals with large amounts of missing data were removed, leaving 81 individuals for linkage mapping. Loci were sorted into linkage groups using a log of odds LOD threshold of 6.0. Ungrouped loci were assigned to groups using the strongest crosslink information in Joinmap. Approximate numbers of linkage groups is known in *A. vazferreirai* (2n = 46) (García et al. 2014) and *A. bellottii* (2n = 48) (García et al. 1993). Loci were removed if they possessed significantly segregation distortion based on a chi-squared test ($P<0.01$) or were identical to other loci in the dataset. Markers were mapped using the regression mapping algorithm. Map distances in centimorgans (cM) were calculated using the Kosambi's mapping function and recombination frequencies. The map was then examined and any

markers with unusually high mean chi-squared contribution were removed and the mapping was repeated until all values were suitable. This process was done for maternal and paternal maps separately.

4.3.5 Genome scan and sex determination

Individuals were scored for sex based on coloration at maturity. Any juvenile individuals with unknown sex were removed from the trait mapping analysis leaving 54 (20 males and 34 females) individuals with known sex. The function *scanone* in the R package qtl (Broman et al. 2003) was used to detect loci associated with sex. Genotype probabilities were calculated with a step size of 1 and an error probability of 0.01. Binary model and non-parametric models were used with a permutation test of 10000 permutations. This produced model-based LOD thresholds above which loci were significantly associated with the trait. Genome scans were conducted separately for the maternal and paternal maps. I also attempted to find sex-linked loci by using the approach performed by Chibalina & Filatov (Chibalina & Filatov 2011). This method identifies SNPs that segregate in either only males or only females in my cross. For example, if a locus has an allele present in the male parent that is then found in all male offspring and no female offspring, this is evidence that this particular locus may be sex-linked.

4.4 Results

4.4.1 ddRAD sequencing and linkage mapping

A total of 495,835,396 sequences were produced by the two lanes of sequencing. After removing sequences with ambiguous barcodes, ambiguous RAD-tags and those sequences of low quality were removed, 450,780,353 (91%) were retained. An average of 3,720,230 RAD-tags were obtained for each individual and RAD-tags were clustered into 41,450 loci. After removing markers that were found in less than 50% of offspring and those that were suitable for pseudo-testcross mapping, 6259 markers remained. These markers were then split into maternal and paternal maps and those with high levels of segregation distortion ($p < 0.01$) and identicals were removed. Preliminary maps were constructed and those markers that had unusually high mean chi-squared contributions or nearest neighbour fit values were removed and mapping was rerun until all values were reasonable. For the maternal map, 2652 markers were assigned to 24 linkage groups (Table 4.1). 1974 markers were assigned to 22 linkage groups to make the paternal map (Table 4.2).

Table 4.1 Summary of the maternal (*A. bellottii)* linkage map with information on number of ddRAD markers per linkage group, the length of linkage groups in centimorgans (cM) and the density of markers on each linkage group.

Maternal Map			
Linkage Group	Number of Markers	Linkage Group Length (cM)	Average Spacing (cM)
1	154	64.5	0.4
2	80	34.3	0.4
3	154	53.6	0.4
4	132	58.6	0.4
5	123	45.3	0.4
6	122	42.2	0.3
7	113	49	0.4
8	115	46.9	0.4
9	102	64.9	0.6
10	98	44.9	0.5
11	158	66.8	0.4
12	128	44.3	0.3
13	95	49.9	0.5
14	135	52.9	0.4
15	90	61	0.7
16	79	88.9	1.1
17	137	61.2	0.5
18	122	53.2	0.4
19	146	57.2	0.4
20	93	54.4	0.6
21	79	48	0.6
22	34	18.2	0.6
23	36	7.9	0.2
24	127	34.1	0.3
Overall	2652	1202.2	0.5

This matched the expected chromosome number in the maternal species *A. bellottii* (2n = 48, (García et al. 1993)) but only 22 linkage groups were constructed for the paternal map of *A. vazferreirai,* one less than expected from previous cytogenetic work (2n = 46, (García et al. 2014)). The length of the paternal linkage groups range from 6.8 to 83.5 cM (Fig. 4.1a) and total 841.1 cM with an average spacing of 0.4 cM. The length of the maternal linkage groups ranged from 7.9 cM to 88.9 cM (Fig. 4.1b) reaching a total length of 1202.2 cM and an average spacing of 0.5 cM. I plotted histograms showing the number of markers in 10cM bins along the paternal (Fig 4.2a) and maternal (Fig. 4.2b) genomes. There are 11 regions with 60 or more markers per 10cM in the paternal genome and just two in the paternal genome. These regions with very high marker numbers indicate that recombination is low in these areas and so are potential sites of recombination suppression. Despite the apparent higher level of marker density variation in the paternal map, the mean number of markers per 10cM region is similar: 24 for the paternal genome and 22 for the maternal genome.

Table 4.2 Summary of the paternal (*A. vazferreirai)* linkage map with information on number of ddRAD markers per linkage group, the length of linkage groups in centimorgans (cM) and the density of markers on each linkage group.

Paternal Map			
Linkage Group	Number of Markers	Linkage Group Length (cM)	Average Spacing (cM)
1	113	44.9	0.4
2	99	21.6	0.2
3	101	25.2	0.3
4	125	57.9	0.5
5	139	39	0.3
6	139	53.6	0.4
7	143	84.3	0.6
8	51	25.5	0.5
9	25	7.8	0.3
10	141	53.2	0.4
11	111	83.5	0.8
12	88	24.8	0.3
13	131	45.8	0.4
14	74	53.9	0.7
15	108	22.6	0.2
16	51	29	0.6
17	32	16.6	0.5
18	138	47.6	0.3
19	79	53.1	0.7
20	38	16.5	0.4
21	29	27.9	1
22	19	6.8	0.4
Overall	1974	841.1	0.4

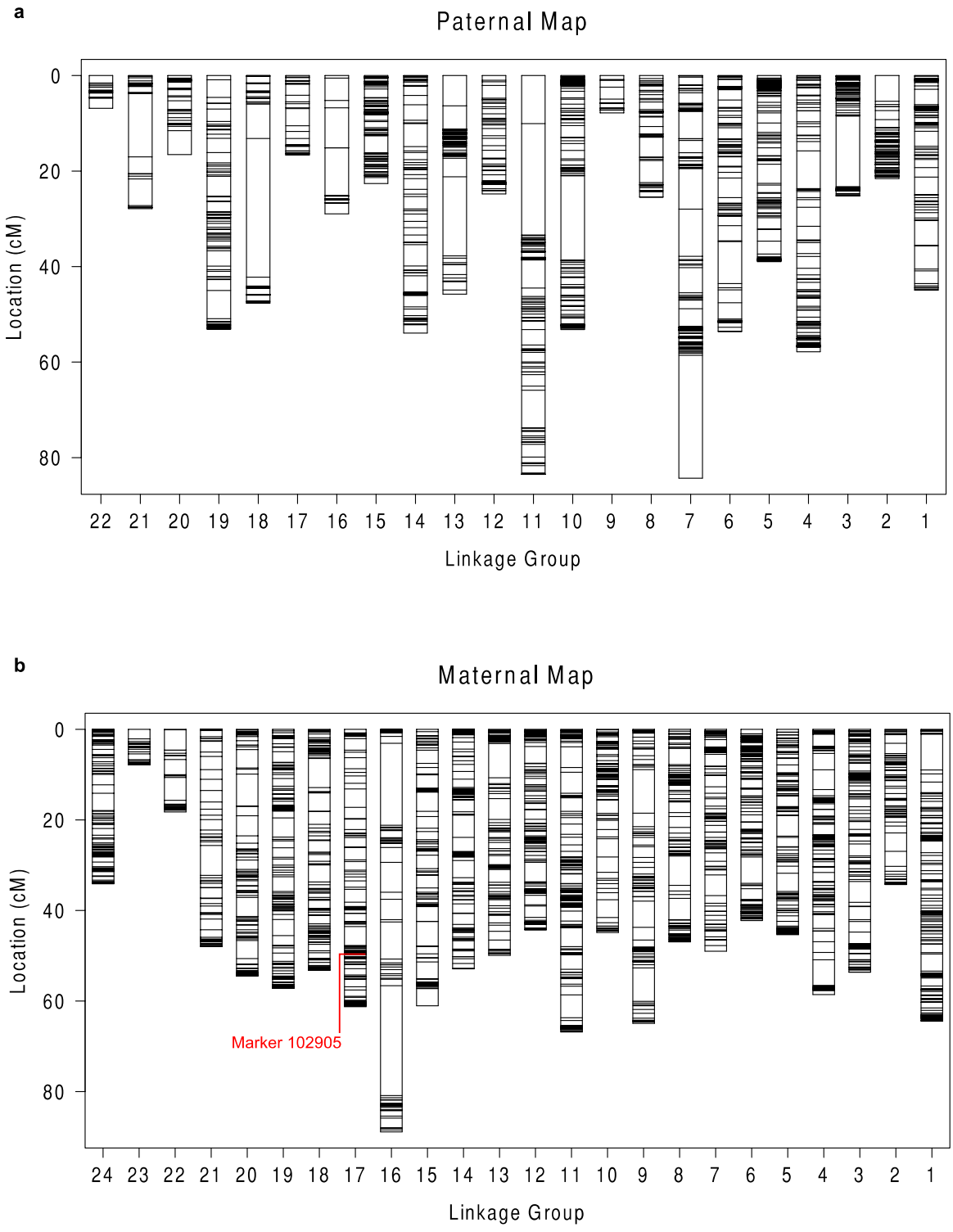

Figure 4.1 The (a**)** paternal and (b**)** maternal genetic maps constructed using the Kosambi regression mapping algorithm and ddRAD markers. Horizontal lines represent mapped markers. Location of marker 102905, associated with sex, is highlighted in red on the maternal linkage map.

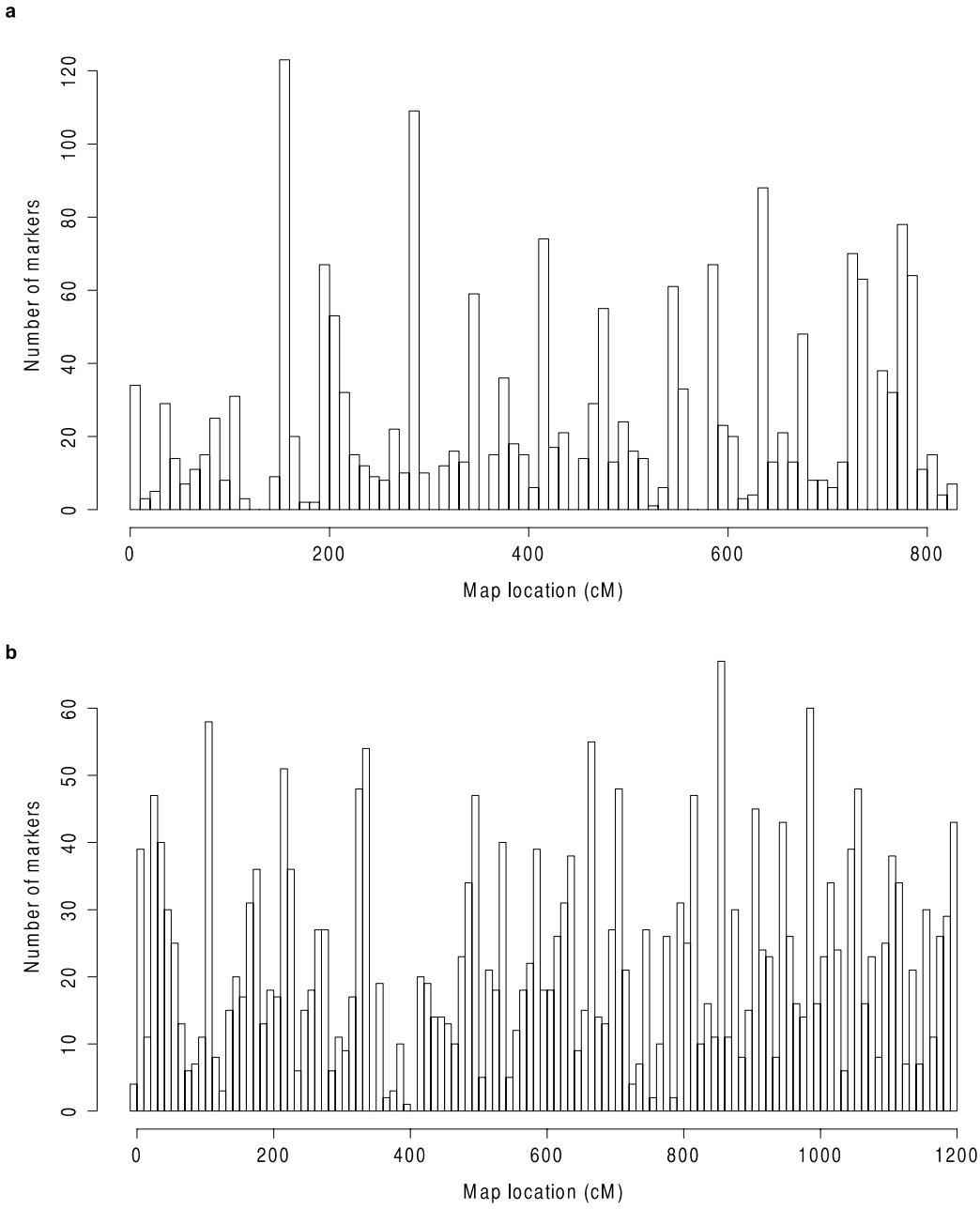

Figure 4.2 Histograms showing the marker density across the (a) paternal genome and (b) maternal genome. Each bin represents a 10cM region of the genome.

4.4.2 Sex determination

The genome scan with a single-qtl binary model revealed that there was a single locus on the maternal map associated with sex and no loci significantly associated with sex in the paternal map. A permutation test of 10,000 permutations was run to get a genome-wide LOD significance threshold for each genome scan and adjusted P values were calculated for inferred QTL. No loci were significant on either parental map at $\alpha = 0.05$. On the maternal map a single locus, 102905, 50.7 cM on linkage group 17 was significantly linked to sex ($\alpha = 0.1$) in both binary (LOD = 2.86, P = 0.0782) and non-parametric models (LOD = 7.91, P = 0.079). The marker lies in a 10cM region containing 31 markers, which is higher than average density (22 markers per 10cM) for the maternal genome. The paired-end sequences of this marker were BLAST (blastn) (Altschul et al. 1997) searched against the *Danio rerio* genome (Howe et al. 2013), the *N. furzeri* genome (Reichwald et al. 2009) and the *N. furzeri* transcriptome (Petzold et al. 2013) with an E-value cutoff of $1e^{-10}$. These searches yielded no matches. The location of this marker on the maternal map is highlighted in Figure 4.1b. The maximum LOD score on the paternal map was at 11 cM on linkage group 3 but was not significant under either binary (LOD = 1.9, P > 0.1) or non-parametric models (LOD = 5.49, P > 0.1). The LOD curves and thresholds calculated using the binary and non-parametric models for each locus are shown in Figure 4.3 for the maternal map and Figure S4.1 for the paternal map. The investigation of patterns of segregation in alleles revealed no SNPs that were present in all males and no females or vice versa.

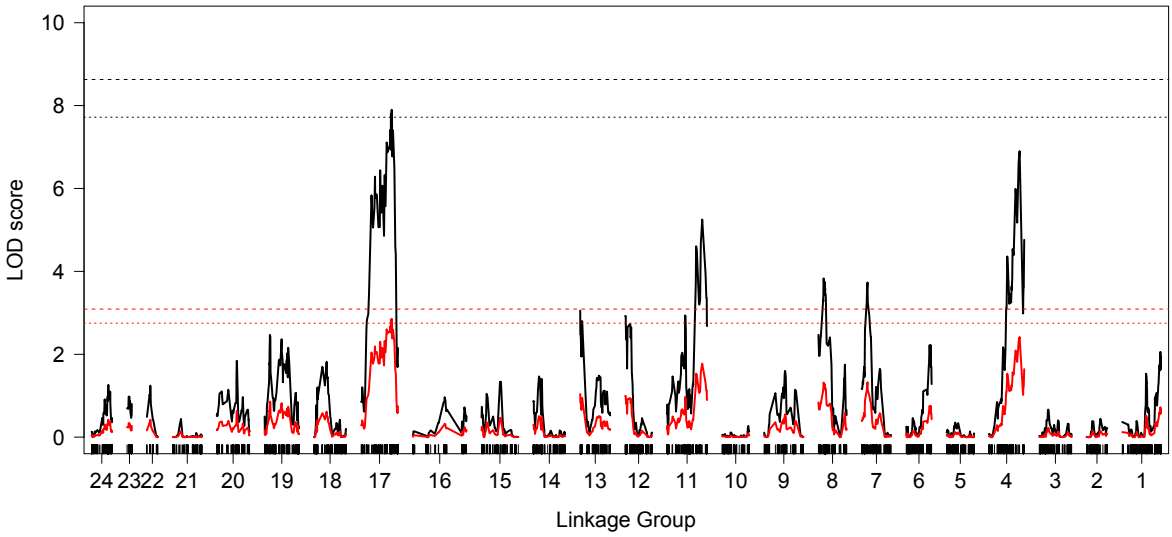

Figure 4.3 Plots of the LOD curves for a genome scan using the single-QTL model, for each linkage group in the maternal map. In black are the LOD curves for the non-parametric model and in red are the curves for the binary model. Dashed lines represent the 5% LOD threshold calculated from a permutation test using 10000 permutations; dotted lines represent the 10% threshold.

4.4.3 Chromosomal correspondence and rearrangements

50 loci were present in both parents revealed correspondence between linkage groups of maternal and paternal maps. Generally, shared loci revealed a one to one correspondence between linkage groups (Table S4.1). Shared markers found in more than one linkage group may indicate that a chromosomal rearrangement such as a fusion or split has occurred. Four markers were found on single linkage groups that matched more than one linkage group (LG) in the other parent. Three of these (27650, 76226 & 50965) did not match a one to one pattern in both parents, and were thus seemed likely to be the result of mapping errors rather than evidence for true fusions. For example, marker 27650 was mapped to LG 1 in the paternal map and LG 14 in the maternal map, which disagreed with multiple other loci that indicated that LG 1 in the paternal map corresponded to LG 9 in the maternal map and that

maternal LG 14 matched paternal LG 18 (Table S4.1). Markers found in paternal LGs 2 and 21 are mapped to maternal LG 6, indicating that there may have been a chromosomal rearrangement. The combined length of paternal LGs 2 (21.6 cM) and 21 (16.5 cM) was 38.1 cM, similar to the length of maternal of LG 6 (42.2 cM), evidence pointing towards fusion of paternal LGs 2 and 21 to make maternal LG 6. Several LGs did not contain any shared markers and thus could not be matched to LGs in the other parent's map.

Pairwise recombination fractions and LOD scores were calculated to identify putative CRs in maternal and paternal maps (Fig. 4.4). Blocks of low levels of recombination are found in both maps, with considerably more in the paternal map (Fig. S4.2). These blocks may be representative of CRs such as inversions. The typical pattern of recombination fraction and LOD along a linkage group is represented in Figure 4.4a and 4.4b, with Figure 4.4c and 4.4d showing examples of the block-like regions where recombination is low and may have been suppressed. Heat maps for recombination fractions and LOD score for all marker pairs can be found in Figures S4.2 and S4.3.

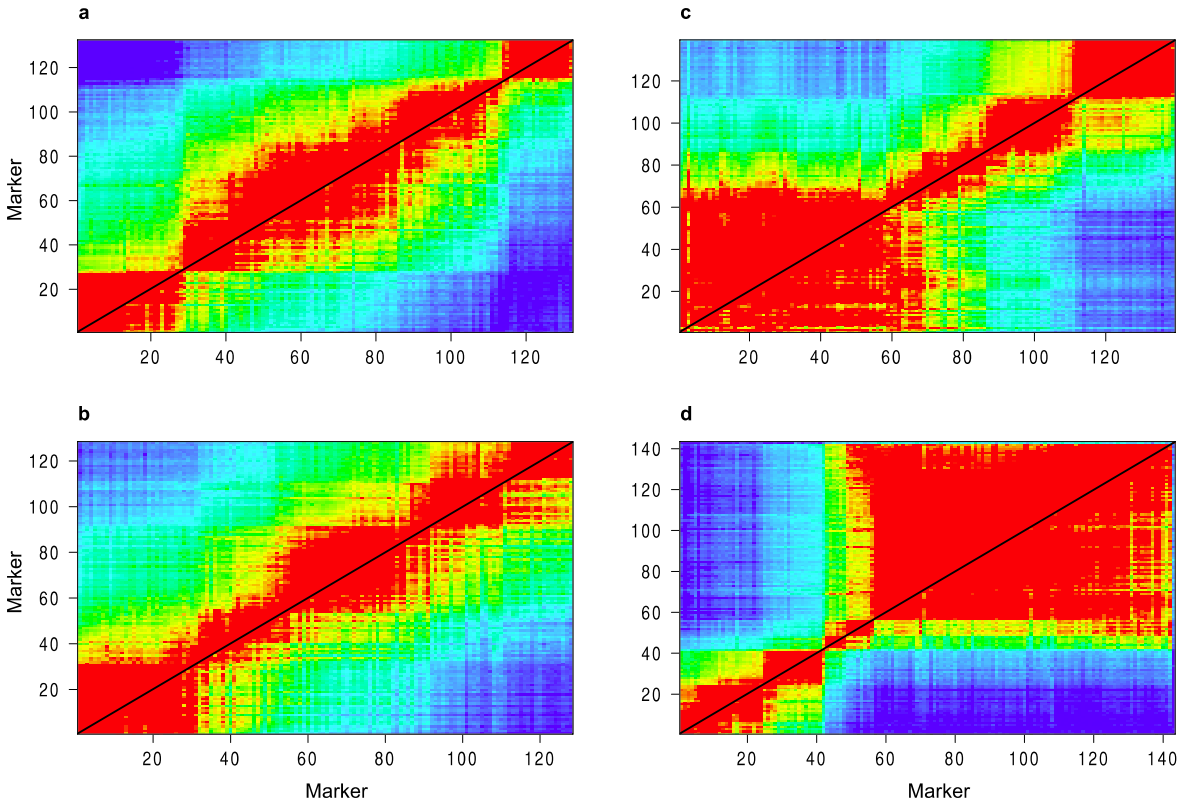

Figure 4.4 Heat maps depicting pairwise recombination fractions (upper left triangle) and LOD scores (lower right triangle) for (a) maternal linkage group 4, (b) maternal linkage group 12, (c) paternal linkage group 5 and (d) paternal linkage group 7. LOD score tests the null hypothesis that the recombination fraction between two markers is 0.5. Low recombination fraction/high LOD score is shaded in red and high recombination fraction/low LOD score is shaded in blue. Large blocks of low recombination are seen in (c**)** and (d)**,** indicating that recombination is low in these regions. Panels (a**)** and (b**)** represent a more typical pattern of recombination.

4.5 Discussion

4.5.1 Linkage map

Here I present the first linkage map of a South American annual killifish. This will act as an important resource for studying genomic regions that underlie phenotypic diversity in the group. Mapped linkage groups matched expected chromosome numbers in *A. bellottii* (2n = 48, (García et al. 1993)) but only 22 linkage groups were mapped of the expected 23 in *A.*

vazferreirai (García et al. 2001). Intrapopulation variation in chromosome number has been observed in *Austrolebias* (García et al. 1993), so I may have captured previously unknown natural variation in chromosome number in *A. vazferreirai.* Additionally, *A. vazferreirai* is sister to *A. cinereus* ((García et al. 2014); chapter 2) and the pair were previously suggested to be the same species (chapter 2). *Austrolebias cinereus* individuals have 22 pairs of chromosomes (García et al. 2001), as reported for *A. vazferreirai* in this study. It may be that chromosome number varies within *A. vazferreirai* and the parent sequenced in this study had a karyotype more similar to *A. cinereus* than other previously recorded *A. vazferreirai* karyotypes.

Several small linkage groups were found in maternal (LG 23) and paternal maps (LGs 9 & 22). These groups may be real or the addition of more markers and meioses may cause these linkage groups to merge with others. The male map (841.1cM) was markedly shorter than the female (1202.2 cM). Differences in linkage group length estimates among paternal and maternal species maps may be due to differences in the physical length of the chromosomes, LG-specific recombination frequencies or marker coverage. This difference in map length may also have been due to the female map having more markers than the male map and thus increasing map length. I also suspect some difference in map length as these maps are from different species. However as the female map is almost 1.5 times larger than the male map it is likely that some of these differences are due to sex-specific recombination rates. Recombination rates are known to vary among sexes in many animals (Lenormand & Dutheil 2005) and in fish specifically, recombination rates have been found to be lower in males of the fugu (*Takifugu rubripes*, (Kai et al. 2011)), the Japanese eel (*Anguilla japonica*, (Kai et al. 2014)) and the zebrafish (*Danio rerio*, (Singer et al. 2002)). The largest difference in sex specific recombination ratio in fish is found in the Atlantic salmon, *Salmo salar*, in which

male/female recombination has a ratio of 1:8.26 (Moen et al. 2004). Recombination was more even across the female map than the male map but regions of low recombination were detected in both. These regions are commonly considered evidence for the existence chromosomal rearrangements.

4.5.2 Chromosomal rearrangements

Chromosomal rearrangements are common among species and may play an important role in adaptive divergence and speciation (M. King 1995; Rieseberg 2001). I found widespread evidence for areas if reduced recombination in the maternal and as well as the paternal map, some of which may be the result of recombination suppression. Areas of recombination suppression are used as evidence that chromosomal rearrangements (e.g. inversions) have taken place, so it is likely that there has been rearrangements since the parental species diverged approximately 10 million years ago (chapter 2). However, with the pseudo-testcross method one can only observe recombination and meiosis within the mother and father. In order to fully understand the reasons behind these areas of low recombination a linkage map with a mapping population down to the F_2 level would need to be constructed. It may also have been that the ddRAD technique sampled at a higher density in some physical regions of the chromosomes than others and produced variable recombination rates along the chromosome. I also found evidence for a single fusion event where markers from two small paternal linkage groups map to a larger maternal linkage group. The frequency of potential rearrangements fits with observations from previous studies where large differences in karyotype structure across the genus were found (García et al. 1993; García et al. 1995; García et al. 2001). In particular, the *A. bellottii-robustus* species group, of which both species in this study are members, is “notorious” for its differences in karyotype structure and

centric fusions are thought to play a major role in repatterning (García et al. 1993; García et al. 1995; García et al. 2014). Study of the physical chromosomes must be conducted to determine whether the putative rearrangements highlighted in this study are real but my observations conclusions of previous cytogenetic studies stating that rearrangements are frequent (García et al. 1993; García et al. 1995; García et al. 2001). Recombination suppression may also be caused by unbalanced gametes which cause non-recombinants to be the only viable gametes or limiting recombination among rearrangements (Borodin et al. 2008). As chromosome numbers are almost certainly different in *A. bellottii* and *A. vazferreirai* this is likely to be the source of some of the observed recombination suppression, though again F_2 individuals would be needed to prove definitively that there is recombination suppression between species.

4.5.3 Sex determination

Surprisingly, I found just a single QTL influencing sex, and this was only significant at a low threshold. I would have expected that marker density was higher in this region as recombination suppression can often be higher in sex determining regions (Kondo et al. 2001; Charlesworth et al. 2005). I did find that the region was higher than average density, but far from the highest across the genome. When this marker was BLAST searched against the zebrafish genome and *N. furzeri* transcriptome/genome it did not match any functional regions, which is not surprising as most RAD-tags will not map to a coding region (Amores et al. 2011). Furthermore, my analysis of segregation patterns (Chibalina & Filatov 2011) also yielded no putatively sex-linked loci. There are several possibilities as to why I found little evidence for genetic sex determination. The first is that there may be little/no genetic influence in the sex determination system of *Austrolebias.* The absence of sex chromosomes

(Garcia 2006) indicated that it was likely that the sex determination system was either governed by homomorphic chromosomes (i.e. not distinguishable and likely to be recent/young) or not entirely genetic. Sex determination may be based more predominantly on differential patterns of gene expression among sexes rather than genetic differences among sexes. Arezo et al. (Arezo et al. 2014) found a sexually dimorphic expression pattern in a single candidate gene purported to be towards the top of the sex determination cascade. Alternatively, environmental variables, plasticity or maternal effects may be important in sex determination as they are in many other species of fish (Devlin & Nagahama 2002). I observed a female biased sex ratio in the common-garden raised individuals where sex was known, which is suggestive of some degree of environmental sex determination that we do not yet understand. As recombination suppression is known to be higher in regions associated with sex determination (Kondo et al. 2001; Charlesworth et al. 2005), a more thorough investigation of the low recombination regions identified in this study could reveal sex-linked loci within. An intraspecific cross could be used to identify additional genomic regions associated with sex determination that were not accessible with the interspecific cross used in this study. This cross could be taken to the F_2 generation, which would allow one to look at recombination in the F_1 individuals instead of only the parents. This extra information could be used to assess the underlying causes of any observed regions of low recombination and to identify whether differences in recombination rate are significant among males and females of the same species. Furthermore, QTL mapping could be used to identify regions influencing size and shape variation among *Austrolebias* species (chapter 2, 3) and determine whether the same regions are causing the convergent evolution in size and shape observed (chapter 3).

4.6 Conclusion

The genetic map of *Austrolebias* provides a starting point for genomic studies using this emerging model genus (Berois et al. 2014). I have found little evidence for a genetic sex determination system, just a single locus. However, I did find a large amount of evidence for putative recombination suppression and chromosomal rearrangements. More regions with low recombination were found in the male map compared to the female map. The widespread karyotypic variation within the genus and evidence for numerous potential chromosomal rearrangements identified in this study and others indicate that these factors may have been important in past speciation events in the genus (García et al. 1993; García et al. 1995; García et al. 2001). *Austrolebias* could therefore act as suitable study system for developing our understanding about how chromosomal rearrangements can generate diversity. Future studies could continue to develop our understanding of the sex determination system in *Austrolebias* or examine the genomic underpinning of other phenotypic traits such as the extensive variation in body size found within the genus (chapter 3).

Chapter 5

Viviparity Stimulates Diversification in an Order of Fish

Adapted from a manuscript of the same title currently in review at Nature Communications

5.1 Abstract

Species richness is distributed unevenly across the tree of life, and this may be influenced by the evolution of novel phenotypes that promote diversification. Viviparity has originated approximately 150 times in vertebrates and is considered to be an adaptation to highly variable environments. Likewise, possessing an annual life cycle is common in plants and insects, where it enables the colonisation of seasonal environments, but rare in vertebrates. The extent to which these reproductive life-history traits have enhanced diversification, and their relative importance in the process remains unknown. In this chapter I show that convergent evolution of viviparity causes large bursts of diversification in fish. I present a new phylogenetic tree of Cyprinodontiformes, an order in which both annualism and viviparity have arisen, and reveal that while both traits have evolved multiple times, only viviparity played a role in shaping patterns of diversity. These results demonstrate that changes in reproductive life-history strategy can stimulate diversification.

5.2 Introduction

The rate at which a clade accumulates species depends on the balance between speciation and extinction. In recent years, phylogenetic studies have shown that such net diversification rates vary immensely. Where the coelocanth genus, *Latimera*, has produced only two known species in the last 80 million years (Amemiya et al. 2013), the Haplochromine cichlids of Lake Victoria may have produced as many as 500 species in as few as 15,000 years (Brawand et al. 2015). Increases in net diversification rate are often thought to be driven by the evolution of novel phenotypes that provide access to new ecological niches (Yoder et al. 2010). However to date, there have been few convincing examples of such phenotypes (Hunter & Jernvall 1995; Ree 2005). To demonstrate the effect of a proposed phenotypic trait on the rate of diversification, it is necessary to show that the evolution of this trait is repeatedly and independently associated with a change in net diversification rate (Maddison & FitzJohn 2015). Using the order Cyprinodontiformes, I tested the hypothesis that two reproductive life-history traits, viviparity and annualism, can drive rapid diversification.

The Cyprinodontiformes are an order of approximately 1,200 ray-finned fish species found primarily in Africa and the Americas. Many of these species are popular in the aquarium hobby, including guppies, mollies and killifish. Living in a wide range of habitats, they have also evolved many different life history strategies. Where most Cyprinodontiformes have external fertilization and are oviparous, approximately 28% of species have internal fertilization and are viviparous or ovoviviparous, which I group together for the remainder of this study and refer to as viviparity (Wourms 1981). Their most remarkable life-history strategy, however, is annualism. Annual species are typically found in seasonal pools and wetlands on the African and South American grasslands, savannahs and forests. When ponds dry out the adults die, but their embryos, which are buried and protected from desiccation by

a thick chorion and an embryonic diapause, survive to hatch during the next wet season (Wourms 1972). About 25% of Cyprinodontiformes are annuals while the rest live and breed for multiple years.

Both traits have the potential to affect diversification in different ways. Viviparity can allow for increased colonisation rates and establishment by single gravid females, providing access to new geographic regions (Meyer & Lydeard 1993). This may lead to geographic isolation eventually giving rise to speciation. Annualism provides access to new niche space previously unoccupied by fish species, i.e. seasonal ponds. Following the colonisation of this new habitat, geographic isolation and adaptation may drive bursts of speciation. Furthermore, the adaptations that enable survival in a seasonal system may act as a buffer against extinction. As a result, I predicted that these extraordinary reproductive life history traits could be associated with increases in diversification rate.

In order to investigate this I first built a generic level phylogenetic tree of Cyprinodontiformes, which I used to identify shifts in the rate of net diversification across the order. Next, I reconstructed ancestral states for both viviparity and annualism to determine when and how often these traits evolved. I then examined whether previously identified diversification rate shifts coincide with the evolution of annualism or viviparity. Finally, I determined whether annual and/or viviparous clades had increased diversification rates relative to the remainder of Cyprinodontiformes.

5.3 Materials and methods

5.3.1 Phylogenetic analysis

Sequences from six nuclear genes and six mitochondrial genes were used to construct the phylogenetic tree of the Cyprinodontiformes. The nuclear genes used comprised of *ENC1*, *GLYT*, *SH3PX3, MYH6, RAG1* and *X-SRC*. The mitochondrial genes used included *cytB, COI, ND1, ND2, 12S* and *16S*. *cytB* was divided by codon position into separate alignments. Sequences for all genes for species assigned to the order Cyprinodontiformes were downloaded from Genbank (accessed September 2014) as well as sequences for seven outgroup species. I reduced the dataset to the longest sequence per gene per species. I then selected one species per genus that possessed sequences for the highest number of genes from the chosen set. The final dataset included sequences from 85% of recognised Cyprinodontiform genera representing 94% of species. Sequences for all genes were aligned using the MAFFT (v1.3 (Katoh et al. 2002)) plugin in Geneious v6.1.6 (Kearse et al. 2012) using the auto alignment method after which the ends were trimmed, totalling up to 12,455 base pairs of sequence data. A table showing the sampled species and the loci used for each species can be found in Table S5.1.

Sequences of 12 genes from 107 Cyprinodontiform species and seven outgroup species were used to build a linked gene tree in BEAST v 1.8.0 (A. J. Drummond & Rambaut 2007). The appropriate nucleotide substitution model for each gene was determined using jModeltest v2.1.4 (Posada 2008), using Akaike information criterion (AIC) model selection. A relaxed lognormal molecular clock model was used for each of the genes, allowing substitution rates to vary between taxa. BEAST was run for 200 x 10^6 generations and trees were sampled every 20,000 generations. Tracer v1.6 (A. J. Drummond & Rambaut 2007) was used to identify at which point stationarity had been reached and that the Effective Sample Size was

greater than 200 for all relevant parameters. I combined the logs and trees from two analyses using LogCombiner v1.8.0 (A. J. Drummond & Rambaut 2007), discarding the appropriate amount of burn-in for each analysis before combining. TreeAnnotator v1.8.0 (A. J. Drummond & Rambaut 2007) was then used to generate a maximum clade credibility tree (MCC) with the highest sum of posterior probabilities for all clades and mean node heights. The tree was calibrated using three secondary calibrations from a recently published tree of bony fishes (Betancur-R et al. 2013) under a truncated normal prior. The most recent common ancestors of Cyprinodontiformes and Perciformes (mean = 97.3, sd = 7.48, upper= 157.3, lower= 37.3), Atheriniformes (mean = 77.4, sd = 11.6, upper= 117.4, lower= 37.4) and Beloniformes (mean = 67.5, sd = 12.1, upper= 107.5, lower= 27.5) were used. Outgroup taxa were then pruned for all subsequent analyses. Ideally one would use fossils rather than secondary calibration points. Betancur-R et al. (Betancur-R et al. 2013) collated 58 fossils of bony fish to use as calibration points. Only two of these could be used in my tree: two cichlids that were dated to the same age of approximately 49 million years (Betancur-R et al. 2013), these fossils were placed accurately among several representatives of cichlids, but this does not apply here given that I have only one cichlid, at the root of the tree. Therefore, I decided to use secondary calibrations.

5.3.2 Ancestral state reconstruction

Data for each trait was collected from FishBase ((Froese & Pauly 2015), accessed September 2014) except in instances where information was not available and alternative sources were used (Table S5.2). Using the MCC tree I reconstructed ancestral states for character traits under a Multiple State Speciation and Extinction (MuSSE) model (FitzJohn 2012). I divided the Cyprinodontiform genera into three character state groups; non-annual viviparous, annual oviparous and non-annual oviparous. Incomplete sampling was accounted for by a state-

dependent sampling factor. I built a model with state-dependent speciation rates, a single extinction rate (as dictated by model simplification, see below) and all transitions rates. The resulting MuSSE model was run in a maximum likelihood framework and the coefficients generated were used to perform ancestral state reconstruction. Additional reconstructions using stochastic character mapping were performed with the make.simmap function in the phytools R package v0.4-31 (Revell 2012). This method fits a continuous-time reversible Markov model for the evolution of the selected trait. It then simulates stochastic character histories using that model and the tip states on the tree (Revell 2012). I simulated 1,000 character histories per trait.

There is one well-known instance of variation in annualism in the genera shown on the phylogenetic tree, i.e. in the genus *Fundulopanchax* (Furness et al. 2015). In the analyses above, *Fundulopanchax* was scored as annual. However, I also reran all BAMM and MuSSE analyses, scoring this genus as non-annual, and it did not affect the results or plots of net diversification (Fig. S5.12).

5.3.3 Diversification rates

I used Bayesian Analysis of Macroevolutionary Mixtures (BAMM) (Rabosky 2014) to estimate rates of speciation and extinction across the phylogeny of Cyprinodontiformes. BAMM allows variation in evolutionary rates through time and among lineages, relaxing the assumption that diversification rates must be time-homogenous as in MEDUSA (Alfaro, Santini, et al. 2009). BAMM allows for the incorporation of incomplete taxonomic sampling at the backbone and clade level for which my tree contains 85% sampling of backbone taxa and varying proportions of species present sampling fractions per clade (Table S5.2). I performed multiple BAMM runs of 30 million generations, sampling every 6000 generations

and checked convergence and stationarity using the CODA package v0.16-1 (Plummer et al. 2006) in R. ESSs of all parameters were greater than 200. The process was repeated three times to ensure convergence of separate runs. I then calculated the mean of the marginal posterior density of speciation, extinction and net diversification rates at all points on each branch of the summary tree. Credible shift sets, Bayes factor calculations and cumulative shift probabilities were obtained with the R package BAMMTools v2.02 (Rabosky, Grundler, et al. 2014). Speciation and extinction rates over time were calculated for each of the three trait groups (non-annual viviparous, annual oviparous and non-annual oviparous) using all samples from the posterior distribution of a single run.

5.3.4 Diversification correlates

I examined differences in speciation, extinction and net diversification rates between viviparous, annual and non-annual oviparous clades using the posterior distribution of state-dependent rates extracted from the BAMM analyses. I modified the getCladeRates () function of BAMMtools to select any required subset of nodes and tips in order to calculate a mean diversification rate across multiple clades of viviparous and annual species. I also calculated diversification rates for all non-annual oviparous clades, including internal branches from the BAMM analyses. State-dependent rates were then compared using the credible intervals of differences to assess significance.

I verified these results by using MuSSE and the MCC tree. MuSSE allows one to associate changes in speciation or extinction with multiple character states and has been developed in order to incorporate the effects of incomplete taxonomic sampling (FitzJohn 2012). MuSSE was implemented using the R package Diversitree. I fit a ML MuSSE model with 12 parameters as a starting point to estimate parameters using a Bayesian framework. I again

accounted for incomplete sampling by using a sampling fraction for each state. I first performed model simplification with MuSSE in a maximum likelihood framework based on likelihood ratio tests. My simplification suggested that the simplest, best fitting MuSSE model comprised of three speciation rates (one for each state), one extinction rate and one transition rate. I then ran a MCMC chain of 10,000 generations using the full model and an exponential prior 1/ (2r), where r is the character independent diversification rate. I removed 10% burn-in and then summarised the MCMC samples to assess variation in state-dependent speciation, extinction and net diversification rates. I calculated statistical significance between character state groups using the credible intervals of differences among posterior distributions of the state-dependent speciation, extinction and net diversification rates.

5.4 Results

5.4.1 Phylogenetic analysis

Using DNA sequence data and Bayesian inference I produced a time-calibrated molecular phylogenetic tree of Cyprinodontiformes for 107 genera (Fig. S5.1). This tree was well resolved with strong support (posterior probabilities > 0.9) for 70% of the nodes (Fig. S5.2). My tree is broadly consistent with previously published phylogenetic trees of a subclade of Poeciliidae (Pollux et al. 2015), the family Goodeidae (S. A. Webb et al. 2004) and suborder Apolcheiloidei (Furness et al. 2015). All currently accepted Cyprinodontiform families were monophyletic except Cyprinodontidae and Poeciliidae (Fig. 5.1), whose taxonomy may, therefore, need to be re-evaluated. These taxonomic uncertainties do not affect my estimates of branching times and diversification rates.

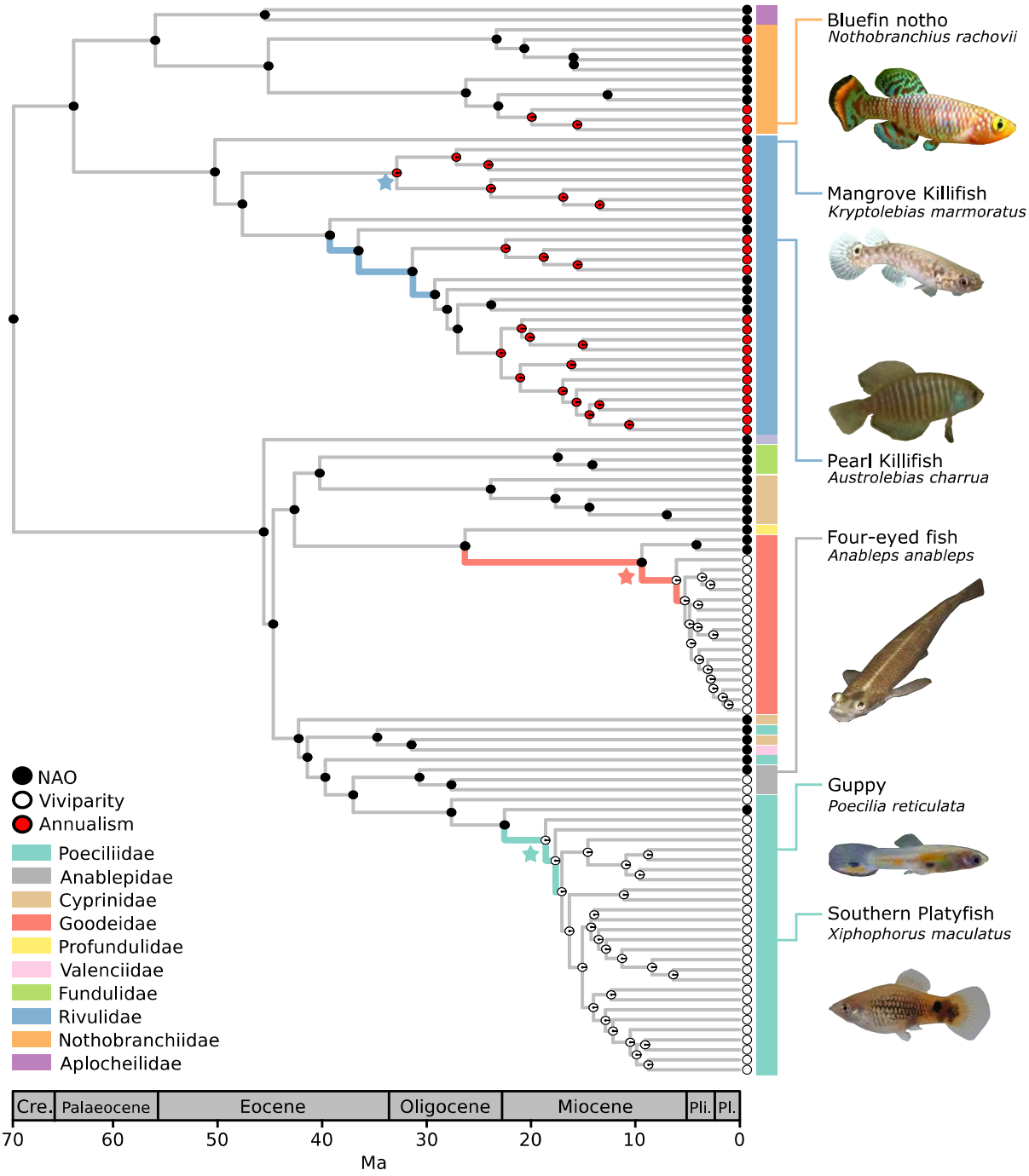

Figure 5.1 Phylogenetic tree of Cyprinodontiformes. A Bayesian maximum clade credibility tree is shown with ancestral reconstructed rates of viviparity and annualism. Pie charts in each node represent MuSSE reconstructed ancestral states (NAO = non-annual oviparous). Branches on which BAMM indicated large support for rate changes (Bayes Factor > 20) are highlighted in colour. Stars denote the node from which clade diversification rates over time were calculated (shown in Fig. 5.2). See supplementary materials for photo credits.

5.4.2 Modelling diversification rates

To model the dynamics of speciation and extinction on this phylogenetic tree I used Bayesian Analysis of Macroevolutionary Mixtures (BAMM) (Rabosky 2014). This analysis revealed several shifts in diversification rates within Cyprinodontiformes (Fig. 5.1, Fig. S5.3). I found strong support for more than one diversification rate across the order; the posterior probability that 2-4 rate shifts have occurred was 0.95. Two primary shifts were recovered consistently in the posterior distribution of shift sets produced by BAMM (Fig. S5.4). The first of these shifts was located at the base of Goodeidae, and the second in Poeciliidae. I calculated branch-specific Bayes factors (BFs) under a model imposing a rate shift for a particular branch versus a model without that shift, and detected eight branches where there was strong support for a rate shift. Two of these branches were located within Rivulidae, three at the base of Goodeidae and three at the base of the livebearing Poeciliidae, highlighting three regions where rate shifts are likely to have occurred (Fig. 5.1). Overall, I found considerable rate variation over the evolutionary history of Cyprinodontiformes for which I can attempt to uncover the underlying causes.

5.4.3 Ancestral state reconstruction

I then used ancestral trait reconstruction (ASR) to determine when and how often annualism and viviparity have evolved in Cyprinodontiformes. ASR methods are often biased towards traits that are associated with increased diversification, preferentially assigning the node state to the trait associated with increased diversification (Maddison 2006). To circumvent this issue I reconstructed traits using a Multiple State Speciation and Extinction (MuSSE) model (FitzJohn 2012). MuSSE reconstructions revealed that both viviparity and annualism (Fig. 5.1) have each evolved in five independent instances. ASR using stochastic character mapping agreed with MuSSE methods, except in Anablepidae and Poeciliidae where there

was substantial uncertainty regarding the origin of viviparity (Figs. S5.5, S5.6). MuSSE reconstructions were considered more reliable because of their ability to cope with differential diversification rates and lack of uncertainty when reconstructing character state. They were therefore used in all subsequent analyses.

5.4.4 Timing of diversification rate shifts

If the reproductive life history traits have caused an increase in diversification I would expect rate shifts to occur during or shortly after a trait has appeared. Combining my ASR and BAMM analyses I found that the evolution of viviparity coincides with the sharp increase in diversification rates seen in Goodeidae and Poeciliidae, while the evolution of annualism did not overlap with increases in diversification (Fig. 5.2a, b, c). The rate shift identified in Poeciliidae was consistently placed at or adjacent to the evolution of viviparity in Poeciliidae as shown in credible shift sets (Fig. S5.4). Modelling diversification rates for the oviparous Empetricthyinae, a subfamily within Goodeidae, proved difficult as BAMM analyses produced a bimodal distribution of rate estimates (Fig. S5.7a). Regardless, cumulative shift probabilities (the probability that a given node has a rate different to that found at the root) indicate that the best support for rate shifts lies immediately after the evolution of viviparity in Goodeidae and Poeciliidae (Fig. S5.8). Additionally, the highest branch specific BFs support a rate shift occurring on the branch leading to the viviparous Goodeidae (upon which viviparity likely evolved) and the branch following the evolution of viviparity in Poeciliidae. These results confirm my expectation that diversification increased when or shortly after viviparity appeared, and show that viviparity has been instrumental in stimulating diversification in these clades. Rate shifts did not overlap with the evolution of annualism in any cases and I therefore conclude that the evolution of annualism has had no causal effect on diversification shifts.

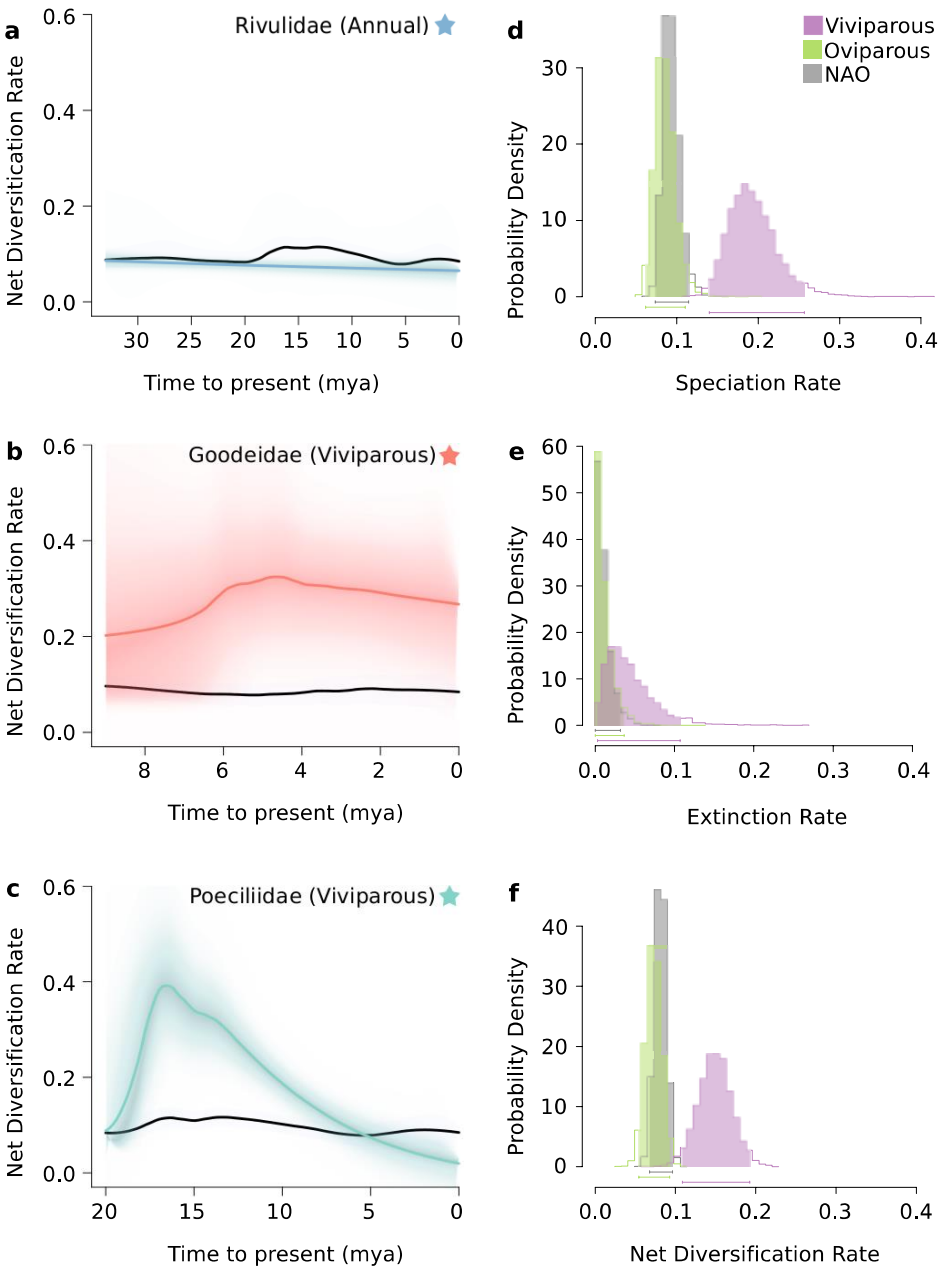

Figure 5.2 State-dependent diversification rates and rate shifts in Cyprinodontiformes. Graphs on the left show net diversification rates over time for three clades in which annualism or viviparity evolved: (a) a clade of annual Rivulidae, (b) Goodeidae and (c) a clade of viviparous Poeciliidae (see stars in Fig. 5.1 and text for details). Coloured lines indicate net diversification rates against background rate (black lines), with shading around coloured lines representing 90% confidence intervals. On the right, state-dependent diversification rates extracted from BAMM analyses fare shown for non-annual viviparous, annual oviparous and non-annual oviparous (NAO) clades. These graphs show the posterior distribution of rates for speciation (d), extinction (e) and net diversification (f), coloured by character state.

5.4.5 Trait-dependent estimates of diversification

Finally, I looked for significant associations between character states and lineage-specific diversification rates using the posterior distribution of state-dependent rates from my BAMM analyses. I separated taxa into three groups depending on character state: non-annual viviparous (viviparous), annual oviparous (oviparous) and non-annual oviparous (NAO). I found that net diversification and speciation rates in viviparous clades were approximately twice those of annual and NAO clades (Fig. 5.2d, f), while extinction rate did not differ between any groups (Fig. 5.2e). There were no significant differences between the diversification and speciation rates of annual clades and NAO clades (Fig. 5.2d, f). Significance was calculated by examining the posterior distribution of differences among groups (Fig. S5.9). I also modelled state-dependent rates using MuSSE (FitzJohn 2012) and the output from these analyses broadly reflected results derived from BAMM (Fig. S5.10 and S5.11). At their maximum rate, viviparous lineages in families Goodeidae and Poeciliidae diversified up to three and four times faster than the background rate, respectively (Fig. 5.2b, c). The notable exceptions to the trend of higher diversification in viviparous clades were the genera *Anableps* and *Jenynsia*, which have diversification rates similar to the background rate (Fig. S5.3). Regardless, the overarching pattern indicates that viviparity is associated with increased diversification rates.

5.5 Discussion

How might viviparity promote diversification in freshwater habitats? As briefly mentioned in the introduction, one obvious way is that unlike oviparous fishes, viviparous females carry fertilized embryos with them. This means that a single, pregnant, viviparous female can colonize a new watershed whereas a single, gravid, oviparous female cannot (Meyer & Lydeard 1993); more frequent colonisation of geographically isolated areas may facilitate

speciation. There are other possibilities, for example, the young of viviparous species are also relatively protected from their environment (Thibault & Schultz 1978; Wourms & Lombardi 1992) and so may have higher survival rates than the young of oviparous species. This, in turn, might make the colonisation of new habitats easier. Finally, viviparity allows for post-fertilization genomic conflicts to occur between mothers and embryos, siblings in the womb and maternal and paternal genomes within embryos (D. W. Zeh & J. A. Zeh 2000). Such conflicts can perpetuate antagonistic coevolution, which may lead to increased post-zygotic reproductive isolation between populations and consequently stimulate speciation. Although I demonstrate a strong link between diversification and viviparity, I cannot disentangle these factors with my data, and future work should aim to discriminate between causal mechanisms. Unusually, the viviparous Anablepidae have diversification rates closer to oviparous taxa, and with the current data I cannot determine the cause of this low diversity. Further work could investigate whether factors, such as vicariance, dispersal, isolation, or available niche space have been notably limited in Anablepidae compared to other viviparous groups.

My finding that the evolution of viviparity has triggered multiple diversification rate shifts contrasts with results from reptiles. Viviparity has also evolved many times in reptiles (Blackburn 2014) where, contrary to my results, it has increased both rates of speciation and extinction, leaving net rates of diversification unaffected (R. A. Pyron & Burbrink 2014). Future studies may expand upon my work to examine the relationship between diversification and viviparity in sharks, amphibians and across all vertebrates.

I show that annualism has no effect on diversification rate, and rates were very similar to non-annual oviparous groups, which was surprising given my initial prediction that

annualism buffers against extinction. One possible explanation is that annualism limits the maximum number of generations per year to one, thereby reducing mutation rate and speciation. Also, the ephemeral nature of seasonal ponds might limit their lifespan and the speed at which advantageous life history traits spread across populations. Finally, I found that neither annualism, nor viviparity has been lost during the evolutionary history of the Cyprinodontiformes. Again, this contrasts with evidence from reptiles showing that transitions from viviparity to oviparity occur, though whether they are common (R. A. Pyron & Burbrink 2014) or rare (B. King & Lee 2015) depends on the analytical approach.

I encountered a number of caveats and challenges. Although my study includes the replication necessary to link the evolution of a trait with a diversification rate shift, it is limited, with only two strong associations. MuSSE-like models are known to incorrectly estimate very low extinction rates (Davis et al. 2013), which may have biased my estimates for annual species. This may also help to explain why my MuSSE analyses indicated that net diversification was significantly higher in annual clades than non-annual oviparous clades while speciation rates did not different significantly. MuSSE-like models have received considerable criticism in recent years because of their low power at low sample sizes and heavy tip bias and its susceptibility to type 1 errors (Davis et al. 2013; Rabosky & Goldberg 2015) so I take caution in interpreting my MuSSE results especially in regard to estimating extinction. I note that the MuSSE model indicates two origins of viviparity in a monophyletic clade of two Anablepidae genera (Fig 5.1). I believe this may be due to lower diversification rates in Anablepidae relative to other viviparous species. When correcting for increased diversification rate in viviparous species, MuSSE may overestimate the number of origins of viviparity in Anablepidae. Precise estimates of diversification rates require accurate dates for cladogenic events and are compromised to the extent that taxon sampling is incomplete.

Although I have a near complete genus-level tree, it encompasses only 8.5% of Cyprinodontiform species. However, I are confident in my conclusions given that MuSSE and BAMM, which are independent methods that account for missing taxa in different ways, gave similar results (compare Fig. 5.2d with Fig. S5.10a; Fig. 5.2e with Fig. S5.10b, and Fig. 5.2f with Fig. S5.10c).

5.6 Conclusion

It is clear that patterns of diversification will only be understood by interpreting my knowledge of organismal and life history traits in view of the space and time patterns of environmental conditions encountered. For example, it may be that viviparity can only promote species diversity when combined with the variety and fragmentation typical of the freshwater habitats of Cyprinodontiformes. Regardless of these specific factors, my results demonstrate how the evolution of viviparity can have drastic effects on the distribution of diversity and go far towards explaining why so many species give birth to live young.

Chapter 6

Rhodopsin Evolution in Cyprinodontiformes

6.1 Abstract

Rhodopsin (*RH1*) is the visual pigment that initiates low-light vision in vertebrates. The structure and function of this opsin has been extensively studied, providing the basis for further investigating the evolution of rhodopsin and low light vision in new groups. Here, I use likelihood-based methods to identify a signature of positive selection across species from 81 genera in Cyprinodontiformes, an order containing many well-known fish groups (guppies, killifish) that are found in a variety of freshwater habitats. I found 12 codon positions within rhodopsin that are putatively under selection. These sites are also found in previous studies where mutations at these positions have been shown to have a functional effect. Substitutions at sites 165, 213 and 266 have been shown to affect retinal release rates in zebrafish and putatively affect rates in cichlids. Others may be important in rhodopsin dimerization (162, 165, 213, 217 and 218) and lie close to the binding site of the protein (297). I also found the substitution Asp83Asn, which is known to affect peak absorbance in many other species, although these were not under significant positive selection in Cyprinodontiformes. Finally, stochastic branch-site models revealed that selection acted in all major groups in Cyprinodontiformes, most notably all amino acid changes I found with a putative effect on retinal release rate were under selection in the splitfins of the Mexican highlands (Goodeidae). I have identified extensive positive selection acting on low light vision in a group of fish found in a variety of habitats and possessing diverse ecological traits.

6.2 Introduction

Understanding how organisms adapt to different environments is a major goal in evolutionary biology. The visual system is well suited to the study the molecular mechanisms of adaptation as there is a very close link between phenotype and environment. Vision has evolved to suit the wide range of ecological niches and photic habitats occupied by vertebrate species (S. Yokoyama & R. Yokoyama 1996). In order for the eye to function, visual pigments must absorb light. The peak spectral frequency of absorption can be changed by amino acid substitutions in pigments to match the light conditions of the local environment (e.g. (Seehausen et al. 2008; S. Yokoyama et al. 2008; Sugawara et al. 2005)). Of the five major classes of visual pigments in vertebrates, four are involved in bright light vision. The final pigment, rhodopsin (*RH1*), is located in the rod cells of the rentina and facilitates low-light vision (Bowmaker 2008). Visual pigments are composed of an opsin protein (a member of the G-protein-coupled receptor family) and a covalently bonded light-absorbing chromophore (Wald 1968), typically 11-*cis*-retinal in *RH1*. The 11-*cis*-retinal chromophore is bound by a Schiff base linkage at the active site K296 (Sakmar et al. 1989) and maintains stability and decreases thermal activation of dark state rhodopsin (Corson et al. 1990). When activated, 11-*cis*-retinal is converted into a stereoisomer – all-*trans*-retinal which causes a number of structural changes that result in metarhodopsin II and the activation of the G protein transducin (Pugh & Lamb 1993). After just milliseconds, the metarhodopsin II is deactivated, ceasing catalytic activity (Gross & Burns 2010). In order for rhodopsin to regenerate after this process, all-*trans*-retinal is released through the hydrolysis of the Schiff base link. New 11-*cis*-retinal can then bind with opsin and restore photosensitivity (Pulvermüller et al. 1997).

Mutations at key amino acids have been shown to alter spectral sensitivity (S. Yokoyama et al. 2008), retinal release rates (rate of reversible Schiff base hydrolysis and dissociation of the retinal chromophore following photobleaching; (Piechnick et al. 2012; Morrow & Chang 2015)) and thermal stability (Janz et al. 2003) of rhodopsin. Determining how particular substitutions may affect the function of rhodopsin is the first step towards understanding the adaptive significance of these amino acid changes.

Changes in dim-light vision have been correlated with changes in the ecology of aquatic organisms and the environment they inhabit. For example, deep sea fishes typically have a peak light absorbance (λ_{max}) between 480 and 485nm matching the narrow range of light that penetrates to the depths they inhabit is approximately 480nm (S. Yokoyama et al. 2008). Meanwhile, fish at the surface or in shallow water have a λ_{max} of 500-507nm, which corresponds to the range of light wavelengths at twilight, 400-500nm (S. Yokoyama et al. 2008). Evidence from African lake cichlids revealed that specific substitutions (e.g. Asp83Asn) lead to a blue shift in the absorbance spectrum of *RH1* (Sugawara et al. 2010). This was suggested to be an adaptation of deep-water cichlids to the blue-green photic environment they inhabit (Sugawara et al. 2010). Numerous sites across rhodopsin have been found to be under selection in different groups (S. Yokoyama et al. 2008). While convergent evolution may have produced parallel substitutions in bats and fish (Sugawara et al. 2010), divergent selection can also act across closely related groups in different environments (Schott et al. 2014). It was previously thought that peak absorbance was the only aspect of rhodopsin that could be under selection, and many changes under selection were found to have no effect on this trait (S. Yokoyama et al. 2008). Recently, work has focused upon phenotypes other than peak absorbance, with studies highlighting the potential effect of substitutions and selection on dimerization, retinal release rate and 3D structure (Schott et al.

2014; Morrow & Chang 2015). The wealth of information available on rhodopsin function makes it possible to go beyond just assessing signatures of natural selection - to inferring possible phenotypic changes caused by the amino acid changes. Much of what we know about rhodopsin evolution in freshwater fishes comes from evidence from African and Neotropical cichlids (Sugawara et al. 2010; Schott et al. 2014; Torres-Dowdall et al. 2015) and to identify broad scale patterns it is necessary to develop our knowledge in different study groups. Here I use another order of fishes, Cyprinodontiformes, to investigate the molecular processes acting upon the rhodopsin and their functional consequences in a new ecological and evolutionary context.

The order Cyprinodontiformes contains approximately 1,200 ray-finned fish species found in Africa, Europe, Asia and the Americas. These species live in a wide range of habitats; from the small freshwater streams typically inhabited by *Poecilia reticulata* to the salt marshes and brackish estuaries of the Atlantic coast where *Fundulus heteroclitus* is found. Remarkable life history adaptations have allowed some Cyprindontiform groups to colonise seasonal ponds in South America and Africa where they survive using a phase of desiccation-resistant diapause during the dry season (Wourms 1972). Two of the most peculiar members of the order are *Kryptolebias marmoratus,* a self-fertilising hermaphrodite that can last for months out of water (Taylor et al. 2008) and *Anableps anableps,* a large live-bearing fish that has a partitioned retina that receives light from above and below the water line (Owens et al. 2012). The diverse ecology, morphology and habitats of Cyprinodontiformes will likely apply different selection pressures upon rhodopsin and thus make this order an appropriate study group for investigating the evolution of low-light vision. Visual pigments have previously been studied in the Cyprinodontiformes, but the work largely focuses on the evolution of colour vision (Fuller & Claricoates 2011; Owens et al. 2012; Tezuka et al. 2014) and little

research has gone into examining evolutionary processes acting on the low-light visual pigment, rhodopsin.

Here, I attempt to determine the extent to which positive selection is acting on rhodopsin in Cyprinodontiformes, at what sites selection is occurring and if changes at these sites will have a functional effect. The considerable range of habitats and ecological differences between lineages of Cyprinodontiformes lead me to expect that selection is acting on *RH1* in this order. I tested this prediction by collating available Cyprinodontiform rhodopsin sequence data and using site-based models of molecular evolution along with a newly produced phylogenetic tree of Cyprinodontiformes (chapter 5) to look for signatures of selection. I then used published empirical evidence to infer the potential phenotypic effects of substitutions at sites under selection. Finally I used stochastic branch-site models to determine which lineages positive selection is acting upon for specific sites. I expect that selection will be acting across the whole tree because of the variety of habitats and geographic locations Cyprinodontiformes occupy.

6.3 Materials and Methods

6.3.1 Sequence acquisition and alignment

All available rhodopsin sequences from the order Cyprinodontiformes were downloaded from Genbank (accessed September 2014). If a rhodopsin sequence was found for the species used in the phylogenetic tree of Cyprinodontiformes (chapter 5), this was used. If no rhodopsin sequence was found on Genbank, the longest sequence of a congeneric species was then used. This approach resulted in 81 species for downstream analyses each with a sequence length between 628 and 921 base pairs (bp). The phylogenetic tree produced in

chapter 5 was pruned to only include genera representing these 81 species. Rhodopsin sequences were then aligned using the MAFFT (Katoh et al. 2002) plugin in Geneious v6.1.6 (Kearse et al. 2012) using the auto alignment method. A table showing the species used for each genus and accession numbers can be found in Table S6.1.

6.3.2 Identifying signatures of selection

Signatures of selection can be identified on a protein-coding DNA sequencing by examining the ratio of nonsynonymous to synonymous nucleotide substitutions (ω). Purifying selection is indicated when $\omega < 1$, $\omega = 1$ suggests neutral evolution and $\omega > 1$ implies positive selection is occurring (Yang 2007). Inference of positive selection is possible by comparing the goodness of fit of a set of nested statistical models; models where that allow ω to vary above 1 are compared with null models where ω is limited between 0 and 1. Statistical significance between models is then assessed using likelihood ratio tests and chi-square distributions (Yang 2007).

Site-based likelihood models were used to infer positive selection acting on rhodopsin. I searched for signatures of positive selection in Cyprinodontiform rhodopsin using the CODEML program of PAML v4.7 (Yang 2007), first using the M7:M8 model comparison. The M7 beta neutral model has eight categories of ω less than one that together form a beta distribution while the M8 model contains an additional ω category that can vary above one and account for positive selection. I followed this by using more stringent model comparisons (M7:M8a, M1a:M2a) to test for positive selection. To identify sites under selection the significance of the ω ratio at each site was calculated using the Bayes Empirical Bayes (BEB)

method as implemented in PAML (Yang 2007), with a 95% significance threshold. I also identified the best fitting structural model to the dataset and built the 3-D structure of Rhodopsin using SWISS-MODEL (Schwede et al. 2003). The model was then visualised and manipulated in PyMOL v0.99rc6 (DeLano 2002).

6.3.3 Lineage and site-specific selection

I used stochastic branch-site models to detect lineage and site-specific positive selection, as implemented in FITMODEL ((Guindon et al. 2004), http://code.google.com/p/fitmodel, last accessed 15 April, 2015). This approach uses stochastic processes to model the variability of selection patterns along lineages and has been shown to perform better than typical branch-site models in exploratory analyses (Lu & Guindon 2014). This approach allowed me to investigate the site-specific shifts between rate ratio classes by modelling switching as a time-reversible Markov process (Guindon et al. 2004). FITMODEL introduces a switching parameter that estimates the rate of change between different selection regimes (purifying, neutral and positive selection). Switching rates were estimated between the three rate classes used in the m2a model (Yang et al. 2005). The S1 model has equal rates of switching between classes while the S2 model allows switching rates to vary to account for unequal rates of switching among classes (Guindon et al. 2004). I conducted likelihood ratio tests between the m2a, m2a + S1 and m2a + S2 to determine the best fitting model, where the degrees of freedom was equal to the difference in parameters estimated between models. I then used FITMODEL to estimate the posterior probabilities (PP) of assigning a codon to the $\omega 3$ rate ratio class (positive selection) for each branch of the gene tree of rhodopsin.

6.4 Results

6.4.1 Signatures of selection

Positive selection on rhodopsin was inferred from all site based model (M7:M8, M8:M8a; M1a:M2a; $P<0.0001$). The BEB analysis identified 12 sites under significant positive selection (Table 6.1). Of these sites, those that had substitutions that caused a change in residue polarity and hydrophobicity included 149, 165, 213, 217, 218, 266 and 304 (Fig. 6.1). Sites where substitutions only changed residue hydrophobicity included 162, 255, 263 and 297 (Fig. 6.1). I also found a single site (25) where a substitution from glutamic acid to aspartic acid did not change polarity or hydrophobicity of the residue.

Table 6.1 Amino acids at sites under selection and their potential functional effects. Stars denote significance of Bayes Emperical Bayes (BEB) inference of amino acid sites under selection where *: P > 95% and **: P >99%.

Codon	Location	Potential effect on RH1 function	Reference	BEB	ω M7:M8 ± SE	Amino Acids
25	N			0.998**	2.497 (0.069)	E,D
149	C-2			0.997**	2.496 (0.081)	G,S,T
162	TM4	Dimerisation interface	Guo et al. (2005), Fotiadis et al. (2006)	0.997**	2.495 (0.085)	I,F,L,V,M
165	TM4	Dimerisation interface, retinal release rate	Guo et al. (2005), Fotiadis et al. (2006), Morrow & Chang (2015)	1.000**	2.500 (0.001)	N,C,A,L,S,G
213	TM5	Dimerisation interface, retinal release rate	Guo et al. (2005), Fotiadis et al. (2006), Morrow & Chang (2015)	1.000**	2.500 (0.010)	C,L,I,V,S
217	TM5	Dimerisation interface	Guo et al. (2005), Fotiadis et al. (2006)	1.000**	2.500 (0.001)	A,F,T,I,V,S,L
218	TM5	Dimerisation interface	Guo et al. (2005), Fotiadis et al. (2006)	0.996**	2.493 (0.107)	V,T,I
255	TM6			1.000**	2.500 (0.016)	V,I
263	TM6			1.000**	2.500 (0.006)	V,I
266	TM6	Retinal release rate	Morrow & Chang (2015)	1.000**	2.500 (0.002)	I,L,C,T
297	TM7	Adjacent to retinal binding site 296		0.999**	2.498 (0.050)	T,S
304	TM7			0.951*	2.420 (0.354)	M,L,V,C,A

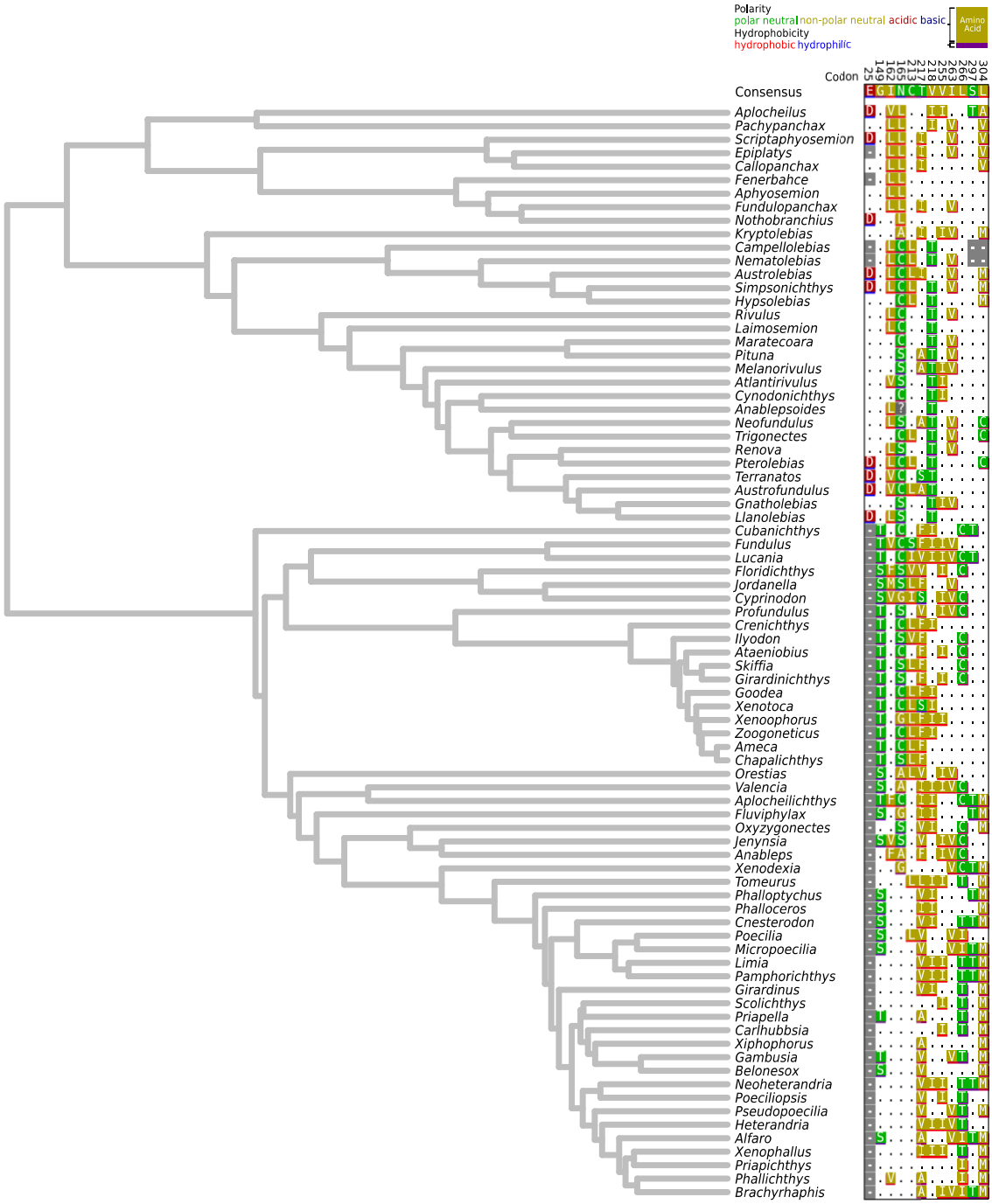

Fig. 6.1. The phylogenetic tree of Cyprinodontiformes with codons under selection. Phylogenetic tree of Cyprinodontiformes (chapter 5) labelled with the name of each genus. Adjacent to the tree are amino acid sites identified using the M7:M8 Bayes Empirical Bayes analysis as under significant positive selection. A majority consensus sequence is provided at the top, with "." indicating the amino acid at that site matches that of the consensus. Polarity is denoted by the colour of the rectangle surrounding each amino acid; hydrophobicity is denoted by the colour of the bar below each amino acid. The key at the top right shows the colours representing each state.

I then used the high-resolution crystal structure of rhodopsin to determine the location of those codons under positive selection. Predicted structural models of rhodopsin protein sequences were modelled against the bovine rhodopsin structure (Okada et al. 2002) (1l9h.3.B; sequence identity = 79.94%) generated using SWISS-MODEL (Schwede et al. 2003). All 12 residues are found at the surface of the protein (Fig. 6.2) and all were located in the trans-membrane domains except Glu25 and Gly149 that were located on the N-terminus and the C-2 loop respectively.

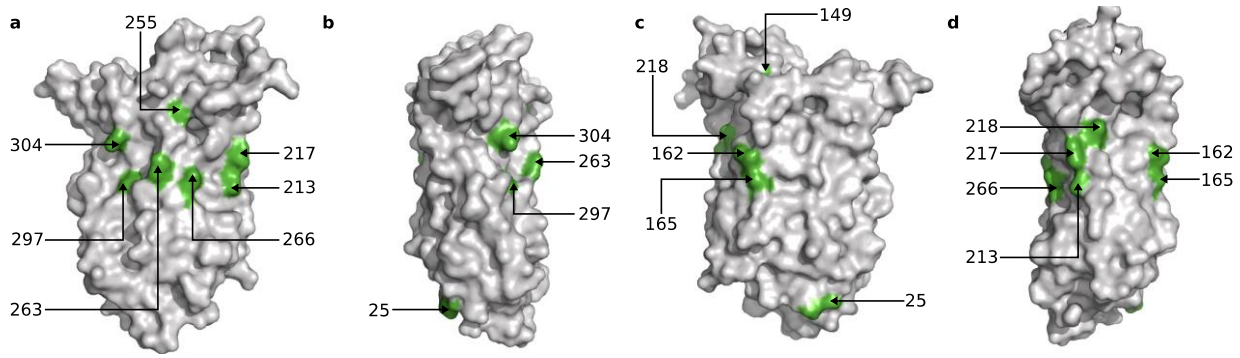

Fig. 6.2. Structural model of rhodopsin. A structural model highlighting the location of codons under selection in Cyprinodontiform rhodopsin. The structural model is rotated 90° around the Y-axis for each panel (a), (b), (c) and (d).

6.4.2 Functional significance of changes at sites under selection

Following this, I examined positively selected sites in the context of previous work conducted on rhodopsin and found that many sites identified as under positive selection in the analyses have been associated with various aspects of rhodopsin function (Table 6.1). Schott et al. (Schott et al. 2014) suggested that dimerization may be an important function of

rhodopsin that could be the target of positive selection. Rhodopsin can form dimers in their natural state (Fotiadis et al. 2003) and intermolecular contact occurs between trans-membrane helices IV and V. Of those under positive selection, residues Ile162, Asn165, Cys213, Thr217, Val218 may have a function in rhodopsin dimerization as they fall on or near the dimerization interface (Guo et al. 2005; Fotiadis et al. 2006).

Residue 213 is near retinal channel B, which gives access to the chromophore binding pocket and provides the opening for retinal release (Wang & Duan 2010). Substitutions that change polarity or size of amino acid residues near the retinal canal may affect the conformation of the retinal channel and consequently alter retinal release rate (Chen et al. 2012). Recent evidence from Morrow & Chang (Morrow & Chang 2015) confirms this observation by showing a number of substitutions in this region of the proteins 3D structure significantly alter retinal release rates. The substitution Phe213Ile lengthened the time taken for retinal release in zebrafish by 1.5 minutes (Morrow & Chang 2015) and I found five different amino acids at this site (Cys, Leu, Ser, Ile and Val) (Fig. 6.1). Morrow & Chang (Morrow & Chang 2015) also found that the substitution Cys165Leu decreased the retinal release rate. These AAs, as well as Asn, Ala, Ser and Gln are found at this residue in the dataset (Fig. 6.1). The substitution Val266Leu was found to increase retinal release rates in zebrafish rhodopsin, while Val, Cys, Thr and Ile were found at this residue in Cyprinodontiform rhodopsin (Fig. 6.1). In addition, additive effects of multiple substitutions (e.g. Phe213Ile and Val266Leu) were observed in Morrow & Chang (Morrow & Chang 2015) and such effects may have taken place in Cyprinodontiformes in genera such as *Austrolebias, Poecilia* and *Cyprinodon* (Fig. 6.1). The range of substitutions at these sites where an effect has already been documented strongly indicates that these sites under selection are having a phenotypic affect.

Yokoyama et al. (S. Yokoyama et al. 2008) identified a large number of amino acid substitutions shown to change peak absorbanc (λ_{max}) across vertebrates. When comparing the substitutions at sites under selection in my dataset to those in (S. Yokoyama et al. 2008) I find several where the effect of the substitution on λ_{max} is unknown (Table S6.2). I also note that although not under selection, I found the substitution Asp83Asn – which is known to affect λ_{max} (Hunt et al. 1996) - in 5 genera; *Campellolebias, Callopanchax, Scriptaphyiosemion, Epiplatys* and *Jordanella*.

6.4.3 Lineage and site-specific selection

Likelihood ratio tests revealed that the m2a+S2 model was the best fitting stochastic branch-site model (Table 6.2).

Table 6.2 Results of likelihood ratio tests of site models and stochastic branch-site models.

Likelihood ratio test	2 Δ l	df	p-value
M1a:M2a	65.932152	2	4.82E-15
M7:M8	111.006642	2	7.86E-25
M8:M8a	101.951264	1	2.85E-24
M0:M3	1275.179716	4	8.01E-275
M3:M3+s1	378.10264	4	1.50E-80
M3s1:M3+s2	27.49473	2	1.07E-06
M1a:M2a	145.729146	2	2.27E-32
M2a:M2a+s1	375.651012	4	5.06E-80
M2a+s1:M2a+s2	11.010354	2	0.00407

The value of ω_3 in the m2a+S2 was estimated to be 5.17, indicating that strong positive selection is acting upon rhodopsin. The switching rate between ω_2 and ω_3 (R_{23}=37.375) was much greater than the rate between ω_1 and ω_2 (R_{12}=2.399) and ω_1 and ω_3 (R_{13}=0.001). This indicates that shifts between neutral selection and positive selection occurred much more frequently than between purifying and neutral or positive selection. All sites previously identified using PAML were found to have branches with high posterior probability (PP > 0.9; Fig. 6.3) along with 5 other sites (19, 39, 50, 112 and 166). Shifts to positive selection were widespread, with most groups experiencing positive selection at one or more codon positions (Fig. 6.3). Analyses revealed that patterns of positive selection were often restricted to single suborders, either Aplocheiloidei (Fig. 6.3a) or Cyprinodontoidei (Fig. 6.3b). Codons also showed similar patterns of positive selection along lineages; positions 255, 266 were subject to positive selection from the root of the gene tree through most of the subfamily Cyprinodontoidei. At codons 149, 217 and 297 positive selection acts on the majority of Cyprinodontoidei. At codons 25 and 162 selection appears to be acting exclusively in the subfamily Aplocheiloidei, while positions 165, 213, 263 appear to be under selection in both subfamilies. There are four groups that are repeatedly subject to positive selection across the codon set; the Goodeidae (Fig. 6.3e), the Poeciliidae (Fig. 6.3d), a clade including members of Anablepidae, Cyprinodontidae, Valenciidae (Fig. 6.3f) and basal Poeciliidae and a clade of Rivulidae including *Austrofundulus and Pterolebias* (Fig. 6.3c). I examined the branches showing signs of positive selection at those sites that have previously found to be important in retinal release rate (165, 213 and 266). At site 165 selection occurred in Rivulidae, Goodeidae, Cyprinodontidae and Anablepidae. At site 213 positive selection was focused on a clade of Rivulidae and the family Goodeidae. This site is unique in that it has a known phenotypic effect on retinal release rate, is involved in rhodopsin dimerization and has two independent changes to rate class ω_3. Both of these instances of positive selection involve

changes from Cys to Leu (Fig. 6.1) and indicate that convergent effects on retinal release rate and/or dimerization may be occurring. At site 266 positive selection appears to be acting across most of Cyprinodontoidei. These results show that positive selection acting on sites that influence retinal release rate is principally found in Cyprinodontoidei, as well as a single clade of Rivulidae and that all sites affecting retinal release rate show signatures of selection in Goodeidae. Selection at sites influencing *RH1* dimerization occurred throughout the Cyprinodontiformes with no group under selection for all sites influencing dimerization.

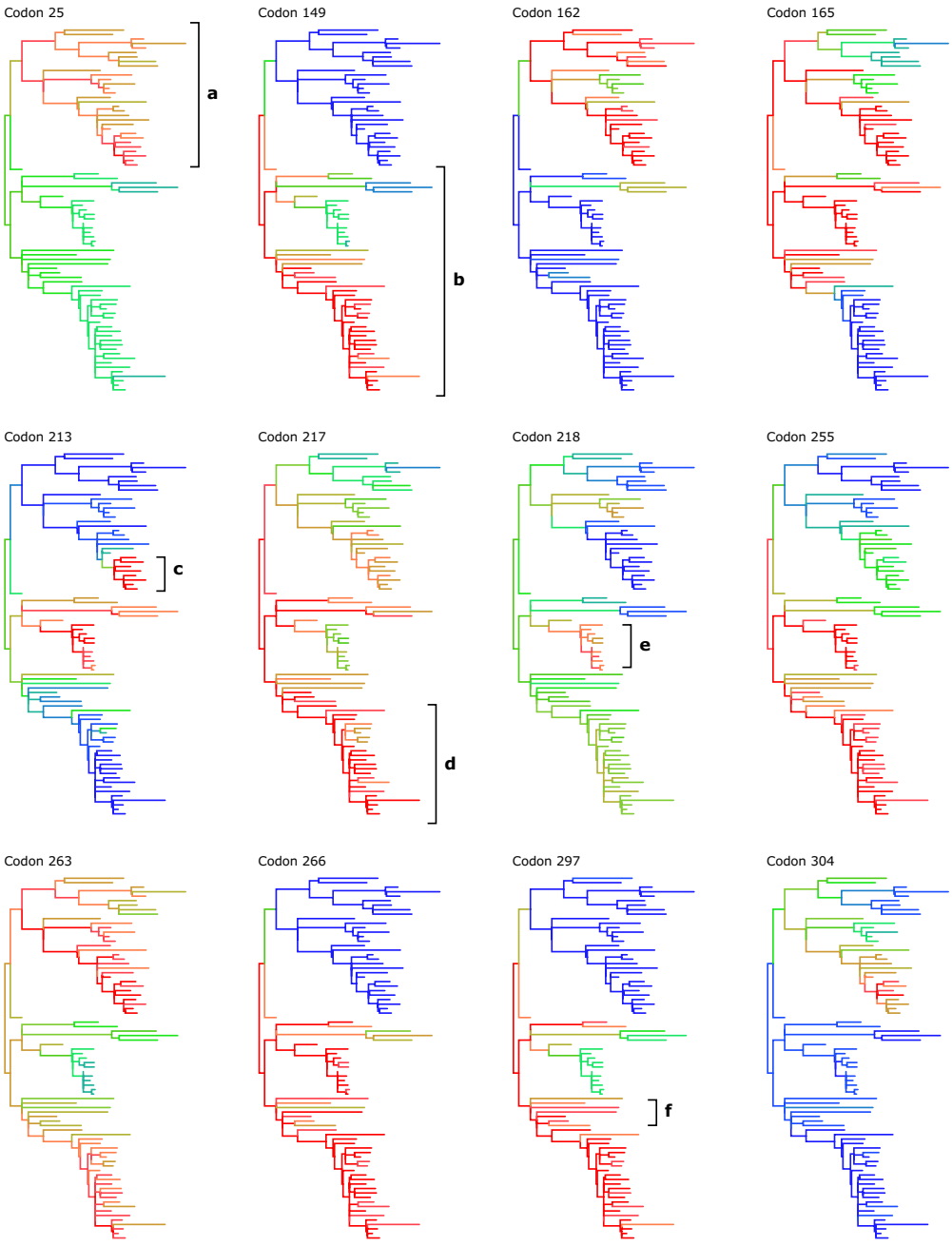

Fig. 6.3. Lineage and site-specific patterns of selection. Gene trees representing site-specific patterns of shifting selection on rhodopsin at sites identified in both site models and stochastic branch-site models as being subject to positive selection. Each tree is labelled with the codon it represents and colours on the tree represent posterior probability of belonging to selection class ω_3. Those branches that are red in colour have a posterior probability (PP) > 90% and have evolved under positive selection. Blue indicates a PP < 20% while intermediate colours represent a PP between 21 and 89%. Brackets show (a) Aplocheiloidei, (b) Cyprinodontoidei, (c) a clade of Rivulidae, (d) Poeciliidae, (e) Goodeidae and (f) a clade containing members of the Anablepidae, Cyprinodontidae, Poeciliidae and Valenciidae.

6.5 Discussion

Through codon-based likelihood analyses I have revealed extensive positive selection acting on rhodopsin in species of Cyprinodontiformes that possess a wide range of ecological characteristics and habitats. Selection appears to be acting across the whole group rather than specific lineages, with substitutions at sites under selection found in all major families. Substitutions at several sites under selection have been linked to functional traits such as dimerization and retinal release rate. Sites 162, 165, 213, 217, 263 and 297 were found to be under selection in Cyprinodontiformes and one or more Cichlid clades (Schott et al. 2014; Torres-Dowdall et al. 2015). Perciformes and Cyprinodontiformes diverged approximately 95 million years ago (Betancur-R et al. 2013) yet share many of the same sites under selection, indicating that these may serve a similar adaptive purpose in both groups. Determining whether selection acts upon these sites in other groups may help to reveal broad scale patterns of selection across vertebrate rhodopsin.

Using stochastic branch-site models (Guindon et al. 2004), I identified lineages where a shift to positive selection was observed (Fig. 6.3). These lineages were spread throughout the phylogenetic tree of Cyprinodontiformes, and while some sites could be grouped into those that have similar selective patterns (e.g. codon 255 & 266 (Fig. 6.3)), selection acted in different lineages among sites. This may be an indicator of divergent selection pressures acting upon different Cyprinodontiform clades. I also note that selection appears to act in large taxonomic groups such as families rather than between small clades, which may be because of a common selection pressure these groups share.

I found several instances of shared amino acids at sites under selection among distantly related Cyprindontiform groups, which may be an indication of convergent evolution. For example, Leu213 is found in Rivulidae and Goodeidae, where stochastic branch-site models indicate selection is acting (Fig. 6.1, 6.3). Multiple amino acids including Phe217, Ala217, Val217 and Ile217 appear to evolve independently in lineages where positive selection is acting, mainly the Poeciliidae, Cyprinodontidae and Anablepidae (Fig. 6.1, 6.3). An investigation into the environmental and ecological characteristics of Cyprinodontiformes may reveal what these species and groups have in common that may drive natural selection and convergent evolution. As I only have one representative per genus it is difficult to know whether the sequence of this individual represents the genus. Any sequence variation within genera will be masked by this approach so additional sequences at species level will reveal interspecific differences in selection and rhodopsin function within genera and may be able to help pinpoint environmental selection pressures.

Although common in many other groups (S. Yokoyama et al. 2008), I found no sites known to affect spectral absorbance to be under selection. It is unlikely that many Cyprinodontiform species frequent deep-water environments, as they are primarily shallow freshwater species, which may be why I see little evidence for selection on peak absorbance. However, I did find the substitution Asp83Asn in the rhodopsin of *Campellolebias, Callopanchax, Scriptaphyiosemion, Epiplatys* and *Jordanella*. This substitution is known to cause a blue-shift in peak absorbance in fish (Hunt et al. 1996), speed up the production of active meta-II state rhodopsin in cichlids (Sugawara et al. 2010) and affect retinal release rates in mammals (Bickelmann et al. 2012). These genera come from a wide range of habitats - *Campellolebias* is an annual freshwater rivulid from South America, *Archaphyosemion*, *Epiplatys* and *Callopanchax* are freshwater African genera with the last being an annual genus. *Jordanella*

is a freshwater fish found in peninsular Florida, USA. If blue shifts in the absorbance peak have occurred in these genera I struggle to find at first glance any shared environmental or ecological traits that may result in similar selection pressures acting on these species. The power of the Bayes Emperical Bayes (BEB) analysis may not have been enough to detect a signal of selection at this site, but further work involving more sequence data would be needed to confirm this.

As a criticism of codon-based models, S. Yokoyama et al. (S. Yokoyama et al. 2008) suggested that many sites found to be under selection in rhodopsin had no functional significance. Many of the sites under selection were located on the surface of the protein, as revealed by my reconstruction (Fig. 6.2), which was the first indication they may have a functional effect. I found many substitutions where mutations at a particular site were known to affect retinal release rate but often amino acids found in my dataset were not tested for their effect in previous studies. In addition, multiple simultaneous substitutions are known to have an additive effect on retinal release rate (Morrow & Chang 2015) and the combination of substitutions in my dataset may produce novel additive effects on this phenotype. Regarding the adaptive significance of changing retinal release rates, it has been suggested that faster retinal release could influence the speed of dark adaptation after bleaching (Ala-Laurila et al. 2006; Morrow & Chang 2015). This could have an important identifying prey or predators, or even potential mates when moving from light to dark areas. Sites that affect retinal release rate are under selection across most of the Cyprinodontoidei; most notably, the Goodeidae are subject to positive selection at every site linked with retinal release rates. These fish live in primarily in the Mexican highlands (S. A. Webb et al. 2004), a rapidly changing environment subject to frequent volcanic activity and tectonic plate movements.

Further research may look into potential selection pressures on retinal release rate and dark adaptation caused by this variable environment.

I also found several substitutions at sites that may be important in dimerization of rhodopsin monomers. These amino acid changes may influence how rhodopsin is packed or affinity between pairs of rhodopsin molecules, although the phenotypic effect these substitutions may have on the visual system is unknown (Schott et al. 2014). The sites that may affect rhodopsin dimerization were under selection in almost all Cyprinodontiform lineages, matching previous work in cichlids where many of the same sites were under selection (Schott et al. 2014; Torres-Dowdall et al. 2015). This indicates that dimerization may be a common target for positive selection in aquatic organisms.

6.6 Conclusion

Rhodopsin is well studied, but the selective pressures that drive positive selection on this visual pigment and any downstream phenotypic effects are still relatively unknown. The wealth of information available for species in the order Cyprinodontiformes provides an ideal opportunity to examine the functional effects of substitutions at sites under selection in rhodopsin. My study has revealed widespread selection acting on at least 12 sites across rhodopsin, some of which can be tied to known phenotypic effects such as retinal release rates or dimerization. My results add to the growing amount of evidence showing that other aspects of rhodopsin function beyond solely spectral absorbance may be the target of positive selection (Schott et al. 2014; Torres-Dowdall et al. 2015). The full extent to which traits other than peak absorbance are shaped by selection is currently unknown. The results of this

chapter highlight the need for species-level analyses and I believe my investigation can act as a platform for future work using Cyprinodontiformes to study the evolution of dim-light vision and adaptation to different environments.

Chapter 7

Thesis Discussion

7.1 Synopsis

This thesis aimed to examine the origins of diversity in the order Cyprinodontiformes, with specific focus on the genus, *Austrolebias*. The project began with the observation that *Austrolebias* annual killifish possessed a peculiar life history that required extreme amounts of local adaptation yet species differed extensively in size and shape. I first aimed to understand the evolutionary relationships among *Austrolebias* species and constructed new phylogenetic trees based on nuclear and mitochondrial DNA markers. I collated the largest dataset of *Austrolebias* occurrence sites to date from a variety of sources in order to build a set of species distribution models based on environmental variables. This information was then used along with phylogenetic independent contrasts to determine how well geographic mode of speciation and body size differences explain the patterns of co-occurrence among species of *Austrolebias*. I then documented the development of 18 species of *Austrolebias* over a 49-day period in order to understand how differences in size and shape arise. Instances of convergent evolution in size and shape were identified using modern phylogenetic comparative methods. I crossed two species of *Austrolebias* to produce an F_1 hybrid offspring family that was sequenced using double digest restriction site associated DNA sequencing. Markers were then used to build linkage maps, which were used to identify any regions associated with sex determination and those with low recombination. The scale of the thesis then changed to examine processes acting in the order to which *Austrolebias* belongs, the egg-laying toothcarps or Cyprinodontiformes. I constructed the most comprehensive phylogenetic tree of this order in an effort to identify shifts in diversification rate and the factors that drove these shifts. Lastly, I used this newly constructed tree to investigate how selection acts upon the low light vision pigment rhodopsin in Cyprinodontiformes. Here I give an overview of the main discussion points of the thesis along with implications for conservation and potential further avenues of research.

7.2 Co-occurrence and body size divergence in *Austrolebias*

In chapter 2 I present a major step forward in understanding the evolutionary relationships among *Austrolebias* species. Previous attempts to build a phylogenetic tree of this genus have relied upon a single mitochondrial gene (García et al. 2014), morphological characters (Costa 2006) or a small number of mitochondrial genes and a single nuclear gene (Van Dooren et al. In review). Here, I assembled separate nuclear and mitochondrial DNA-based trees, each using multiple loci. I found multiple hard incongruences between nuclear-based and mitochondrial-based trees. Accurately determining the factors that lead to these incongruences was not possible with the data from this study but incomplete lineage sorting and/or hybridisation may have played a role. As nuclear DNA is more likely to represent the true relationships among taxa (Ballard & Whitlock 2004) I chose to continue my analysis using the nuclear DNA-based tree only. This tree revealed recovered major groups similar to the previously published trees (García et al. 2014; Van Dooren et al. In review) though species relationships within these clades were different.

I used two different approaches (Bayesian Binary Method (BBM) and S-DEC, a Bayesian implementation of the lagrange method (Yu et al. 2015) to reconstruct the biogeographic history of the group using discrete classifications based on previously identified regions of endemism (Costa 2010). This revealed that the genus has originated in the Patos Lagoon or the Patos Lagoon & Negro River regions, depending on method used. Multiple dispersal events then followed with species moving east and north into the Rio Negro, La Plata and Western Paraguay regions.

I then examined species ranges at a finer scale by collating over 500 occurrence points of *Austrolebias* from various sources to understand how these species are distributed throughout South America. Using 19 bioclimatic variables and altitude, I built species distribution models to estimate the range of each species. The estimated ranges allowed me to assess the degree of geographic isolation during speciation events by performing an age-range correlation (Barraclough & Vogler 2000) and using similar methodology to assess the relationship between size differences and range overlap. Recently diverged species were found to be in allopatry more often than sympatry (chapter 2, Fig. 2.5b). This was somewhat expected as allopatric speciation is generally considered to be the more common mode (Coyne & Orr 2004). The degree of sympatry in divergence events increased through time, though this may have been an artefact of the age-range correlation methodology, which is not without its drawbacks (Barraclough & Vogler 2000; Fitzpatrick & Turelli 2006).

I found a positive relationship between body size contrast and range overlap, indicating that at nodes where range overlap was higher, there was a larger difference in body size. I expanded upon this by attempting to classify nodes by mode of speciation, and found that a mixture model with a single component best explained the data, suggesting that the effects of size were present regardless of speciation mode. This suggests that size is an important factor in determining the patterns of co-occurrence in *Austrolebias*. The only node to be classified as sympatric was the divergence of *A. luteoflammulatus* from the clade containing large bodied species including *A. cheradophilus* & *A. elongatus.* Historical biogeographic reconstructions indicated that this divergence took place in the same region (Patos Lagoon) and this node had the highest levels of range overlap and body size contrast in the tree. Furthermore, *A. luteoflammulatus* and *A. cheradophilus* are known to occur in the same ponds in the wild (Laufer et al. 2009). Evidence from other studies points to a change in diet

along with size as *A. luteoflammulatus* is a crustivore, *A. cheradophilus* a generalist and *A. prognathus* a piscivore (Laufer et al. 2009; Costa 2009). I therefore suggest that character displacement may have driven size divergence in this clade, as larger species were able to eat a larger variety of food and became specialised piscivores. Large body size differences have also evolved between the co-occurring sister species pair *A. wolterstorffi* and *A. gymnoventris* but this was not classified as in sympatry like a previous effort from Van Dooren et al. (Van Dooren et al. In review). They suggested an alternative explanation, that speciation by cannibalism may have been a mechanism through which large body size could have arisen in the seasonal pond system.

In all studies using the phylogenetic comparative method, it is hard to distinguish correlation from causation (Garamszegi 2014). For example, Stuart and Losos (Stuart & Losos 2013) showed that in studies that cite ecological character displacement as an explanation for patterns observed, just 9 of 144 cases have effectively ruled out other explanations. Moreover, two recent reviews (Warren et al. 2014; Mittelbach & Schemske 2015) have highlighted that recent studies of community phylogenetics do not adequately consider the role of the geography of speciation as an explanation. New methods are needed to overcome the shortcomings of those used in chapter 2. If further work is done at a finer scale, e.g. examining historical patterns of gene flow between pairs of species, alternative scenarios for how species assemblages based on size could be ruled out. Regardless, the evidence I present in chapter 2 strongly indicates that body size has played a key role in determining patterns of co-occurrence in *Austrolebias*.

7.3 Variation and convergence growth, size and morphology in *Austrolebias*

After I found that body size was of critical importance in dictating patterns of co-occurrence I aimed to quantify the variation in growth, size and shape among *Austrolebias* species. Previous efforts to examine growth in annual killifish had been made in the African genus *Nothobranchius* (Blažek et al. 2013) or in select species of *Austrolebias* (Fonseca et al. 2012). Chapter 3 is the first large-scale, common garden assessment of interspecific variation in growth and morphology among annual killifish species, which took measurements from 18 species of *Austrolebias* and over 300 individuals. My study aimed to determine how differences in growth, size and shape arise in these fish that inhabit a seasonal pond system and whether convergent evolution has occurred.

Size at hatching was found to be one of the principal factors driving differences in growth, size and shape. Hatching size of hybrid species was typically intermediate but in cases where species with larger differences in initial size were crossed, the hatching size of offspring more closely resembled the mothers. This indicates that maternal effects could have played a role in the evolution of large body size in *Austrolebias*. Analysis taking into account shared ancestry revealed that shape variation was closely linked to body size variation. Differences in diet among large and small *Austrolebias* have already been documented (Laufer et al. 2009; Costa 2009) and I suggested that this difference in size and shape is closely linked to divergence in diet among *Austrolebias* species. Larger species were typically more elongated and streamlined, which is indicative of a more predatory role in the ephemeral pond ecosystem. The size differences in *Austrolebias* while not as varied, are reminiscent of the morphological specialisation found in East African (Muschick et al. 2012) and Neotropical crater lake cichlids (Elmer et al. 2010).

I observed evidence for convergent evolution in both size and shape in two groups of *Austrolebias* - the clade containing the largest species in the genus (*A. cheradophilus, A. elongatus*, *monstrosus* and *prognathus*) and *A. wolterstorffi*. Both groups have evolved towards an optimum of a larger, more elongated body most likely adapted to piscivory or mulloscivory in the case of *A. wolterstorffi* (Costa 2009). Evidence from chapter 2 indicated that speciation in both these groups occurred with high levels of range overlap, although only in one case was divergence found to be in sympatry. The convergent evolution found in this chapter likely played a major role in generating the variation in size that is important in determining patterns of range overlap in *Austrolebias* (chapter 3). This convergence could provide an excellent opportunity to study the mechanisms of evolution and natural selection by asking whether the same genes or genomic regions underlie these similar phenotypes (Elmer & Meyer 2011).

7.4 Linkage mapping, chromosomal rearrangements and sex determination

This thesis presents the first linkage map of a South American annual killifish. Two species that diverged approximately 10 mya (chapter 2) were hybridised and offspring were sequenced using double-digest restriction-site associated sequencing (ddRAD). Paternal and maternal maps were constructed separately in this pseudo-testcross design. The paternal map was 841.1 cM long and consisted of 22 linkage groups, one less than expected in *A. vazferreirai* (García et al. 2014). The maternal map spanned 1202.2 cM across 24 linkage groups. There was little evidence for a genetic sex determination system from this mapping analysis, with a single locus detected at a lower significance threshold ($\alpha = 0.1$). This locus did not map to any regions on the *Nothobranchius furzeri* (Reichwald et al. 2009; Petzold et al. 2013) or *Danio rerio* (Howe et al. 2013) genomes, which is not unexpected as by the

nature of the RAD methodology many markers are located in intragenic regions. The lack of sex chromosomes in *Austrolebias* is not surprising, just 10% of fishes have cytogenetically district sex chromosomes (Devlin & Nagahama 2002). However, because of evidence for a simple genetic sex determination mechanism in *Nothobranchius* (Valenzano et al. 2009), I did expect to find a similar result in *Austrolebias*. As evidence went against my expectations, I suggested that sex determination in *Austrolebias* might rely more on the environment as in many other fish species (Devlin & Nagahama 2002) or differences in gene expression as previous evidence from an assessment of candidate genes has pointed to (Arezo et al. 2014). I found that there were many more regions of low recombination in the male map than the female map, with some regions containing over 120 markers per 10cM. The considerable time since the divergence of *A. bellottii* and *A. vazferreirai* may have caused some of the observed regions of low recombination and/or difficulties isolating sex determining regions through genomic compatibilities that arise from a heterokaryotypic cross (Borodin et al. 2008). However, as chromosomal rearrangements are common in *Austrolebias* (García et al. 1993; García et al. 1995; García et al. 2001), some of these low recombination regions are likely to be the result of recombination suppression caused by rearrangements. Regions of recombination suppression can be important in the process of speciation, as they are often sources of divergence that can accumulate incompatibilities faster than recombining collinear regions (Rieseberg 2001; Noor et al. 2001; Faria & Navarro 2010). The genomes of *Austrolebias* are very large (García et al. 2014) and variable at both interspecific and intraspecific levels (García et al. 1993; García et al. 1995; García et al. 2001). This linkage map is a major step forward in understanding how these characteristics of the genome have shaped the evolution of diversity in *Austrolebias* and information from this linkage map can be used as a genomic resource to help answer other questions about *Austrolebias* evolution.

In an initial pilot study I carried out a number of other interspecific crosses but these did not produce any viable F_1 offspring and the F_1 individuals of the cross used in chapter 4 were also paired up – eggs were produced but no viable offspring hatched, suggesting that incompatibilities may have been present. Future work could use the recently developed phylogenetic tree (chapter 2) to design a cross between two more closely related species in order to assess chromosomal rearrangements without the noise and complications extended divergence times among parental species undoubtedly introduce.

7.5 Diversification trends in Cyprinodontiformes

There have been a number of attempts to reconstruct the evolutionary history of the Cyprinodontiformes but these have either limited to suborder (Murphy & Collier 1997; Furness et al. 2015) or family (Hrbek & Larson 1999). An initial attempt at reconstructing the evolution of viviparity (Meyer & Lydeard 1993) paved the way for future work but used just 22 taxa. Newly available sequence data from over 100 species and improved ancestral state reconstruction techniques (Maddison et al. 2007; Revell 2013) have revealed viviparity evolved four or five times rather than three suggested by Meyer et al. (Meyer & Lydeard 1993). The evolutionary history of diapause II (Wourms 1972) was recently reconstructed by Furness et al. (Furness et al. 2015) who identified seven clades in which it had evolved. However, Diapause II does not directly equate to annualism but is required to complete an annual life cycle. The five cases I found where annualism evolved cannot be directly compared to instances of diapause II, though all five clades recovered were found in the Furness (Furness et al. 2015) paper. I suspected that annualism might have affected diversification through providing ecological opportunity by opening up new niches and geographic regions linked to the seasonal pond system. The chapter 5 analyses did not reveal

any significant differences in diversification rate among annual groups and non-annual oviparous groups. I suggested that this might be because of the unique life-history of annual killifish which is limited to one generation per year. Increased generation times can slow the rate of evolution and thus potentially speciation, and this phenomenon has been observed in other groups (W.-H. Li et al. 1996; J. A. Thomas et al. 2010).

The generic-level approach used in chapter 5 presented a number of challenges, the most obvious of which is dealing with the high level of incomplete sampling. It is not uncommon to attempt to calculate diversification rates from poorly-sampled or 'backbone' phylogenetic trees that consist of one representative from a single group of interest (M. G. Weber & Agrawal 2014; Estep et al. 2014). This introduces a large amount of error in the estimation of diversification rates but our ability to deal with this issue is improving (FitzJohn et al. 2009; Stadler & Bokma 2013). Associating a shift in diversification is difficult as there may be many alternative factors that are acting simultaneously with the trait believed to drive diversification. Multiple instances of association between rate shift and trait are required to reliably pinpoint a causal mechanism (Maddison & FitzJohn 2015). The association between increased diversification rates and viviparity is repeated in two independent instances and is further supported by temporal evidence; rate shifts occur during or soon after the evolution of viviparity. Aided by BAMM's (Rabosky, Donnellan, et al. 2014) ability to estimate rate changes along branches, I was able to provide a second angle of evidence that is not common in studies of this nature. I suggested that the observed association between viviparity and diversification might be due to increased colonisation success and subsequent geographic isolation. Single females from livebearing species do not require external fertilization of eggs from a conspecific male and thus could colonise a new area with the offspring they carry. Furthermore, superfetation, where mothers can carry multiple litters from different fathers

simultaneously (Pollux et al. 2009; Evans et al. 2011) could increase genetic variation within colonisers and thus reduce the chance of inbreeding depression. In chapter 5 I believe I present one of the strongest cases for a trait that stimulates diversification in viviparity and show how reproductive life history traits can shape diversity.

7.6 Selection and low light vision

Selection on visual pigments is known to common in various fish species including gobies (Ebert & Andrew 2009), guppies (Tezuka et al. 2014) and cichlids (Schott et al. 2014) and has been shown to be a driving force in the process of speciation (Seehausen et al. 2008). In chapter 6 I used the newly developed phylogenetic tree of Cyprinodontiformes (chapter 5) to look at patterns of selection on rhodopsin (*RH1*), a visual pigment critical for the mediation of low-light vision in vertebrates (Palczewski et al. 2000; Burns & Baylor 2001; Morrow & Chang 2015). A considerable amount is known about the function of rhodopsin but comparatively little about how selection acts upon the gene and the functional consequences of this selection, especially going beyond spectral absorbance (S. Yokoyama et al. 2008; Schott et al. 2014). Signatures of selection were found in rhodopsin across all major groups of Cyprinodontiformes and found at 12 amino acid sites across rhodopsin. These sites have previously been shown in zebrafish (Morrow & Chang 2015) and cichlids (Schott et al. 2014) to have functional effects on retinal release rate and *RH1* dimerisation. Sites affecting retinal release were conspicuously under selection in the Goodeidae in all cases, indicating that selection pressures for this trait may be the strongest within this group. Substitutions at sites known to affect peak spectral absorbance in taxa as wide ranging as bats, elephants and guinea pigs as well as fish (Sugawara et al. 2010; S. Yokoyama et al. 2005) were also found among Cyprinodontiform groups but these sites did not possess signatures of selection. It was

thought that peak absorbance (λ_{max}) was the only important function of rhodopsin that selection acted upon (S. Yokoyama et al. 2008) but chapter 6 and studies in cichlids (Schott et al. 2014; Torres-Dowdall et al. 2015) have found evidence for selection upon other functional aspects like retinal release rate and dimerisation. Future studies should take into account other traits beyond spectral absorbance, such as retinal release, if we wish to truly understand pigment evolution.

The vast amount of genetic data available for Cyprinodontiformes enabled this study but this work only examined patterns at the genus level. Traits could not be effectively linked to broad scale ecological differences among the genera sampled, indicating that the selection observed may be due to variation in rhodopsin within genera or unconsidered environmental or ecological variables. The order Cyprinodontiformes contains species from a huge variety of geographic regions, peculiar habitats and life histories (Parenti 1981) that experience different photic environments and thus I believe they would make an excellent model system for understanding how selection acts upon the visual system. This study is the first step towards using this order to understand broad scale patterns of selection rhodopsin.

7.7 Conservation and annual killifish

Annual killifish species are inherently vulnerable to climate change. During my collection trip to Uruguay we failed to find *A. elongatus,* one of the largest species of *Austrolebias*, despite finding smaller congenerics in a pond *A. elongatus* was known to inhabit. When I asked my guide, Heber Salvia, why we weren't finding any fish he replied that as it was late in the season (October), the water level was dropping and this made the fish easier targets for

predatory birds. He continued by saying that the largest species were the first to be eaten, as they could not hide as easily as the smaller species. Climate change could shorten the life of these ponds – higher temperatures may cause water to evaporate earlier in the year. This would put considerable pressure on annual killifish, especially the less common larger species. A number of species are already conservation concerns with some red-listed in certain areas (Volcan et al. 2011; Fonseca et al. 2012; Lanés et al. 2014). Furthermore, it has been shown in *A. wolterstorffi* that high temperatures have a detrimental effect on growth, which is critical to survival in the seasonal pond system (Fonseca et al. 2012).

By expanding our knowledge of killifish ecology we can hope to better focus our conservation efforts. The occurrence data and species distribution models used in this thesis can provide a better idea of where undiscovered populations of these endangered fish may be. Models may also be expanded upon to examine the effect of climate change on species ranges by using bioclimatic data from future climate projections. This would allow us to determine which species are in most need of conservation effort. Understanding the evolutionary relationships between species is also an important step towards better conservation. For example, *A. cinereus* is on the IUCN red list and known only from a single locality (Loureiro et al. 2007) but there is some indication to suggest that it is simply a subspecies of *A. vazferreirai*. Information on gene flow between these two species and better resolved evolutionary relationships will be able to direct conservation effort where it is needed.

7.8 The emergence of new two new model systems and future directions

The *Austrolebias* are an exciting study group that could potentially provide a significant contribution to our understanding of many fields of evolutionary research. Attempts to highlight the suitability of *Austrolebias* to the study of various aspects of biology have already been made (Berois et al. 2014). I hope that my thesis has shown how the biology of this genus is well suited for work on the evolution of diversity. However, I believe that going forward, the biggest challenge that must be conquered before *Austrolebias* can be used as a model system is accurately assessing how gene flow acts within this system to help inform species delimitation and classification. What is the level of inbreeding within a single isolated pond? How often to conspecifics from different ponds come into contact? If introgression and/or hybridisiation does occur, how often does it happen? Answering questions such as these would allow the revision of species classification in *Austrolebias* through a more thorough examination of morphological and genetic data. Estimates of gene flow and more accurate species classification would improve analyses of patterns of co-occurrence. The non-monophyly of some species and the hard incongurences between mitochondrial and nuclear DNA-based trees (chapter 2) demonstrates this major issue. There are potential solutions though - high-throughput sequencing can provide huge amounts of genetic data that can reliably reconstruct evolutionary relationships with very good support (see (Jones et al. 2013) or (DaCosta & Sorenson 2015) and accurately assess levels of gene flow among populations or species (Keller et al. 2012; Sousa & Hey 2013).

Chapters 2 and 3 use data from up to 26 recognised species of *Austrolebias* while the most recent estimates suggest there are more than 40 species described (García et al. 2014; Volcan et al. 2014). Inclusion of these species would improve analyses by adding more comparisons

and therefore more power. However, species not included in this study are mostly rare, often only occurring at a small number locations (Loureiro et al. 2011; Volcan et al. 2014) so more thorough sampling could be conducted to determine whether more locations exist. This thesis and previous studies have suggested that some recently diverged sister species pairs such as *A. vazferreirai* & *A. cinereus* and *A. apaii* & *A. bellottii* (García et al. 2012) should be classified as a single species. A review of species classification and delimitation is needed to fully understand interspecific interactions in *Austrolebias*.

The linkage maps produced in chapter 4 pave the way for further genomic analyses in *Austrolebias*. I have shown that interspecific hybridisation is possible in this genus, despite the frequency of chromosomal rearrangements ((García et al. 2001); chapter 4). Another natural step forward would be to cross large and small species to reveal those regions that are associated variation in size and shape across the genus. By using the latest phylogenetic tree of *Austrolebias* (chapter 2) one could select species closely related but divergent in the trait of interest. Quantitative trait locus (QTL) mapping could be used to assess the genomic regions that influence body size and growth, which has been done in a number of fish species including the Japanese flounder (Song et al. 2012) and *Takifugu* (Hosoya et al. 2013), and assess whether these regions are under selection. As I found convergent evolution towards large, streamlined bodies, one could use genomic approaches to determine whether the same regions have lead to this convergence, as in cichlids (Kautt et al. 2012) and sticklebacks (Hohenlohe et al. 2011). The linkage maps from chapter 4 could also be used to see how the large and variable genomes of *Austrolebias* (García et al. 2014) compare to more distantly related taxa or other *Austrolebias* species.

The order Cyprinodontiformes contains many model organisms (e.g. *Nothobranchius furzeri* (Genade et al. 2005) or *Xiphophorus maculatus* (Schartl et al. 2013) and numerous studies have been conducted on specific families or genera (Hrbek & Larson 1999; Ritchie et al. 2005; Pollux et al. 2015), with some newer studies examining patterns at a broader taxonomic scale (chapter 5,6; (Furness et al. 2015)). I believe Cyprinodontiformes are well suited to studying patterns of evolution at this higher level. A huge amount of genetic data is available; a simple genbank search for Cyprinodontiformes yields 673,173 results (http://www.ncbi.nlm.nih.gov/genbank/, accessed 21/09/2015). Databases that I have used in this thesis such as FishBase (Froese & Pauly 2015) or GBIF (http://www.gbif.org/) can provide accurate trait and environmental data alongside the primary literature. A major next step would be to fill in the current gaps in large skeleton trees ((Furness et al. 2015; Campanella et al. 2015); chapter 5) to improve the reliability of analyses of diversification by removing the challenges associated with using incomplete phylogenetic trees (FitzJohn et al. 2009; Stadler & Bokma 2013).

The five annual clades I have highlighted in chapter 5 could be the subject for the study of convergent evolution in annualism. With the development of an *Austrolebias* linkage map and a draft genome of the African annual *Nothobranchius furzeri* (Reichwald et al. 2009) and three additional annual groups to use for comparison, there is scope for investigating the genomic basis of annualism and whether the same genomic regions are found to be govern this remarkable life history adaptation. The use of groups where there is known variation in annualism (*Fundulopanchax*, chapter 5) may allow for crossing experiments and trait mapping to identify genomic regions associated with annualism. There is also evidence for convergent evolution of piscivory in the African annual genus *Nothobranchius* and *Austrolebias* (Costa 2011). The approach taken in this thesis could reveal whether the same

selective pressures have lead to piscivory in *Nothobranchius* and whether the increased size and streamlined shape that comes with this predatory niche develops in a similar way.

An unprecedented amount of selection on the rhodopsin gene was found across the Cyprinodontiformes. The next logical step forward would be to correlate positive selection with environmental or ecological variables to determine what drives selection on Cyprinodontiform rhodopsin. This will likely involve looking in depth at particular groups where a change in selection regime has taken place, for example in the Goodeidae, where all sites known to affect retinal release rate were under selection (chapter 6). Beyond this, assessing the effect of amino acid changes by measuring λ max and retinal release rate in expressed rhodopsin, as has been done in other studies (S. Yokoyama et al. 2008; Morrow & Chang 2015) will reveal the true functional significance of key substitutions identified in chapter 6.

7.9 Conclusion

Diversity can be observed everywhere in the natural world, but it is the task of evolutionary biologists to understand how it arises and the processes that shape it. My thesis has studied the evolution of diversity at different levels. I have used cutting edge, high-throughput sequencing techniques to build genetic maps of a hybrid cross of members of the annual killifish genus, *Austrolebias.* I have examined molecular evolution and its functional consequences in the visual pigment rhodopsin using the order Cyprinodontiformes. I have generated sequence data to construct phylogenetic trees of *Austrolebias* and used them to demonstrate that size is a major factor determining patterns of co-occurrence among

members of this genus. I have revealed how variation in size and shape has arisen across *Austrolebias* and found evidence for convergent evolution towards large, streamlined bodies. Finally, I have shown how a reproductive life history trait, viviparity, can shape patterns of species diversity by stimulating speciation in multiple groups of Cyprinodontiformes. All of these have added to our understanding of how diversity evolves in these groups, be it genetic diversity, trait diversity or species diversity. Specifically for *Austrolebias* and Cyprinodontiformes, I have provided significant steps forward for the study of evolution in these groups as well as new tools, such as location datasets, phylogenetic trees and linkage maps, to be used by others. I believe this thesis has shown how both *Austrolebias* and Cyprinodontiformes are excellent study groups that can be used to further our understanding of the evolution of diversity. However, with the ever-looming presence of climate change it may not be too long before some of this diversity disappears through the extinction of the more vulnerable species. I hope that the data I provide in this study can be used to inform conservation efforts in these groups. Further study using novel approaches will be able to reveal more about the evolution of diversity in *Austrolebias* and Cyprinodontiformes and add to our growing understanding of patterns and processes that generate diversity.

Bibliography

Abel, D.C., Koenig, C.C. & Davis, W.P., 1987. Emersion in the mangrove forest fish *Rivulus marmoratus*: a unique response to hydrogen sulfide. Environmental Biology of Fishes, 18(1), pp.67–72.

Adams, D.C., 2014. A method for assessing phylogenetic least squares models for shape and other high-dimensional multivariate data. Evolution, 68(9), pp.2675–2688.

Adkins-Regan, E. & Reeve, H.K., 2014. Sexual Dimorphism in Body Size and the Origin of Sex-Determination Systems. The American Naturalist, 183(4), pp.519–536.

Ala-Laurila, P. et al., 2006. Visual cycle: Dependence of retinol production and removal on photoproduct decay and cell morphology. The Journal of General Physiology, 128(2), pp.153–169.

Alfaro, M.E., Brock, C.D., et al., 2009. Does evolutionary innovation in pharyngeal jaws lead to rapid lineage diversification in labrid fishes? BMC Evolutionary Biology, 9(1), p.255.

Alfaro, M.E., Santini, F., et al., 2009. Nine exceptional radiations plus high turnover explain species diversity in jawed vertebrates. Proceedings of the National Academy of Sciences, 106(32), pp.13410–13414.

Altschul, S.F. et al., 1997. Gapped BLAST and PSI-BLAST: a new generation of protein database search programs. Nucleic Acids Research, 25(17), pp.3389–3402.

Amemiya, C.T. et al., 2013. The African coelacanth genome provides insights into tetrapod evolution. Nature, 496(7445), pp.311–316.

Amores, A. et al., 2011. Genome Evolution and Meiotic Maps by Massively Parallel DNA Sequencing: Spotted Gar, an Outgroup for the Teleost Genome Duplication. Genetics, 188(4), pp.799–808.

Anderson, J.L. et al., 2012. Multiple Sex-Associated Regions and a Putative Sex Chromosome in Zebrafish Revealed by RAD Mapping and Population Genomics PLoS ONE, 7(7), pp.e40701–14.

Arezo, M.J. et al., 2014. Sex determination in annual fishes: searching for the master sex-determining gene in *Austrolebias charrua* (Cyprinodontiformes, Rivulidae). Genetics and Molecular Biology, 37(2), pp.364–374.

Ballard, J.W.O. & Whitlock, M.C., 2004. The incomplete natural history of mitochondria. Molecular Ecology, 13(4), pp.729–744.

Barluenga, M. et al., 2006. Sympatric speciation in Nicaraguan crater lake cichlid fish. Nature, 439(7077), pp.719–723.

Barraclough, T.G. & Vogler, A.P., 2000. Detecting the Geographical Pattern of Speciation from Species- Level Phylogenies. The American Naturalist, 155(4), pp.419–434.

Barraclough, T.G., Vogler, A.P. & Harvey, P.H., 1998. Revealing the factors that promote

speciation. Philosophical Transactions of the Royal Society B: Biological Sciences, 353(1366), pp.241–249.

Bartoszek, K. et al., 2012. A phylogenetic comparative method for studying multivariate adaptation. Journal of Theoretical Biology, 314, pp.204–215.

Bates, D. et al., 2015. Fitting Linear Mixed-Effects Models using lme4. Available at: arXiv:1406.5823v1.

Beaulieu, J.M. & O'Meara, B.C., 2015. Detecting hidden diversification shifts in models of trait-dependent speciation and extinction. bioRxiv. doi: http://dx.doi.org/10.1101/016386

Beaulieu, J.M. et al., 2012. Modeling stabilizing selection: expanding the Ornstein-Uhlenbeck model of adaptive evolution. Evolution, 66(8), pp.2369–2383.

Berk, M., 2015. Smoothing-splines Mixed-effects Models in R. Available at: https://cran.r-project.org/web/packages/sme/sme.pdf.

Berois, N., Arezo, M.J. & de Sá, R.O., 2014. The Neotropical Genus Austrolebias: An Emerging Model of Annual Killifishes. Cell Dev Biol, 3(2).

Betancur-R, R. et al., 2013. The Tree of Life and a New Classification of Bony Fishes. PLoS Currents.

Bickelmann, C. et al., 2012. Functional characterization of the rod visual pigment of the echidna (Tachyglossus aculeatus), a basal mammal. Visual Neuroscience, 29(4-5), pp.211–217.

Blackburn, D.G., 2014. Evolution of vertebrate viviparity and specializations for fetal nutrition: A quantitative and qualitative analysis. Journal of Morphology, 276(8), pp.961–990.

Blackburn, D.G., 2015. Evolution of viviparity in squamate reptiles: Reversibility reconsidered. Journal of Experimental Zoology Part B: Molecular and Developmental Evolution, 324(6), pp.473–486.

Blanckenhorn, W., 2000. The evolution of body size: what keeps organisms small? Quarterly Review of Biology, 75(4), pp.385–407.

Blažek, R., Polacik, M. & Reichard, M., 2013. Rapid growth, early maturation and short generation time in African annual fishes. EvoDevo, 4(1), p.24.

Blomberg, S.P. et al., 2012. Independent Contrasts and PGLS Regression Estimators Are Equivalent. Systematic Biology, 61(3), pp.382–391.

Bolnick, D.I. & Fitzpatrick, B.M., 2007. Sympatric speciation: models and empirical evidence. Annual Review of Ecology, 38, pp.459–487.

Borodin, P.M. et al., 2008. Recombination map of the common shrew, Sorex araneus (Eulipotyphla, Mammalia). Genetics, 178(2), pp.621–632.

Bowers, M.A. & Brown, J.H., 1982. Body Size and Coexistence in Desert Rodents: Chance

or Community Structure? Ecology, 63(2), p.391.

Bowmaker, J.K., 2008. Evolution of vertebrate visual pigments. Vision Research, 48(20), pp.2022–2041.

Brawand, D. et al., 2015. The genomic substrate for adaptive radiation in African cichlid fish. Nature, 513(7518), pp.375–381.

Bretz, F., Hothorn, T. & Westfall, P., 2010. Multiple comparisons using R, CRC Press, Boca Raton.

Broman, K.W. et al., 2003. R/qtl: QTL mapping in experimental crosses. Bioinformatics, 19(7), pp.889–890.

Brown, W.L. & Wilson, E.O., 1956. Character displacement. Systematic zoology, 5(2), p.49.

Burns, M.E. & Baylor, D.A., 2001. Activation, deactivation, and adaptation in vertebrate photoreceptor cells. Annual review of neuroscience, 24, pp.779–805.

Butler, M.A. & King, A.A., 2004. Phylogenetic Comparative Analysis: A Modeling Approach for Adaptive Evolution. The American Naturalist, 164(6), pp.683–695.

Butlin, R., 1987. Speciation by reinforcement. Trends in Ecology & Evolution, 2(1), pp.8–13.

Campanella, D. et al., 2015. Multi-locus fossil-calibrated phylogeny of Atheriniformes (Teleostei, Ovalentaria). Molecular Phylogenetics and Evolution, 86, pp.8–23.

Canavero, A. et al., 2013. Patterns of co-occurrences in a killifish metacommunity are more related with body size than with species identity. Austral Ecology, 39(4), pp.455–461.

Catchen, J.M. et al., 2011. Stacks: Building and Genotyping Loci De Novo From Short-Read Sequences. G3 Genes|Genomes|Genetics, 1(3), pp.171–182.

Cellerino, A., Valenzano, D.R. & Reichard, M., 2015. From the bush to the bench: the annual *Nothobranchius* fishes as a new model system in biology. Biological Reviews.

Chambers, R.C. & Leggett, W.C., 1996. Maternal Influences on Variation in Egg Sizes in Temperate Marine Fishes. American Zoologist, 36(2), pp.180–196.

Chan, Y.F. et al., 2010. Adaptive Evolution of Pelvic Reduction in Sticklebacks by Recurrent Deletion of a Pitx1 Enhancer. Science, 327(5963), pp.302–305.

Charlesworth, D., Charlesworth, B. & Marais, G., 2005. Steps in the evolution of heteromorphic sex chromosomes. Heredity, 95(2), pp.118–128.

Chase, J.M. & Myers, J.A., 2011. Disentangling the importance of ecological niches from stochastic processes across scales. Philosophical Transactions of the Royal Society B: Biological Sciences, 366(1576), pp.2351–2363.

Chen, M.-H. et al., 2012. Rapid Release of Retinal from a Cone Visual Pigment following Photoactivation. Biochemistry, 51(20), pp.4117–4125.

Chibalina, M.V. & Filatov, D.A., 2011. Plant Y Chromosome Degeneration Is Retarded by Haploid Purifying Selection. Current Biology, 21(17), pp.1475–1479.

Colosimo, P.F. et al., 2004. The Genetic Architecture of Parallel Armor Plate Reduction in Threespine Sticklebacks. PLoS Biology, 2(5), p.e109.

Colosimo, P.F., Hosemann, K.E. & Balabhadra, S., 2005. Widespread parallel evolution in sticklebacks by repeated fixation of ectodysplasin alleles. Science, 307(5717), pp.1928–1933.

Connell, J., 1961. The influence of interspecific competition and other factors on the distribution of the barnacle *Chthamalus stellatus*. Ecology, 42(4), pp.710–723.

Corson, D.W. et al., 1990. Sensitization of bleached rod photoreceptors by 11-cis-locked analogues of retinal. Proceedings of the National Academy of Sciences, 87(17), pp.6823–6827.

Costa, W.J.E.M., 2014. *Austrolebias araucarianus*, a new seasonal killifish from the Iguacu river drainage, southern Brazilian Araucarian Plateau Forest (Cyprinodontiformes: Rivulidae). Ichthyological Exploration of Freshwaters, 25(2), pp.97–101.

Costa, W.J.E.M., 2013. Historical biogeography of aplocheiloid killifishes (Teleostei: Cyprinodontiformes). Vertebrate Zoology, 63(2), pp.139–154.

Costa, W.J.E.M., 2010. Historical biogeography of cynolebiasine annual killifishes inferred from dispersal-vicariance analysis. Journal of Biogeography, 37(10), pp.1995–2004.

Costa, W.J.E.M., 2011. Parallel evolution in ichthyophagous annual killifishes of South America and Africa. Cybium, 35(1), pp.49–46.

Costa, W.J.E.M., 1998. Phylogeny and classification of Rivulidae revisited: origin and evolution of annualism and miniaturization in rivulid fishes (Cyprinodontiformes: Aplocheiloidei). Journal of Comparative Biology, 3(1), pp.33–92.

Costa, W.J.E.M., 2006. The South American annual killifish genus *Austrolebias* (Teleostei: Cyprinodontiformes: Rivulidae): phylogenetic relationships, descriptive morphology and taxonomic revision, Zootaxa.

Costa, W.J.E.M., 2009. Trophic radiation in the South American annual killifish genus *Austrolebias* (Cyprinodontiformes: Rivulidae). Ichthyological Exploration of Freshwaters, 20(2), pp.179–191.

Costa, W.J.E.M., Reis, R.E. & Behr, E.R., 2004. *Austrolebias varzeae*, a new annual fish from the upper rio Uruguay basin, southern Brazil (Cyprinodontiformes: Rivulidae). Neotropical Ichthyology, 2(1), pp.13–17.

Coyne, J.A. & Orr, H.A., 2004. Speciation. Sinauer Associates.

DaCosta, J.M. & Sorenson, M.D., 2015. ddRAD-seq phylogenetics based on nucleotide, indel, and presence-absence polymorphisms: Analyses of two avian genera with contrasting histories. Molecular Phylogenetics and Evolution. In Press.

Darwin, C., 1859. The Origin of Species: By Means of Natural Selection, Or the Preservation of Favoured Races in the Struggle for Life. Cambridge University Press.

Davies, T.J. et al., 2007. Species co- existence and character divergence across carnivores. Ecology Letters, 10(2), pp.146–152.

Davis, M.P., Midford, P.E. & Maddison, W., 2013. Exploring power and parameter estimation of the BiSSE method for analyzing species diversification. BMC Evolutionary Biology, 13(1), p.38.

DeLano, W.L., 2002. The PyMOL Molecular Graphics System, DeLano Scientific, San Carlos, CA, USA, 2002,

Devlin, R.H. & Nagahama, Y., 2002. Sex determination and sex differentiation in fish: an overview of genetic, physiological, and environmental influences. Aquaculture, 208(3-4), pp.191–364.

Dobzhansky, T., 1937. Genetics and the Origin of Species, Columbia University Press.

Dorn, A. et al., 2011. Phylogeny, genetic variability and colour polymorphism of an emerging animal model: The short-lived annual Nothobranchius fishes from southern Mozambique. Molecular Phylogenetics and Evolution, 61(3), pp.739–749.

Drummond, A.J. & Rambaut, A., 2007. BEAST: Bayesian evolutionary analysis by sampling trees. BMC Evolutionary Biology, 7(1), p.214.

Drummond, A.J. et al., 2012. Bayesian phylogenetics with BEAUti and the BEAST 1.7. Molecular Biology and Evolution, 29(8), pp.1969–1973.

Drummond, C.S. et al., 2012. Multiple continental radiations and correlates of diversification in *Lupinus* (Leguminosae): testing for key innovation with incomplete taxon sampling. Systematic Biology, 61(3), pp.443–460.

Duarte, C.M. & Alcaraz, M., 1989. To produce many small or few large eggs: a size-independent reproductive tactic of fish. Oecologia, 80(3), pp.401–404.

Dunning, L.T. et al., 2013. Positive selection in glycolysis among Australasian stick insects. BMC Evolutionary Biology, 13(1), pp.1–1.

Eastman, J.M. et al., 2011. A novel comparative method for identifying shifts in the rate of character evolution of trees. Evolution, 65(12), pp.3578–3589.

Ebert, D. & Andrew, R.L., 2009. Rhodopsin population genetics and local adaptation: variable dim- light vision in sand gobies is illuminated. Molecular Ecology, 18, pp.4140–4142.

Eisler, R., 1971. Cadmium Poisoning in *Fundulus heteroclitus* (Pisces: Cyprinodontidae) and other Marine Organisms. Journal of the Fisheries Research Board of Canada, 28(9), pp.1225–1234.

Elith, J. et al., 2011. A statistical explanation of MaxEnt for ecologists. Diversity and Distributions, 17(1), pp.43–57.

Elith, J. et al., 2006. Novel methods improve prediction of species' distributions from occurrence data. Ecography, 29(2), pp.129–151.

Elliot, M.G. & Mooers, A.Ø., 2014. Inferring ancestral states without assuming neutrality or gradualism using a stable model of continuous character evolution. BMC Evolutionary Biology, 14(1), p.226.

Elmer, K.R. & Meyer, A., 2011. Adaptation in the age of ecological genomics: insights from parallelism and convergence. Trends in Ecology & Evolution, 26(6), pp.298–306.

Elmer, K.R. et al., 2010. Local variation and parallel evolution: morphological and genetic diversity across a species complex of neotropical crater lake cichlid fishes. Philosophical Transactions of the Royal Society B: Biological Sciences, 365(1547), pp.1763–1782.

Endler, J.A., 1984. Natural and sexual selection on color patterns in poeciliid fishes. In Evolutionary ecology of neotropical freshwater fishes. Developments in environmental biology of fishes. Dordrecht: Springer Netherlands, pp. 95–111.

Estep, M.C. et al., 2014. Allopolyploidy, diversification, and the Miocene grassland expansion. Proceedings of the National Academy of Sciences, 111(42), pp.15149–15154.

Evans, J.P., Pilastro, A. & Schlupp, I., 2011. Ecology and evolution of poeciliid fishes, The University of Chicago Press

Fan, S., Elmer, K.R. & Meyer, A., 2012. Genomics of adaptation and speciation in cichlid fishes: recent advances and analyses in African and Neotropical lineages. Philosophical Transactions of the Royal Society B: Biological Sciences, 367(1587), pp.385–394. Available at: http://rstb.royalsocietypublishing.org/cgi/doi/10.1098/rstb.2011.0247.

Fan, S., Elmer, K.R. & Meyer, A., 2011. Positive Darwinian Selection Drives the Evolution of the Morphology-Related Gene, EPCAM, in Particularly Species-Rich Lineages of African Cichlid Fishes. Journal of Molecular Evolution, 73(1-2), pp.1–9.

Faria, R. & Navarro, A., 2010. Chromosomal speciation revisited: rearranging theory with pieces of evidence. Proceedings of the Biological Society of Washington, 25(11), pp.660–669. Available at: http://linkinghub.elsevier.com/retrieve/pii/S0169534710001795.

Feder, J., Egan, S. & Nosil, P., 2012. The genomics of speciation-with-gene-flow. Trends in Genetics.

Felsenstein, J., 1985. Phylogenies and the comparative method. American Naturalist, 125(1), pp.1–15.

Felsenstein, J., 1981. Skepticism towards Santa Rosalia, or why are there so few kinds of animals? Evolution, 35(1), p.124.

Ferrer, J., Malabarba, L.R. & Costa, W.J.E.M., 2007. *Austrolebias paucisquama* (Cyprinodontiformes: Rivulidae), a new species of annual killifish from southern Brazil. Neotropical Ichthyology, 6(2), pp.175–180.

FitzJohn, R.G., 2012. Diversitree: comparative phylogenetic analyses of diversification in R.

Methods in Ecology and Evolution, 3(6), pp.1084–1092.

FitzJohn, R.G., 2010. Quantitative traits and diversification. Systematic Biology, 59(6), pp.619–633.

FitzJohn, R.G., Maddison, W.P. & Otto, S.P., 2009. Estimating Trait-Dependent Speciation and Extinction Rates from Incompletely Resolved Phylogenies. Systematic Biology, 58(6), pp.595–611.

Fitzpatrick, B.M. & Turelli, M., 2006. The geography of mammalian speciation: mixed signals from phylogenies and range maps. Evolution, 60(3), pp.601–16.

Fonseca, A.P.D. et al., 2012. Growth of Critically Endangered annual fish *Austrolebias wolterstorffi* (Cyprinodontiformes: Rivulidae) at different temperatures. Neotropical Ichthyology, 11(4), pp.837–844.

Fotiadis, D. et al., 2003. Atomic-force microscopy: rhodopsin dimers in native disc membranes. Nature, 421(6919), pp.127–128.

Fotiadis, D. et al., 2006. Structure of the rhodopsin dimer: a working model for G-protein-coupled receptors. Current Opinion in Structural Biology, 16(2), pp.252–259.

Fraley, C. et al., 2012. mclust Version 4 for R: normal mixture modeling for model-based clustering, classification. Density Estimation Technical Report, 597

Freckleton, R.P., Harvey, P.H. & Pagel, M., 2002. Phylogenetic Analysis and Comparative Data: A Test and Review of Evidence. The American Naturalist, 160(6), pp.712–726.

Froese, R. & Pauly, D. eds., 2015. FishBase. Available at: www.fishbase.org [Accessed September 21, 2015].

Fuller, R.C. & Claricoates, K.M., 2011. Rapid light-induced shifts in opsin expression: finding new opsins, discerning mechanisms of change, and implications for visual sensitivity. Molecular Ecology, 20(16), pp.3321–3335.

Furness, A.I. et al., 2015. Convergent evolution of alternative developmental trajectories associated with diapause in African and South American killifish. Proceedings of the Royal Society B: Biological Sciences, 282.

Futuyma, D. & Mayer, G., 1980. Non-allopatric speciation in animals. Systematic Biology. 29(3), pp.254-271.

Garamszegi, L.Z., 2014. Modern phylogenetic comparative methods and their application in evolutionary biology. Springer-Verlag Berlin Heidelberg.

Garcia, G., 2006. Multiple simultaneous speciation in killifishes of the *Cynolebias adloffi* species complex (Cyprinodontiformes, Rivulidae) from phylogeography and chromosome data. Journal of Zoological Systematics and Evolutionary Research, 44(1), pp.75–87.

García, G. et al., 1993. Analysis of Karyotypic Evolution in Natural Populations of *Cynolebias* (Pisces: Cyprinodontiformes, Rivulidae) Using Banding Techniques.

Cytologia, 58(1), pp.85–94.

García, G. et al., 2014. Burst speciation processes and genomic expansion in the neotropical annual killifish genus *Austrolebias* (Cyprinodontiformes, Rivulidae). Genetica, 142(1), pp.87–98.

García, G. et al., 2001. Chromosome evolution in the annual killifish genus Cynolebias and mitochondrial phylogenetic analysis. Chromosome Research, 9(6), pp.437–448.

García, G. et al., 2012. Patterns of population differentiation in annual killifishes from the Paraná-Uruguay-La Plata Basin: the role of vicariance and dispersal. Journal of Biogeography, 39(9), pp.1707–1719.

García, G., Scvortzoff, E. & Hernández, A., 1995. Karyotypic Heterogeneity in South American Annual Killifishes of the Genus Cynolebias (Pisces, Cyprinodontiformes Rivulidae). Cytologia, 60(2), pp.103–110.

Garland, T., Harvey, P.H. & Ives, A.R., 1992. Procedures for the Analysis of Comparative Data Using Phylogenetically Independent Contrasts. Systematic Biology, 41(1), pp.18–32.

Gatesy, J. & Springer, M.S., 2014. Phylogenetic analysis at deep timescales: Unreliable gene trees, bypassed hidden support, and the coalescence/concatalescence conundrum. Molecular Phylogenetics and Evolution, 80, pp.231–266.

Genade, T. et al., 2005. Annual fishes of the genus *Nothobranchius* as a model system for aging research. Aging Cell, 4(5), pp.223–233.

Goldberg, E.E., Lancaster, L.T. & Ree, R.H., 2011. Phylogenetic inference of reciprocal effects between geographic range evolution and diversification. Systematic Biology, 60(4), pp.451–465.

Grada, A. & Weinbrecht, K., 2013. Next-Generation Sequencing: Methodology and Application. Journal of Investigative Dermatology, 133(8), pp.e11–14.

Grafen, A., 1989. The phylogenetic regression. Philosophical Transactions of the Royal Society of London. Series B, Biological Sciences, 326, pp.119–157.

Grandcolas, P. et al., 2011. Mapping extrinsic traits such as extinction risks or modelled bioclimatic niches on phylogenies: does it make sense at all? Cladistics, 27(2), pp.181–185.

Grant, P.R., 1972. Convergent and divergent character displacement. Biological Journal of the Linnean Society, 4, pp.39–68.

Grant, P.R., 1999. Ecology and Evolution of Darwin's Finches, Princeton University Press.

Grant, P.R. & Grant, B.R., 2006. Evolution of Character Displacement in Darwin's Finches. Science, 313(5784), pp.224–226.

Gross, O.P. & Burns, M.E., 2010. Control of rhodopsin's active lifetime by arrestin-1 expression in mammalian rods. Journal of neuroscience, 30(9), pp.3450–3457.

Grün, B. & Leisch, F., 2008. FlexMix Version 2: Finite Mixtures with Concomitant Variables and Varying and Constant Parameters. Journal of Statistical Software, 28(1), pp.1–35.

Guindon, S., Rodrigo, A.G. & Dyer, K.A., 2004. Modeling the site-specific variation of selection patterns along lineages. Proceedings of the National Academy of Sciences, 101(35), pp.12957–12962.

Guo, W. et al., 2005. Crosstalk in G protein-coupled receptors: Changes at the transmembrane homodimer interface determine activation. Proceedings of the National Academy of Sciences, 102(48), pp.17495–17500.

Hansen, T.F., 1997. Stabilizing Selection and the Comparative Analysis of Adaptation. Evolution, 51(5), p.1341.

Hardenberg, A.V. & Gonzalez Voyer, A., 2013. Disentangling evolutionary cause-effect relationships with phylogenetic confirmatory path analysis. Evolution, 67(2), pp.378–387.

Hardin, G., 1960. The competitive exclusion principle. Science. 131(3409), pp.1292-1297.

Harmon, L.J., Losos, J.B. & Davies, T.J., 2010. Early bursts of body size and shape evolution are rare in comparative data. Evolution, 64(8), pp.2385–2396.

Harvey, P.H. & Pagel, M.D., 1991. The Comparative Method in Evolutionary Biology, Oxford University Press.

Heled, J. & Drummond, A.J., 2010. Bayesian Inference of Species Trees from Multilocus Data. Molecular Biology and Evolution, 27(3), pp.570–580.

Hinchliff, C.E. et al., 2015. Synthesis of phylogeny and taxonomy into a comprehensive tree of life. Proceedings of the National Academy of Sciences. In Press.

Hodges, S.A. & Arnold, M.L., 1995. Spurring plant diversification: are floral nectar spurs a key innovation? Proceedings of the Royal Society B: Biological Sciences, 262, pp.343–348.

Hohenlohe, P.A. et al., 2011. Extensive linkage disequilibrium and parallel adaptive divergence across threespine stickleback genomes. Philosophical Transactions of the Royal Society B: Biological Sciences, 367(1587), pp.395–408.

Hoskin, C. et al., 2005. Reinforcement drives rapid allopatric speciation. Nature, 437(7063), pp.1353–1356.

Hosoya, S. et al., 2013. The genetic architecture of growth rate in juvenile Takifugu species. Evolution, 67(2), pp.590–598.

Housworth, E.A., Martins, E.P. & Lynch, M., 2004. The Phylogenetic Mixed Model. The American Naturalist, 163(1), pp.84–96.

Howe, K. et al., 2013. The zebrafish reference genome sequence and its relationship to the human genome. Nature, 496(7446), pp.498–503.

Hrbek, T. & Larson, A., 1999. The evolution of diapause in the killifish family Rivulidae (Atherinomorpha, Cyprinodontiformes): a molecular phylogenetic and biogeographic perspective. Evolution, 53(4), p.1200.

Hubbell, S.P., 2001. The Unified Neutral Theory of Biodiversity and Biogeography, Princeton University Press.

Hugall, A.F. & Stuart-Fox, D., 2013. Accelerated speciation in colour-polymorphic birds. Nature, 485(7400), pp.631–634.

Hunt, D.M., Fitzgibbon, J. & Slobodyanyuk, S.J., 1996. Spectral tuning and molecular evolution of rod visual pigments in the species flock of cottoid fish in Lake Baikal. Vision Research, 36(9), pp.1217–1224.

Hunter, J.P., 1998. Key innovations and the ecology of macroevolution. Trends in Ecology & Evolution, 13(1), pp.31–36.

Hunter, J.P. & Jernvall, J., 1995. The hypocone as a key innovation in mammalian evolution. Bioinformatics, 96(23), pp.10718–10722.

Ingram, T. & Mahler, D.L., 2013. SURFACE: detecting convergent evolution from comparative data by fitting Ornstein- Uhlenbeck models with stepwise Akaike Information Criterion T. Hansen, ed. Methods in Ecology and Evolution, 4(5), pp.416–425.

Janz, J.M., Fay, J.F. & Farrens, D.L., 2003. Stability of dark state rhodopsin is mediated by a conserved ion pair in intradiscal loop E-2. Journal of Biological Chemistry, 278(19), pp.16982–16991.

Jetz, W. et al., 2012. The global diversity of birds in space and time. Nature, 491(7424), pp.444–448.

Johnston, S.E. et al., 2011. Genome-wide association mapping identifies the genetic basis of discrete and quantitative variation in sexual weaponry in a wild sheep population. Molecular Ecology, 20(12), pp.2555–2566.

Jones, J.C. et al., 2013. The evolutionary history of *Xiphophorus* fish and their sexually selected sword: a genome-wide approach using restriction site-associated DNA sequencing. Molecular Ecology, 22(11), pp.2986–3001.

Kai, W. et al., 2014. A ddRAD-based genetic map and its integration with the genome assembly of Japanese eel (*Anguilla japonica*) provides insights into genome evolution after the teleost-specific genome duplication. BMC Genomics, 15(1), p.233.

Kai, W. et al., 2011. Integration of the Genetic Map and Genome Assembly of *Fugu* Facilitates Insights into Distinct Features of Genome Evolution in Teleosts and Mammals. Genome Biology and Evolution, 3, pp.424–442.

Kamler, E., 2005. Parent–egg–progeny Relationships in Teleost Fishes: An Energetics Perspective. Reviews in Fish Biology and Fisheries, 15(4), pp.399–421.

Katoh, K. et al., 2002. MAFFT: a novel method for rapid multiple sequence alignment based

on fast Fourier transform. Nucleic Acids Research, 30(14), pp.3059–3066.

Kautt, A.F., Elmer, K.R. & Meyer, A., 2012. Genomic signatures of divergent selection and speciation patterns in a "natural experiment," the young parallel radiations of Nicaraguan crater lake cichlid fishes. Molecular Ecology, 21(19), pp.4770–4786.

Kearse, M. et al., 2012. Geneious Basic: an integrated and extendable desktop software platform for the organization and analysis of sequence data. Bioinformatics, 28(12), pp.1647–1649.

Keller, I. et al., 2012. Population genomic signatures of divergent adaptation, gene flow and hybrid speciation in the rapid radiation of Lake Victoria cichlid fishes. Molecular Ecology, 22(11), pp.2848–2863.

King, B. & Lee, M.S.Y., 2015. Ancestral State Reconstruction, Rate Heterogeneity, and the Evolution of Reptile Viviparity. Systematic Biology, 64(3), pp.532–544.

King, M., 1995. species evolution: the role of chromosome change. Cambridge University Press.

Kirkpatrick, M., 2006. Chromosome Inversions, Local Adaptation and Speciation. Genetics, 173(1), pp.419–434.

Kocher, T.D., 2004. Adaptive evolution and explosive speciation: the cichlid fish model. Nature Reviews Genetics, 5(4), pp.288–298.

Kondo, M. et al., 2001. Differences in recombination frequencies during female and male meioses of the sex chromosomes of the medaka, Oryzias latipes. Genetical research, 78(01), pp.23–30.

Lanés, L. & Maltchik, L., 2010. Discovery of the critically endangered annual killifish, *Austrolebias wolterstorffi* (Ahl, 1924) (Rivulidae: Cyprinodontiformes) in Lagoa do Peixe National Park, Rio Grande do Sul, southern Brazil. Journal of Threatened Taxa, 2(11), pp.1282–1285.

Lanés, L., Gonçalves, Â. & Volcan, M., 2014. Discovery of endangered annual killifish *Austrolebias cheradophilus* (Aplocheiloidei: Rivulidae) in Brazil, with comments on habitat, population structure and conservation status. Neotropical Ichthyology, 12(1), pp.117–124.

Lanfear, R. et al., 2012. Partitionfinder: combined selection of partitioning schemes and substitution models for phylogenetic analyses. Molecular Biology and Evolution, 29(6), pp.1695–1701.

Laufer, G. et al., 2009. Diet of four annual killifishes: an intra and interspecific comparison. Neotropical Ichthyology, 7(1), pp.77–86.

Lebrija-Trejos, E., Pérez-García, E.A. & Meave, J.A., 2010. Functional traits and environmental filtering drive community assembly in a species-rich tropical system. Ecology, 91(2), pp.386–398.

Lenormand, T. & Dutheil, J., 2005. Recombination Difference between Sexes: A Role for

Haploid Selection. PLoS Biology, 3(3), p.e63.

Leroi, A.M., Rose, M.R. & Lauder, G.V., 1994. What does the comparative method reveal about adaptation? American Naturalist, 143(3), pp.381–402.

Li, C. et al., 2007. A practical approach to phylogenomics: the phylogeny of ray-finned fish (Actinopterygii) as a case study. BMC Evolutionary Biology, 7(1), p.44.

Li, W.-H. et al., 1996. Rates of Nucleotide Substitution in Primates and Rodents and the Generation–Time Effect Hypothesis. Molecular Phylogenetics and Evolution, 5(1), pp.182–187.

Liu, L., Yu, L. & Pearl, D.K., 2009. Maximum tree: a consistent estimator of the species tree. Journal of Mathematical Biology, 60(1), pp.95–106.

Lohmann, G.P., 1983. Eigenshape analysis of microfossils: A general morphometric procedure for describing changes in shape. Mathematical Geology, 15(6), pp.659–672.

Losos, J., 1990a. Ecomorphology, performance capability, and scaling of West Indian Anolis lizards: an evolutionary analysis. Ecological Monographs, 60(3), pp.369–388.

Losos, J.B., 1990b. A phylogenetic analysis of character displacement in Caribbean Anolis lizards. Evolution, 44(3), p.558.

Losos, J.B., 2011. Convergence, adaptation and constraint. Evolution, 65(7), pp.1827–1840.

Losos, J.B., 2009. Lizards in an evolutionary tree: ecology and adaptive radiation of anoles,

Loureiro, M. et al., 2007. The IUCN Red List of Threatened Species. Austrolebias cinereus. 2015 ed.,

Loureiro, M., Duarte, A. & Zarucki, M., 2011. A new species of *Austrolebias* Costa (Cyprinodontiformes: Rivulidae) from northeastern Uruguay, with comments on distribution patterns. Neotropical Ichthyology, 9(2), pp.335–342.

Lowry, D.B. & Willis, J.H., 2010. A Widespread Chromosomal Inversion Polymorphism Contributes to a Major Life-History Transition, Local Adaptation, and Reproductive Isolation N. H. Barton, ed. PLoS Biology, 8(9), p.e1000500.

Lu, A. & Guindon, S., 2014. Performance of Standard and Stochastic Branch-Site Models for Detecting Positive Selection among Coding Sequences. Molecular Biology and Evolution, 31(2), pp.484–495.

MacArthur, R. & Levins, R., 1967. The limiting similarity, convergence, and divergence of coexisting species. American Naturalist, 101(921), pp.377–385.

MacLeod, N., 1999. Generalizing and extending the eigenshape method of shape space visualization and analysis. Paleobiology, 25(1), pp.107–138.

Maddison, W.P., 2006. Confounding Asymmetries in Evolutionary Diversification and Character Change. Evolution, 60(8), p.1743.

Maddison, W.P. & FitzJohn, R.G., 2015. The unsolved challenge to phylogenetic correlation tests for categorical characters. Systematic Biology, 64(1), pp.127–136.

Maddison, W.P., Midford, P.E. & Otto, S.P., 2007. Estimating a binary character's effect on speciation and extinction. Systematic Biology, 56(5), pp.701–710.

Mallet, J. et al., 2009. Space, sympatry and speciation. Journal of Evolutionary Biology, 22(11), pp.2332–2341.

Martin, C.H. et al., 2015. Complex histories of repeated gene flow in Cameroon crater lake cichlids cast doubt on one of the clearest examples of sympatric speciation. Evolution, 69(6), pp.1406–1422.

Martins, E P & Hansen, T.F., 1997. Phylogenies and the comparative method: a general approach to incorporating phylogenetic information into the analysis of interspecific data. American Naturalist, 194(4), pp.646–667.

Martins, Emília P, 2000. Adaptation and the comparative method. Trends in Ecology & Evolution, 15(7), pp.296–299.

Matsuda, M. et al., 2002. DMY is a Y-specific DM-domain gene required for male development in the medaka fish. Nature, 417(6888), pp.559–563.

May, R.M. & MacArthur, R.H., 1972. Niche overlap as a function of environmental variability. In Proceedings of the National Academy of Sciences. pp. 1109–1113.

Mayhew, P.J., 2002. Shifts in hexapod diversification and what Haldane could have said. Proceedings of the Royal Society B: Biological Sciences, 269(1494), pp.969–974.

Mayr, E., 1982. Speciation and Macroevolution. Evolution, 36(6), p.1119.

McGaugh, S.E. & Noor, M.A.F., 2012. Genomic impacts of chromosomal inversions in parapatric Drosophila species. Philosophical Transactions of the Royal Society B: Biological Sciences, 367(1587), pp.422–429.

McGuire, J.A. et al., 2014. Molecular Phylogenetics and the Diversification of Hummingbirds. Current Biology, 24(8), pp.910–916.

Meyer, A. & Lydeard, C., 1993. The evolution of copulatory organs, internal fertilization, placentae and viviparity in killifishes (Cyprinodontiformes) inferred from a DNA phylogeny of the tyrosine kinase gene X-src. Proceedings of the Royal Society B: Biological Sciences, 254(1340), pp.153–162.

Miller, P.J., 1978. Fish phenology. In Zoological Society London. Academic Press.

Mittelbach, G.G. & Schemske, D.W., 2015. Ecological and evolutionary perspectives on community assembly. Trends in Ecology & Evolution, 30(5), pp.241–247.

Moen, T. et al., 2004. A linkage map of Atlantic salmon (*Salmo salar*) reveals an uncommonly large difference in recombination rate between the sexes. Animal genetics, 35(2), pp.81–92.

Mooers, A.O. & Heard, S.B., 1997. Macroevolution and the shape of phylogenetic trees. Quarterly Review of Biology, 72, pp.31–54.

Morlon, H., 2014. Phylogenetic approaches for studying diversification. Ecology Letters, 17(4), pp.508–525.

Morrow, J.M. & Chang, B.S.W., 2015. Comparative Mutagenesis Studies of Retinal Release in Light-Activated Zebrafish Rhodopsin Using Fluorescence Spectroscopy. Biochemistry, 54(29), pp.4507–4518.

Moshgani, M. & Dooren, T.J., 2011. Maternal and paternal contributions to egg size and egg number variation in the blackfin pearl killifish Austrolebias nigripinnis. Evolutionary Ecology, 25(5), pp.1179–1195.

Mouillot, D., Dumay, O. & Tomasini, J.A., 2007. Limiting similarity, niche filtering and functional diversity in coastal lagoon fish communities. Estuarine, Coastal and Shelf Science, 71(3-4), pp.443–456.

Mousseau, T.A. & Roff, D.A., 1989. Adaptation to seasonality in a cricket: patterns of phenotypic and genotypic variation in body size and diapause expression along a cline in season length. Evolution, 43(7), p.1483.

Murphy, W.J. & Collier, G.E., 1997. A molecular phylogeny for aplocheiloid fishes (Atherinomorpha, Cyprinodontiformes): the role of vicariance and the origins of annualism. Molecular Biology and Evolution, 14(8), pp.790–799.

Muschick, M., Indermaur, A. & Salzburger, W., 2012. Convergent Evolution within an Adaptive Radiation of Cichlid Fishes. Current Biology, 22(24), pp.2362–2368.

Nagel, L. & Schluter, D., 1998. Body size, natural selection, and speciation in sticklebacks. Evolution, 52(1), pp.209–218.

Navarro, A. & Barton, N.H., 2003. Chromosomal Speciation and Molecular Divergence--Accelerated Evolution in Rearranged Chromosomes. Science, 300(5617), pp.321–324.

Noor, M.A. et al., 2001. Chromosomal inversions and the reproductive isolation of species. Proceedings of the National Academy of Sciences, 98(21), pp.12084–12088.

Nosil, P., 2012. Ecological Speciation, Oxford University Press.

O'Meara, B.C. et al., 2006. Testing for different rates of continuous trait evolution using likelihood. Evolution, 60(5), pp.922–933.

Okada, T. et al., 2002. Functional role of internal water molecules in rhodopsin revealed by x-ray crystallography. Proceedings of the National Academy of Sciences, 99(9), pp.5982–5987.

Orme, D., 2013. The caper package: comparative analysis of phylogenetics and evolution in R. R package version 5.2.

Ortíz-Barrientos, D. et al., 2002. Recombination and the divergence of hybridizing species. In Genetics of Mate Choice: From Sexual Selection to Sexual Isolation. Contemporary

Issues in Genetics and Evolution. Dordrecht: Springer Netherlands, pp. 167–178.

Osinaga, K., 2006. Nuevo registro para Bolivia de Austrolebias monstrosus (Huber, 1995 Rivulidae). Kempffiana.

Oviedo Alcoba, S., 2009. Posibles mecanismos genómicos de aislamiento postcigótico en especies del género *Austrolebias* (Cyprinodontiformes, Rivulidae). Universidad de la Republica Uruguay.

Owens, G.L. et al., 2012. In the four-eyed fish (*Anableps anableps*), the regions of the retina exposed to aquatic and aerial light do not express the same set of opsin genes. Biology Letters, 8(1), pp.86–89.

Pagel, M., 1997. Inferring evolutionary processes from phylogenies. Zoologica Scripta, 26(4), pp.331–348.

Pagel, M., 1999. Inferring the historical patterns of biological evolution. Nature, 401(6756), pp.877–884.

Pagel, M. & Meade, A., 2006. Bayesian Analysis of Correlated Evolution of Discrete Characters by Reversible- Jump Markov Chain Monte Carlo. The American Naturalist, 167(6), pp.808–825.

Palaiokostas, C., Bekaert, M. & Khan, M., 2015. A novel sex-determining QTL in Nile tilapia (Oreochromis niloticus). BMC Genomics, 16(1), p.171.

Palczewski, K. et al., 2000. Crystal Structure of Rhodopsin: A G Protein-Coupled Receptor. Science, 289(5480), pp.739–745.

Papadopulos, A.S. et al., 2011. Speciation with gene flow on Lord Howe Island. Proceedings of the National Academy of Sciences, 108(32), pp.13188–13193.

Paradis, E., 2014. An Introduction to the Phylogenetic Comparative Method. In Modern Phylogenetic Comparative Methods and Their Application in Evolutionary Biology. Springer Berlin Heidelberg, pp. 3–18.

Paradis, E., Claude, J. & Strimmer, K., 2004. APE: Analyses of Phylogenetics and Evolution in R language. Bioinformatics, 20(2), pp.289–290.

Parenti, L.R., 1981. A phylogenetic and biogeographic analysis of cyprinodontiform fishes (Teleostei, Atherinomorpha). Bulletin of the AMNH; v. 168, article 4.

Pearson, R.G. et al., 2006. Predicting species distributions from small numbers of occurrence records: a test case using cryptic geckos in Madagascar. Journal of Biogeography, 34(1), pp.102–117.

Peterson, B.K. et al., 2012. Double Digest RADseq: An Inexpensive Method for De Novo SNP Discovery and Genotyping in Model and Non-Model Species. PLoS ONE, 7(5), p.e37135.

Petzold, A. et al., 2013. The transcript catalogue of the short-lived fish *Nothobranchius* furzeri provides insights into age-dependent changes of mRNA levels. BMC Genomics,

14(1), p.185.

Pfennig, K.S. & Simovich, M.A., 2002. Differential selection to avoid hybridization in two toad species. Evolution, 56(9), pp.1840–1848.

Phillips, S.J. & Dudík, M., 2008. Modeling of species distributions with Maxent: new extensions and a comprehensive evaluation. Ecography, 31(1), pp.161–175.

Phillips, S.J., Anderson, R.P. & Schapire, R.E., 2006. Maximum entropy modeling of species geographic distributions. Ecological Modelling, 190(3-4), pp.231–259.

Piechnick, R., Ritter, E. & Hildebrand, P.W., 2012. Effect of channel mutations on the uptake and release of the retinal ligand in opsin. Proceedings of the National Academy of Sciences, 109(14), pp.5247–5252.

Pigot, A.L. & Tobias, J.A., 2012. Species interactions constrain geographic range expansion over evolutionary time. Ecology Letters, 16(3), pp.330–338.

Plummer, M. et al., 2006. CODA: convergence diagnosis and output analysis for MCMC. Available at: http://cran.r-project.org/web/packages/coda/coda.pdf.

Pollux, B.J.A. et al., 2009. Evolution of Placentas in the Fish Family Poeciliidae: An Empirical Study of Macroevolution. Annual Review of Ecology, Evolution, and Systematics, 40(1), pp.271–289.

Pollux, B.J.A. et al., 2015. The evolution of the placenta drives a shift in sexual selection in livebearing fish. Nature, 513(7517), pp.233–236.

Posada, D., 2008. jModelTest: phylogenetic model averaging. Molecular Biology and Evolution, 25(7), pp.1253–1256.

Price, T.D., 1984. Sexual selection on body size, territory and plumage variables in a population of Darwin's finches. Evolution, 38(2), pp.327–341.

Pugh, E.N. & Lamb, T.D., 1993. Amplification and kinetics of the activation steps in phototransduction. Biochimica et Biophysica Acta (BBA)-Bioenergetics, 1141(2-3), pp.111–149.

Pulvermüller, A. et al., 1997. Functional Differences in the Interaction of Arrestin and Its Splice Variant, p44, with Rhodopsin. Biochemistry, 36(30), pp.9253–9260.

Pyron, M., 1999. Relationships between geographical range size, body size, local abundance, and habitat breadth in North American suckers and sunfishes. Journal of Biogeography, 26(3), pp.549–558.

Pyron, R.A. & Burbrink, F.T., 2014. Early origin of viviparity and multiple reversions to oviparity in squamate reptiles. Ecology Letters, 17(1), pp.13–21.

Pyron, R.A., Burbrink, F.T. & Wiens, J.J., 2013. A phylogeny and revised classification of Squamata, including 4161 species of lizards and snakes. BMC Evolutionary Biology, 13(1), p.93.

Rabosky, D.L., 2014. Automatic Detection of Key Innovations, Rate Shifts, and Diversity-Dependence on Phylogenetic Trees. PLoS ONE, 9(2), p.e89543.

Rabosky, D.L., 2009. Extinction rates should not be estimated from molecular phylogenies. Evolution, 64(6), pp.1816–1824.

Rabosky, D.L. & Goldberg, E.E., 2015. Model inadequacy and mistaken inferences of trait-dependent speciation. Systematic Biology, 64(2), pp.340–355.

Rabosky, D.L. & Huang, H., 2015. A Robust Semi-Parametric Test for Detecting Trait-Dependent Diversification. Systematic Biology, p.syv066.

Rabosky, D.L. et al., 2013. Rates of speciation and morphological evolution are correlated across the largest vertebrate radiation. Nature Communications, 4, pp.1–8.

Rabosky, D.L., Donnellan, S.C., et al., 2014. Analysis and visualization of complex macroevolutionary dynamics: an example from Australian scincid lizards. Systematic Biology, 63(4), pp.610–627.

Rabosky, D.L., Grundler, M., et al., 2014. BAMMtools: an R package for the analysis of evolutionary dynamics on phylogenetic trees. Methods in Ecology and Evolution, 5(7), pp.701–707.

Raup, D.M. et al., 1973. Stochastic models of phylogeny and the evolution of diversity. The Journal of Geology, 81(5), pp.525–542.

Ree, R.H., 2005. Detecting the historical signature of key innovations using stochastic models of character evolution and cladogenesis. Evolution, 59(2), pp.257–265.

Ree, R.H. & Smith, S.A., 2008. Maximum likelihood inference of geographic range evolution by dispersal, local extinction, and cladogenesis. Systematic Biology, 57(1), pp.4–14.

Reichwald, K. et al., 2009. High tandem repeat content in the genome of the short-lived annual fish *Nothobranchius furzeri*: a new vertebrate model for aging research. Genome Biology, 10(2), p.R16. Available at: http://genomebiology.com/content/10/2/R16.

Revell, L.J., 2010. Phylogenetic signal and linear regression on species data. Methods in Ecology and Evolution, 1(4), pp.319–329.

Revell, L.J., 2012. phytools: an R package for phylogenetic comparative biology (and other things). Methods in Ecology and Evolution, 3(2), pp.217–223.

Revell, L.J., 2013. Two new graphical methods for mapping trait evolution on phylogenies. Methods in Ecology and Evolution, 4(8), pp.754–759.

Revell, L.J. et al., 2012. A new phylogenetic method for identifying exceptional phenotypic diversification. Evolution, 66(1), pp.135–146.

Reznick, D.A., Bryga, H. & Endler, J.A., 1990. Experimentally induced life-history evolution in a natural population. Nature, 346, pp.357–359.

Ricklefs, R.E., 2007. Estimating diversification rates from phylogenetic information. Trends in Ecology & Evolution, 22(11), pp.601–610.

Rieseberg, L.H., 2001. Chromosomal rearrangements and speciation. Proceedings of the Biological Society of Washington, 16(7), pp.351–358.

Rieseberg, L.H. et al., 2003. Major ecological transitions in wild sunflowers facilitated by hybridization. Science, 301(5637), pp.1211–1216.

Rieseberg, L.H., Archer, M.A. & Wayne, R.K., 1999. Transgressive segregation, adaptation and speciation. Heredity, 83(4), pp.363–372.

Rieseberg, L.H., Whitton, J. & Gardner, K., 1999. Hybrid Zones and the Genetic Architecture of a Barrier to Gene Flow Between Two Sunflower Species. Genetics, 152(2), pp.713–727.

Ritchie, M.G. et al., 2005. Patterns of speciation in endemic Mexican Goodeid fish: sexual conflict or early radiation? Journal of Evolutionary Biology, 18(4), pp.922–929.

Roch, S. & Warnow, T., 2015. On the Robustness to Gene Tree Estimation Error (or lack thereof) of Coalescent-Based Species Tree Methods. Systematic Biology, 64(4), pp.663–676.

Ronquist, F. & Huelsenbeck, J.P., 2003. MrBayes 3: Bayesian phylogenetic inference under mixed models. Bioinformatics, 19(12), pp.1572–1574.

Roughgarden, J., Heckel, D.G. & Fuentes, E.R., 1983. Coevolutionary theory and the biogeography and community structure of *Anolis*. In Lizard ecology : Studies of a model organism. Harvard Univ.Pr., pp. 371–410.

Römer, U. & Beisenherz, W., 1996. Environmental determination of sex in *Apistogrammai* (Cichlidae) and two other freshwater fishes (Teleostei). Journal of Fish Biology, 48(4), pp.714–725.

Rubinoff, D. & Holland, B., 2005. Between Two Extremes: Mitochondrial DNA is neither the Panacea nor the Nemesis of Phylogenetic and Taxonomic Inference. Systematic Biology, 54(6), pp.952–961.

Sakmar, T.P., Franke, R.R. & Khorana, H.G., 1989. Glutamic acid-113 serves as the retinylidene Schiff base counterion in bovine rhodopsin. Proceedings of the National Academy of Sciences, 86(21), pp.8309–8313.

Savolainen, V. et al., 2006. Sympatric speciation in palms on an oceanic island. Nature, 441(7090), pp.210–213.

Schartl, M. et al., 2013. The genome of the platyfish, *Xiphophorus maculatus*, provides insights into evolutionary adaptation and several complex traits. Nature Genetics, 45(5), pp.567–572.

Scheipl, F., Greven, S. & Küchenhoff, H., 2008. Size and power of tests for a zero random effect variance or polynomial regression in additive and linear mixed models. Computational Statistics & Data Analysis, 52(7), pp.3283–3299.

Schliewen, U.K. et al., 2006. Evolutionary Biology: Evidence for sympatric speciation? Nature, 444(7120), pp.E12–E13.

Schluter, D., 1993. Adaptive radiation in sticklebacks: size, shape, and habitat use efficiency. Ecology, 74(3), p.699.

Schluter, D., 2000. The Ecology of Adaptive Radiation, Oxford University Press.

Schluter, D. & McPhail, J.D., 1992. Ecological character displacement and speciation in sticklebacks. American Naturalist, 140(1), pp.85–108.

Schluter, D., Price, T.D. & Grant, P.R., 1985. Ecological Character Displacement in Darwin's Finches. Science, 227(4690), pp.1056–1059.

Schlüter, A., Parzefall, J. & Schlupp, I., 1998. Female preference for symmetrical vertical bars in male sailfin mollies. Animal Behaviour, 56(1), pp.147–153.

Schott, R.K. et al., 2014. Divergent Positive Selection in Rhodopsin from Lake and Riverine Cichlid Fishes. Molecular Biology and Evolution, 31(5), pp.1149–1165.

Schwede, T. et al., 2003. SWISS-MODEL: An automated protein homology-modeling server. Nucleic Acids Research, 31(13), pp.3381–3385.

Seehausen, O., 2004. Hybridization and adaptive radiation. Trends in Ecology & Evolution, 19(4), pp.198–207.

Seehausen, O. et al., 2008. Speciation through sensory drive in cichlid fish. Nature, 455(7213), pp.620–626.

Sexton, J.P. et al., 2009. Evolution and Ecology of Species Range Limits. Annual Review of Ecology, Evolution, and Systematics, 40(1), pp.415–436.

Shapiro, M. et al., 2004. Genetic and developmental basis of evolutionary pelvic reduction in threespine sticklebacks. Nature, 428(6984), pp.717–723.

Shaw, K.L., 2002. Conflict between nuclear and mitochondrial DNA phylogenies of a recent species radiation: What mtDNA reveals and conceals about modes of speciation in Hawaiian crickets. Proceedings of the National Academy of Sciences, 99(25), pp.16122–16127.

Singer, A. et al., 2002. Sex-specific recombination rates in zebrafish (*Danio rerio*). Genetics, 160(2), pp.649–657.

Sivak, J.G., 1976. Optics of the eye of the “four-eyed fish” (*Anableps anableps*). Vision Research, 16(5), pp.531–534.

Song, W. et al., 2012. Construction of High-Density Genetic Linkage Maps and Mapping of Growth-Related Quantitative Trail Loci in the Japanese Flounder (*Paralichthys olivaceus*) PLoS ONE, 7(11), pp.e50404–9.

Sousa, V. & Hey, J., 2013. Understanding the origin of species with genome-scale data: modelling gene flow. Nature Reviews Genetics, 14(6), pp.404–414.

Spady, T.C. et al., 2005. Adaptive molecular evolution in the opsin genes of rapidly speciating cichlid species. Molecular Biology and Evolution, 22(6), pp.1412–1422.

Stadler, T., 2011. Mammalian phylogeny reveals recent diversification rate shifts. Journal of Evolutionary Biology, 108(15), pp.6187–6192.

Stadler, T. & Bokma, F., 2013. Estimating speciation and extinction rates for phylogenies of higher taxa. Systematic Biology, 62(2), pp.220–230.

Stamatakis, A., 2006. RAxML-VI-HPC: maximum likelihood-based phylogenetic analyses with thousands of taxa and mixed models. Bioinformatics, 22(21), pp.2688–2690.

Stapley, J. et al., 2010. Adaptation genomics: the next generation. Proceedings of the Biological Society of Washington, 25(12), pp.705–712.

Stuart, Y.E. & Losos, J.B., 2013. Ecological character displacement: glass half full or half empty? Trends in Ecology & Evolution, 28(7), pp.402–408.

Stuessy, T.F., 2006. Evolutionary biology: Sympatric plant speciation in islands? Nature, 443(7114), pp.E12–E12.

Sugawara, T. et al., 2010. Vertebrate Rhodopsin Adaptation to Dim Light via Rapid Meta-II Intermediate Formation. Molecular Biology and Evolution, 27(3), pp.506–519.

Sugawara, T., Terai, Y. & Imai, H., 2005. Parallelism of amino acid changes at the RH1 affecting spectral sensitivity among deep-water cichlids from Lakes Tanganyika and Malawi. Proceedings of the National Academy of Sciences, 102(15), pp.5448–5453.

Sugawara, T., Terai, Y. & Okada, N., 2002. Natural selection of the rhodopsin gene during the adaptive radiation of East African Great Lakes cichlid fishes. Molecular Biology and Evolution, 19(10), pp.1807–1811.

Taylor, D.S. et al., 2008. A Novel Terrestrial Fish Habitat inside Emergent Logs. The American Naturalist, 171(2), pp.263–266.

Tezuka, A. et al., 2014. Divergent selection for opsin gene variation in guppy (Poecilia reticulata) populations of Trinidad and Tobago. Heredity, 113, pp.381–389.

The Marie Curie SPECIATION Network, 2012. What do we need to know about speciation? Proceedings of the Biological Society of Washington, 27(1), pp.27–39.

Thibault, R.E. & Schultz, R.J., 1978. Reproductive adaptations among viviparous fishes (Cyprinodontiformes: Poeciliidae). Evolution, 32(2), pp.320–333.

Thomas, G.H. & Freckleton, R.P., 2011. MOTMOT: models of trait macroevolution on trees. Methods in Ecology and Evolution, 3(1), pp.145–151.

Thomas, J.A. et al., 2010. A Generation Time Effect on the Rate of Molecular Evolution in Invertebrates. Molecular Biology and Evolution, 27(5), pp.1173–1180.

Torres-Dowdall, J., Henning, F. & Elmer, K.R., 2015. Ecological and lineage specific factors drive the molecular evolution of rhodopsin in cichlid fishes. Molecular Biology and

Evolution. In press.

Tregenza, T. & Butlin, R.K., 1999. Speciation without isolation. Nature, 400(6742), pp.311–312.

Tripathi, N. et al., 2009. Genetic linkage map of the guppy, *Poecilia reticulata*, and quantitative trait loci analysis of male size and colour variation. Proceedings of the Royal Society B: Biological Sciences, 276(1665), pp.2195–2208.

Untergasser, A. et al., 2012. Primer3--new capabilities and interfaces. Nucleic Acids Research, 40(15), p.e115.

Valenzano, D.R. et al., 2009. Mapping loci associated with tail color and sex determination in the short-lived fish Nothobranchius furzeri. Genetics, 183(4), pp.1385–1395.

Vamosi, S.M. & Vamosi, J.C., 2005. Endless tests: guidelines for analysing non-nested sister-group comparisons. Evolutionary Ecology Research, 7(4), pp.567–579.

Van Dooren, T.J.M. et al., Speciation by cannibalism in *Austrolebias* South American annual killifish. Evolution. In review.

Van Ooijen, J.W., 2006. JoinMap 4, Kyazma B.V.

Van't Hof, A.E. et al., 2012. Linkage map of the peppered moth, *Biston betularia* (Lepidoptera, Geometridae): a model of industrial melanism. 110(3), pp.283–295.

Venditti, C., Meade, A. & Pagel, M., 2011. Multiple routes to mammalian diversity. Nature, 479(7373), pp.393–396.

Via, S., 2001. Sympatric speciation in animals: the ugly duckling grows up. Proceedings of the Biological Society of Washington, 16(7), pp.381–390.

Volcan, M., Gonçalves, Â. & Lanés, L., 2011. Distribution, habitat and conservation status of two threatened annual fishes (Rivulidae) from southern Brazil. Endangered Species Research, 13(1), pp.79–85.

Volcan, M.V., Lanés, L. & Gonçalves, Â.C., 2014. *Austrolebias bagual*, a new species of annual fish (Cyprinodontiformes: Rivulidae) from southern Brazil. aqua, 20, pp.4–15.

Volcan, M.V., Lanés, L. & Gonçalves, Â.C., 2010. Pisces, Cyprinodontiformes, Rivulidae, Austrolebias periodicus (Costa, 1999): Distribution extension in state of Rio Grande do Sul, southern Brazil. CheckList.

Walter, R.B. et al., 2004. A microsatellite genetic linkage map for Xiphophorus. Genetics, 168(1), pp.363–372.

Wang, T. & Duan, Y., 2010. Retinal release from opsin in molecular dynamics simulations. Journal of Molecular Recognition, 24(2), pp.350–358.

Warren, D.L. et al., 2014. Mistaking geography for biology: inferring processes from species distributions. Trends in Ecology & Evolution, 29(10), pp.572–580.

Warton, D.I. & Hui, F.K.C., 2011. The arcsine is asinine: the analysis of proportions in ecology. Ecology, 92(1), pp.3–10.

Webb, C.O. et al., 2002. Phylogenies and community ecology. Annual Review of Ecology and Systematics, 33(1), pp.475–505.

Webb, S.A. et al., 2004. Molecular phylogeny of the livebearing Goodeidae (Cyprinodontiformes). Molecular Phylogenetics and Evolution, 30(3), pp.527–544.

Weber, J.N., Peterson, B.K. & Hoekstra, H.E., 2014. Discrete genetic modules are responsible for complex burrow evolution in *Peromyscus* mice. Nature, 493(7432), pp.402–405.

Weber, M.G. & Agrawal, A.A., 2014. Defense mutualisms enhance plant diversification. Proceedings of the National Academy of Sciences, 11(46), pp.16442–16447.

Weitzman, S.H. & Vari, R.P., 1988. Miniaturization in South American freshwater fishes; an overview and discussion. Proceedings of the Biological Society of Washington, 101(2), pp.444–465.

Wiens, J.J., 2011. The niche, biogeography and species interactions. Philosophical Transactions of the Royal Society B: Biological Sciences, 366(1576), pp.2336–2350.

Wilson, M.A. & Makova, K.D., 2009. Evolution and Survival on Eutherian Sex Chromosomes T. Gojobori, ed. PLoS Genetics, 5(7), p.e1000568.

Woodward, G. & Hildrew, A.G., 2002. Body- size determinants of niche overlap and intraguild predation within a complex food web. Journal of Animal Ecology, 71(6), pp.1063–1074.

Wourms, J.P., 1972. The developmental biology of annual fishes. III. Pre- embryonic and embryonic diapause of variable duration in the eggs of annual fishes. Journal of Experimental Zoology, 182(3), pp.389–414.

Wourms, J.P., 1981. Viviparity: The Maternal-Fetal Relationship in Fishes. American Zoologist, 21(2), pp.473–515.

Wourms, J.P. & Lombardi, J., 1992. Reflections on the evolution of piscine viviparity. American Zoologist, 32, pp.276–293.

Wright, A.M. et al., 2015. Which came first: The lizard or the egg? Robustness in phylogenetic reconstruction of ancestral states. Journal of Experimental Zoology Part B: Molecular and Developmental Evolution, 324(6), pp.504–516.

Wu, S. et al., 2013. Reply to Gatesy and Springer: the multispecies coalescent model can effectively handle recombination and gene tree heterogeneity. Proceedings of the National Academy of Sciences, 110(13), pp.E1180–E1180.

Yang, Z., 2007. PAML 4: phylogenetic analysis by maximum likelihood. Molecular Biology and Evolution, 24(8), pp.1586–1591.

Yang, Z., 2005. The power of phylogenetic comparison in revealing protein function.

Proceedings of the National Academy of Sciences, 102(9), pp.3179–3180.

Yang, Z., Wong, W.S.W. & Nielsen, R., 2005. Bayes empirical bayes inference of amino acid sites under positive selection. Molecular Biology and Evolution, 22(4), pp.1107–1118.

Yoder, J.B., Clancey, E. & Roches, des, S., 2010. Ecological opportunity and the origin of adaptive radiations. Journal of Evolutionary Biology, 23, pp.1581–1596.

Yokoyama, S. & Yokoyama, R., 1996. Adaptive evolution of photoreceptors and visual pigments in vertebrates. Annual Review of Ecology and Systematics, 27, pp.543–567.

Yokoyama, S. et al., 2005. Elephants and human color-blind deuteranopes have identical sets of visual pigments. Genetics, 170(1), pp.335–344.

Yokoyama, S. et al., 2008. Elucidation of phenotypic adaptations: Molecular analyses of dim-light vision proteins in vertebrates. Proceedings of the National Academy of Sciences, 105(36), pp.13480–13485.

Yu, Y. et al., 2015. RASP (Reconstruct Ancestral State in Phylogenies): A tool for historical biogeography. Molecular Phylogenetics and Evolution, 87, pp.46–49.

Zahn, C. & Roskies, R., 1972. Fourier descriptors for plane closed curves. IEEE Transactions on Computers, c-21(3), pp.269-281.

Zaret, T.M. & Rand, A.S., 1971. Competition in tropical stream fishes: support for the competitive exclusion principle. Ecology, 52(2), pp.336–342.

Zeh, D.W. & Zeh, J.A., 2000. Reproductive mode and speciation: the viviparity-driven conflict hypothesis. Bioessays, 22(10), pp.938–946.

Appendix I Supplementary material for chapter 2

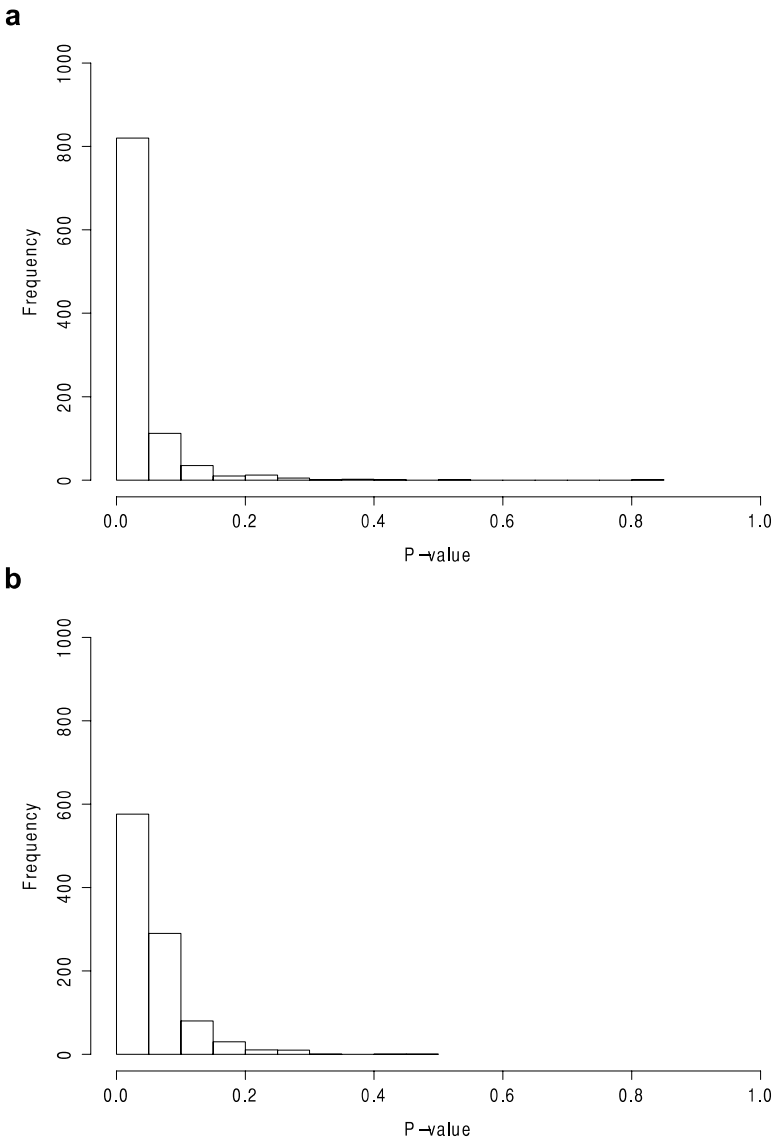

Figure S2.1 Histogram of P-values from 1000 trees randomly sampled for the posterior distribution the nDNA BEAST run. Histogram (a) is size x range overlap, (b) is node age x range overlap.

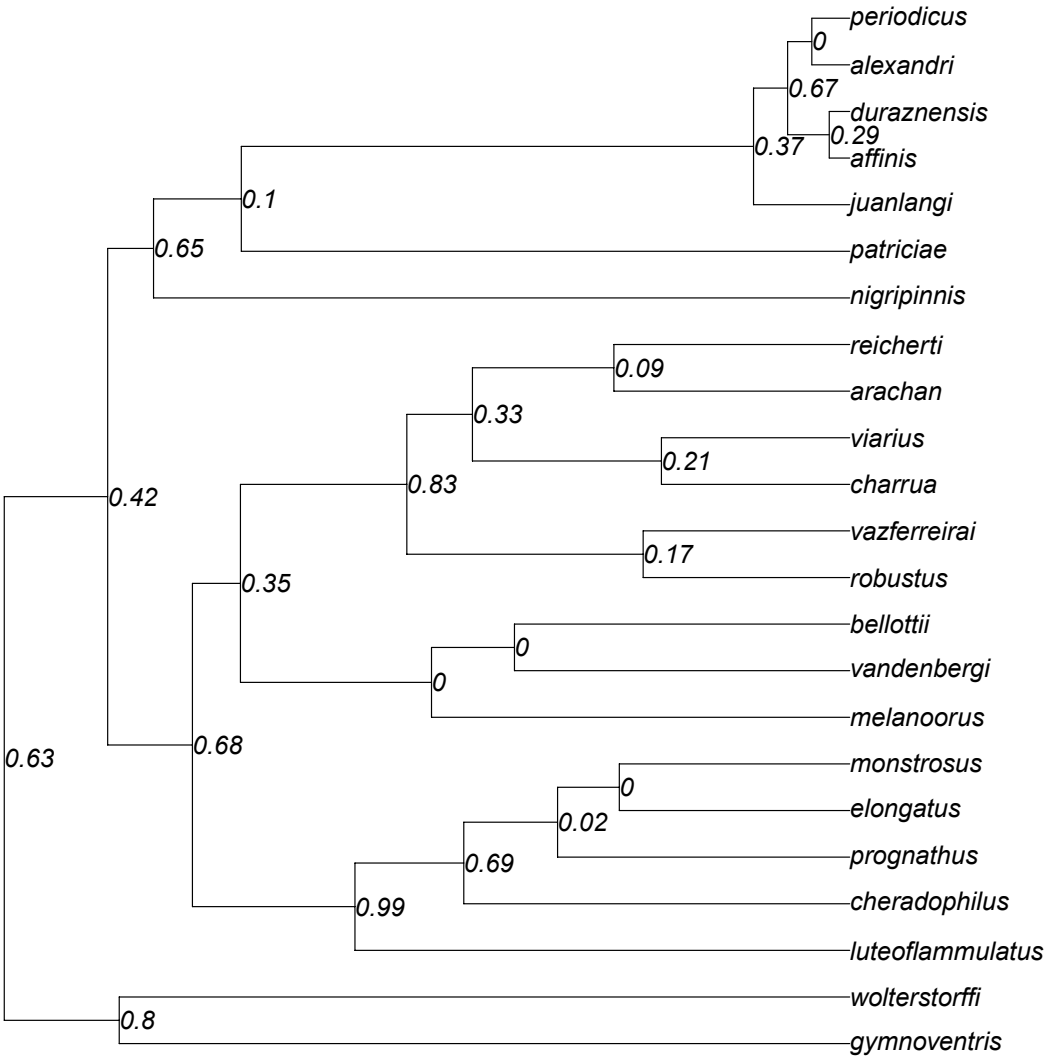

Figure S2.2 GLASS species tree with values of range overlap (untransformed) on each node.

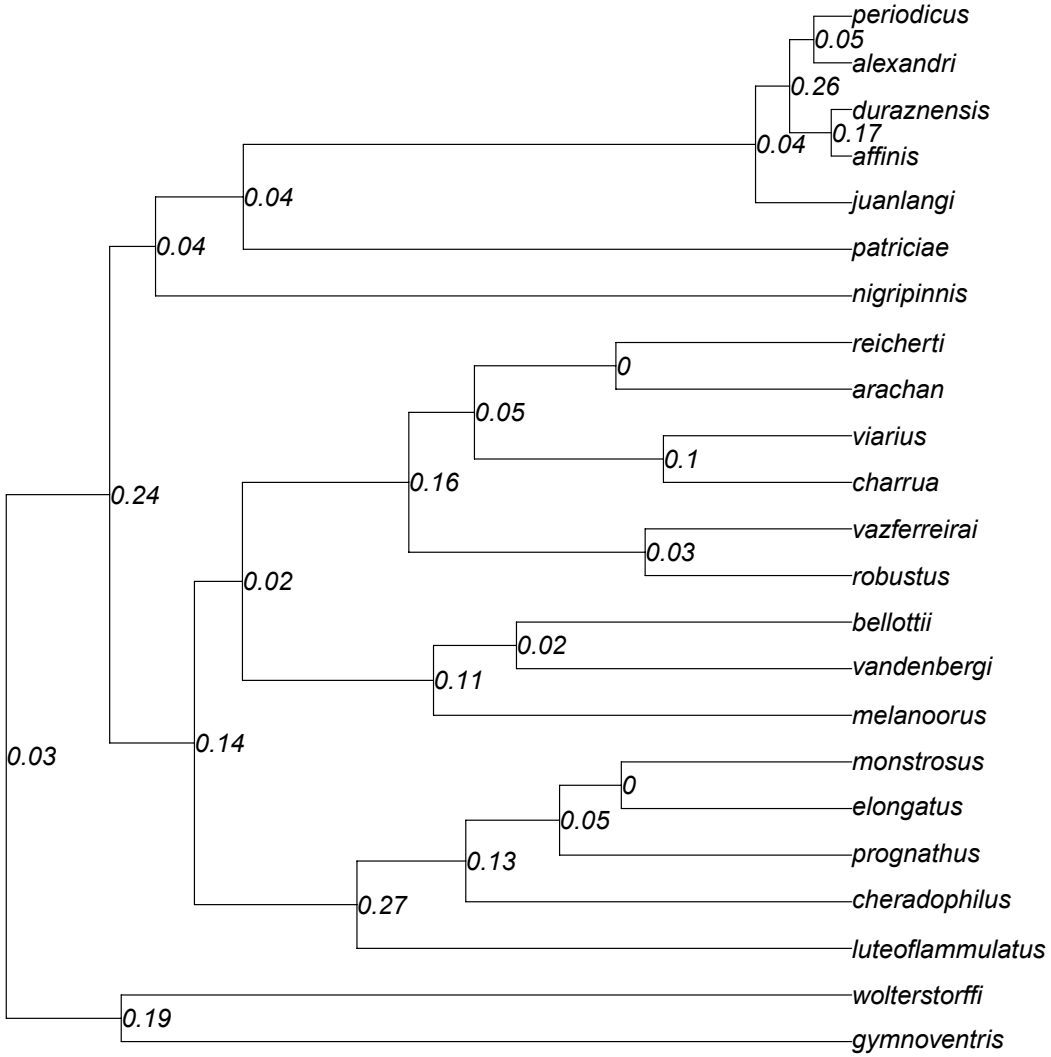

Figure S2.3 GLASS phylogenetic tree with values of log body size (SL) contrasts on each node.

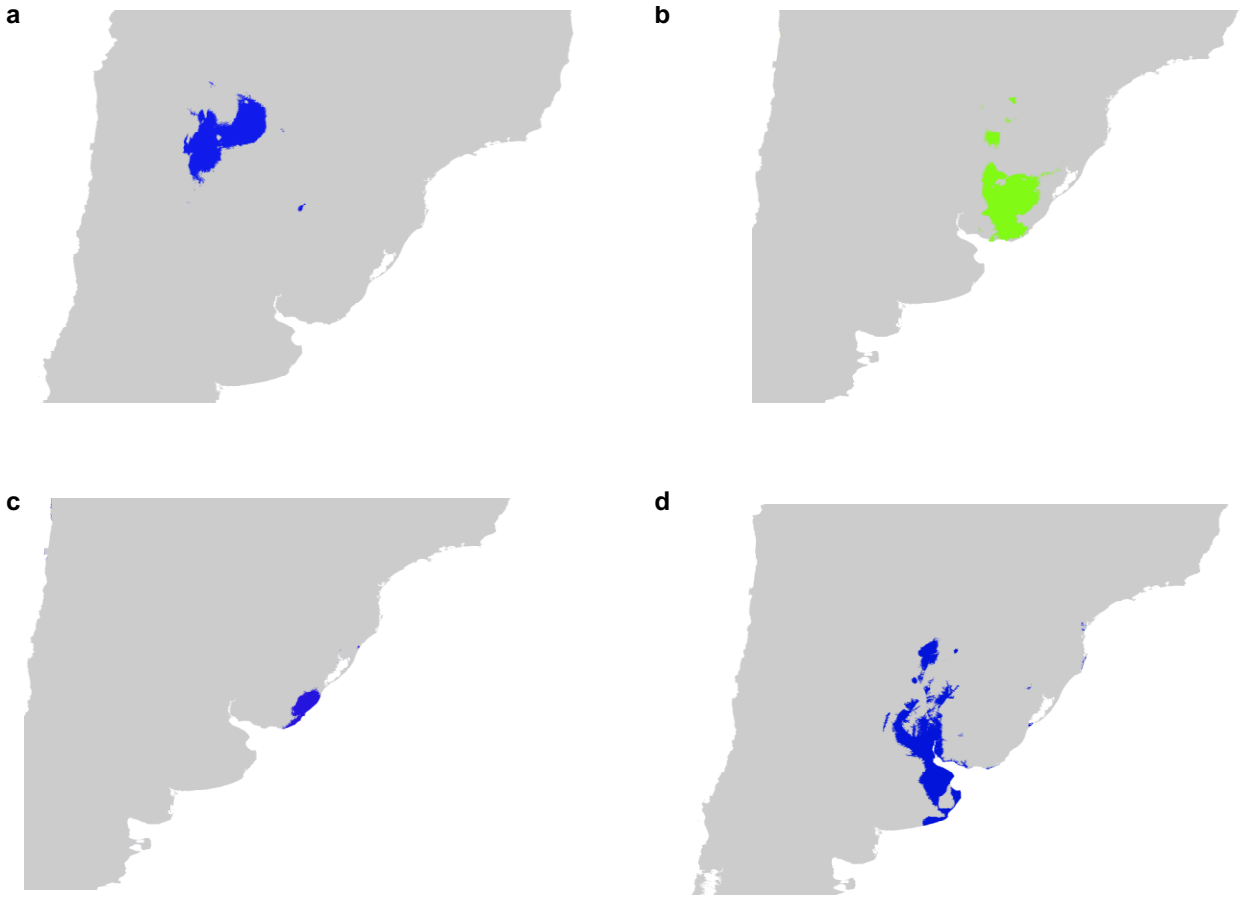

Figure S2.4 Examples of binary maps from MaxEnt for (a) *Austrolebias vandenbergi*, (b) *A. melanoorus*, (c) *A. cheradophilus* and (d) *A. bellottii*.

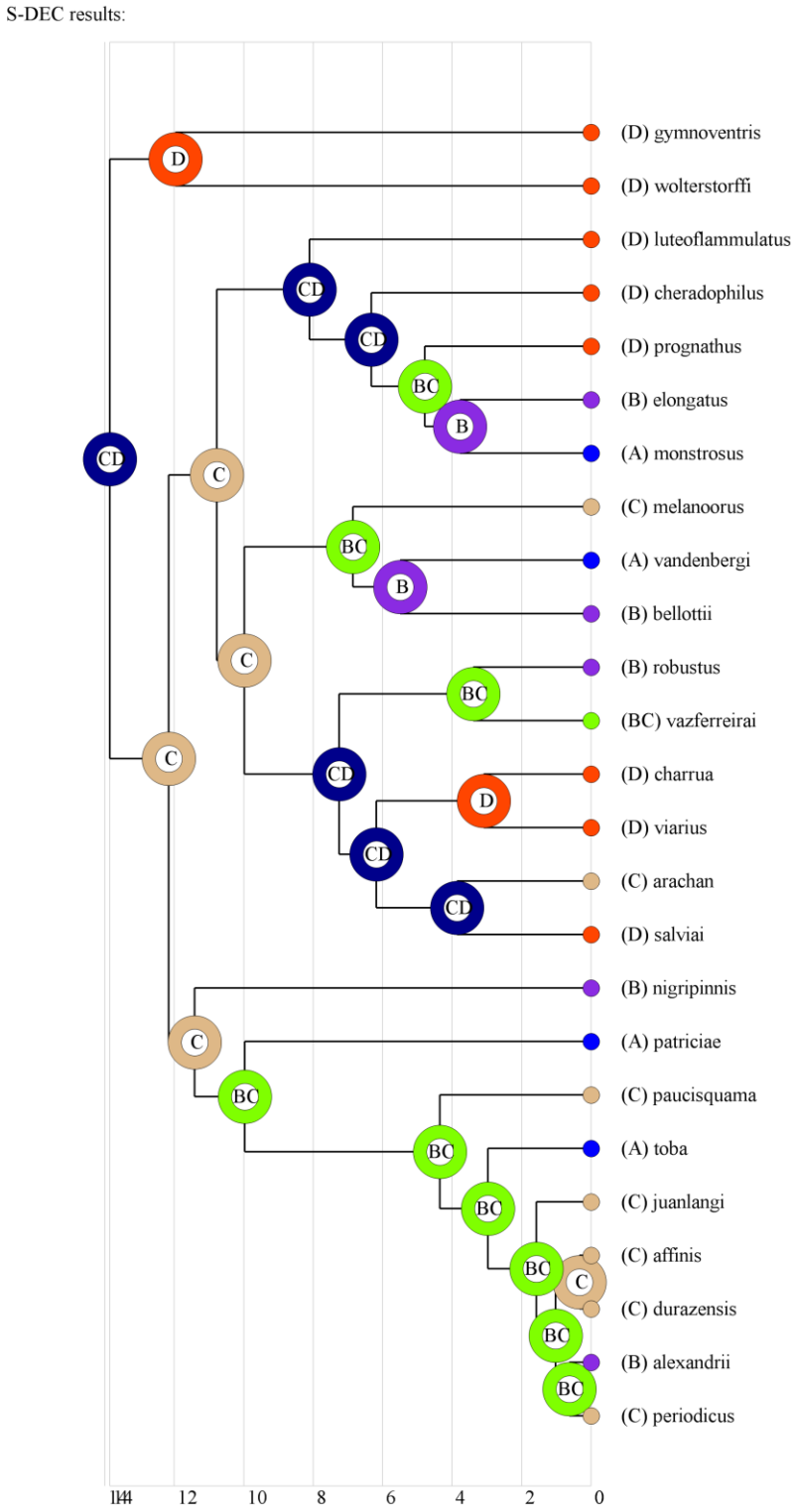

Figure S2.5 Results from the S-DEC analysis. Labels on nodes correspond to the most likely states. A = Western Paraguay, B = La Plata, C = Rio Negro and D = Patos Lagoon.

Table S2.1 Sequencing primers.

Gene	Direction	Sequence (5' - 3')
ENC1	F	GACATGCTGGAGTTTCAGGA
ENC1	R	ACTTGTTRGCMACTGGGTCAAA
RAG1	F	AGCTTCTCCCTGGCTTTCAC
RAG1	R	GAACGGGTTGGTTCTCCAGA
28S c1c2	F	ACCCGCTGAATTTAAGCAT
28S c1c2	R	TGAACTCTCTCTTCAAAGTTCTTTTC
28S c6c7	F	TCACCTGCCGAATCAACTAGC
28S c6c7	R	ACTACCACCAAGATCTGCAC
28S c12d12	F	TTATGACTGAACGCCTCTAAG
28S c12d12	R	TGACTTTCAATAGATCGCAG
RH1	F	TGTCAACCCAGCAGCCTATG
RH1	R	TGGTCTCAGACTCCTGCTGA
SH3PX3	F	TGCTCCATTGAAGACCCCAC
SH3PX3	R	TGTCGTCCATCTTCTTGGCA
16S	SARL	CGCCTGTTTATCAAAAACAT
16S	SBRH	CCGGTCTGAACTCAGATCACGT
12S	F	AAAAAGCTTCAAACTGGGATTAGATACCCCACTAT
12S	R	TGACTGCAGAGGGTGACGGGCGGTGTGT
cytB	F	GGCAAATAGGAARTATCATTC
cytB	R	TGACTTGAARAACCAYCGTTG

Table S2.2 Sequence sources. All ENC1, SH3PX3, RAG1 and RH1 sequences were sequenced for chapter 2.

Tip Name	Gene	Source
alexandrii_sanjavier	12S	Van Dooren et al. In review
arachan_parquerivera2	12S	Van Dooren et al. In review
bellottii_sol	12S	Van Dooren et al. In review
charrua_ca	12S	Van Dooren et al. In review
charrua_ca2	12S	Van Dooren et al. In review
cheradophilus_castillos	12S	Van Dooren et al. In review
cheradophilus_castillos2	12S	Van Dooren et al. In review
cheradophilus_lp	12S	Van Dooren et al. In review
cinereus_1	12S	Van Dooren et al. In review
cinereus_arroyoviboras	12S	Van Dooren et al. In review
elongatus_villasoriano	12S	Van Dooren et al. In review
gymnoventris_salamanca4	12S	Van Dooren et al. In review
gymnoventris_velasquez	12S	Van Dooren et al. In review
luteoflammulatus_1	12S	Van Dooren et al. In review
nigripinnis_ceibas	12S	Van Dooren et al. In review
periodicus_1	12S	Van Dooren et al. In review
prognathus_salamanca	12S	Van Dooren et al. In review
pterolebias_longipinnis	12S	Van Dooren et al. In review
robustus_1	12S	Van Dooren et al. In review
s_magnificus	12S	Van Dooren et al. In review
alexandrii_sanjavier	16S	Van Dooren et al. In review
arachan_parquerivera2	16S	Van Dooren et al. In review
bellottii_sol	16S	Van Dooren et al. In review
charrua_ca2	16S	Van Dooren et al. In review
cheradophilus_castillos	16S	Van Dooren et al. In review
cheradophilus_castillos2	16S	Van Dooren et al. In review
cheradophilus_lp	16S	Van Dooren et al. In review
cinereus_1	16S	Van Dooren et al. In review
cinereus_arroyoviboras	16S	Van Dooren et al. In review
gymnoventris_salamanca4	16S	Van Dooren et al. In review
gymnoventris_velasquez	16S	Van Dooren et al. In review
luteoflammulatus_1	16S	Van Dooren et al. In review
nigripinnis_ceibas	16S	Van Dooren et al. In review
periodicus_1	16S	Van Dooren et al. In review
pterolebias_longipinnis	16S	Van Dooren et al. In review
robustus_1	16S	Van Dooren et al. In review
s_magnificus	16S	Van Dooren et al. In review
affinis_1	28S c12d12	Van Dooren et al. In review

alexandrii_sanjavier	28S c12d12	Van Dooren et al. In review
arachan_parquerivera2	28S c12d12	Van Dooren et al. In review
charrua_ca	28S c12d12	Van Dooren et al. In review
charrua_ca2	28S c12d12	Van Dooren et al. In review
cheradophilus_castillos	28S c12d12	Van Dooren et al. In review
cheradophilus_castillos2	28S c12d12	Van Dooren et al. In review
cheradophilus_lp	28S c12d12	Van Dooren et al. In review
cinereus_arroyoviboras	28S c12d12	Van Dooren et al. In review
elongatus_villasoriano	28S c12d12	Van Dooren et al. In review
gymnoventris_salamanca4	28S c12d12	Van Dooren et al. In review
gymnoventris_velasquez	28S c12d12	Van Dooren et al. In review
luteoflammulatus_1	28S c12d12	Van Dooren et al. In review
melanoorus_1	28S c12d12	Van Dooren et al. In review
nigripinnis_ceibas	28S c12d12	Van Dooren et al. In review
periodicus_1	28S c12d12	Van Dooren et al. In review
pterolebias_longipinnis	28S c12d12	Van Dooren et al. In review
robustus_1	28S c12d12	Van Dooren et al. In review
vandenbergi_paloboraccio3	28S c12d12	Van Dooren et al. In review
affinis_1	cytB	Van Dooren et al. In review
arachan_parquerivera2	cytB	Van Dooren et al. In review
bellottii_sol	cytB	Van Dooren et al. In review
charrua_ca2	cytB	Van Dooren et al. In review
cheradophilus_castillos	cytB	Van Dooren et al. In review
cheradophilus_castillos2	cytB	Van Dooren et al. In review
cinereus_1	cytB	Van Dooren et al. In review
cinereus_2	cytB	Van Dooren et al. In review
cinereus_arroyoviboras	cytB	Van Dooren et al. In review
elongatus_gc	cytB	Van Dooren et al. In review
elongatus_villasoriano	cytB	Van Dooren et al. In review
gymnoventris_salamanca4	cytB	Van Dooren et al. In review
gymnoventris_velasquez	cytB	Van Dooren et al. In review
luteoflammulatus_velasquez	cytB	Van Dooren et al. In review
nigripinnis_ceibas	cytB	Van Dooren et al. In review
periodicus_1	cytB	Van Dooren et al. In review
prognathus_salamanca	cytB	Van Dooren et al. In review
pterolebias_longipinnis	cytB	Van Dooren et al. In review
robustus_1	cytB	Van Dooren et al. In review
s_magnificus	cytB	Van Dooren et al. In review
salviai_pdd	cytB	Van Dooren et al. In review
wolterstorffi_elbagre2	cytB	Van Dooren et al. In review
pterolebias_longipinnis	28S c1c2	Van Dooren et al. In review

affinis_1	28S c1c2	Van Dooren et al. In review
alexandrii_sanjavier	28S c1c2	Van Dooren et al. In review
arachan_parquerivera2	28S c1c2	Van Dooren et al. In review
charrua_ca	28S c1c2	Van Dooren et al. In review
cheradophilus_castillos2	28S c1c2	Van Dooren et al. In review
cinereus_1	28S c1c2	Van Dooren et al. In review
cinereus_2	28S c1c2	Van Dooren et al. In review
gymnoventris_velasquez	28S c1c2	Van Dooren et al. In review
luteoflammulatus_1	28S c1c2	Van Dooren et al. In review
melanoorus_1	28S c1c2	Van Dooren et al. In review
periodicus_1	28S c1c2	Van Dooren et al. In review
robustus_1	28S c1c2	Van Dooren et al. In review
bellottii_sol	28S c1c2	Van Dooren et al. In review
cinereus_arroyoviboras	28S c1c2	Van Dooren et al. In review
prognathus_salamanca2	28S c1c2	Van Dooren et al. In review
wolterstorffi_velasquez2	28S c1c2	Van Dooren et al. In review
nigripinnis_ceibas	28S c6c7	Van Dooren et al. In review
charrua_ca2	28S c6c7	Van Dooren et al. In review
cheradophilus_castillos	28S c6c7	Van Dooren et al. In review
cinereus_3	28S c6c7	Van Dooren et al. In review
elongatus_villasoriano	28S c6c7	Van Dooren et al. In review
gymnoventris_salamanca4	28S c6c7	Van Dooren et al. In review
pterolebias_longipinnis	28S c6c7	Van Dooren et al. In review
affinis_1	28S c6c7	Van Dooren et al. In review
alexandrii_sanjavier	28S c6c7	Van Dooren et al. In review
arachan_parquerivera2	28S c6c7	Van Dooren et al. In review
charrua_ca	28S c6c7	Van Dooren et al. In review
cheradophilus_castillos2	28S c6c7	Van Dooren et al. In review
cinereus_1	28S c6c7	Van Dooren et al. In review
cinereus_2	28S c6c7	Van Dooren et al. In review
gymnoventris_velasquez	28S c6c7	Van Dooren et al. In review
luteoflammulatus_1	28S c6c7	Van Dooren et al. In review
melanoorus_1	28S c6c7	Van Dooren et al. In review
periodicus_1	28S c6c7	Van Dooren et al. In review
robustus_1	28S c6c7	Van Dooren et al. In review
apaii_villasoriano2	28S c1c2	This study
apaii_villasoriano3	28S c1c2	This study
arachan_chuy	28S c1c2	This study
bellottii_maschwitz2	28S c1c2	This study
bellottii_maschwitz3	28S c1c2	This study
cheradophilus_lp2	28S c1c2	This study

cinereus2	28S c1c2	This study
durazensis_lc	28S c1c2	This study
elongatus_ezeiza2	28S c1c2	This study
elongatus_gc	28S c1c2	This study
gymnoventris_castillos	28S c1c2	This study
juanlangi_bm	28S c1c2	This study
juanlangi_pr	28S c1c2	This study
luteoflammulatus_ca	28S c1c2	This study
luteoflammulatus_velasquez	28S c1c2	This study
monstrosus_lobo	28S c1c2	This study
monstrosus_lobo2	28S c1c2	This study
monstrosus_lobo3	28S c1c2	This study
nigripinnis_sanjuan	28S c1c2	This study
nigripinnis_sanjuan2	28S c1c2	This study
patriciae_fontane	28S c1c2	This study
patriciae_fontane2	28S c1c2	This study
patriciae_fontane3	28S c1c2	This study
paucisquama_saosepe	28S c1c2	This study
paucisquama_saosepe2	28S c1c2	This study
paucisquama_saosepe3	28S c1c2	This study
salviai_pdd	28S c1c2	This study
salviai_pdd2	28S c1c2	This study
salviai_pdd3	28S c1c2	This study
toba_puertobeniejo	28S c1c2	This study
toba_puertobeniejo2	28S c1c2	This study
vandenbergi_paloboraccio	28S c1c2	This study
vandenbergi_paloboraccio2	28S c1c2	This study
vandenbergi_paloboraccio3	28S c1c2	This study
vazferrerai_parquerivera	28S c1c2	This study
vazferrerai_parquerivera2	28S c1c2	This study
viarius_castillos2	28S c1c2	This study
viarius_castillos3	28S c1c2	This study
wolterstorffi_elbagre	28S c1c2	This study
wolterstorffi_elbagre2	28S c1c2	This study
wolterstorffi_velasquez	28S c1c2	This study
affinis_1	16S	This study
apaii_villasoriano2	16S	This study
apaii_villasoriano3	16S	This study
arachan_chuy	16S	This study
bellottii_maschwitz2	16S	This study
bellottii_maschwitz3	16S	This study

cheradophilus_lp2	16S	This study
cinereus_2	16S	This study
durazensis_lc	16S	This study
elongatus_ezeiza2	16S	This study
elongatus_gc	16S	This study
gymnoventris_castillos	16S	This study
juanlangi_bm	16S	This study
juanlangi_pr	16S	This study
luteoflammulatus_ca	16S	This study
luteoflammulatus_velasquez	16S	This study
melanoorus_1	16S	This study
monstrosus_lobo	16S	This study
monstrosus_lobo2	16S	This study
monstrosus_lobo3	16S	This study
nigripinnis_sanjuan	16S	This study
nigripinnis_sanjuan2	16S	This study
patriciae_fontane	16S	This study
patriciae_fontane2	16S	This study
patriciae_fontane3	16S	This study
paucisquama_saosepe	16S	This study
paucisquama_saosepe2	16S	This study
paucisquama_saosepe3	16S	This study
prognathus_salamanca2	16S	This study
salviai_pdd	16S	This study
salviai_pdd2	16S	This study
salviai_pdd3	16S	This study
toba_puertobeniejo	16S	This study
toba_puertobeniejo2	16S	This study
vandenbergi_paloboraccio	16S	This study
vandenbergi_paloboraccio2	16S	This study
vandenbergi_paloboraccio3	16S	This study
vazferrerai_parquerivera	16S	This study
vazferrerai_parquerivera2	16S	This study
viarius_castillos2	16S	This study
viarius_castillos3	16S	This study
wolterstorffi_elbagre	16S	This study
wolterstorffi_elbagre2	16S	This study
wolterstorffi_velasquez	16S	This study
wolterstorffi_velasquez2	16S	This study
affinis_1	12S	This study
apaii_villasoriano2	12S	This study

apaii_villasoriano3	12S	This study
arachan_chuy	12S	This study
bellottii_maschwitz2	12S	This study
bellottii_maschwitz3	12S	This study
cheradophilus_lp2	12S	This study
cinereus_2	12S	This study
durazensis_lc	12S	This study
elongatus_ezeiza2	12S	This study
elongatus_gc	12S	This study
gymnoventris_castillos	12S	This study
juanlangi_bm	12S	This study
juanlangi_pr	12S	This study
luteoflammulatus_ca	12S	This study
luteoflammulatus_velasquez	12S	This study
melanoorus_1	12S	This study
monstrosus_lobo	12S	This study
monstrosus_lobo2	12S	This study
monstrosus_lobo3	12S	This study
nigripinnis_sanjuan	12S	This study
nigripinnis_sanjuan2	12S	This study
patriciae_fontane	12S	This study
patriciae_fontane2	12S	This study
patriciae_fontane3	12S	This study
paucisquama_saosepe	12S	This study
paucisquama_saosepe2	12S	This study
paucisquama_saosepe3	12S	This study
prognathus_salamanca2	12S	This study
salviai_pdd	12S	This study
salviai_pdd2	12S	This study
salviai_pdd3	12S	This study
toba_puertobeniejo	12S	This study
toba_puertobeniejo2	12S	This study
vandenbergi_paloboraccio	12S	This study
vandenbergi_paloboraccio2	12S	This study
vandenbergi_paloboraccio3	12S	This study
vazferrerai_parquerivera	12S	This study
vazferrerai_parquerivera2	12S	This study
viarius_castillos2	12S	This study
viarius_castillos3	12S	This study
wolterstorffi_elbagre	12S	This study
wolterstorffi_elbagre2	12S	This study

wolterstorffi_velasquez	12S	This study
wolterstorffi_velasquez2	12S	This study
apaii_villasoriano3	cytB	This study
arachan_chuy	cytB	This study
bellottii_maschwitz2	cytB	This study
bellottii_maschwitz3	cytB	This study
cheradophilus_lp2	cytB	This study
cinereus2	cytB	This study
durazensis_lc	cytB	This study
elongatus_ezeiza2	cytB	This study
juanlangi_bm	cytB	This study
juanlangi_pr	cytB	This study
luteoflammulatus_ca	cytB	This study
luteoflmmulatus_velasquez	cytB	This study
monstrosus_lobo	cytB	This study
monstrosus_lobo2	cytB	This study
monstrosus_lobo3	cytB	This study
nigripinnis_sanjuan	cytB	This study
nigripinnis_sanjuan2	cytB	This study
patriciae_fontane	cytB	This study
patriciae_fontane2	cytB	This study
patriciae_fontane3	cytB	This study
paucisquama_saosepe	cytB	This study
paucisquama_saosepe2	cytB	This study
paucisquama_saosepe3	cytB	This study
prognathus_salamanca2	cytB	This study
salviai_pdd2	cytB	This study
salviai_pdd3	cytB	This study
toba_puertobeniejo	cytB	This study
toba_puertobeniejo2	cytB	This study
vandenbergi_paloboraccio	cytB	This study
vandenbergi_paloboraccio2	cytB	This study
vandenbergi_paloboraccio3	cytB	This study
vazferrerai_parquerivera	cytB	This study
vazferrerai_parquerivera2	cytB	This study
viarius_castillos2	cytB	This study
viarius_castillos3	cytB	This study
wolterstorffi_elbagre	cytB	This study
wolterstorffi_velasquez	cytB	This study
wolterstorffi_velasquez2	cytB	This study
apaii_villasoriano2	28S c12d12	This study

apaii_villasoriano3	28S c12d12	This study
arachan_chuy	28S c12d12	This study
bellottii_maschwitz3	28S c12d12	This study
cheradophilus_lp2	28S c12d12	This study
durazensis_lc	28S c12d12	This study
elongatus_ezeiza2	28S c12d12	This study
elongatus_gc	28S c12d12	This study
gymnoventris_castillos	28S c12d12	This study
juanlangi_bm	28S c12d12	This study
juanlangi_pr	28S c12d12	This study
luteoflammulatus_ca	28S c12d12	This study
luteoflammulatus_velasquez	28S c12d12	This study
monstrosus_lobo	28S c12d12	This study
monstrosus_lobo2	28S c12d12	This study
monstrosus_lobo3	28S c12d12	This study
nigripinnis_sanjuan	28S c12d12	This study
nigripinnis_sanjuan2	28S c12d12	This study
patriciae_fontane	28S c12d12	This study
patriciae_fontane3	28S c12d12	This study
paucisquama_saosepe	28S c12d12	This study
paucisquama_saosepe2	28S c12d12	This study
paucisquama_saosepe3	28S c12d12	This study
prognathus_salamanca2	28S c12d12	This study
salviai_pdd	28S c12d12	This study
toba_puertobeniejo	28S c12d12	This study
toba_puertobeniejo2	28S c12d12	This study
vandenbergi_paloboraccio2	28S c12d12	This study
vazferrerai_parquerivera2	28S c12d12	This study
viarius_castillos2	28S c12d12	This study
wolterstorffi_elbagre	28S c12d12	This study
wolterstorffi_elbagre2	28S c12d12	This study
wolterstorffi_velasquez	28S c12d12	This study
wolterstorffi_velasquez2	28S c12d12	This study
apaii_villasoriano2	28S c6c7	This study
apaii_villasoriano3	28S c6c7	This study
arachan_chuy	28S c6c7	This study
bellottii_maschwitz2	28S c6c7	This study
bellottii_maschwitz3	28S c6c7	This study
cheradophilus_lp2	28S c6c7	This study
cinereus2	28S c6c7	This study
durazensis_lc	28S c6c7	This study

elongatus_ezeiza2	28S c6c7	This study
elongatus_gc	28S c6c7	This study
gymnoventris_castillos	28S c6c7	This study
juanlangi_bm	28S c6c7	This study
juanlangi_pr	28S c6c7	This study
luteoflammulatus_ca	28S c6c7	This study
luteoflammulatus_velasquez	28S c6c7	This study
monstrosus_lobo	28S c6c7	This study
monstrosus_lobo2	28S c6c7	This study
monstrosus_lobo3	28S c6c7	This study
nigripinnis_sanjuan	28S c6c7	This study
nigripinnis_sanjuan2	28S c6c7	This study
patriciae_fontane	28S c6c7	This study
patriciae_fontane2	28S c6c7	This study
patriciae_fontane3	28S c6c7	This study
paucisquama_saosepe	28S c6c7	This study
paucisquama_saosepe2	28S c6c7	This study
paucisquama_saosepe3	28S c6c7	This study
prognathus_salamanca2	28S c6c7	This study
salviai_pdd	28S c6c7	This study
salviai_pdd2	28S c6c7	This study
salviai_pdd3	28S c6c7	This study
toba_puertobeniejo	28S c6c7	This study
toba_puertobeniejo2	28S c6c7	This study
vandenbergi_paloboraccio	28S c6c7	This study
vandenbergi_paloboraccio2	28S c6c7	This study
vandenbergi_paloboraccio3	28S c6c7	This study
vazferrerai_parquerivera	28S c6c7	This study
vazferrerai_parquerivera2	28S c6c7	This study
viarius_castillos2	28S c6c7	This study
viarius_castillos3	28S c6c7	This study
wolterstorffi_elbagre	28S c6c7	This study
wolterstorffi_elbagre2	28S c6c7	This study
wolterstorffi_velasquez	28S c6c7	This study
wolterstorffi_velasquez2	28S c6c7	This study

Table S2.3 Substitution models and codon positions from Partitionfinder.

Gene	Codon position	Substitution Model
RAG1	1+3	K80+G
RAG1	2	K80+G
ENC1	1+2	K80+I
ENC1	3	K80+G
RH1	1+2	K80+I
RH1	3	HKY+G
SH3PX3	1+2	HKY+I
SH3PX3	3	HKY+G
28s c1c2+c6c7	1+2+3	GTR+I+G
28s c12d12	1+2+3	TrNef+G
CYTB	1+2	HKY+I+G
CYTB	3	GTR+I+G
16S	1+2+3	TrN+G
12S	1+2+3	SYM+G

Table S2.4 Collated *Austrolebias* occurrence data points

Species	Site	Long.	Lat.
Austrolebias adloffi	S‹o Leopoldo /OR/ temporary swamp near the road BR-116, S‹o Leopoldo	-29.73821	-51.131927
Austrolebias adloffi	Canoas	-29.888858	-51.240042
Austrolebias adloffi	Area Inundada No Distrito Industrial De Alvorada, Rs Drenagem Do Rio Gravatai,_jacui. /OR/ Gravata’	-29.910564	-51.024003
Austrolebias adloffi	swamp close to the road RS-118, about 500 m from the road BR-290	-29.962638	-51.002455
Austrolebias adloffi	Brazil: Rio Grande do Sul: laguna dos Patos system, Porto Alegre /OR/ Porto Alegre /OR/ Porto Alegre, Rio Grande do Sul, Brazil /OR/ SÌÏDAMERIKA, OSO-, BRASILIEN, OSO-, PORTO ALEGRE* ,	-29.964404	-51.132673
Austrolebias affinis	FYMNSA	-31.1075	-55.7465
Austrolebias affinis	Ruta 30 Tranqueras /OR/ Tranqueras /OR/ Tranqueras, Ruta 30	-31.176667	-55.764667
Austrolebias affinis	CTL1178	-31.186667	-55.7805
Austrolebias affinis	CTL1173	-31.193333	-55.789167
Austrolebias affinis	Rivera	-31.233833	-55.844833
Austrolebias affinis	Paso LambarŽ	-31.5315	-55.960667
Austrolebias affinis	Tacuarembo /OR/ Tacuaremb—	-31.649528	-55.899806
Austrolebias affinis	floodplains of arroyo Tres Cruces /OR/ R5 KM 399 /OR/ R5 KM 399 /OR/ Ruta 5 km 399 /OR/ Ruta 5 km 399,5 /OR/ Ruta5km399 /OR/ swamp at the arroyo Tres Cruces, Ruta 5, km 399.5 /OR/ Tres Cruces	-31.651833	-55.900167
Austrolebias affinis	Ruta 26 Km. 252	-31.727656	-55.799251
Austrolebias affinis	Ansina	-31.884667	-55.492
Austrolebias affinis	Pueblo Ansina	-31.885556	-55.4925
Austrolebias alexandri	Uruguaiana /OR/ Uruguaiana, road BR-472, close to arroio Salso I, a small tributary of rio Uruguay	-29.799431	-57.092181
Austrolebias alexandri	Sauce-R.8 Rio Guayquiraro	-30.142791	-58.808186
Austrolebias alexandri	Franquia /OR/ Fraquia /OR/ Fraquia	-30.205384	-57.616185
Austrolebias alexandri	El Pingo	-31.580016	-59.892354
Austrolebias alexandri	Mar’a Grande	-31.656941	-59.888716

Austrolebias alexandri	Los Lapachitos	-32.077483	-60.464421
Austrolebias alexandri	Rosario del Tala AAK 12/15\	-32.30723	-59.092669
Austrolebias alexandri	Banco Pelay - Boca Falsa	-32.449936	-58.217717
Austrolebias alexandri	San Cipriano	-32.541	-60.1082
Austrolebias alexandri	San Javier /OR/ San Javier /OR/ San Javier, r'o Uruguay basin	-32.655667	-58.128833
Austrolebias alexandri	Rinc—n de Nogoy‡	-32.748193	-59.936351
Austrolebias alexandri	Parque UnzuŽ, Gualeguaychu	-33.01372	-58.496341
Austrolebias alexandri	Gualeguaychu /OR/ Gualeguaychœ /OR/ Gualeguaychœ City, Entre R'os Province, Argentina	-33.015652	-58.483834
Austrolebias alexandri	La Guarderia	-33.019999	-58.501393
Austrolebias alexandri	Arroyo Tajamar /OR/ Arroyo Tajamar (Ruta 12)	-33.0333	-58.7333
Austrolebias alexandri	Gualeguay	-33.149963	-59.366667
Austrolebias alexandri	Camino P. Ruiz	-33.18241	-59.346375
Austrolebias alexandri	Arroyo Coria	-33.4	-58.75
Austrolebias alexandri	Medanos /OR/ MŽdanos	-33.428569	-59.078884
Austrolebias alexandri	Ceibas /OR/ Ceibas Town, Entre R'os Province, Argentina /OR/ Estaci—n Shell	-33.455857	-58.802767
Austrolebias apaii	Argentina: Prov'ncia de Entre R'os. La Salamanca, Concepci—n del Uruguay	-32.471221	-58.231357
Austrolebias apaii	Puerto Viejo, San Javier Town, Rio Negro Department, Uruguay	-32.637189	-58.142999
Austrolebias apaii	Estero de Farrapos, San Javier Town, R'o Negro Department, Uruguay	-32.751225	-58.088279
Austrolebias apaii	Gualeguaychu /OR/ Gualeguaychœ /OR/ Gualeguaychœ City, Entre R'os Province, Argentina	-33.015652	-58.483834
Austrolebias apaii	Ruta 96, km 8 /OR/ Soriano, Ruta 96, km 8 /OR/ Uruguay: Soriano. Ruta 96, km 8 /OR/ Villa Soriano /OR/ Villa Soriano Town, Soriano Department, Uruguay	-33.438333	-58.2765
Austrolebias apaii	Villa SorianoA	-33.439583	-58.277528
Austrolebias apaii	Villa SorianoB	-33.443194	-58.313528
Austrolebias apaii	Ceibas /OR/ Ceibas Town, Entre R'os Province, Argentina /OR/ Estaci—n Shell	-33.455857	-58.802767
Austrolebias apaii	Rio San Salvador, Soriano Department, Uruguay	-33.512345	-58.201006
Austrolebias apaii	Nueva Palmira /OR/ Nueva Palmira City, Colonia Department, Uruguay	-33.86	-58.39

Austrolebias apaii	Carmelo /OR/ Carmelo Town, Colonia Department, Uruguay /OR/ Uruguay: Colonia: Carmelo	-34.005167	-58.283333
Austrolebias apaii	Uruguay: Colonia. Swamp in front of Cassino de Carmelo	-34.011166	-58.287858
Austrolebias arachan	Pedras Altas	-32.061389	-53.724444
Austrolebias arachan	Banado de los Cinco Sauces, Route 26	-32.089794	-55.152868
Austrolebias arachan	Ruta 26, km 331 /OR/ Ruta 26 km 331 /OR/ Ruta 26, km 331 /OR/ Tacuaremb—: Ruta 26, km 331, r'o Negro drainage, r'o Uruguay basin /OR/ temporary swamp in, ca–ada Los Cinco Sauces, rio Negro system [r'o Uruguay basin], km 331 of the road Ruta 26, Departamento de Tacuaremb—,northeastern Uruguay /OR/ Ruta26KM331	-32.090833	-55.148333
Austrolebias arachan	Paso de Mazangano, Ruta 44 /OR/ Paso de Mazangano, Ruta 44, r'o Negro floodplains /OR/ temporary pool near r'o Negro, Paso de Mazangano, Ruta 44 /OR/ Paso de Mazangano, Ruta 44	-32.111333	-54.666
Austrolebias arachan	Arroyo Chuy, Ruta 7 /OR/ ba–ados A. Chuy /OR/ temporary pool near arroyo Chuy /OR/ temporary pond close to ruta 7 and arroyo chuy /OR/ R.7 Km.17 Ba–ado del arroyo Chuy	-32.24339	-54.06221
Austrolebias arachan	Ruta 26 y R'o Negro	-32.286702	-54.821146
Austrolebias arachan	Ruta 26, km 372 /OR/ Ruta 26, km 372 /OR/ Ruta 26, km 372, r'o Negro drainage, r'o Uruguay basin /OR/ Ruta26KM372	-32.288167	-54.8045
Austrolebias arachan	Melo, Parque Rivera, r'o Tacuar' drainage, laguna dos Patos system /OR/ Parque de Rivera /OR/ Parque Rivera /OR/ temporary pool in Parque Rivera, Melo	-32.374333	-54.188667
Austrolebias arachan	Arroyo Chuy Ruta 7 -2	-32.777778	-54.062222
Austrolebias bagual	Encruzilhada do Sul	-30.853333	-52.571111
Austrolebias bellottii	Puerto Bermejo /OR/ Puerto Bermejo, Chaco, Argentina /OR/ Rio Bermejo /OR/ Ruta 3, Puerto Bermejo	-26.924858	-58.510875
Austrolebias bellottii	Arroyo Cangui Chico	-26.986446	-58.549578
Austrolebias bellottii	Las Palmas	-27.050503	-58.924423
Austrolebias bellottii	Route 11, 21km S from Rio de Oro, Chaco Province, Argentina	-27.07035	-58.941955
Austrolebias bellottii	Colonia Benitez AAK 12/26\	-27.330226	-58.924836
Austrolebias bellottii	Puerto Tirol /OR/ Puerto Tirol City, Chaco Province, Argentina	-27.376518	-59.043592
Austrolebias bellottii	Riacho InŽ	-27.449229	-58.854227
Austrolebias bellottii	Resistencia, Chaco	-27.45	-58.983333

Austrolebias bellottii	Puerto Vilelas City, Chaco Province, Argentina	-27.519055	-58.94744
Austrolebias bellottii	Esteros de Iber‡, Corrientes Province, Argentina	-27.717967	-56.677991
Austrolebias bellottii	Arroyo Palometa AAK 12/25\	-28.294623	-59.217222
Austrolebias bellottii	Sauce-R.8 Rio Guayquiraro	-30.142791	-58.808186
Austrolebias bellottii	Bella Union City, Artigas Department, Uruguay	-30.235195	-57.577311
Austrolebias bellottii	Ruta 34 KM 274 Palacios	-30.820206	-61.601825
Austrolebias bellottii	Tacural /OR/ Tacural, Santa FŽ Province, Argentina	-30.850671	-61.578978
Austrolebias bellottii	Salto City, Salto Department, Uruguay	-31.403458	-57.925994
Austrolebias bellottii	Ruta 34 KM 202 Rafaela	-31.43524	-61.54183
Austrolebias bellottii	La Rosada	-31.496149	-58.002866
Austrolebias bellottii	Ruta 34 KM 188 Rafaela	-31.558172	-61.533032
Austrolebias bellottii	Sauce Viejo	-31.760967	-60.839943
Austrolebias bellottii	Estancia La Argentina	-32.2667	-60.2167
Austrolebias bellottii	Banco Pelay - Boca Falsa	-32.449936	-58.217717
Austrolebias bellottii	Argentina: Rio Parana, Above Rosario	-32.829	-60.69
Austrolebias bellottii	Gualeguaychu /OR/ Gualeguaychœ /OR/ Gualeguaychœ City, Entre R'os Province, Argentina	-33.015652	-58.483834
Austrolebias bellottii	La Guarderia	-33.019999	-58.501393
Austrolebias bellottii	Arroyo Tajamar /OR/ Arroyo Tajamar (Ruta 12)	-33.0333	-58.7333
Austrolebias bellottii	Gualeguay-Evita Capitana /OR/ Gualeguay-Pomelo es rock	-33.149963	-59.299399
Austrolebias bellottii	Gualeguay	-33.149963	-59.366667
Austrolebias bellottii	Arroyo Coria	-33.4	-58.75
Austrolebias bellottii	Medanos /OR/ MŽdanos	-33.428569	-59.078884
Austrolebias bellottii	Ruta 96, km 8 /OR/ Soriano, Ruta 96, km 8 /OR/ Uruguay: Soriano. Ruta 96, km 8 /OR/ Villa Soriano /OR/ Villa Soriano Town, Soriano Department, Uruguay	-33.438333	-58.2765
Austrolebias bellottii	Ceibas /OR/ Ceibas Town, Entre R'os Province, Argentina /OR/ Estaci—n Shell	-33.455857	-58.802767
Austrolebias bellottii	Arroyo Pericos	-33.67327	-58.839662

Austrolebias bellottii	Tranquera Azul - V». Paranacito	-33.711114	-58.655283
Austrolebias bellottii	A¼ El Tala (San Pedro)	-33.75	-59.6333
Austrolebias bellottii	Ibicuicito /OR/ Ibicuisito /OR/ Ibicuycito /OR/ Ibicuysito	-33.833525	-58.877414
Austrolebias bellottii	Ruta 9 Km 124 Lima	-33.97142	-59.386141
Austrolebias bellottii	Carmelo /OR/ Carmelo Town, Colonia Department, Uruguay /OR/ Uruguay: Colonia: Carmelo	-34.005167	-58.283333
Austrolebias bellottii	La Trinidad	-34.1	-61.1333
Austrolebias bellottii	Campana /OR/ Otamendi /OR/ Otamendi (Ruta 9 Km 57)	-34.262146	-58.90187
Austrolebias bellottii	Camino de la Via Muerta	-34.364	-58.700367
Austrolebias bellottii	Dique Lujan /OR/ Dique Lujan/Maschwitz	-34.365209	-58.718661
Austrolebias bellottii	Ingeniero Maschwitz, Argentina /OR/ Maschwitz	-34.36599	-58.718787
Austrolebias bellottii	Tigre /OR/ Tigre, r'o Luj‡n floodplains	-34.406288	-58.581832
Austrolebias bellottii	Benavidez	-34.420685	-58.676001
Austrolebias bellottii	La Aguada, Ezeiza	-34.748979	-58.521103
Austrolebias bellottii	Berazategui	-34.751488	-58.201207
Austrolebias bellottii	Ezeiza /OR/ Ezeiza	-34.769157	-58.523542
Austrolebias bellottii	Hudson	-34.79229	-58.135647
Austrolebias bellottii	Florencio Varela	-34.797735	-58.272386
Austrolebias bellottii	Villa Elisa /OR/ Villa Elisa, about 10 mi. s. of city of Buenos Aires, about 2 mi. inland.	-34.8166	-58.045
Austrolebias bellottii	Punta Lara /OR/ Punta Lara, Buenos Aires Province, Argentina	-34.820047	-57.971648
Austrolebias bellottii	Villars	-34.827574	-58.925814
Austrolebias bellottii	Haras Federal, Ezeiza	-34.862341	-58.567901
Austrolebias bellottii	carretera Villa Elisa-Punta Lara /OR/ road between Villa Elisa and Punta Lara, Argentina /OR/ temporary pool road between Villa Elisa and Punta Lara	-34.869413	-57.991579
Austrolebias bellottii	Las Heras, r'o Salado basin	-34.873381	-58.904539
Austrolebias bellottii	San Vicente	-35.018679	-58.401926
Austrolebias bellottii	Canuelas /OR/ Ca–uelas	-35.034083	-58.720705

Austrolebias bellottii	road La Plata-Magdalena /OR/ Swamp on the road, Ruta Nacional 11, coming from Magdalena /OR/ swamp on the road Ruta Nacional 11, coming from Magdalena /OR/ temporary pool, road Ruta Nacional 11,between Magdalena and La Plata	-35.064958	-57.573454
Austrolebias bellottii	Poblet	-35.071389	-57.962673
Austrolebias bellottii	Brandsen	-35.16724	-58.215384
Austrolebias bellottii	swamp, road Ruta Provincial 29, km 6 of the section Brandsen-Ranchos	-35.221822	-58.203053
Austrolebias bellottii	temporary pool, road Ruta 11, between Punta Indio and Veronica	-35.310293	-57.214651
Austrolebias bellottii	swamp close to Base Aeronaval de Punta Indio	-35.339916	-57.27501
Austrolebias bellottii	Altamirano	-35.356432	-58.151518
Austrolebias bellottii	Punta Piedras	-35.406666	-57.159872
Austrolebias bellottii	San Miguel del Monte /OR/ San Miguel del Monte, Buenos Aires, Argentina	-35.43887	-58.79161
Austrolebias bellottii	Pipinas	-35.521067	-57.329759
Austrolebias bellottii	Ranchos /OR/ road Ruta Provincial 29, between General Belgrano and Ranchos	-35.595	-58.423
Austrolebias bellottii	small road 10 km of the road Ruta Provincial 29, between General Belgrano and Chas	-35.673418	-58.477455
Austrolebias bellottii	Route 2 Km 145.2, Argentina	-35.778142	-57.927682
Austrolebias bellottii	Las Flores	-36.040249	-59.105252
Austrolebias bellottii	Dolores /OR/ Dolores City, Argentina	-36.303009	-57.701307
Austrolebias bellottii	Cachar' (Azul) /OR/ Cachar', Partido de Azul	-36.395568	-59.475644
Austrolebias bellottii	General Conesa /OR/ Ruta Prov. 11 - Gral. Conesa	-36.487279	-57.326809
Austrolebias bellottii	Los Yngleses /OR/ Cabo San Antonio /OR/ Cabo San Antonio, Argentina	-36.511275	-56.817273
Austrolebias bellottii	11 Road, Santa Teresita, Buenos Aires Province, Argentina	-36.542304	-56.716733
Austrolebias bellottii	Estacion Sol	-36.710246	-56.701585
Austrolebias bellottii	Fanazul (Azul)	-37.1287	-59.697993
Austrolebias bellottii	Nahuel Ruca	-37.637333	-57.468718
Austrolebias bellottii	13 from the Ruta 2, Vivorat‡ /OR/ Argentina: Prov'ncia de Buenos, arroyo Vivorat‡ /OR/ arroyo Vivorat‡, Mar Chiquita, Provincia de Buenos Aires, Argentina /OR/ Ruta Nacional 2 km276 Near arroyo vivorata /OR/ small road 13 km from Ruta Nacional 2, near arroyo Vivorat‡ /OR/ Viborota City, Buenos Aires Province, Argentina /OR/ Vivorata /OR/ km 276, road Ruta Nacional 2, near arroyo Vivorat‡	-37.660289	-57.670694

Austrolebias bellottii	small road 13 km of the road Ruta Nacional 2, near arroyo Vivorat‡	-37.717637	-57.524066
Austrolebias bellottii	Mar Chiquita	-37.739777	-57.452158
Austrolebias bellottii	Mar de Cobo /OR/ Mar de Cobo, Buenos Aires Province, Argentina	-37.769	-57.4637
Austrolebias bellottii	Balcarce	-37.825666	-58.255752
Austrolebias carvalhoi	highlands of the rio Iguassu, near Porto Uniao	-26.272997	-51.054657
Austrolebias bellottii	Ibarreta /OR/ Ibarreta Norte	-25.188084	-59.874021
Austrolebias charrua	north of Vergara /OR/ Road 18 close to Vergara town /OR/ Vergara	-32.9225	-53.91361111
Austrolebias charrua	temporary pool 2 km N of Curral Alto	-32.924782	-52.78292
Austrolebias charrua	Road 91, close to Corrales del Parao stream /OR/ Merin Lagoon Drainage: Route 91	-33.00166667	-53.87277778
Austrolebias charrua	Road 91 10 km to the North of Charqueada town	-33.15111111	-53.87416667
Austrolebias charrua	Treinta y Tres	-33.22131	-54.39904
Austrolebias charrua	arroyo Yerbal /OR/ Uruguay: Treinta y Tres: temporary swamp close to arroyo Yerbal	-33.221667	-54.398833
Austrolebias charrua	Road 8, close to treinta y tres city	-33.22555556	-54.39583333
Austrolebias charrua	Cebollati	-33.250313	-53.770064
Austrolebias charrua	Road 15 km 173	-33.47027778	-53.86972222
Austrolebias charrua	Road 15 km 151.5	-33.58444444	-54.06944444
Austrolebias charrua	Road 19 km close to San Luis stream /OR/ Rocha, San Luis /OR/ Ruta19 San Luis /OR/ San Luis /OR/ San Luis, Ruta 19, km 29.5; /OR/ Merin Lagoon Drainage: Route 19 San Luis creek	-33.60083333	-53.72472222
Austrolebias charrua	R.15 Km.146	-33.60527	-54.04857
Austrolebias charrua	r'o Cebollat', north to Lascano /OR/ Ruta 14, km 270 north to Lascano	-33.613667	-54.3
Austrolebias charrua	Los Naranjales /OR/ Los Naranjales Rio Cebollat'	-33.617538	-54.331414
Austrolebias charrua	Ruta 19, between 18 de Julio and San Luis /OR/ between 18 de Julio and San Luis, Ruta 19	-33.624398	-53.627671
Austrolebias charrua	Ruta 14, km 269 /OR/ Ruta 14, km 269, north to Lascano /OR/ Merin Lagoon Drainage: Route 14 km 269.2	-33.62705	-54.292275
Austrolebias charrua	temporary pool, 3 km N of Chu'	-33.657648	-53.433474
Austrolebias charrua	3 km N of Chu', road BR-471	-33.6654	-53.4379

Austrolebias charrua	Ruta19 km13	-33.66722	-53.57361
Austrolebias charrua	CIMC 8933, charco localizado na v‡rzea do arroio Chu' /OR/ CIMC 8942, charco localizado na v‡rzea do arroio Chu' /OR/ CIMC 9487, v‡rzea do arroio Chu' /OR/ CIMC 9488, v‡rzea do arroio Chu'	-33.669543	-53.431311
Austrolebias charrua	CIMC 8938, charco pr—ximo ˆ v‡rzea do arroio Chu'	-33.677043	-53.440366
Austrolebias charrua	CIMC 8924, aproximadamente 100 metros do lote CIMC 8895, na v‡rzea do arroio Chu'	-33.686149	-53.440194
Austrolebias charrua	CIMC 9481, estrada marginal ao arroio S‹o Miguel	-33.687911	-53.520961
Austrolebias charrua	Banado San Miguel	-33.688467	-53.535714
Austrolebias charrua	Road 19 km 6.5Ð7 /OR/ Merin Lagoon Drainage: Route 19 San Miguel creek	-33.68861111	-53.52666667
Austrolebias charrua	temporary swamp close to arroyo San Miguel, Chuy	-33.688905	-53.534383
Austrolebias charrua	temporary pool close to arroio Chu', road to Barra do Chu'	-33.689788	-53.436536
Austrolebias charrua	CIMC 9483, estrada vicinal pr—xima ˆ ponte do arroio Chu' /OR/ CIMC 9507, estrada vicinal pr—xima ˆ ponte do arroio Chu'	-33.690006	-53.443413
Austrolebias charrua	CIMC 8895, charco marginal ao arroio Chu' a 100 metros da ponte da estrada da Barra do Chu' /OR/ CIMC 8920, mesmo local do lote CIMC 8895	-33.69222	-53.441954
Austrolebias charrua	ditch at road side, km 3 of the road between Chu' and Barra do Chu'	-33.701484	-53.421168
Austrolebias charrua	Rocha R-9, Km. 316,1 Chui /OR/ Ruta 9 Km 315 /OR/ Ruta 9 Km 316.1 /OR/ Ruta 9 KM361.1	-33.701605	-53.453568
Austrolebias charrua	Rocha R-9, Km. 316,1 Chui /OR/ Ruta 9 Km 315 /OR/ Ruta 9 Km 316.1 /OR/ Ruta 9 KM361.1	-33.701605	-53.453568
Austrolebias charrua	CIMC 9485, estrada da Barra do Chu' em frente ˆ entrada da fazenda Charrua /OR/ CIMC 9486, estrada da Barra do Chu' em frente ˆ entrada da fazenda Charrua,	-33.708512	-53.412471
Austrolebias charrua	CIMC 8908, charco marginal ˆ estrada da Barra do Chu'	-33.715223	-53.402343
Austrolebias charrua	CIMC 8902, charco marginal ˆ estrada da Barra do Chu' /OR/ CIMC 8905, charco marginal ˆ estrada da Barra do Chu'	-33.715795	-53.414702
Austrolebias charrua	temporary pool km 5.5 of road Chu'-Barra do Chu', Brazil: Rio Grande do Sul /OR/ temporary swamp, km 5.5 of the road between Chu' and Barra do Chu'	-33.716465	-53.401014
Austrolebias charrua	R.9 Km. 331.5, Estancia La Horqueta	-33.71841	-53.46636
Austrolebias charrua	CIMC 8916, charco marginal ˆ estrada da Barra do Chu'	-33.723362	-53.392043
Austrolebias charrua	CIMC 8912, charco marginal ˆ estrada da Barra do Chu'	-33.726503	-53.406806
Austrolebias charrua	Ruta 9, KM 334.7	-33.74698	-53.47806

Austrolebias charrua	Road 9 km 336.5	-33.75527778	-53.43583333
Austrolebias charrua	R.14 Ba–ado India muerta	-33.75926	-54.10941
Austrolebias charrua	Road 14 km 489.5	-33.904619	-53.699066
Austrolebias charrua	La Coronilla /OR/ Merin Lagoon Drainage: La Coronilla	-33.9054	-53.525391
Austrolebias charrua	Canal Andreoni /OR/ Rocha: temporary swamp near canal Andreoni /OR/ Ruta14 KM 504 /OR/ temporary swamp near canal Andreoni /OR/ Temporary swamp near Canal Andreoni, Ruta 14, km 504	-33.920167	-53.5435
Austrolebias charrua	R.9 Km.310	-33.92988	-53.53742
Austrolebias charrua	Road 16 km 34.5	-33.99666667	-53.8175
Austrolebias charrua	Road 9 km 302	-34.0275	-53.59305556
Austrolebias charrua	arroyo India Muerta floodplains, 150 m from bridge on Ruta 13 and 50 m from the road to Southeast, near Vel‡zquez, Rocha, Uruguay /OR/ Velasquez /OR/ Velazquez	-34.056	-54.243167
Austrolebias charrua	Road 13 and Road 16 /OR/ Ruta 16 Km. 27 /OR/ Ruta13 y 16	-34.05944444	-53.85472222
Austrolebias charrua	Road 9 km 272b	-34.205	-53.77444444
Austrolebias charrua	Road 9 km 272 /OR/ Merin Lagoon Drainage: Route 9 km 272	-34.215	-53.77166667
Austrolebias cheradophilus	Jaguar‹oSite2	-32.55	-53.333333
Austrolebias cheradophilus	Jaguar‹oSite1	-32.55	-53.35
Austrolebias cheradophilus	Laguna Mer’n	-32.734722	-53.258333
Austrolebias cheradophilus	Road 13 and Road 16 /OR/ Ruta 16 Km. 27 /OR/ Ruta13 y 16	-34.05944444	-53.85472222
Austrolebias cheradophilus	Castillos /OR/ Castillos /OR/ Ruta 9, km 254.8 /OR/ R9 Km 254 Castillos /OR/ Ruta 9 Castillos /OR/ Ruta 9 Km 254.5 /OR/ Ruta 9, km 254.8 /OR/ Rutal 9 Castillos /OR/ temporary pool, near Ruta 9, km 254.8	-34.2205	-53.954333
Austrolebias cheradophilus	Arroyo Valisas /OR/ Arroyo Valizas /OR/ Ruta 10 Km 268 /OR/ Ruta 10, close to arroyo Valizas; /OR/ Temporary swamp near arroyo Valizas, Ruta 10, km 267 /OR/ Temporary swamp near arroyo, Valizas, Rocha, Uruguay /OR/ Valisas /OR/ Valizas /OR/ Valizas, Ruta 10 Km 267	-34.359221	-53.844422
Austrolebias cheradophilus	La Paloma	-34.63733	-54.165344
Austrolebias cinereus	Arroyo de las Viboras /OR/ Las Viboras /OR/ Las Vivoras /OR/ Route 21, Viboras stream, Colonia Department, Uruguay	-33.94	-58.369333
Austrolebias cinereus	Carmelo /OR/ Carmelo Town, Colonia Department, Uruguay /OR/ Uruguay: Colonia: Carmelo	-34.005167	-58.283333

Austrolebias cyaneus	Rio Pardo Dom Marcos Stream P6	-29.96805556	-52.39361111
Austrolebias cyaneus	Rio Pardo Capivari Stream P4	-30.06638889	-52.27805556
Austrolebias cyaneus	Rio Pardo Dom Marcos Stream P6	-30.07805556	-52.26
Austrolebias cyaneus	Rio Pardo Capivari Stream P5	-30.09305556	-52.23722222
Austrolebias cyaneus	Minas do Le‹o Francisquinho Stream P1	-30.10666667	-52.16138889
Austrolebias cyaneus	Minas do Le‹o Francisquinho Stream P2	-30.12777778	-52.16416667
Austrolebias cyaneus	arroio Dom Marcos floodplains, road BR-290 /OR/ Dom Marcos	-30.21049	-52.527166
Austrolebias duraznensis	Parque Guernika, Mercedes	-33.2455	-58.052
Austrolebias duraznensis	Sarandi Del Yi, Proximidades Del Rio Yi, Departamento De Durazno, Uruguay. Basin: Rio Negro, Rio Uruguay	-33.3409	-55.6181
Austrolebias duraznensis	Durazno /OR/ Durazno /OR/ La Cordobeza	-33.392486	-56.611043
Austrolebias duraznensis	Durazno /OR/ Durazno /OR/ La Cordobeza	-33.392486	-56.611043
Austrolebias duraznensis	Paso de San Borja /OR/ Paso San Borjas	-33.415833	-56.4325
Austrolebias elongatus	Ruta 96, km 8 /OR/ Soriano, Ruta 96, km 8 /OR/ Uruguay: Soriano. Ruta 96, km 8 /OR/ Villa Soriano /OR/ Villa Soriano Town, Soriano Department, Uruguay	-33.438333	-58.2765
Austrolebias elongatus	Villa SorianoA	-33.439583	-58.277528
Austrolebias elongatus	Villa SorianoB	-33.443194	-58.313528
Austrolebias elongatus	La Aguada, Ezeiza	-34.748979	-58.521103
Austrolebias elongatus	Ezeiza /OR/ Ezeiza	-34.769157	-58.523542
Austrolebias elongatus	Villa Elisa /OR/ Villa Elisa, about 10 mi. s. of city of Buenos Aires, about 2 mi. inland.	-34.8166	-58.045
Austrolebias elongatus	carretera Villa Elisa-Punta Lara /OR/ road between Villa Elisa and Punta Lara, Argentina /OR/ temporary pool road between Villa Elisa and Punta Lara	-34.869413	-57.991579
Austrolebias elongatus	Argentina: Buenos Aires, La Plata	-34.913	-57.934
Austrolebias elongatus	Argentina: Prov’ncia de Buenos Aires, r’o de la Plata	-34.98	-57.67
Austrolebias elongatus	road La Plata-Magdalena /OR/ Swamp on the road, Ruta Nacional 11, coming from Magdalena /OR/ swamp on the road Ruta Nacional 11, coming from Magdalena /OR/ temporary pool, road Ruta Nacional 11,between Magdalena and La Plata	-35.064958	-57.573454
Austrolebias elongatus	Punta Piedras	-35.406666	-57.159872
Austrolebias elongatus	Patricios	-35.444983	-60.730084

Austrolebias elongatus	laguna de Chascomœs	-35.601604	-58.054376
Austrolebias elongatus	pila	-36.015307	-58.121431
Austrolebias elongatus	General Conesa /OR/ Ruta Prov. 11 - Gral. Conesa	-36.487279	-57.326809
Austrolebias elongatus	Los Yngleses /OR/ Cabo San Antonio /OR/ Cabo San Antonio, Argentina	-36.511275	-56.817273
Austrolebias elongatus	Fanazul (Azul)	-37.1287	-59.697993
Austrolebias elongatus	13 from the Ruta 2, Vivorat‡ /OR/ Argentina: Prov'ncia de Buenos, arroyo Vivorat‡ /OR/ arroyo Vivorat‡, Mar Chiquita, Provincia de Buenos Aires, Argentina /OR/ Ruta Nacional 2 km276 Near arroyo vivorata /OR/ small road 13 km from Ruta Nacional 2, near arroyo Vivorat‡ /OR/ Viborota City, Buenos Aires Province, Argentina /OR/ Vivorata /OR/ km 276, road Ruta Nacional 2, near arroyo Vivorat‡	-37.660289	-57.670694
Austrolebias elongatus	Alzaga	-37.864088	-59.95103
Austrolebias gymnoventris	Cebollati	-33.250313	-53.770064
Austrolebias gymnoventris	temporary pool near arroyo India Muerta, Ruta 13, km 251	-34.051782	-54.033268
Austrolebias gymnoventris	arroyo India Muerta floodplains, 150 m from bridge on Ruta 13 and 50 m from the road to Southeast, near Vel‡zquez, Rocha, Uruguay /OR/ Velasquez /OR/ Velazquez	-34.056	-54.243167
Austrolebias gymnoventris	Salamanca	-34.10536	-54.60083
Austrolebias gymnoventris	Castillos /OR/ Castillos /OR/ Ruta 9, km 254.8 /OR/ R9 Km 254 Castillos /OR/ Ruta 9 Castillos /OR/ Ruta 9 Km 254.5 /OR/ Ruta 9, km 254.8 /OR/ Rutal 9 Castillos /OR/ temporary pool, near Ruta 9, km 254.8	-34.2205	-53.954333
Austrolebias ibicuiensis	rio Toropi floodplains, a tributary of rio Ibicu', rio Uruguay basin road BR-287, 34 km W of S‹o Pedro do Sul /OR/ Rio Torpi	-29.650512	-54.541594
Austrolebias ibicuiensis	rio Ibicu'-Mirim, road BR-287, between S‹o Pedro do Sul and Santa Maria	-29.663628	-54.115743
Austrolebias jaegari	swamp at banhado do Timba, Corredor das Tropas	-31.5	-52.333333
Austrolebias juanlangi	temporary pool 9 km S of Bage, road BR-153	-31.42878	-54.137207
Austrolebias juanlangi	temporary pool 19 km S of Bage, road BR-153	-31.517	-54.138
Austrolebias juanlangi	temporary pool 27 km S of Bage, road BR-153	-31.578269	-54.139704
Austrolebias juanlangi	Hulha Negra Jaguar‹o River P2	-31.58083333	-53.97166667
Austrolebias juanlangi	swamp near banhado do Minuano, road BR-153, rio Jaguar‹o	-31.68	-54.145833
Austrolebias juanlangi	temporary pool 42 km S of BagŽ, road BR-153	-31.716737	-54.154911
Austrolebias juanlangi	Acegu‡P1	-31.736111	-54.019167

Austrolebias juanlangi	Acegu‡P2	-31.763611	-54.036389
Austrolebias juanlangi	Acegu‡P3	-31.765	-54.039444
Austrolebias juanlangi	Isidoro Noblia	-31.951195	-54.142312
Austrolebias juanlangi	Pedras Altas Jaguar‹o River P1	-32.01555556	-53.77444444
Austrolebias juanlangi	Banado de los Cinco Sauces, Route 26	-32.089794	-55.152868
Austrolebias juanlangi	Ruta 26, km 331 /OR/ Ruta 26 km 331 /OR/ Ruta 26, km 331 /OR/ Tacuaremb—: Ruta 26, km 331, r'o Negro drainage, r'o Uruguay basin /OR/ temporary swamp in, ca–ada Los Cinco Sauces, rio Negro system [r'o Uruguay basin], km 331 of the road Ruta 26, Departamento de Tacuaremb—,northeastern Uruguay /OR/ Ruta26KM331	-32.090833	-55.148333
Austrolebias juanlangi	Paso de Mazangano, Ruta 44 /OR/ Paso de Mazangano, Ruta 44, r'o Negro floodplains /OR/ temporary pool near r'o Negro, Paso de Mazangano, Ruta 44 /OR/ Paso de Mazangano, Ruta 44	-32.111333	-54.666
Austrolebias juanlangi	AJH1 /OR/ AJH2	-32.112194	-54.665444
Austrolebias juanlangi	Herval Jaguar‹o River P3	-32.12444444	-53.72611111
Austrolebias juanlangi	km 44 of the road Ruta 44, from Melo to Rivera , Departamento Cerro-Largo, North Eastern, Uruguay, r'o Negro drainage, r'o Uruguay basin /OR/ Ruta 44 km 44.4 /OR/ Uruguay: Cerro Largo, Ruta 44, km 44.4, r'o Negro drainage, r'o Uruguay basin	-32.173	-54.5345
Austrolebias juanlangi	Ruta 26 y R'o Negro	-32.286702	-54.821146
Austrolebias juanlangi	Ruta 26, km 372 /OR/ Ruta 26, km 372 /OR/ Ruta 26, km 372, r'o Negro drainage, r'o Uruguay basin /OR/ Ruta26KM372	-32.288167	-54.8045
Austrolebias juanlangi	Ba–ados Conventos /OR/ Ba–ados Conventos, r'o Tacuar' basin	-32.353333	-54.237
Austrolebias juanlangi	Ruta 26, km 405, area between upper r'o Negro and r'o Tacuar' basins	-32.365167	-54.474833
Austrolebias juanlangi	Ruta 26, km 406, area between upper r'o Negro and r'o Tacuar' basins	-32.368333	-54.462667
Austrolebias juanlangi	Melo, Parque Rivera, r'o Tacuar' drainage, laguna dos Patos system /OR/ Parque de Rivera /OR/ Parque Rivera /OR/ temporary pool in Parque Rivera, Melo	-32.374333	-54.188667
Austrolebias juanlangi	Melo /OR/ Melo, r'o Tacuar' drainage, laguna dos Patos system	-32.3745	-54.205333
Austrolebias juanlangi	Telho /OR/ Telho, about 21 km from the city of Jaguar‹o /OR/ temporary swamp near arroio Telho, Jaguar‹o	-32.378828	-53.444228
Austrolebias juanlangi	Banado Medina	-32.397455	-54.352614
Austrolebias juanlangi	Paso del Dragon /OR/ Paso del Drag—n /OR/ Paso Del Dragon /OR/ temporary pool near r'o Tacuar', Paso del Drag—n /OR/ R.18 Km.370 Paso del drag—n	-32.765833	-53.719833

Austrolebias litzi	2.5 km of arroio Arenal, about 12 km from Santa Maria, road BR-392 /OR/ Santa Maria	-29.78462	-53.782959
Austrolebias litzi	floodplains of a stream tributary of rio Vacaca', 6 km NW of Vila Block, road BR-392	-29.94606	-53.703841
Austrolebias luteoflammulatus	Road 18 km 369.5 /OR/ Merin Lagoon Drainage: Route 18 km 369.\5	-32.78083333	-53.64444444
Austrolebias luteoflammulatus	Ruta 18 KM367	-32.781389	-53.759444
Austrolebias luteoflammulatus	Road 91, close to Corrales del Parao stream /OR/ Merin Lagoon Drainage: Route 91	-33.00166667	-53.87277778
Austrolebias luteoflammulatus	Ruta 91 B	-33.14639	-53.88333
Austrolebias luteoflammulatus	Cebollati	-33.250313	-53.770064
Austrolebias luteoflammulatus	Merin Lagoon Drainage: Route 15 km, 156	-33.566066	-54.027902
Austrolebias luteoflammulatus	Road 19 km close to San Luis stream /OR/ Rocha, San Luis /OR/ Ruta19 San Luis /OR/ San Luis /OR/ San Luis, Ruta 19, km 29.5; /OR/ Merin Lagoon Drainage: Route 19 San Luis creek	-33.60083333	-53.72472222
Austrolebias luteoflammulatus	r'o Cebollat', north to Lascano /OR/ Ruta 14, km 270 north to Lascano	-33.613667	-54.3
Austrolebias luteoflammulatus	Ruta 19, between 18 de Julio and San Luis /OR/ between 18 de Julio and San Luis, Ruta 19	-33.624398	-53.627671
Austrolebias luteoflammulatus	Ruta 14, km 269 /OR/ Ruta 14, km 269, north to Lascano /OR/ Merin Lagoon Drainage: Route 14 km 269.2	-33.62705	-54.292275
Austrolebias luteoflammulatus	Ruta19 km13	-33.66722	-53.57361
Austrolebias luteoflammulatus	CIMC 8933, charco localizado na v‡rzea do arroio Chu' /OR/ CIMC 8942, charco localizado na v‡rzea do arroio Chu' /OR/ CIMC 9487, v‡rzea do arroio Chu' /OR/ CIMC 9488, v‡rzea do arroio Chu'	-33.669543	-53.431311
Austrolebias luteoflammulatus	CIMC 9482, estrada marginal ao arroio S‹o Miguel	-33.687411	-53.515639
Austrolebias luteoflammulatus	Road 19 km 6.5Ð7 /OR/ Merin Lagoon Drainage: Route 19 San Miguel creek	-33.68861111	-53.52666667
Austrolebias luteoflammulatus	CIMC 9483, estrada vicinal pr—xima ˆ ponte do arroio Chu' /OR/ CIMC 9507, estrada vicinal pr—xima ˆ ponte do arroio Chu'	-33.690006	-53.443413
Austrolebias luteoflammulatus	CIMC 8895, charco marginal ao arroio Chu' a 100 metros da ponte da estrada da Barra do Chu' /OR/ CIMC 8920, mesmo local do lote CIMC 8895	-33.69222	-53.441954
Austrolebias luteoflammulatus	CIMC 8586, charco na v‡rzea do arroio Chu' /OR/ CIMC 8626, coletado no mesmo local do lote CIMC 8593 /OR/ CIMC 8899, charco marginal ao arroio Chu' /OR/ CIMC 8928, charco marginal ao arroio Chu'	-33.695397	-53.439636
Austrolebias luteoflammulatus	Rocha R-9, Km. 316,1 Chui /OR/ Ruta 9 Km 315 /OR/ Ruta 9 Km 316.1 /OR/ Ruta 9 KM361.1	-33.701605	-53.453568
Austrolebias luteoflammulatus	CIMC 9485, estrada da Barra do Chu' em frente ˆ entrada da fazenda Charrua /OR/	-33.708512	-53.412471

	CIMC 9486, estrada da Barra do Chu' em frente ˆ entrada da fazenda Charrua,		
Austrolebias luteoflammulatus	CIMC 8902, charco marginal ˆ estrada da Barra do Chu' /OR/ CIMC 8905, charco marginal ˆ estrada da Barra do Chu'	-33.715795	-53.414702
Austrolebias luteoflammulatus	temporary pool km 5.5 of road Chu'-Barra do Chu', Brazil: Rio Grande do Sul /OR/ temporary swamp, km 5.5 of the road between Chu' and Barra do Chu'	-33.716465	-53.401014
Austrolebias luteoflammulatus	R.14 Ba–ado India muerta	-33.75926	-54.10941
Austrolebias luteoflammulatus	Ruta 14 El Bagre	-33.860686	-53.902776
Austrolebias luteoflammulatus	Ruta 14, Camino de los Indios, Departamento de Rocha, Uruguay. Temporary pond	-33.8907	-53.804
Austrolebias luteoflammulatus	La Coronilla /OR/ Merin Lagoon Drainage: La Coronilla	-33.9054	-53.525391
Austrolebias luteoflammulatus	Canal Andreoni /OR/ Rocha: temporary swamp near canal Andreoni /OR/ Ruta14 KM 504 /OR/ temporary swamp near canal Andreoni /OR/ Temporary swamp near Canal Andreoni, Ruta 14, km 504	-33.920167	-53.5435
Austrolebias luteoflammulatus	R.9 Km.310	-33.92988	-53.53742
Austrolebias luteoflammulatus	arroyo India Muerta floodplains, 150 m from bridge on Ruta 13 and 50 m from the road to Southeast, near Vel‡zquez, Rocha, Uruguay /OR/ Velasquez /OR/ Velazquez	-34.056	-54.243167
Austrolebias luteoflammulatus	Road 9 km 272 /OR/ Merin Lagoon Drainage: Route 9 km 272	-34.215	-53.77166667
Austrolebias luteoflammulatus	Castillos /OR/ Castillos /OR/ Ruta 9, km 254.8 /OR/ R9 Km 254 Castillos /OR/ Ruta 9 Castillos /OR/ Ruta 9 Km 254.5 /OR/ Ruta 9, km 254.8 /OR/ Rutal 9 Castillos /OR/ temporary pool, near Ruta 9, km 254.8	-34.2205	-53.954333
Austrolebias luteoflammulatus	Charco de Los Sauces /OR/ Castillos Lagoon drainage: Route 10 Los Sauces	-34.250911	-53.813366
Austrolebias luteoflammulatus	Castillos Lagoon Drainage: Route 10 next to Valizas Road	-34.323097	-53.830348
Austrolebias luteoflammulatus	temporary swamp near arroyo Valizas, Ruta 10, km 267	-34.359167	-53.844
Austrolebias luteoflammulatus	Arroyo Valisas /OR/ Arroyo Valizas /OR/ Ruta 10 Km 268 /OR/ Ruta 10, close to arroyo Valizas; /OR/ Temporary swamp near arroyo Valizas, Ruta 10, km 267 /OR/ Temporary swamp near arroyo, Valizas, Rocha, Uruguay /OR/ Valisas /OR/ Valizas /OR/ Valizas, Ruta 10 Km 267	-34.359221	-53.844422
Austrolebias luteoflammulatus	Ruta 10 km 265 /OR/ Castillos lagoon drainage: Route 10 Vivero Forestal Cabo Polonio	-34.388792	-53.854056
Austrolebias luteoflammulatus	Castillos Lagoon Drainage: Route 9 Km 230	-34.39458	-54.108697
Austrolebias luteoflammulatus	Road 9 km 228.5 /OR/ Castillos Lagoon Drainage: Route 9 km 228.5	-34.40277778	-54.12388889
Austrolebias luteoflammulatus	R.9 Km. 229	-34.41556	-54.09139

Austrolebias luteoflammulatus	Castillos lagoon drainage: Route 10 Palmeras Gemelas	-34.419716	-53.895691
Austrolebias luteoflammulatus	Rocha R-9, Km 205 /OR/ Ruta 9 km 205 /OR/ Ruta 9, km 205 /OR/ Ruta 9, Km. 205 /OR/ Rocha Lagoon Drainage: Route 9 km 205	-34.502667	-54.334333
Austrolebias luteoflammulatus	Rocha Lagoon Drainage: road to puerto de los Botes	-34.516878	-54.330021
Austrolebias luteoflammulatus	Ruta 10 Km 226	-34.600369	-54.142853
Austrolebias luteoflammulatus	Ruta 15 km 7.5	-34.605833	-54.1765
Austrolebias luteoflammulatus	Ruta 10 Km 225, Arachania /OR/ Rocha Lagoon Drainage: Route 10 km 225	-34.609718	-54.152952
Austrolebias luteoflammulatus	La Pedrera /OR/ La Pedrera /OR/ La Pedrera, Ruta 10	-34.612833	-54.158667
Austrolebias melanoorus	temporary swamp near r'o Tacuaremb—	-31.087	-55.697833
Austrolebias melanoorus	CTL1196	-31.095167	-55.686833
Austrolebias melanoorus	FYMNSA	-31.1075	-55.7465
Austrolebias melanoorus	Ruta 30 Tranqueras /OR/ Tranqueras /OR/ Tranqueras, Ruta 30	-31.176667	-55.764667
Austrolebias melanoorus	Seival1	-31.431389	-53.681667
Austrolebias melanoorus	Seival2	-31.432222	-53.717778
Austrolebias melanoorus	Seival3	-31.4375	-53.699167
Austrolebias melanoorus	Tacuarembo /OR/ Tacuaremb—	-31.649528	-55.899806
Austrolebias melanoorus	floodplains of arroyo Tres Cruces /OR/ R5 KM 399 /OR/ R5 KM 399 /OR/ Ruta 5 km 399 /OR/ Ruta 5 km 399,5 /OR/ Ruta5km399 /OR/ swamp at the arroyo Tres Cruces, Ruta 5, km 399.5 /OR/ Tres Cruces	-31.651833	-55.900167
Austrolebias melanoorus	Candiota2	-31.73944444	-53.76777778
Austrolebias melanoorus	Candiota1	-31.74055556	-53.77472222
Austrolebias melanoorus	Candiota3	-31.74555556	-53.77638889
Austrolebias melanoorus	Ansina	-31.884667	-55.492
Austrolebias melanoorus	Pueblo Ansina	-31.885556	-55.4925
Austrolebias minuano	Talha Mar	-31.255978	-50.982639
Austrolebias minuano	swamp at the road BR-101, Tavares	-31.290804	-51.073502
Austrolebias minuano	swamp at the road BR-101, 2 km from Tavares	-31.48381	-51.252128
Austrolebias minuano	temporary swamp in Cap‹o do Meio, S‹o JosŽ do Norte	-31.513988	-51.270728

Austrolebias minuano	3 km S of Bojuru, S‹o JosŽ do Norte	-31.648279	-51.438615
Austrolebias minuano	swamp 3 km S of Bojuru, S‹o JosŽ do Norte	-31.65473	-51.442311
Austrolebias minuano	temporary swamp in S‹o Caetano, 20 km NE of S‹o JosŽ do Norte /OR/ temporary swamp in S‹o Caetano, 20 km NE S‹o JosŽ do Norte	-31.894128	-51.910864
Austrolebias minuano	temporary lagoon about 4.5 km N of Quinta /OR/ Quinta Rio Grande	-32.034749	-52.286096
Austrolebias minuano	Mata Paludosa estudada.	-32.128797	-52.151288
Austrolebias minuano	ÔEstrada VelhaÕ	-32.129389	-52.153083
Austrolebias minuano	road to Cassino, 6 km before the city	-32.130354	-52.186445
Austrolebias minuano	banhado do Ma□arico, 8 km of the road BR-471, distrito da Quinta	-32.275192	-52.451986
Austrolebias monstrosus	92 km N. Mariscal to Americo Picco /OR/ R'o Paraguay drainage: 92 Km N of Mariscal Estigarribia on road to AmŽrico Picco	-21.18567	-60.549803
Austrolebias monstrosus	25 km N. Faro Moro to Montania	-21.326934	-59.84124
Austrolebias monstrosus	15 km N. Faro Moro to Montania	-21.373	-59.862
Austrolebias monstrosus	15 km Tte Montania to Madrejon, Boqueron, Par	-21.868912	-59.939016
Austrolebias monstrosus	19.3 km Mariscal EstigarribiaÊ	-22.050871	-60.311761
Austrolebias monstrosus	Santa Mar'a	-22.167129	-62.812397
Austrolebias monstrosus	Fortin Toledo /OR/ Province of Presidente Hayes, near Fort'n Toledo /OR/ RÌÄå_o Paraguay drainage: near FortÌÄå_n Toledo /OR/ RÌ_o Paraguay drainage: near FortÌ_n Toledo /OR/ Toledo /OR/ Toledo (LV23), N.W. Paraguay	-22.27	-60.54
Austrolebias monstrosus	32.3 km S. Transchaco HiWayÊ	-22.376342	-60.211496
Austrolebias monstrosus	la serena /OR/ La Serena, 6 km R220 to Montania /OR/ Provincia de Boqueron, near La Serena, upper Chaco basin, Paraguay /OR/ La Serena, 6 km R220 to Montania	-22.55137	-59.941279
Austrolebias monstrosus	100km SW of Filadelfia, Boqueron	-23.087224	-61.483489
Austrolebias monstrosus	Hickmann /OR/ Hickmann, northern Argentina /OR/ Ruta Nacional 81, Hickmann /OR/ \ Puente de Hickmann AAK 13/37\ /OR/ \ Puente de Hickmann AAK 13/37\	-23.209801	-63.573449
Austrolebias monstrosus	Las Moras	-23.836128	-63.453686
Austrolebias monstrosus	Charco Lobo, Rivadavia	-24.273364	-62.911389
Austrolebias monstrosus	Laguna Yema /OR/ Laguna Yema, Dto Bermejo, Formosa, Argent.	-24.315091	-61.161047
Austrolebias monstrosus	Palo borrachio, Rivadavia	-24.3615278	-62.9894722

Austrolebias monstrosus	Ruta Provincial 52, General de San Martin	-24.682997	-63.961733
Austrolebias monstrosus	Ituzaing—	-27.6	-56.683333
Austrolebias nachtigalli	Rio Grande do Sul: Arroio Grande	-32.25	-53.083333
Austrolebias nachtigalli	temporary pool close to arroio Grande, 10 km E of the road BR-116	-32.318301	-53.013514
Austrolebias nachtigalli	temporary pool at km 11 of the road Arroio Grande-lagoa Mirim	-32.318462	-52.952261
Austrolebias nachtigalli	26 km E of the road BR-116	-32.370527	-52.859959
Austrolebias nachtigalli	12 km NE of Jaguar‹o, road BR-116 /OR/ Rio Grande do Sul, Brazil Road BR 116 km 15	-32.47218	-53.291592
Austrolebias nachtigalli	rua 27 de novembro, between the second and third bridge, about 10 km from the road BR-116, Jaguar‹o /OR/ rua 27 de Novembro, between the second and the third bridge, about 10 km from the road BR-116	-32.473899	-53.435301
Austrolebias nigripinnis	R’o de Oro, KCA 34/05	-26.9138889	-59.0244444
Austrolebias nigripinnis	Arroyo Zapir‡n	-27.084444	-58.949722
Austrolebias nigripinnis	Riacho InŽ	-27.449229	-58.854227
Austrolebias nigripinnis	Resistencia, Chaco	-27.45	-58.983333
Austrolebias nigripinnis	Ituzaing—	-27.6	-56.683333
Austrolebias nigripinnis	El Sombrero	-27.701592	-58.76544
Austrolebias nigripinnis	San Javier Misiones	-27.883333	-55.133333
Austrolebias nigripinnis	Virasoro	-28.069389	-56.016659
Austrolebias nigripinnis	Tacuarend’	-28.416667	-59.3
Austrolebias nigripinnis	Laguna Iber‡	-28.516667	-57.116667
Austrolebias nigripinnis	R’o Aguapey	-29.101389	-56.608056
Austrolebias nigripinnis	R’o Guavirav’	-29.466667	-56.833333
Austrolebias nigripinnis	A¡ Curuzœ Cuati‡	-29.998333	-57.717778
Austrolebias nigripinnis	Sauce-R.8 Rio Guayquiraro	-30.142791	-58.808186
Austrolebias nigripinnis	Franquia /OR/ Fraquia /OR/ Fraquia	-30.205384	-57.616185
Austrolebias nigripinnis	Sagastome	-32.048778	-58.746443
Austrolebias nigripinnis	San Fabi‡n	-32.122061	-60.980915

Austrolebias nigripinnis	Estancia La Argentina	-32.2667	-60.2167
Austrolebias nigripinnis	Rosario del Tala AAK 12/15\	-32.30723	-59.092669
Austrolebias nigripinnis	Paysandu	-32.342513	-58.069477
Austrolebias nigripinnis	Banco Pelay - Boca Falsa	-32.449936	-58.217717
Austrolebias nigripinnis	Arroyo Ceibo	-32.61319	-60.121546
Austrolebias nigripinnis	San Javier /OR/ San Javier /OR/ San Javier, r'o Uruguay basin	-32.655667	-58.128833
Austrolebias nigripinnis	Argentina: Rio Parana, Above Rosario	-32.829	-60.69
Austrolebias nigripinnis	San Marcos	-32.882636	-60.64019
Austrolebias nigripinnis	Gualeguaychu /OR/ Gualeguaychœ /OR/ Gualeguaychœ City, Entre R'os Province, Argentina	-33.015652	-58.483834
Austrolebias nigripinnis	La Guarderia	-33.019999	-58.501393
Austrolebias nigripinnis	Arroyo Tajamar /OR/ Arroyo Tajamar (Ruta 12)	-33.0333	-58.7333
Austrolebias nigripinnis	Gualeguay	-33.149963	-59.366667
Austrolebias nigripinnis	Berisso	-33.230644	-59.210992
Austrolebias nigripinnis	Nancay	-33.394249	-58.747197
Austrolebias nigripinnis	Arroyo Coria	-33.4	-58.75
Austrolebias nigripinnis	Medanos /OR/ MŽdanos	-33.428569	-59.078884
Austrolebias nigripinnis	Ruta 96, km 8 /OR/ Soriano, Ruta 96, km 8 /OR/ Uruguay: Soriano. Ruta 96, km 8 /OR/ Villa Soriano /OR/ Villa Soriano Town, Soriano Department, Uruguay	-33.438333	-58.2765
Austrolebias nigripinnis	Ceibas /OR/ Ceibas Town, Entre R'os Province, Argentina /OR/ Estaci—n Shell	-33.455857	-58.802767
Austrolebias nigripinnis	La Peregrina	-33.496111	-58.861944
Austrolebias nigripinnis	Ruta 45 KM 3 Rio Paranacito	-33.662958	-58.85302
Austrolebias nigripinnis	Arroyo Pericos	-33.67327	-58.839662
Austrolebias nigripinnis	Tranquera Azul - V». Paranacito	-33.711114	-58.655283
Austrolebias nigripinnis	A¼ El Tala (San Pedro)	-33.75	-59.6333
Austrolebias nigripinnis	Brazo Largo	-33.783172	-58.600084
Austrolebias nigripinnis	Ibicuicito /OR/ Ibicuisito /OR/ Ibicuycito /OR/ Ibicuysito	-33.833525	-58.877414

Austrolebias nigripinnis	Nueva Palmira /OR/ Nueva Palmira City, Colonia Department, Uruguay	-33.86	-58.39
Austrolebias nigripinnis	Arroyo Higueritas, Ciudad De Nueva Palmira, Departamento De Colonia, Uruguay.	-33.879745	-58.41095
Austrolebias nigripinnis	Arroyo de las Viboras /OR/ Las Viboras /OR/ Las Vivoras /OR/ Route 21, Viboras stream, Colonia Department, Uruguay	-33.94	-58.369333
Austrolebias nigripinnis	Carmelo /OR/ Carmelo Town, Colonia Department, Uruguay /OR/ Uruguay: Colonia: Carmelo	-34.005167	-58.283333
Austrolebias nigripinnis	Delta del Paran‡, Estaci—n Experimental INTA	-34.170179	-58.86681
Austrolebias nigripinnis	Campana /OR/ Otamendi /OR/ Otamendi (Ruta 9 Km 57)	-34.262146	-58.90187
Austrolebias nigripinnis	Escobar	-34.317574	-58.737448
Austrolebias nigripinnis	Camino de la Via Muerta	-34.364	-58.700367
Austrolebias nigripinnis	Ingeniero Maschwitz, Argentina /OR/ Maschwitz	-34.36599	-58.718787
Austrolebias nigripinnis	Tigre /OR/ Tigre, r'o Luj‡n floodplains	-34.406288	-58.581832
Austrolebias nigripinnis	Cufre /OR/ R.1 Km.101 Boca del CufrŽ	-34.43583	-57.10944
Austrolebias nigripinnis	Punta Lara /OR/ Punta Lara, Buenos Aires Province, Argentina	-34.820047	-57.971648
Austrolebias nigripinnis	carretera Villa Elisa-Punta Lara /OR/ road between Villa Elisa and Punta Lara, Argentina /OR/ temporary pool road between Villa Elisa and Punta Lara	-34.869413	-57.991579
Austrolebias nigripinnis	La Balandra	-34.963071	-57.754416
Austrolebias nigripinnis	road La Plata-Magdalena /OR/ Swamp on the road, Ruta Nacional 11, coming from Magdalena /OR/ swamp on the road Ruta Nacional 11, coming from Magdalena /OR/ temporary pool, road Ruta Nacional 11,between Magdalena and La Plata	-35.064958	-57.573454
Austrolebias nigripinnis	Ruta 11, 5km s of Magdalena	-35.083333	-57.466667
Austrolebias nigrofasciatus	temporary swamp in EMBRAPA near arroio Padre Doutor, canal de S‹o Gon□alo drainage, Cap‹o do Le‹o	-31.6825	-52.446
Austrolebias nigrofasciatus	Pontal da Barra, praia de Laranjal, Pelotas /OR/ Ponta de Barra /OR/ temporary pool in Pontal da Barra, praia de Laranjal, canal de S‹o Gon□alo floodplains, Pelotas	-31.7651	-52.2414
Austrolebias nigrofasciatus	wetland between S‹o Gon□alo channel and Pelotas stream	-31.778611	-52.266944
Austrolebias nigrofasciatus	Padre Doutour	-31.8	-52.416667
Austrolebias nigrofasciatus	Padre Doutourb	-31.806944	-52.419722
Austrolebias nigrofasciatus	temporary pool, road BR-116, 43 km NE of Arroio Grande;	-31.952762	-52.767024

Austrolebias nonoiuliensis	9 de Julio /OR/ Next to 9 de Julio City, Buenos Aires Province, Argentina /OR/ Nueve de Julio, provincia de Buenos Aires, Argentina /OR/ Nuevo de Julio /OR/ SÌÏDAMERIKA, OSO-, ARGENTINIEN, O-, BUENOS AIRES, NUEVE DE JULIO, NAC.RT. 5 ,	-35.507206	-60.921723
Austrolebias paranaensis	Ayolas /OR/ r'o Paran‡, about 2 km E of Ayolas	-27.355124	-56.772999
Austrolebias patriciae	5 km S of Ramanso in the road to Clorinda	-25.189932	-57.613578
Austrolebias patriciae	Prov'ncia de Presidente Hayes, Paraguay	-25.25	-57.67
Austrolebias patriciae	Ditch along the road to Clorinda, Presidente Hayes Prov., ca. 500 m	-25.255939	-57.715748
Austrolebias patriciae	El Fiscal AAK 12/13\	-26.6506	-58.7881
Austrolebias patriciae	Zapir‡n AAK 12/11\	-26.862193	-58.760311
Austrolebias patriciae	R'o de Oro /OR/ Rio de Oro, Ruta 11 /OR/ \ Rio de Oro AAK 12/07\	-26.880508	-58.77761
Austrolebias patriciae	Gral. Vedia /OR/ Vedia	-26.920859	-58.650082
Austrolebias patriciae	Las Palmas	-27.050503	-58.924423
Austrolebias patriciae	Makalle Sur AAK 12/19\	-27.228471	-59.274578
Austrolebias patriciae	Colonia Benitez AAK 12/26\	-27.330226	-58.924836
Austrolebias patriciae	Fontana /OR/ Fontana, Chaco, Argentina /OR/ Fontana AAK 11/02\	-27.405779	-59.031598
Austrolebias patriciae	Cruce Rutas 11 y 16 Chaco AAK 12/09\	-27.410668	-58.996658
Austrolebias patriciae	Rio Tragadero AAK 12/18\	-27.451422	-58.881582
Austrolebias patriciae	Ruta 34 KM 274 Palacios	-30.820206	-61.601825
Austrolebias patriciae	Tacural /OR/ Tacural, Santa FŽ Province, Argentina	-30.850671	-61.578978
Austrolebias paucisquama	S‹o SepŽ	-30.374167	-53.561667
Austrolebias periodicus	6 km W of Ros‡rio do Sul, rio Ibicu' de Armada drainage, road BR-290	-30.238	-55.007
Austrolebias periodicus	Santo Ant™nio floodplains, a tributary of rio Ibicu' de Armada	-30.302325	-54.992088
Austrolebias periodicus	Las Cabas /OR/ Las Cavas /OR/ Las Cavas Artigas /OR/ Las Cavas, r'o Cuareim drainage, r'o Uruguay basin /OR/ r'o Cuareim, tributary of the r'o Uruguay, near Artigas, Uruguay	-30.416667	-56.4505
Austrolebias periodicus	Swamp 300 m of rio Ibirapuit‹	-30.553611	-55.672778
Austrolebias periodicus	Dom Pedrito /OR/ road BR-293, 4 km W from Dom Pedrito	-30.9432	-54.729

Austrolebias periodicus	5km north of the Passo do Valente	-31.416667	-54.133333
Austrolebias prognathus	Road 19 km close to San Luis stream /OR/ Rocha, San Luis /OR/ Ruta19 San Luis /OR/ San Luis /OR/ San Luis, Ruta 19, km 29.5; /OR/ Merin Lagoon Drainage: Route 19 San Luis creek	-33.60083333	-53.72472222
Austrolebias prognathus	Los Naranjales /OR/ Los Naranjales Rio Cebollat'	-33.617538	-54.331414
Austrolebias prognathus	Arroyo Chui Floodplains	-33.6805	-53.4353
Austrolebias prognathus	San Miguel	-33.688879	-53.534768
Austrolebias prognathus	CIMC 8586, charco na v‡rzea do arroio Chu' /OR/ CIMC 8626, coletado no mesmo local do lote CIMC 8593 /OR/ CIMC 8899, charco marginal ao arroio Chu' /OR/ CIMC 8928, charco marginal ao arroio Chu'	-33.695397	-53.439636
Austrolebias prognathus	Las Maravillas /OR/ Maravillas floodplains /OR/ Maravillas floodplains at Ruta 14, 13 km from the Ruta 9	-33.903786	-53.67892
Austrolebias prognathus	Canal Andreoni /OR/ Rocha: temporary swamp near canal Andreoni /OR/ Ruta14 KM 504 /OR/ temporary swamp near canal Andreoni /OR/ Temporary swamp near Canal Andreoni, Ruta 14, km 504	-33.920167	-53.5435
Austrolebias prognathus	Salamanca	-34.10536	-54.60083
Austrolebias quirogai	Acegu‡P1	-31.736111	-54.019167
Austrolebias quirogai	Acegu‡P2	-31.763611	-54.036389
Austrolebias quirogai	Acegu‡P3	-31.765	-54.039444
Austrolebias reicherti	Road 26 5 km from Rio Branco city	-32.57611111	-53.43888889
Austrolebias reicherti	Road to Lago Mer'n town	-32.70111111	-53.30888889
Austrolebias reicherti	Laguna Mer'n	-32.734722	-53.258333
Austrolebias reicherti	Paso del Dragon /OR/ Paso del Drag—n /OR/ Paso Del Dragon /OR/ temporary pool near r'o Tacuar', Paso del Drag—n /OR/ R.18 Km.370 Paso del drag—n	-32.765833	-53.719833
Austrolebias reicherti	Road 18 km 369.5 /OR/ Merin Lagoon Drainage: Route 18 km 369.\5	-32.78083333	-53.64444444
Austrolebias reicherti	north of Vergara /OR/ Road 18 close to Vergara town /OR/ Vergara	-32.9225	-53.91361111
Austrolebias reicherti	Road 91, 39 km North of Charqueada town	-33.02611111	-53.87944444
Austrolebias robustus	PerezMiles1	-34.95	-59.12
Austrolebias robustus	PerezMiles2	-35.92	-60.64
Austrolebias robustus	General Conesa /OR/ Ruta Prov. 11 - Gral. Conesa	-36.487279	-57.326809

Austrolebias robustus	Los Yngleses /OR/ Cabo San Antonio /OR/ Cabo San Antonio, Argentina	-36.511275	-56.817273
Austrolebias robustus	Las Armas	-37.117097	-57.823499
Austrolebias robustus	13 from the Ruta 2, Vivorat‡ /OR/ Argentina: Prov'ncia de Buenos, arroyo Vivorat‡ /OR/ arroyo Vivorat‡, Mar Chiquita, Provincia de Buenos Aires, Argentina /OR/ Ruta Nacional 2 km276 Near arroyo vivorata /OR/ small road 13 km from Ruta Nacional 2, near arroyo Vivorat‡ /OR/ Viborota City, Buenos Aires Province, Argentina /OR/ Vivorata /OR/ km 276, road Ruta Nacional 2, near arroyo Vivorat‡	-37.660289	-57.670694
Austrolebias robustus	Mar Chiquita	-37.739777	-57.452158
Austrolebias robustus	Alzaga	-37.864088	-59.95103
Austrolebias robustus	Alzaga	-37.864088	-59.95103
Austrolebias robustus	A¡ Malacara	-38.322209	-58.327314
Austrolebias robustus	Ruta 88 Km74 /OR/ Ruta88km74	-38.324558	-58.334037
Austrolebias toba	R'o de Oro /OR/ Rio de Oro, Ruta 11 /OR/ \ Rio de Oro AAK 12/07\	-26.880508	-58.77761
Austrolebias toba	Puerto Bermejo /OR/ Puerto Bermejo, Chaco, Argentina /OR/ Rio Bermejo /OR/ Ruta 3, Puerto Bermejo	-26.924858	-58.510875
Austrolebias univentripinnis	Telho /OR/ Telho, about 21 km from the city of Jaguar‹o /OR/ temporary swamp near arroio Telho, Jaguar‹o	-32.378828	-53.444228
Austrolebias univentripinnis	rua 27 de novembro, between the second and third bridge, about 10 km from the road BR-116, Jaguar‹o /OR/ rua 27 de Novembro, between the second and the third bridge, about 10 km from the road BR-116	-32.473899	-53.435301
Austrolebias univentripinnis	laguna dos Patos system, Jaguar‹o, Rio Grande do Sul, Brazil	-32.555431	-53.408771
Austrolebias vandenbergi	Isoce–o community of Kuaridenda-1	-19.17336	-62.58801
Austrolebias vandenbergi	Isoce–o community of Kuaridenda-2	-19.1763	-62.5892
Austrolebias vandenbergi	R'o Paraguay drainage: 2.6 km from Madrej—n on road to Filadelfia	-20.652336	-59.881508
Austrolebias vandenbergi	R'o Paraguay drainage: 4.7 km on road from Madrej—n to Filadelfia	-20.705694	-59.887671
Austrolebias vandenbergi	faro moro	-21.718198	-59.916417
Austrolebias vandenbergi	N. W. Mariscal /OR/ RÌÄå_o Paraguay drainage: roadside pond 35km NW of Mariscal Estigarribia /OR/ R'o Paraguay drainage: roadside pond 35km NW of Mariscal Estigarribia	-21.8331	-60.8608
Austrolebias vandenbergi	RÌÄå_o Paraguay drainage: 53km NNE of Filadelfia on road to FortÌÄå_n MadrejÌÄå_n, about 1km S of Col. Jesudi-ar /OR/ R'o Paraguay drainage: 53km NNE of Filadelfia on road to Fort'n Madrej—n, about 1km S of Col. Jesudi-ar /OR/ 53 km	-21.8803	-59.9397

	N.N.E. Filadelfia to Fortin Madrejon		
Austrolebias vandenbergi	Santa Mar’a	-22.167129	-62.812397
Austrolebias vandenbergi	RÌÄå_o Paraguay drainage: Estancia Aroma, roadside pond/ditch at crossroad to road Filadelfia - FortÌÄå_n Teniente /OR/ RÌ_o Paraguay drainage: Estancia Aroma, roadside pond/ditch at crossroad to road Filadelfia - FortÌ_n Teniente	-22.179916	-60.070551
Austrolebias vandenbergi	Fort’n Teniente /OR/ RÌÄå_o Paraguay drainage: roadside pond + small ditch at road Filadelfia - FortÌÄå_n Teniente /OR/ RÌ_o Paraguay drainage: roadside pond + small ditch at road Filadelfia - FortÌ_n Teniente	-22.2364	-60.0611
Austrolebias vandenbergi	Fortin Toledo /OR/ Province of Presidente Hayes, near Fort’n Toledo /OR/ RÌÄå_o Paraguay drainage: near FortÌÄå_n Toledo /OR/ RÌ_o Paraguay drainage: near FortÌ_n Toledo /OR/ Toledo /OR/ Toledo (LV23), N.W. Paraguay	-22.27	-60.54
Austrolebias vandenbergi	Finca Alcoba	-22.446919	-63.592623
Austrolebias vandenbergi	Ruta 81 km 1841	-23.099813	-63.806762
Austrolebias vandenbergi	Ruta 81 km 1840	-23.114438	-63.777923
Austrolebias vandenbergi	Ruta 81km 1832	-23.159902	-63.68894
Austrolebias vandenbergi	Hickmann /OR/ Hickmann, northern Argentina /OR/ Ruta Nacional 81, Hickmann /OR/ \ Puente de Hickmann AAK 13/37\ /OR/ \ Puente de Hickmann AAK 13/37\	-23.209801	-63.573449
Austrolebias vandenbergi	Dragones /OR/ \ Dragones AAK 13/39\	-23.244934	-63.361703
Austrolebias vandenbergi	Luna Muerta, San Mart’n	-23.332689	-63.622926
Austrolebias vandenbergi	Pluma de Pato	-23.366095	-63.10844
Austrolebias vandenbergi	Ruta 13, Charco 1	-23.80175	-63.5526944
Austrolebias vandenbergi	Las Moras	-23.836128	-63.453686
Austrolebias vandenbergi	Ingeniero Juarez /OR/ Ingeniero Ju‡rez	-23.922836	-61.869287
Austrolebias vandenbergi	Laguna Yema /OR/ Laguna Yema, Dto Bermejo, Formosa, Argent.	-24.315091	-61.161047
Austrolebias vandenbergi	Palo borrachio, Rivadavia	-24.3615278	-62.9894722
Austrolebias vandenbergi	Ruta Provincial 52, General de San Martin	-24.682997	-63.961733
Austrolebias vandenbergi	Ituzaing—	-27.6	-56.683333
Austrolebias varzeae	Fazenda dos Branda /OR/ Fazenda dos Branda, Carazinho, rio Uruguay basin	-28.269102	-52.671914
Austrolebias vazferreirai	5km north of the Passo do Valente	-31.416667	-54.133333

Austrolebias vazferreirai	Ansina	-31.884667	-55.492
Austrolebias vazferreirai	Banado de los Cinco Sauces, Route 26	-32.089794	-55.152868
Austrolebias vazferreirai	Banado de los Cinco Sauces, Route 26	-32.089794	-55.152868
Austrolebias vazferreirai	Ruta 26, km 331 /OR/ Ruta 26 km 331 /OR/ Ruta 26, km 331 /OR/ Tacuaremb—: Ruta 26, km 331, r'o Negro drainage, r'o Uruguay basin /OR/ temporary swamp in, ca–ada Los Cinco Sauces, rio Negro system [r'o Uruguay basin], km 331 of the road Ruta 26, Departamento de Tacuaremb—,northeastern Uruguay /OR/ Ruta26KM331	-32.090833	-55.148333
Austrolebias vazferreirai	Paso de Mazangano, Ruta 44 /OR/ Paso de Mazangano, Ruta 44, r'o Negro floodplains /OR/ temporary pool near r'o Negro, Paso de Mazangano, Ruta 44 /OR/ Paso de Mazangano, Ruta 44	-32.111333	-54.666
Austrolebias vazferreirai	AJH1 /OR/ AJH2	-32.112194	-54.665444
Austrolebias vazferreirai	km 44 of the road Ruta 44, from Melo to Rivera , Departamento Cerro-Largo, North Eastern, Uruguay, r'o Negro drainage, r'o Uruguay basin /OR/ Ruta 44 km 44.4 /OR/ Uruguay: Cerro Largo, Ruta 44, km 44.4, r'o Negro drainage, r'o Uruguay basin	-32.173	-54.5345
Austrolebias vazferreirai	AJH3	-32.173361	-54.534611
Austrolebias vazferreirai	Ruta 26 y R'o Negro	-32.286702	-54.821146
Austrolebias vazferreirai	Ruta 26, km 372 /OR/ Ruta 26, km 372 /OR/ Ruta 26, km 372, r'o Negro drainage, r'o Uruguay basin /OR/ Ruta26KM372	-32.288167	-54.8045
Austrolebias vazferreirai	Ba–ados Conventos /OR/ Ba–ados Conventos, r'o Tacuar' basin	-32.353333	-54.237
Austrolebias vazferreirai	Melo, Parque Rivera, r'o Tacuar' drainage, laguna dos Patos system /OR/ Parque de Rivera /OR/ Parque Rivera /OR/ temporary pool in Parque Rivera, Melo	-32.374333	-54.188667
Austrolebias vazferreirai	Melo, Parque Rivera, r'o Tacuar' drainage, laguna dos Patos system /OR/ Parque de Rivera /OR/ Parque Rivera /OR/ temporary pool in Parque Rivera, Melo	-32.374333	-54.188667
Austrolebias vazferreirai	Melo /OR/ Melo, r'o Tacuar' drainage, laguna dos Patos system	-32.3745	-54.205333
Austrolebias vazferreirai	Banado Medina	-32.397455	-54.352614
Austrolebias viarius	Road 8 close to Piraraj‡ stream	-33.70861111	-54.713056
Austrolebias viarius	Road 9 km 272d	-34.21222222	-53.77527778
Austrolebias viarius	Road 9 km 272c	-34.21527778	-53.72111111
Austrolebias viarius	Castillos /OR/ Castillos /OR/ Ruta 9, km 254.8 /OR/ R9 Km 254 Castillos /OR/ Ruta 9 Castillos /OR/ Ruta 9 Km 254.5 /OR/ Ruta 9, km 254.8 /OR/ Rutal 9 Castillos /OR/ temporary pool, near Ruta 9, km 254.8	-34.2205	-53.954333
Austrolebias viarius	Road 16 km 2.5	-34.27166667	-53.79944444

Austrolebias viarius	arroyo Valizas and balneario Aguas Dulces	-34.273329	-53.797711
Austrolebias viarius	Cruce Ruta 10 Y Ruta 16, Departamento De Rocha, Uruguay. Basin: Laguna Castillos, Oceano Atlantico. /OR/ Road 10 and Road 16	-34.27333333	-53.7975
Austrolebias viarius	temporary swamp in Barra de Valisas	-34.322333	-53.822667
Austrolebias viarius	temporary swamp near arroyo Valizas, Ruta 10, km 267	-34.359167	-53.844
Austrolebias viarius	Arroyo Valisas /OR/ Arroyo Valizas /OR/ Ruta 10 Km 268 /OR/ Ruta 10, close to arroyo Valizas; /OR/ Temporary swamp near arroyo Valizas, Ruta 10, km 267 /OR/ Temporary swamp near arroyo, Valizas, Rocha, Uruguay /OR/ Valisas /OR/ Valizas /OR/ Valizas, Ruta 10 Km 267	-34.359221	-53.844422
Austrolebias viarius	Road 10 km 266.5	-34.36916667	-53.84222222
Austrolebias viarius	Cabo Polonio	-34.380907	-53.844207
Austrolebias viarius	Road 9 km 228.5 /OR/ Castillos Lagoon Drainage: Route 9 km 228.5	-34.40277778	-54.12388889
Austrolebias viarius	Ruta 9 Km 227	-34.411407	-54.131858
Austrolebias viarius	R.9 Km. 229	-34.41556	-54.09139
Austrolebias viarius	Ruta 10 Km 259	-34.433881	-53.915597
Austrolebias viarius	R.10 Km.25.700	-34.44949	-53.94152
Austrolebias viarius	Road 10 km 253.5	-34.4525	-53.94361111
Austrolebias viarius	Road 10 km 250 /OR/ Ruta 10 Km 250	-34.47638889	-53.99722222
Austrolebias viarius	Rocha R-9, Km 205 /OR/ Ruta 9 km 205 /OR/ Ruta 9, km 205 /OR/ Ruta 9, Km. 205 /OR/ Rocha Lagoon Drainage: Route 9 km 205	-34.502667	-54.334333
Austrolebias wolterstorffi	S‹o Leopoldo /OR/ temporary swamp near the road BR-116, S‹o Leopoldo	-29.73821	-51.131927
Austrolebias wolterstorffi	rio Ca' floodplains, rio Jacu' basin, road Taba'-Canoas, km 427, Triunfo	-29.815113	-51.410413
Austrolebias wolterstorffi	Cachoeirinha, swamp near the road BR-290, km 82, rio Gravata' floodplains	-29.957028	-51.083638
Austrolebias wolterstorffi	temporary swamp at rio Gravata' floodplains, near the road RS-118 and about 500 m from the road BR-290	-29.9636116	-51.01166534
Austrolebias wolterstorffi	Brazil: Rio Grande do Sul: laguna dos Patos system, Porto Alegre /OR/ Porto Alegre /OR/ Porto Alegre, Rio Grande do Sul, Brazil /OR/ SÌÏDAMERIKA, OSO-, BRASILIEN, OSO-, PORTO ALEGRE* ,	-29.964404	-51.132673
Austrolebias wolterstorffi	Lagoa do Peixe National Park	-31.115278	-50.849167
Austrolebias wolterstorffi	Pontal da Barra, praia de Laranjal, Pelotas /OR/ Ponta de Barra /OR/ temporary pool in	-31.7651	-52.2414

	Pontal da Barra, praia de Laranjal, canal de S‹o Gon□alo floodplains, Pelotas		
Austrolebias wolterstorffi	wetland between S‹o Gon□alo channel and Pelotas stream	-31.778611	-52.266944
Austrolebias wolterstorffi	temporary swamp in S‹o Caetano, 20 km NE of S‹o JosŽ do Norte /OR/ temporary swamp in S‹o Caetano, 20 km NE S‹o JosŽ do Norte	-31.894128	-51.910864
Austrolebias wolterstorffi	swamp close to the road BR-471, Vila do Povo Novo, Rio Grande	-31.933176	-52.312237
Austrolebias wolterstorffi	Mata Paludosa estudada.	-32.128797	-52.151288
Austrolebias wolterstorffi	ÔEstrada VelhaÕ	-32.129389	-52.153083
Austrolebias wolterstorffi	arroyo Yerbal /OR/ Uruguay: Treinta y Tres: temporary swamp close to arroyo Yerbal	-33.221667	-54.398833
Austrolebias wolterstorffi	El bagre	-33.615001	-54.323604
Austrolebias wolterstorffi	Canal Andreoni /OR/ Rocha: temporary swamp near canal Andreoni /OR/ Ruta14 KM 504 /OR/ temporary swamp near canal Andreoni /OR/ Temporary swamp near Canal Andreoni, Ruta 14, km 504	-33.920167	-53.5435
Austrolebias wolterstorffi	R.9 Km.310	-33.92988	-53.53742
Austrolebias wolterstorffi	arroyo India Muerta floodplains, 150 m from bridge on Ruta 13 and 50 m from the road to Southeast, near Vel‡zquez, Rocha, Uruguay /OR/ Velasquez /OR/ Velazquez	-34.056	-54.243167

Table S2.5 Maximum standard length measurements and their sources

Species	SL (mm)	Source
affinis	32.3	Costa, W., 2006. The South American annual killifish genus Austrolebias (Teleostei: Cyprinodontiformes: Rivulidae): phylogenetic relationships, descriptive morphology and taxonomic revision. Zootaxa.
alexandrii	43	Costa, W., 2006. The South American annual killifish genus Austrolebias (Teleostei: Cyprinodontiformes: Rivulidae): phylogenetic relationships, descriptive morphology and taxonomic revision. Zootaxa.
arachan	44	Loureiro, M., M. de las M. Azpelicueta and G. Garcia, 2004. Austrolebias arachan (Cyprinodontiformes, Rivulidae), a new species of annual fish from northeastern Uruguay. Rev. Suisse Zool. 111(1):21-30.
bellottii	84	Costa, W., 2006. The South American annual killifish genus Austrolebias (Teleostei: Cyprinodontiformes: Rivulidae): phylogenetic relationships, descriptive morphology and taxonomic revision. Zootaxa.
charrua	47.2	Costa, W., 2006. The South American annual killifish genus Austrolebias (Teleostei: Cyprinodontiformes: Rivulidae): phylogenetic relationships, descriptive morphology and taxonomic revision. Zootaxa.
cheradophilus	95.07	Tom JM Van Dooren Field Experiment 2008
durazensis	34.8	Costa, W., 2006. The South American annual killifish genus Austrolebias (Teleostei: Cyprinodontiformes: Rivulidae): phylogenetic relationships, descriptive morphology and taxonomic revision. Zootaxa.
elongatus	151.9	Costa, W., 2006. The South American annual killifish genus Austrolebias (Teleostei: Cyprinodontiformes: Rivulidae): phylogenetic relationships, descriptive morphology and taxonomic revision. Zootaxa.
gymnoventris	30.8	Costa, W., 2006. The South American annual killifish genus Austrolebias (Teleostei: Cyprinodontiformes: Rivulidae): phylogenetic relationships, descriptive morphology and taxonomic revision. Zootaxa.
juanlangi	33.7	Costa, W., 2006. The South American annual killifish genus Austrolebias (Teleostei: Cyprinodontiformes: Rivulidae): phylogenetic relationships, descriptive morphology and taxonomic revision. Zootaxa.
luteoflammulatus	48.3	Costa, W., 2006. The South American annual killifish genus Austrolebias (Teleostei: Cyprinodontiformes: Rivulidae): phylogenetic relationships, descriptive morphology and taxonomic revision. Zootaxa.
melanoorus	50	Costa, W., 2006. The South American annual killifish genus Austrolebias (Teleostei: Cyprinodontiformes: Rivulidae): phylogenetic relationships, descriptive morphology and taxonomic revision. Zootaxa.
monstrosus	150	Osinaga, K., 2006. Nuevo registro para Bolivia de Austrolebias monstrosus (Huber, 1995 Rivulidae). Kempffiana.
nigripinnis	46.6	Huber, J.H., 1996. Killi-Data 1996. Updated checklist of taxonomic names, collecting localities and bibliographic references of oviparous Cyprinodont fishes (Atherinomorpha, Pisces). Societe Francaise d'Ichtyologie, Museum National d'Histoire Naturelle, Paris, France, 399 p.
patriciae	41	Costa, W., 2006. The South American annual killifish genus Austrolebias (Teleostei: Cyprinodontiformes: Rivulidae): phylogenetic relationships, descriptive morphology and taxonomic revision. Zootaxa.
paucisquama	34.2	Ferrer, J., Malabarba, L.R. & Costa, W.J.E.M., 2007. Austrolebias paucisquama (Cyprinodontiformes: Rivulidae), a new species of annual killifish from southern Brazil. Neotropical Ichthyology, 6(2), pp.175-180.

periodicus	40.5	Perujo, E., Calvino, P.A. & Salvia, H., 2005. Austrolebias luzardoi (Cyprinodontiformes: Rivulidae), una especie nueva de pez anual de la cuenca del rio Cuareim, Repœblica Oriental del Uruguay. Volcan, M.V., LanŽs, L. & Goncalves, C., 2010. Pisces, Cyprinodontiformes, Rivulidae, Austrolebias periodicus (Costa, 1999): Distribution extension in state of Rio Grande do Sul, southern Brazil. CheckList.
prognathus	130	Volcan, M. V. Photo
robustus	72	Killi Club Argentino January 2003
reicherti	45.9	Costa, W., 2006. The South American annual killifish genus Austrolebias (Teleostei: Cyprinodontiformes: Rivulidae): phylogenetic relationships, descriptive morphology and taxonomic revision. Zootaxa.
toba	45.5	Costa, W., 2006. The South American annual killifish genus Austrolebias (Teleostei: Cyprinodontiformes: Rivulidae): phylogenetic relationships, descriptive morphology and taxonomic revision. Zootaxa.
vandenbergi	76	Photo, Halbluetzel, P., http://www.fishbase.de/summary/Austrolebias-vandenbergi.html accessed 11.10.14
vazferreirai	83.2	Costa, W., 2006. The South American annual killifish genus Austrolebias (Teleostei: Cyprinodontiformes: Rivulidae): phylogenetic relationships, descriptive morphology and taxonomic revision. Zootaxa.
viarius	61	Costa, W., 2006. The South American annual killifish genus Austrolebias (Teleostei: Cyprinodontiformes: Rivulidae): phylogenetic relationships, descriptive morphology and taxonomic revision. Zootaxa.
wolterstorffi	77.5	Costa, W., 2006. The South American annual killifish genus Austrolebias (Teleostei: Cyprinodontiformes: Rivulidae): phylogenetic relationships, descriptive morphology and taxonomic revision. Zootaxa.

Table S2.6 Output from Maxent run. Training area under curve (AUC), Test AUC and 10 percentile threshold.

Species	Training AUC	Test AUC	10 Percentile Threshold
affinis	0.9977	0.9882	0.4423
alexandri	0.9934	0.9887	0.2795
arachan	0.9987	0.9982	0.4224
bellottii	0.986	0.9758	0.2133
charrua	0.9976	0.9973	0.4462
cheradophilus	0.9982	0.998	0.3727
duraznensis	0.995	0.9307	0.4797
elongatus	0.9924	0.9902	0.1618
gymnoventris	0.9985	0.9956	0.4945
juanlangi	0.9979	0.9976	0.295
luteoflammulatus	0.9975	0.9973	0.4037
melanoorus	0.9881	0.9831	0.5001
monstrosus	0.9864	0.9445	0.2042
nigripinnis	0.9886	0.9846	0.257
patriciae	0.9905	0.9875	0.2204
periodicus	0.9876	0.9808	0.4096
prognathus	0.9989	0.9982	0.2049
reicherti	0.9991	0.9988	0.4413
robustus	0.9875	0.9771	0.2426
vandenbergi	0.9889	0.9561	0.2589
vazferreirai	0.9966	0.9953	0.239
viarius	0.9987	0.9982	0.5575
wolterstorffi	0.9957	0.9943	0.3006

Appendix II Supplementary material for chapter 3

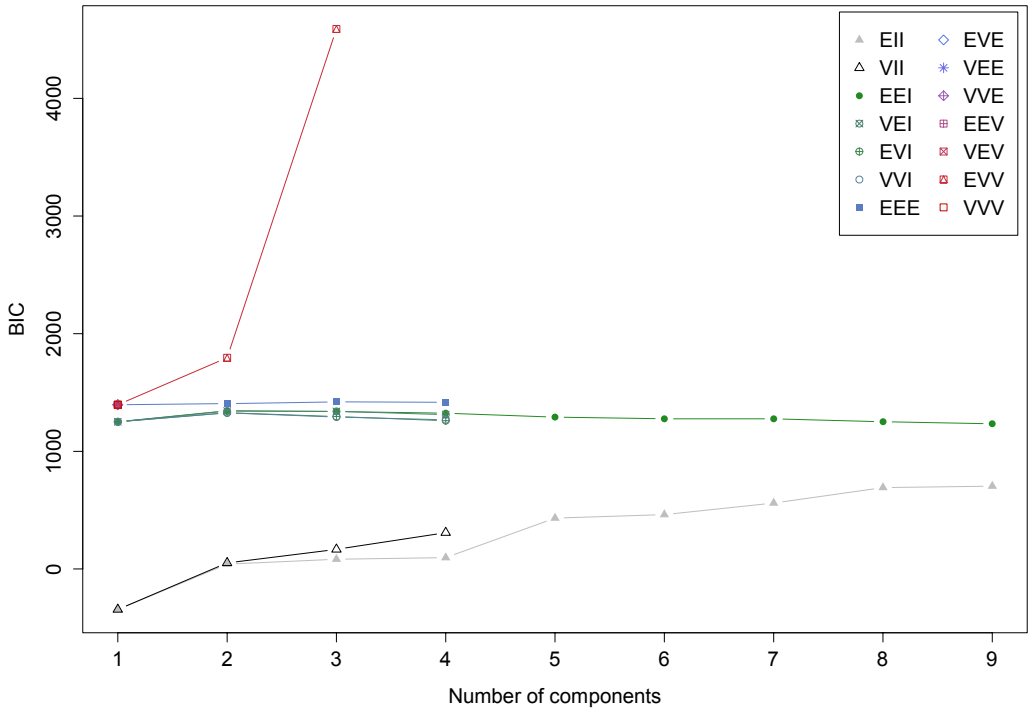

Figure S3.1 Bayesian information criterion (BIC) for parameterised normal mixtures models fitted for size and shape data. Results indicate that a model three components is best.

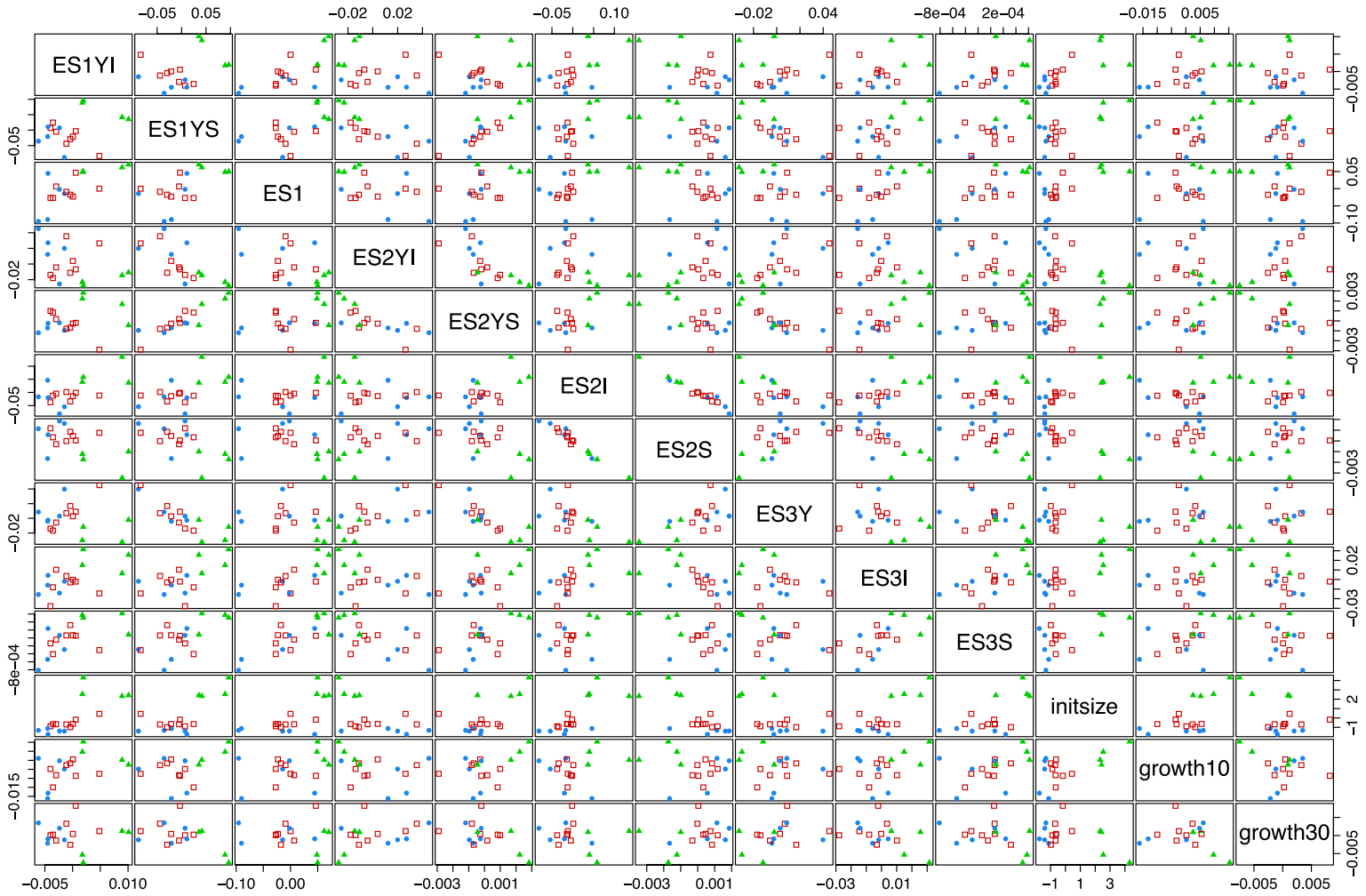

Figure S3.2 Mixture analysis using best fitting model of three clusters for all size and shape variables. Clusters denoted by colour.

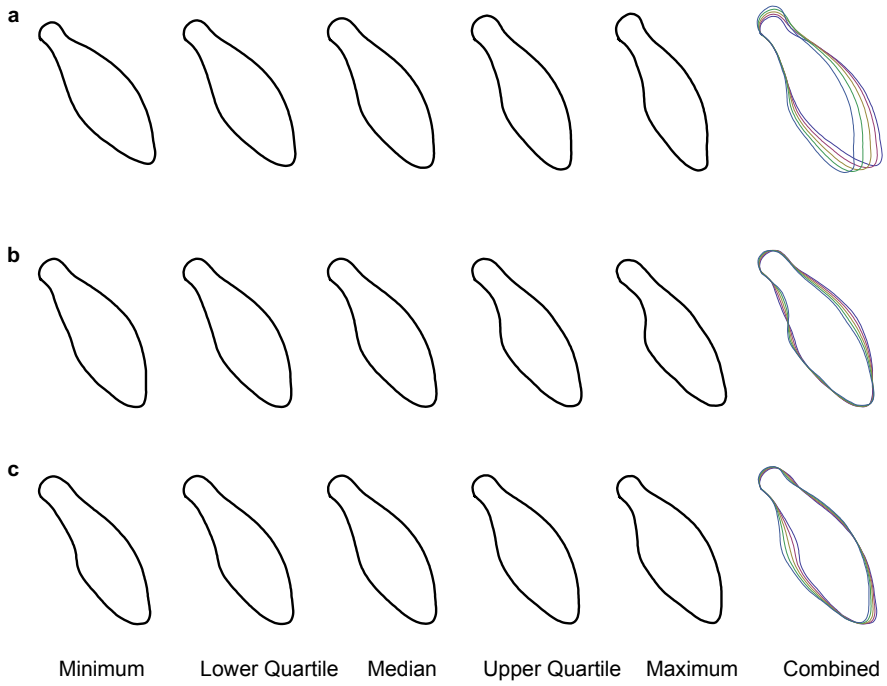

Fig S3.3 Models of eigenshape vectors from field data. (**a**) ES1, (**b**) ES2 and (**c**) ES3 that explain a total of 48.6% of the shape variation in field caught *Austrolebias* adult males.

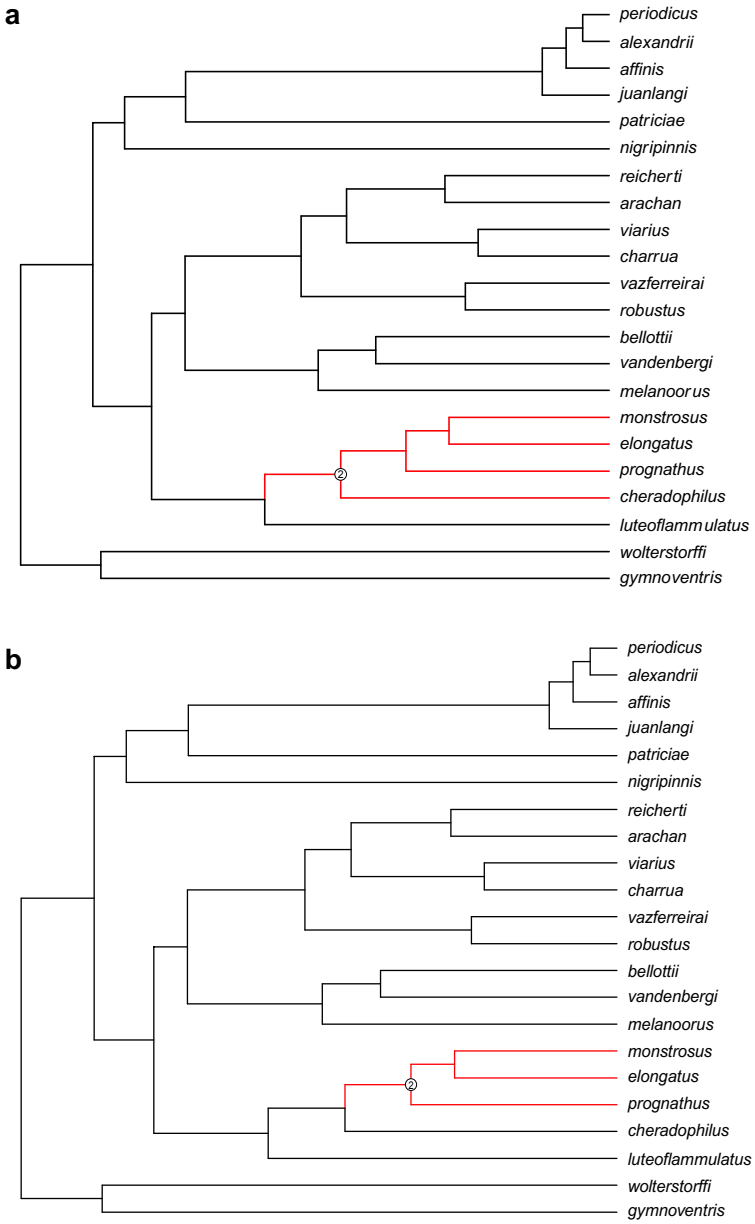

Figure S3.4 Phylogenetic trees of *Austrolebias* showing regime shifts in size and shape identified using the program SURFACE. Panel (a) shows a single regime shift identified using size and shape data taken from field caught adult males. Panel (b) shows the regime shift returned for only size data of field caught adult males.

Appendix III Supplementary material for chapter 4

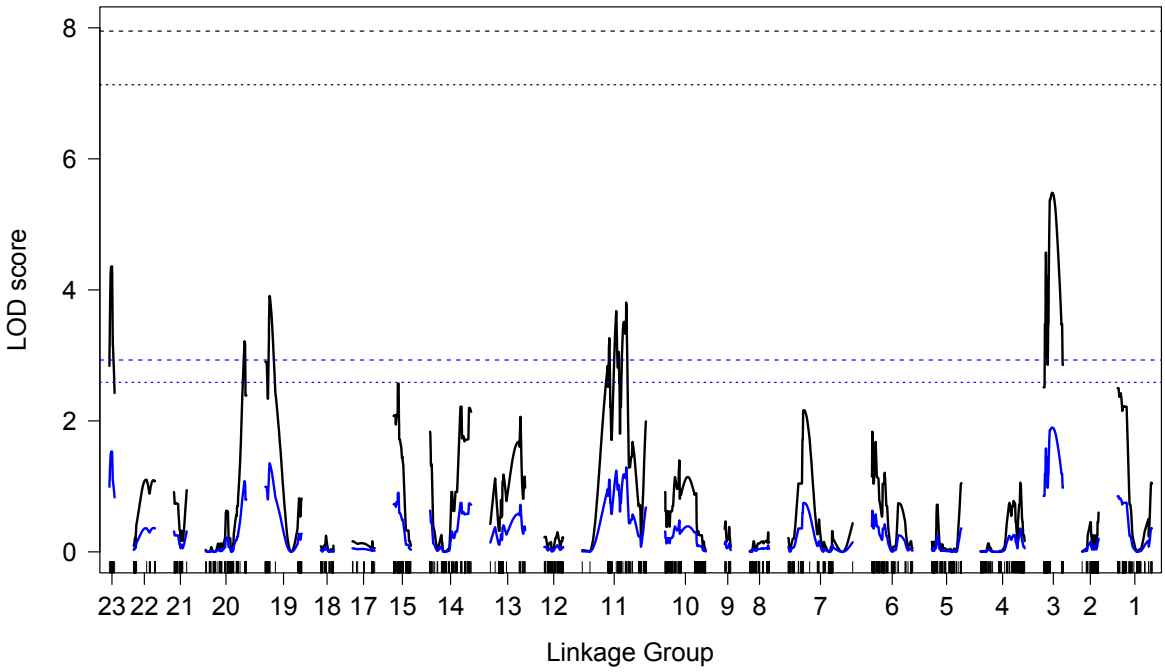

Figure S4.1 Plots of the LOD curves for a genome scan using the single-QTL model, for each linkage group in the paternal map. In black are the LOD curves for the non-parametric model and in blue are the curves for the binary model. Dashed lines represent the 5% LOD threshold calculated from a permutation test using 10000 permutations; dotted lines represent the 10% threshold.

Figure S4.2 Heat maps depicting pairwise recombination fractions (upper left triangle of each box) and LOD scores (lower right triangle) for all 22 linkage groups of the paternal map. LOD score tests the null hypothesis that the recombination fraction between two markers is 0.5. Low recombination fraction/high LOD score is shaded in red and high recombination fraction/low LOD score is shaded in blue. Extensive recombination suppression is revealed across the paternal map.

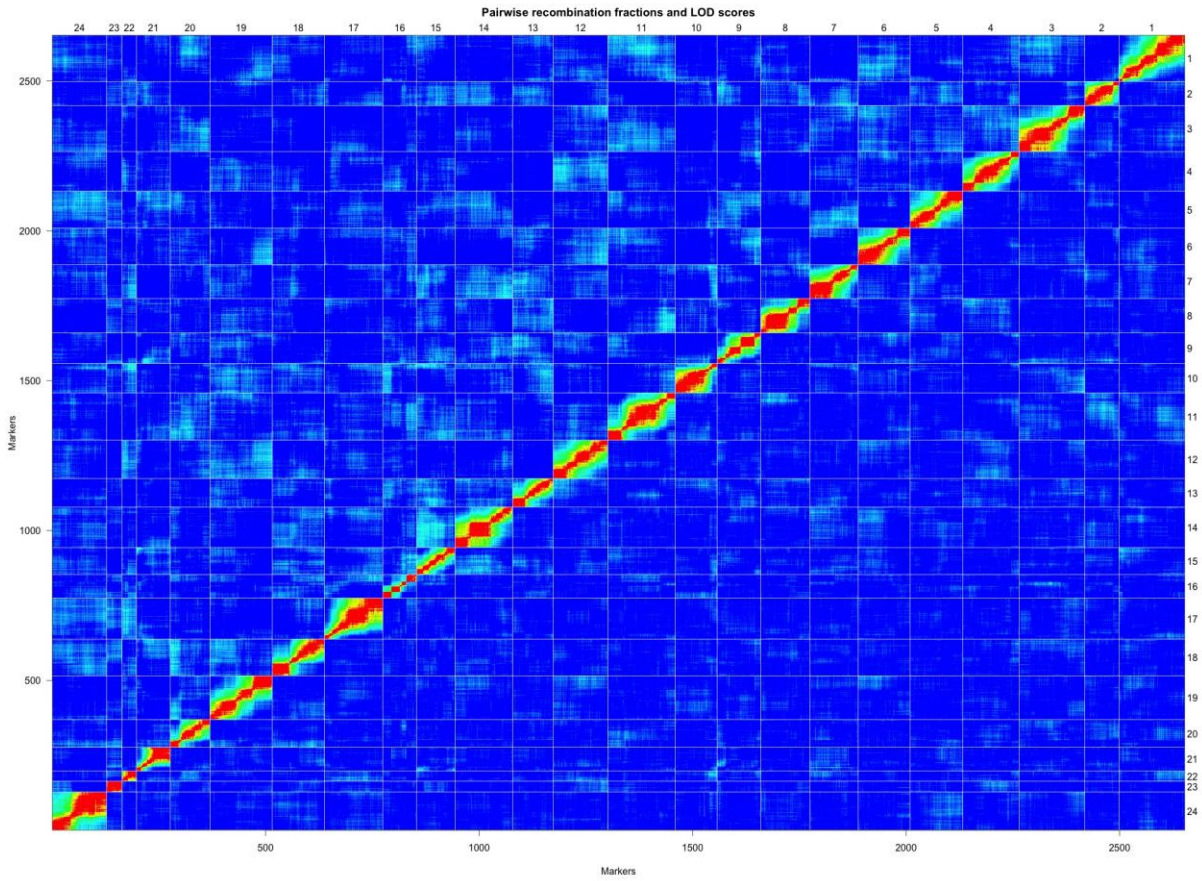

Figure S4.3 Heat maps depicting pairwise recombination fractions (upper left triangle of each box) and LOD scores (lower right triangle) for all 24 linkage groups of the maternal map. LOD score tests the null hypothesis that the recombination fraction between two markers is 0.5. Low recombination fraction/high LOD score is shaded in red and high recombination fraction/low LOD score is shaded in blue. Extensive recombination suppression is revealed across the paternal map.

Table S4.1 Shared markers among male and female linkage maps and the maternal and paternal linkage groups (LGs) on which they were mapped.

Locus	Paternal LG	Maternal LG
27650	1	14
1195	1	9
27863	1	9
64783	1	9
85412	1	9
51559	2	6
65519	2	6
75875	2	6
32464	4	11
41847	4	11
45593	4	11
54232	4	11
60438	4	11
77896	4	11
64694	5	4
94000	5	4
44074	6	20
66682	6	20
76266	6	20
31762	7	21
6165	8	1
61751	8	1
66743	8	1
80810	9	12
38643	10	16
76226	10	15
31384	11	7
32253	11	7
61508	11	7
21987	12	5
36012	12	5
37851	12	5
63131	12	5
68561	12	5
69658	12	5
91932	12	5

50965	13	19
56125	13	15
68062	13	15
91993	13	15
5071	14	10
38324	15	19
65531	15	19
33413	18	14
39333	18	14
63802	18	14
68856	18	14
70965	21	6
96653	22	23
88057	23	13

Appendix IV Supplementary material for chapter 5

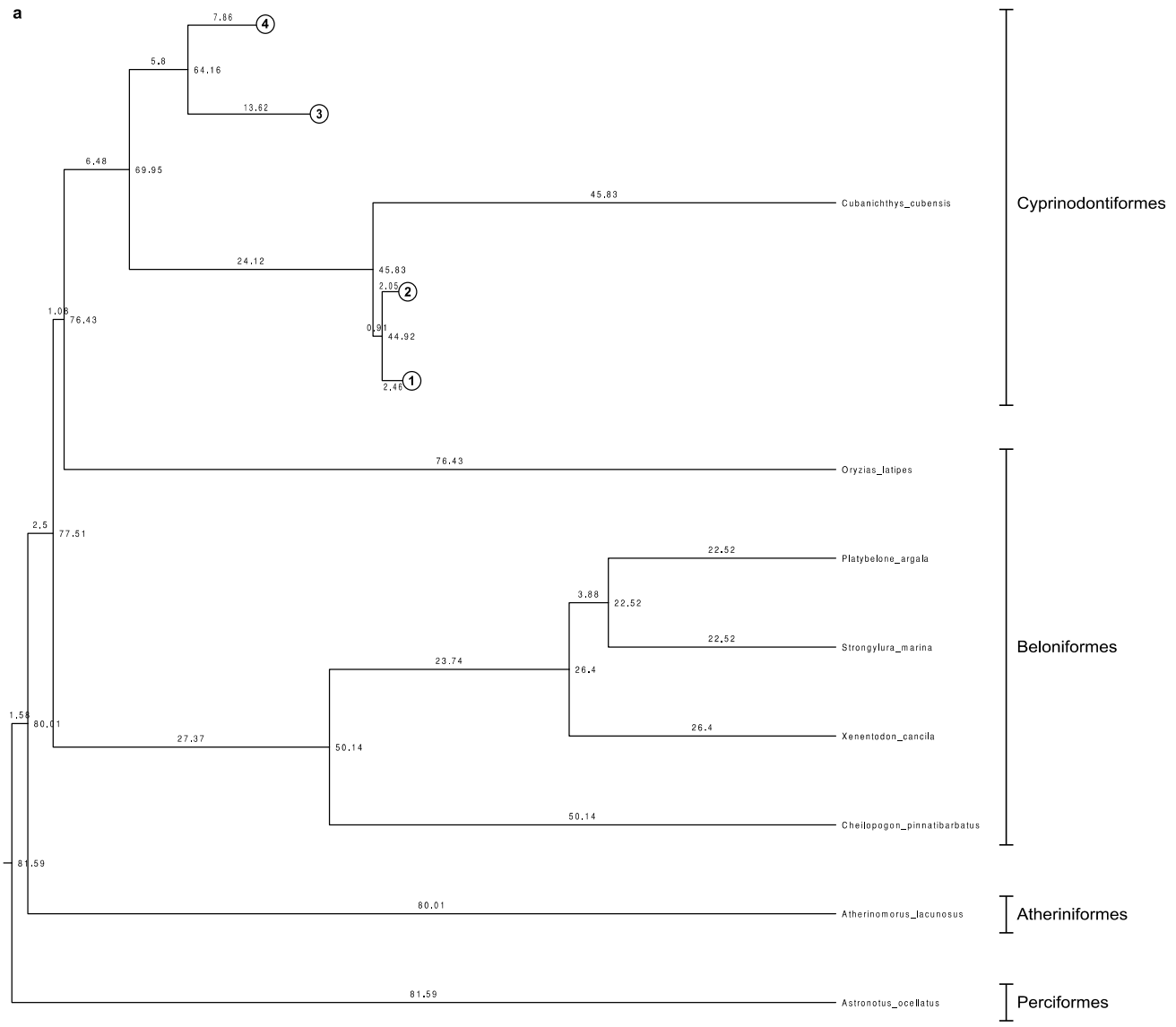
a
7.86
4
5.8
64.16
13.62
3
6.48
69.95
45.83
Cubanichthys_cubensis
24.12
45.83
2.05
2
1.08
76.43
0.91
44.92
2.46
1
76.43
Oryzias_latipes
2.5
77.51
22.52
Platybelone_argala
3.88
22.52
22.52
Strongylura_marina
23.74
26.4
1.58
80.01
26.4
Xenentodon_cancila
27.37
50.14
50.14
Cheilopogon_pinnatibarbatus
81.59
80.01
Atherinomorus_lacunosus
81.59
Astronotus_ocellatus
Cyprinodontiformes
Beloniformes
Atheriniformes
Perciformes

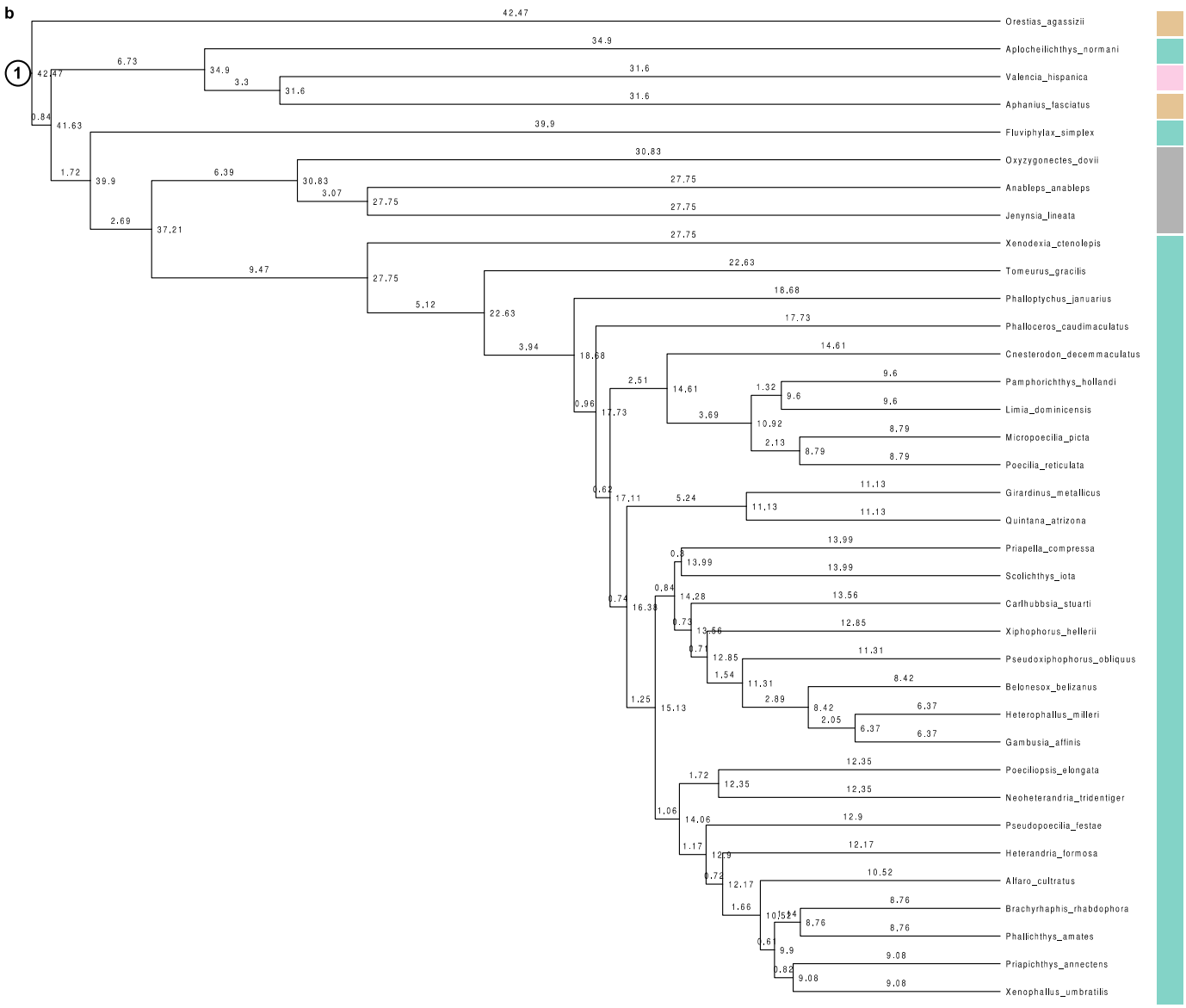
b
1
Orestias_agassizii
Aplocheilichthys_normani
Valencia_hispanica
Aphanius_fasciatus
Fluviphylax_simplex
Oxyzygonectes_dovii
Anableps_anableps
Jenynsia_lineata
Xenodexia_ctenolepis
Tomeurus_gracilis
Phalloptychus_januarius
Phalloceros_caudimaculatus
Cnesterodon_decemmaculatus
Pamphorichthys_hollandi
Limia_dominicensis
Micropoecilia_picta
Poecilia_reticulata
Girardinus_metallicus
Quintana_atrizona
Priapella_compressa
Scolichthys_iota
Carlhubbsia_stuarti
Xiphophorus_hellerii
Pseudoxiphophorus_obliquus
Belonesox_belizanus
Heterophallus_milleri
Gambusia_affinis
Poeciliopsis_elongata
Neoheterandria_tridentiger
Pseudopoecilia_festae
Heterandria_formosa
Alfaro_cultratus
Brachyrhaphis_rhabdophora
Phallichthys_amates
Priapichthys_annectens
Xenophallus_umbratilis

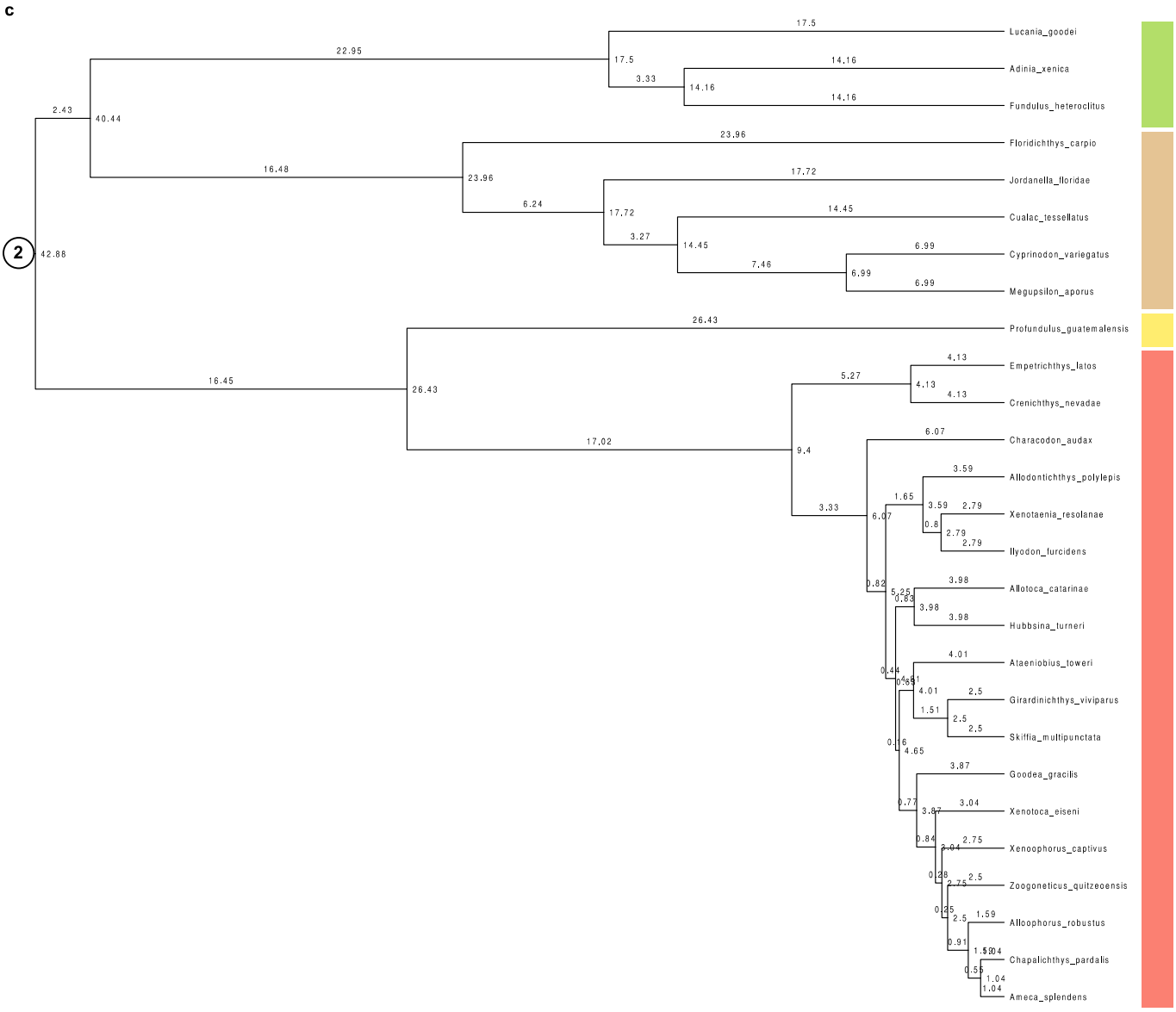
c
2
42.88
2.43
40.44
22.95
17.5
17.5
3.33
14.16
14.16
14.16
Lucania_goodei
Adinia_xenica
Fundulus_heteroclitus
16.48
23.96
23.96
6.24
17.72
3.27
14.45
7.46
6.99
23.96
17.72
14.45
6.99
6.99
Floridichthys_carpio
Jordanella_floridae
Cualac_tessellatus
Cyprinodon_variegatus
Megupsilon_aporus
16.45
26.43
26.43
17.02
Profundulus_guatemalensis
5.27
4.13
4.13
4.13
Empetrichthys_latos
Crenichthys_nevadae
9.4
6.07
Characodon_audax
3.33
6.07
1.65
3.59
3.59
2.79
0.8
2.79
2.79
Allodontichthys_polylepis
Xenotaenia_resolanae
Ilyodon_furcidens
0.82
5.25
0.83
3.98
3.98
3.98
Allotoca_catarinae
Hubbsina_turneri
0.44
0.69
0.51
4.01
4.01
1.51
2.5
2.5
2.5
Ataeniobius_toweri
Girardinichthys_viviparus
Skiffia_multipunctata
0.16
4.65
3.87
Goodea_gracilis
0.77
3.87
3.04
Xenotoca_eiseni
0.84
2.04
2.75
Xenoophorus_captivus
0.28
2.75
2.5
Zoogoneticus_quitzeoensis
0.25
2.5
1.59
Alloophorus_robustus
0.91
1.59
1.04
Chapalichthys_pardalis
0.55
1.04
1.04
Ameca_splendens

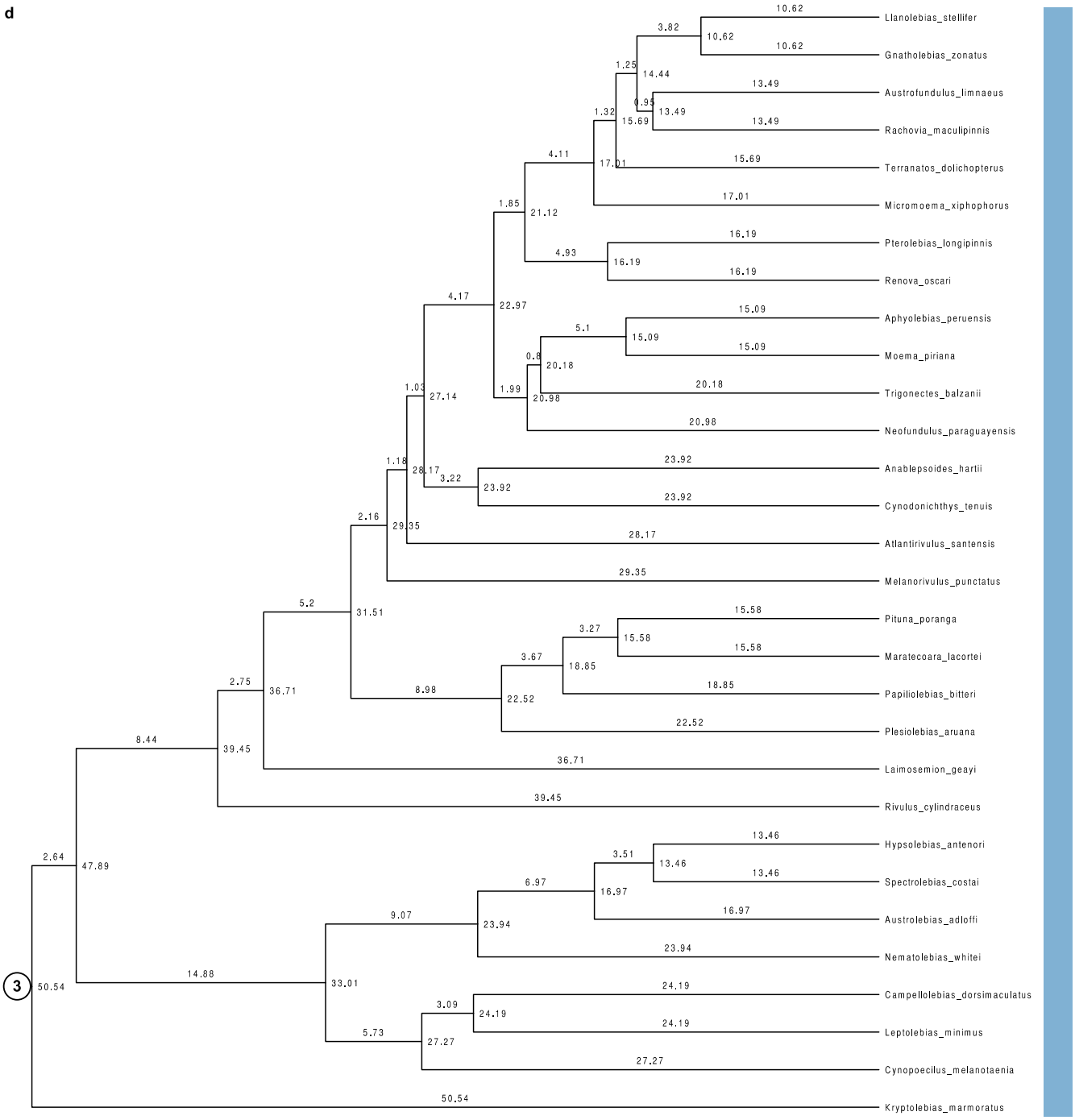
d
Llanolebias_stellifer
Gnatholebias_zonatus
Austrofundulus_limnaeus
Rachovia_maculipinnis
Terranatos_dolichopterus
Micromoema_xiphophorus
Pterolebias_longipinnis
Renova_oscari
Aphyolebias_peruensis
Moema_piriana
Trigonectes_balzanii
Neofundulus_paraguayensis
Anablepsoides_hartii
Cynodonichthys_tenuis
Atlantirivulus_santensis
Melanorivulus_punctatus
Pituna_poranga
Maratecoara_lacortei
Papiliolebias_bitteri
Plesiolebias_aruana
Laimosemion_geayi
Rivulus_cylindraceus
Hypsolebias_antenori
Spectrolebias_costai
Austrolebias_adloffi
Nematolebias_whitei
Campellolebias_dorsimaculatus
Leptolebias_minimus
Cynopoecilus_melanotaenia
Kryptolebias_marmoratus
3

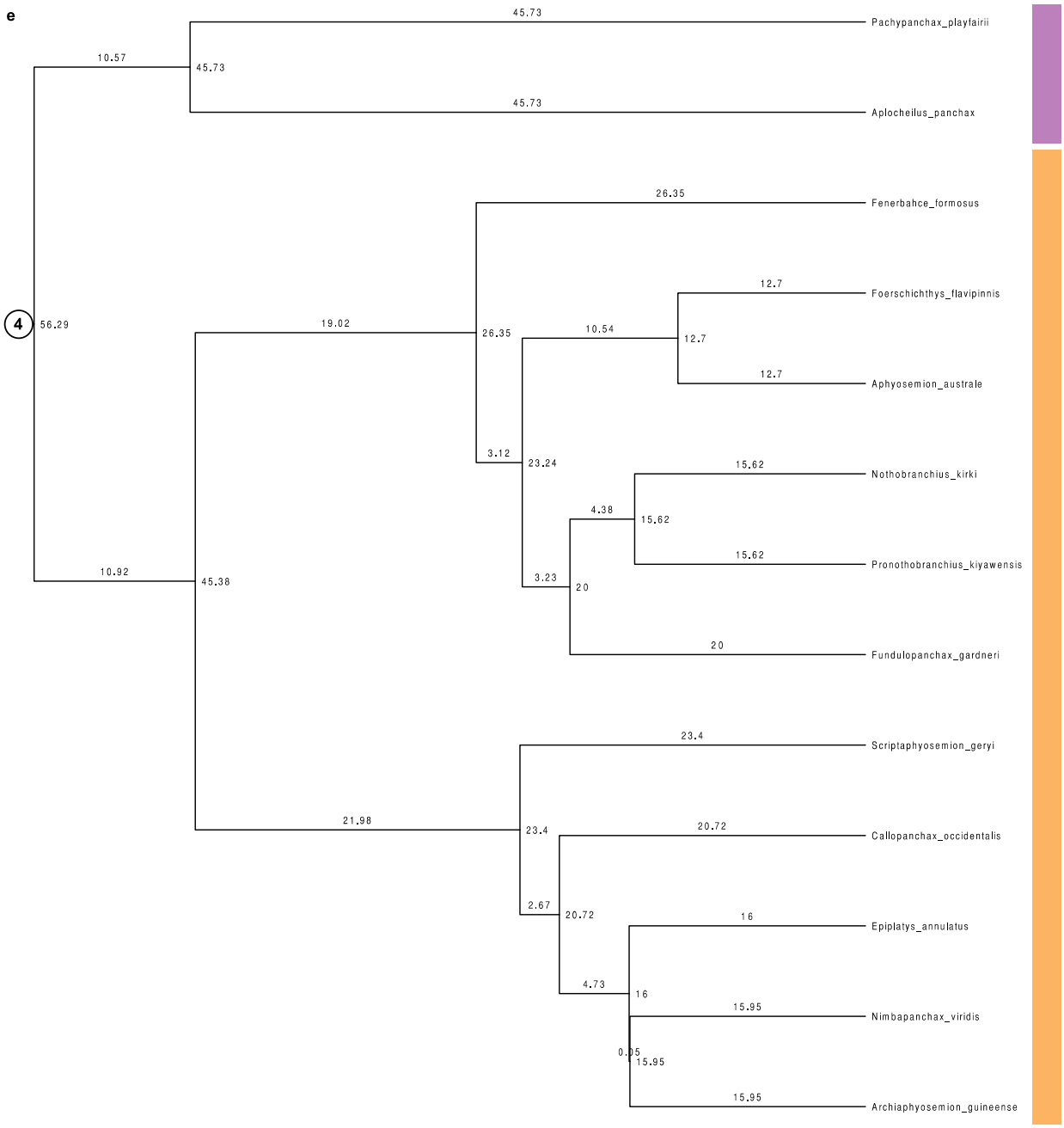

Figure S5.1 MCC phylogenetic tree split into subtrees. Branch lengths and node ages in Ma shown. Panel (a) shows a skeleton tree with the position of each subtree (1,2,3,4) labeled on the branch upon which it is found. The order each tip belongs to is shown on the right. Panels (b), (c), (d) and (e) show the subtrees where colours correspond to the family colur code used in Fig. 5.1. Tip labels show the species molecular data was taken from.

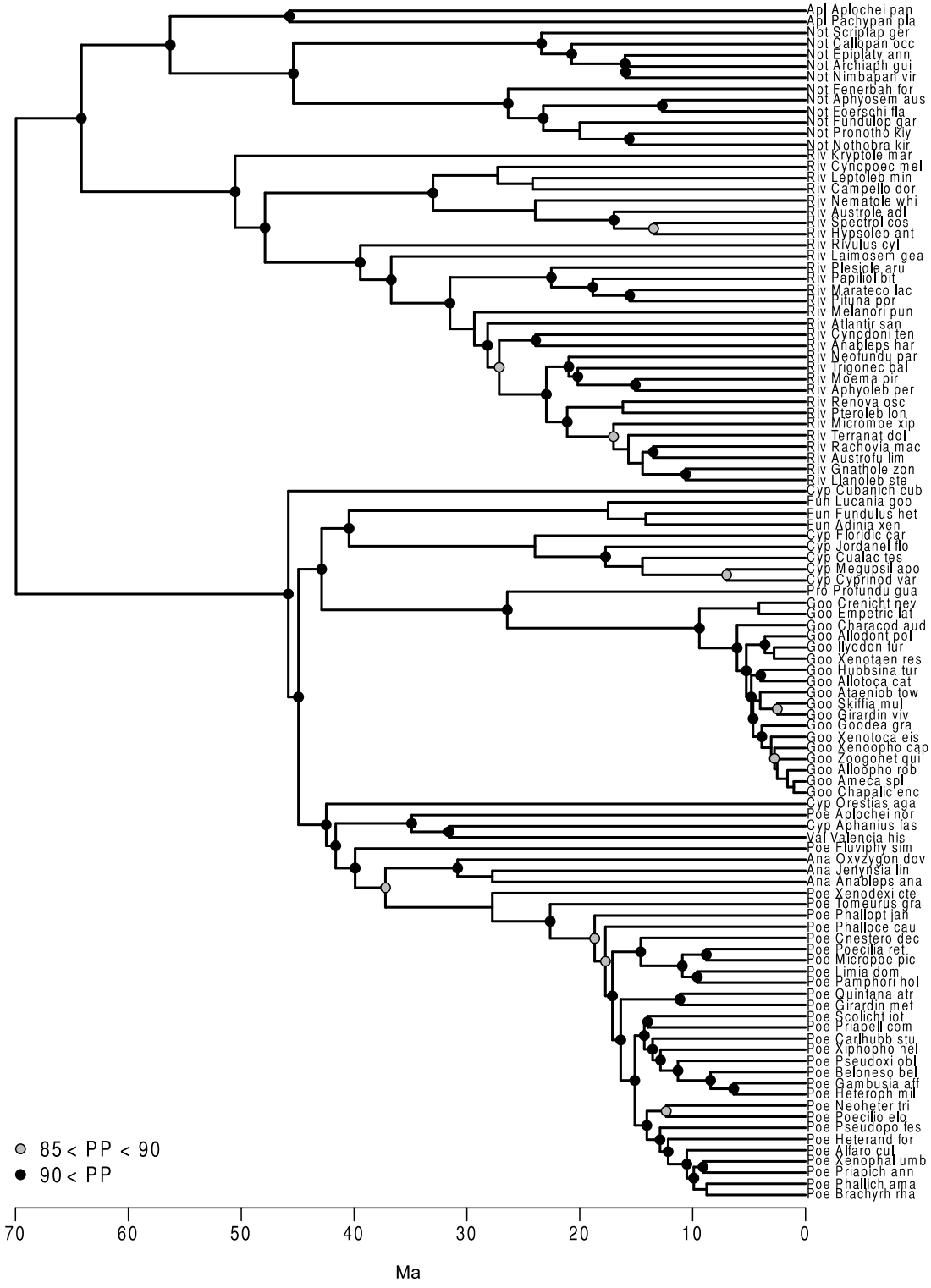

Figure S5.2 MCC phylogenetic tree with node support. Posterior probability (PP) labeled on nodes. Black circles represent PP over 0.9, grey circles represent PP from 0.85-0.9, no circles represent PP under 0.8. Tip labels are abbreviated to Family_Genus_Species of the organism sequence data was taken from.

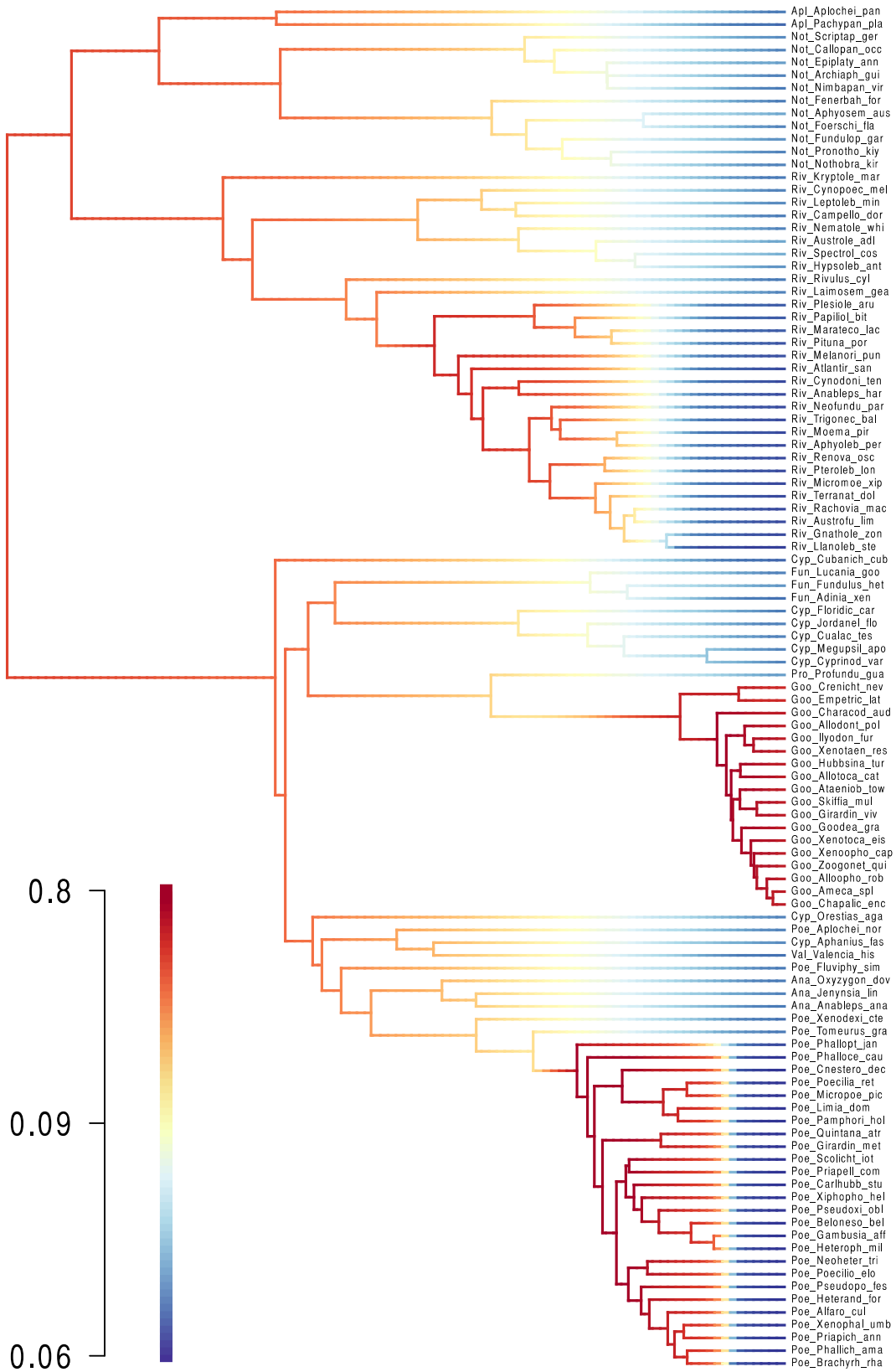

Figure S5.3 Mean phylorate plot of net diversification from BAMM analysis. Tip labels are abbreviated to Family_Genus_Species of the organism sequence data was taken from.

Figure S5.4 The nine most common Credible Shift Sets from the BAMM analysis. Red circles indicate where rate shifts take place. The size of the circle indicates the strength of the rate shift and the red colour indicates rate acceleration. 'f' is the posterior probability of each shift configuration.

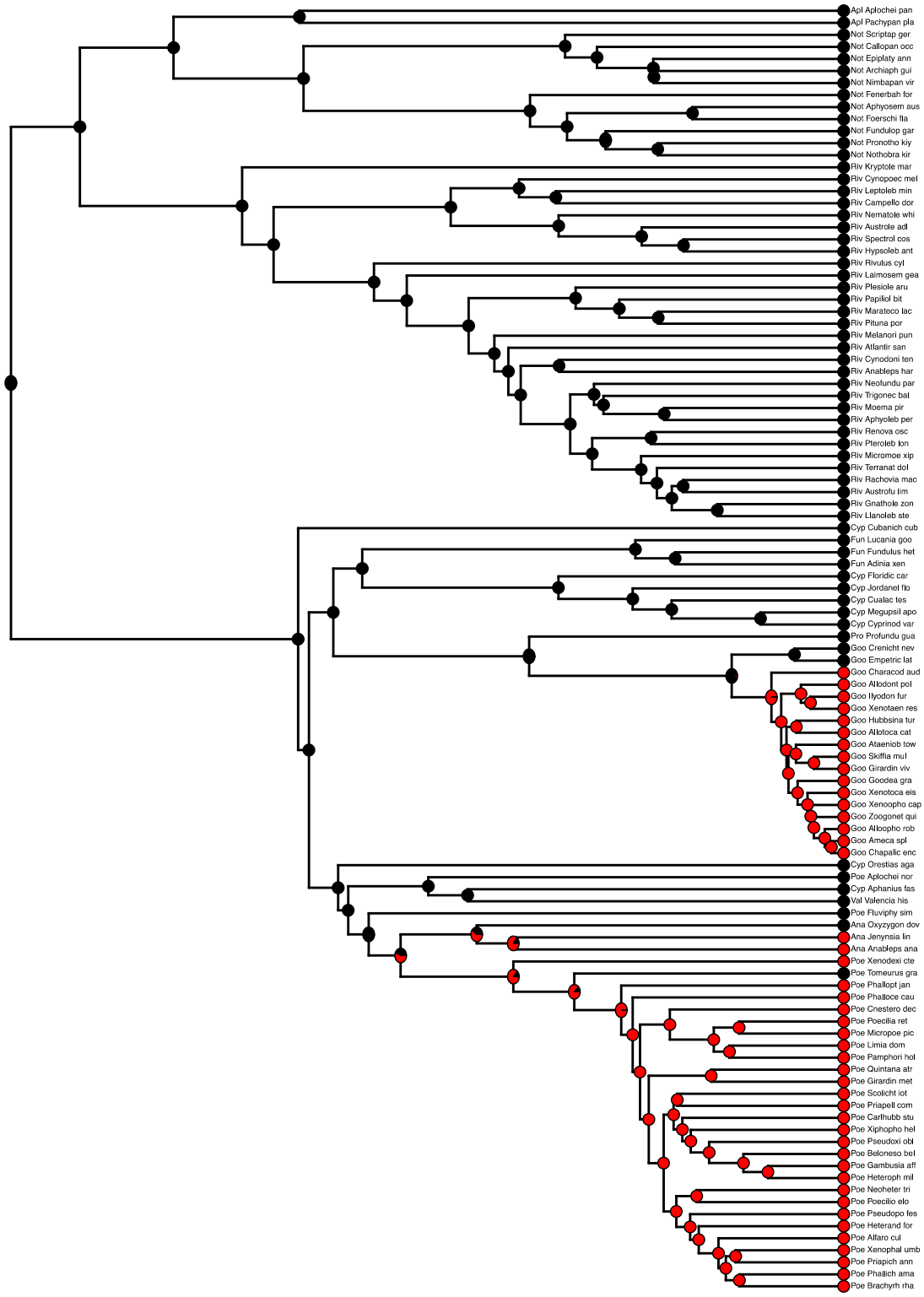

Figure S5.5 Ancestral state reconstructions of viviparity using stochastic character mapping. Red circles denote viviparity and black circles denote oviparity. Tip labels are abbreviated to Family_Genus_Species of the organism sequence data was taken from.

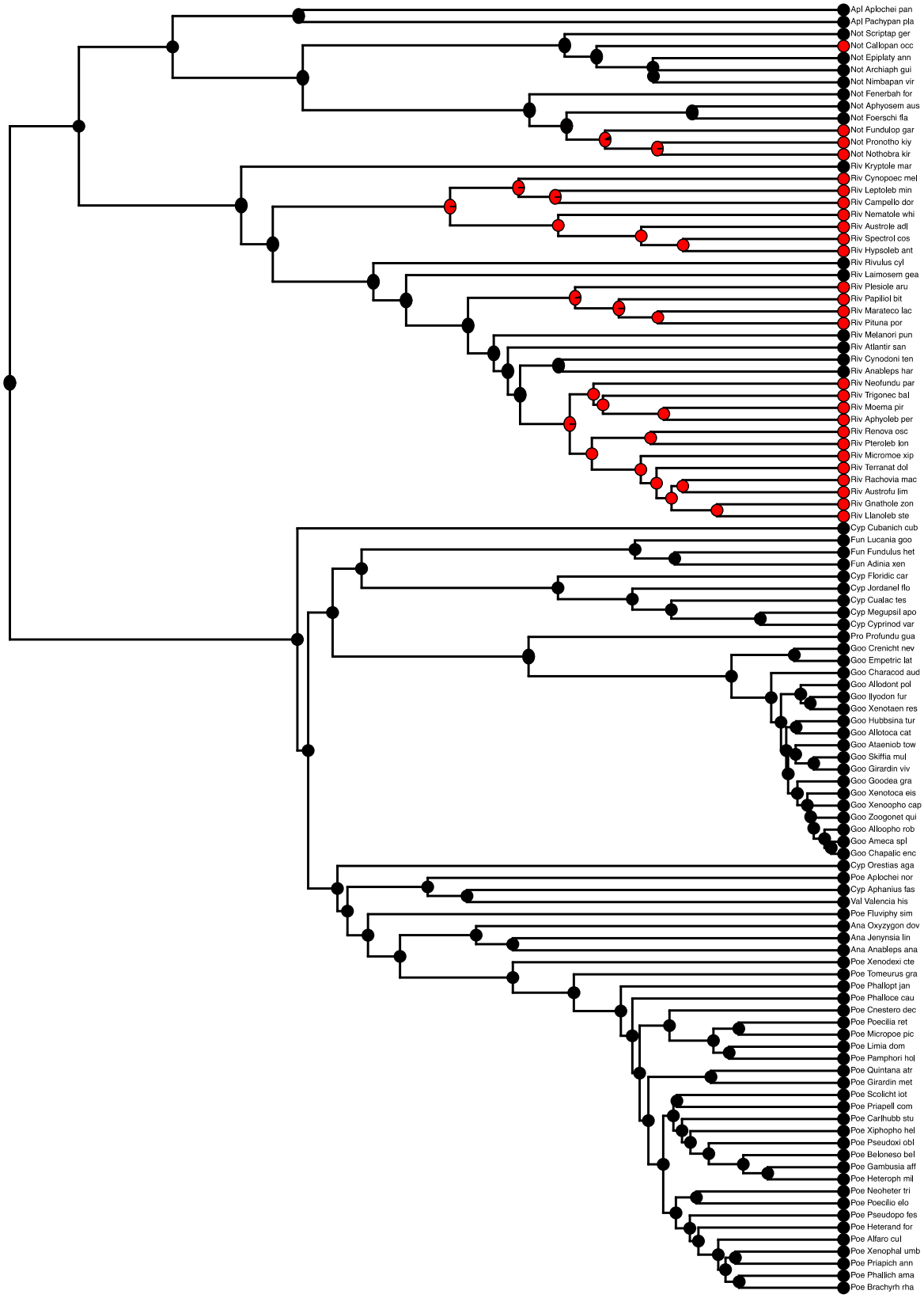

Figure S5.6 Ancestral state reconstructions of annualism using stochastic character mapping**.** Red circles denote annualism and black circles denote non-annualism. Tip labels are abbreviated to Family_Genus_Species of the organism sequence data was taken from.

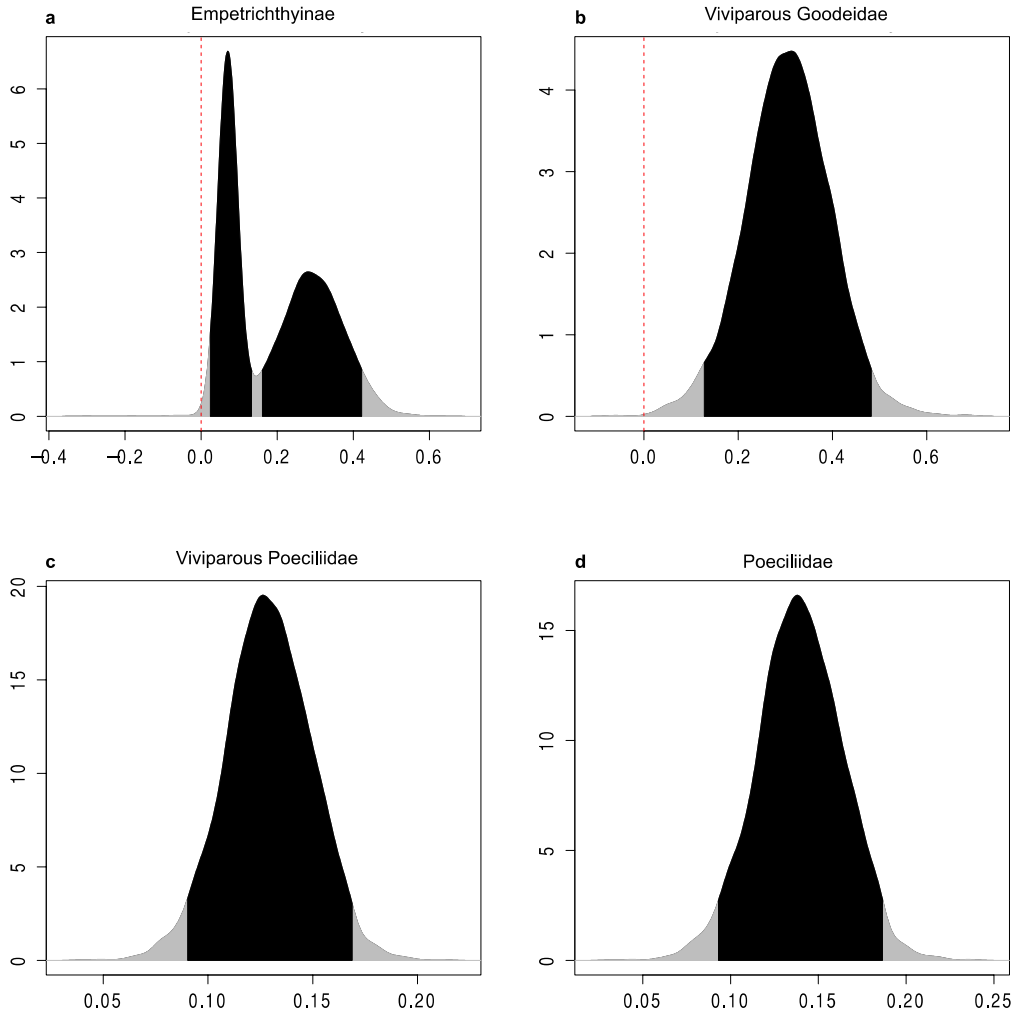

Figure Figure S5.7 Credible intervals of posterior samples from BAMM analyses for net diversification rate of four different clades. (a) The oviparous goodeid subfamily Empetrichthyinae, (b) All viviparous lineages in Goodeidae, (c) The major monophyletic group of viviparous Poeciliidae and (d) all Poeciliidae of the major monophyletic clade. Black regions represent 95% confidence intervals, dotted vertical line marks 0.

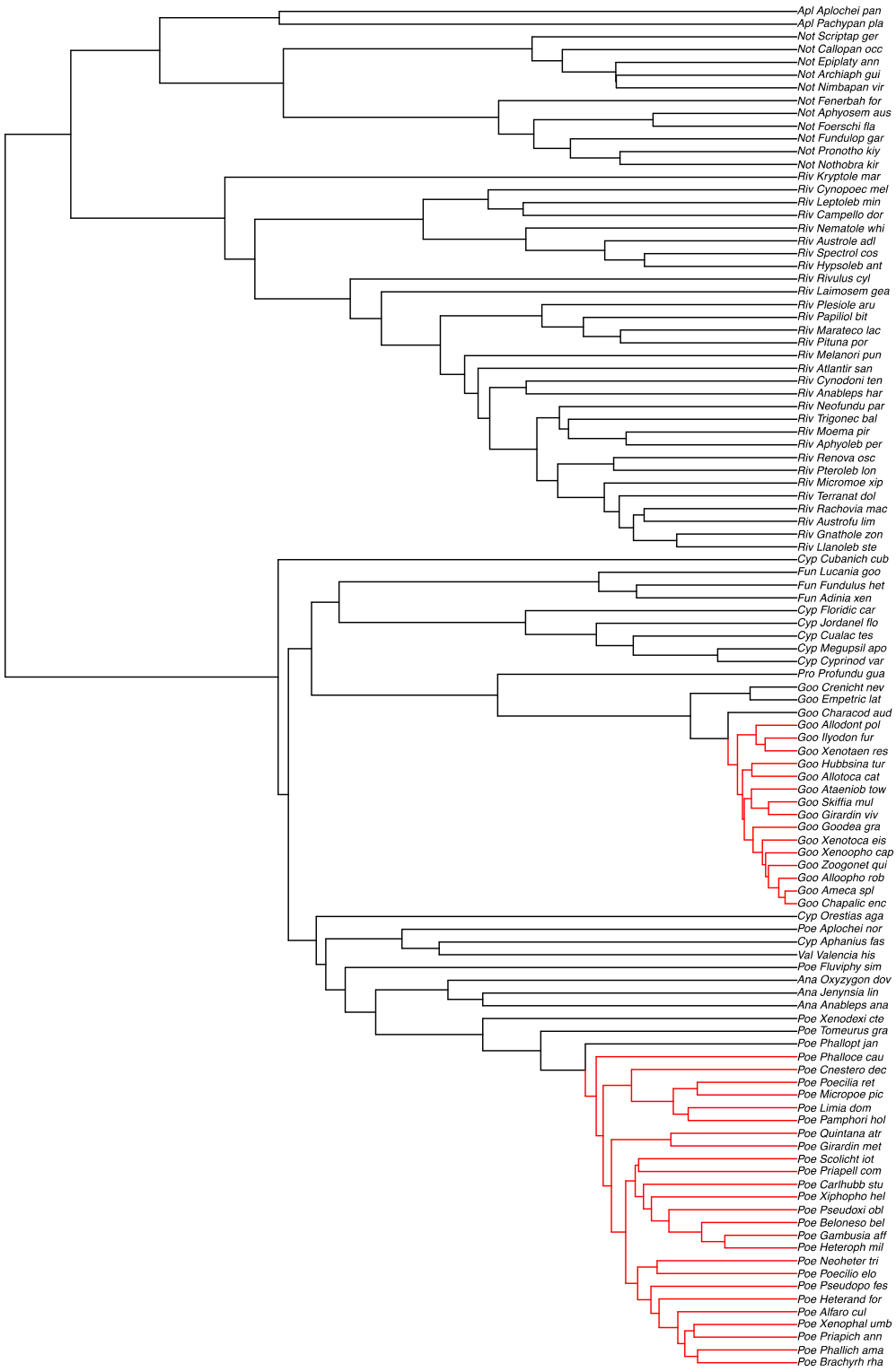

Figure S5.8 Cumulative shift probability. Branches in red indicate a rate shift has occurred between that branch and the root of the tree. Tip labels are abbreviated to Family_Genus_Species of the organism sequence data was taken from.

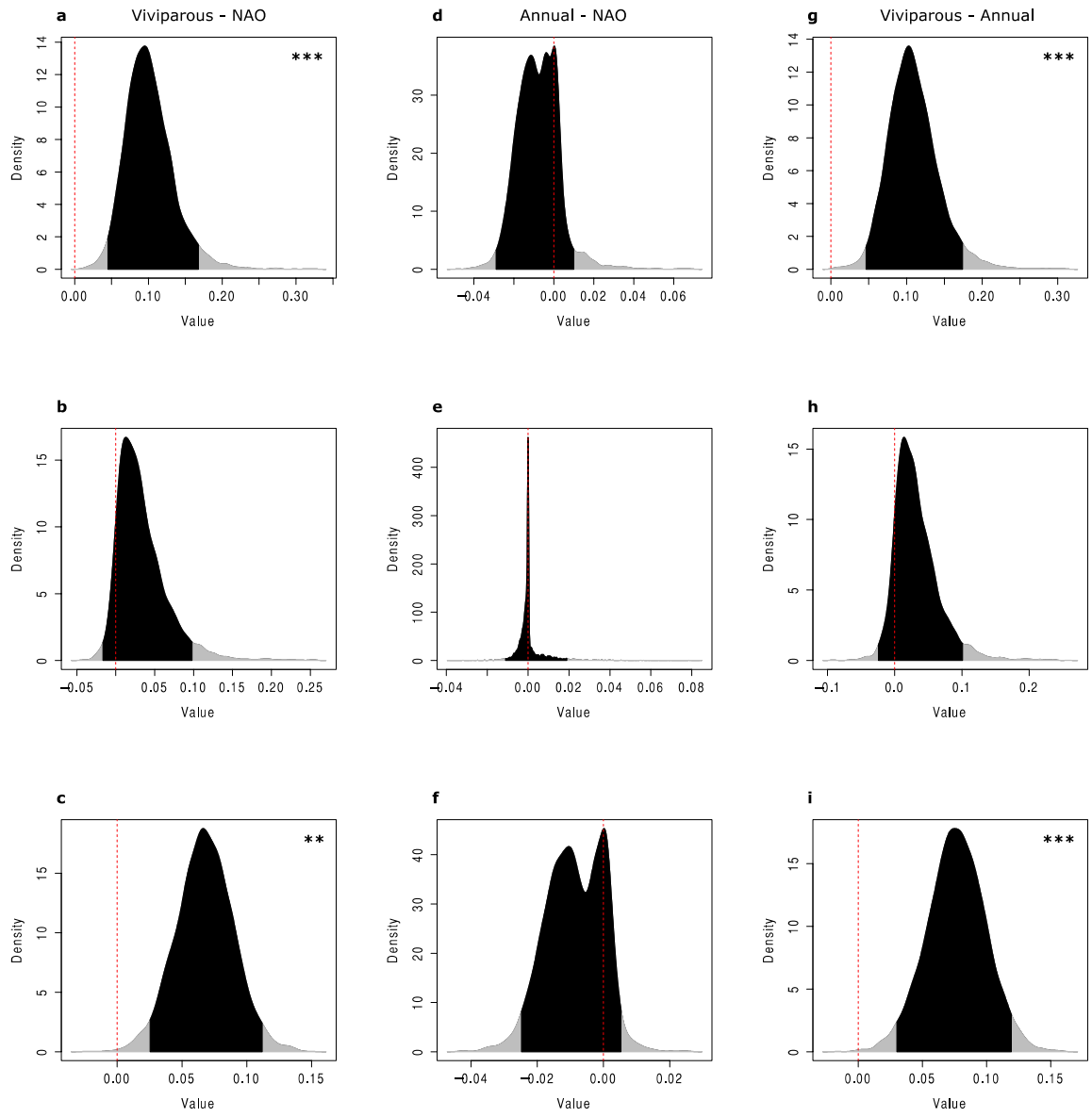

Figure S5.9 Credible intervals of differences from posterior distribution of samples taken from BAMM analyses for the three character groups. Graphs in the left column compare viviparous and non-annual oviparous groups for (a) speciation rate, (b) extinction rate and (c) net diversification rate. Graphs in the middle column compare (d) speciation rate, (e) extinction rate and (f) net diversification rate of annual and non-annual oviparous groups. Graphs in the right column compare (g) speciation rate, (h) extinction rate and (i) net diversification rate for viviparous and annual groups. Dotted red line indicates 0 difference between samples. Black regions represent 95% confidence intervals. Significance is calculated as the percentage of credible differences that do not overlap with zero, represented as * = >95%, ** = >99% and *** = >99.9%; one-tailed.

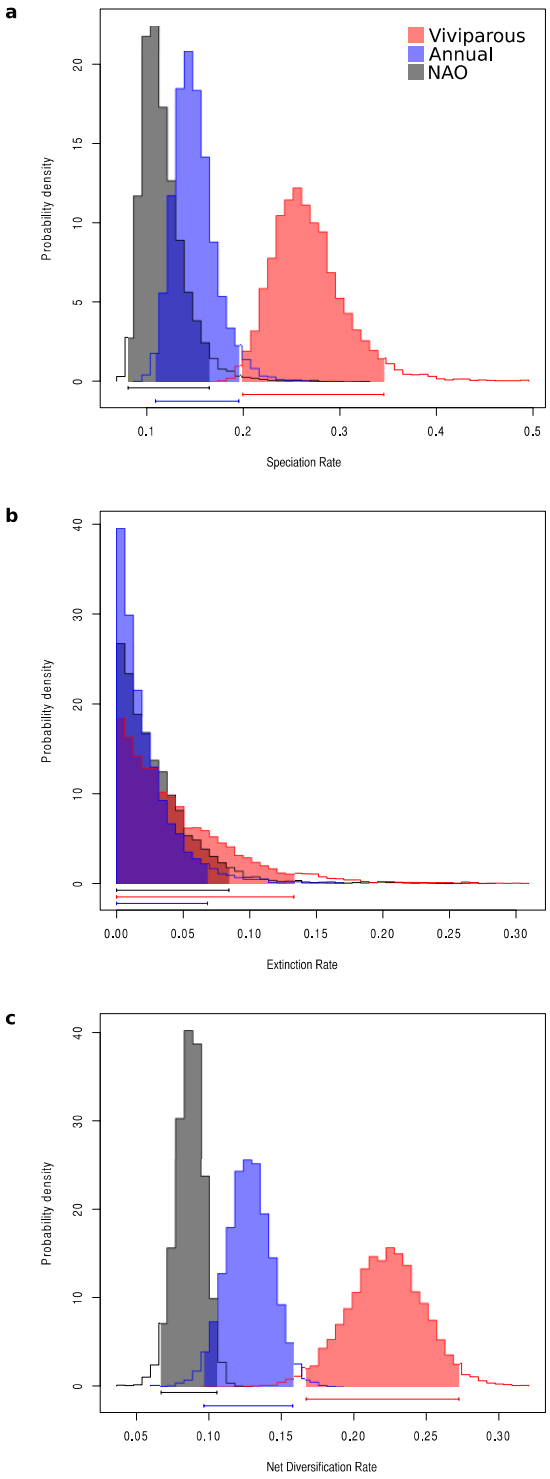

Figure S5.10 Posterior distribution of state-dependent rates. taken from a full 12 parameter MuSSE model. Graphs are separated into (a) speciation rate, (b) extinction rate and (c) net diversification rate for viviparous (red), annual (blue) and non-annual oviparous (NAO, grey).

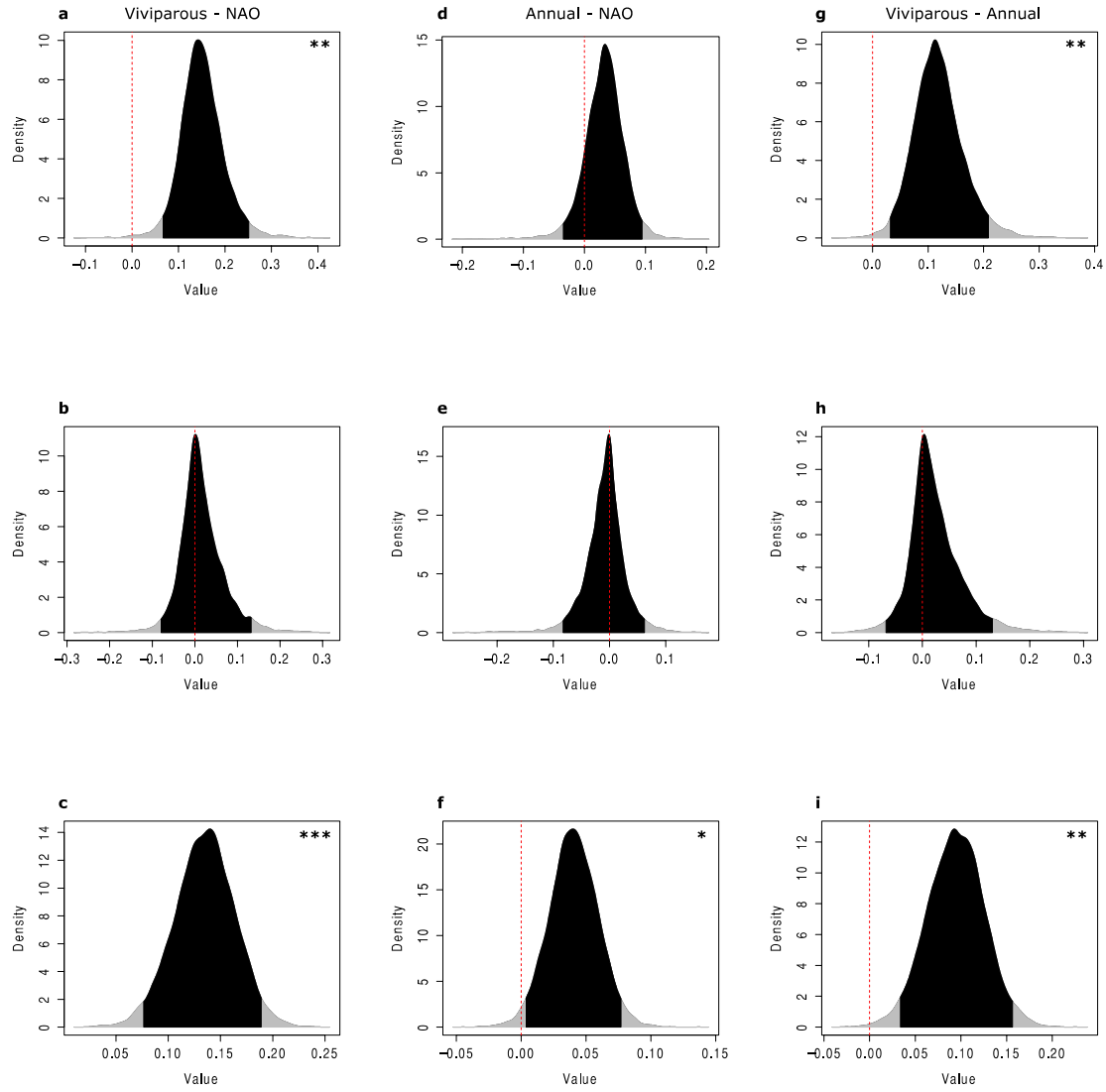

Figure S5.11 Credible intervals of differences from posterior distribution of samples taken from MuSSE analyses for the three character groups. Graphs in the left column compare viviparous and non-annual oviparous groups for (a) speciation rate, (b) extinction rate and (c) net diversification rate. Graphs in the middle column compare (d) speciation rate, (e) extinction rate and (f) net diversification rate of annual and non-annual oviparous groups. Graphs in the right column compare (g) speciation rate, (h) extinction rate and i net diversification rate for viviparous and annual groups. Dotted red line indicates 0 difference between samples. Black regions represent 95% confidence intervals. Significance is calculated as the percentage of credible differences that do not overlap with zero, represented as * = >95%, ** = >99% and *** = >99.9%; one-tailed.

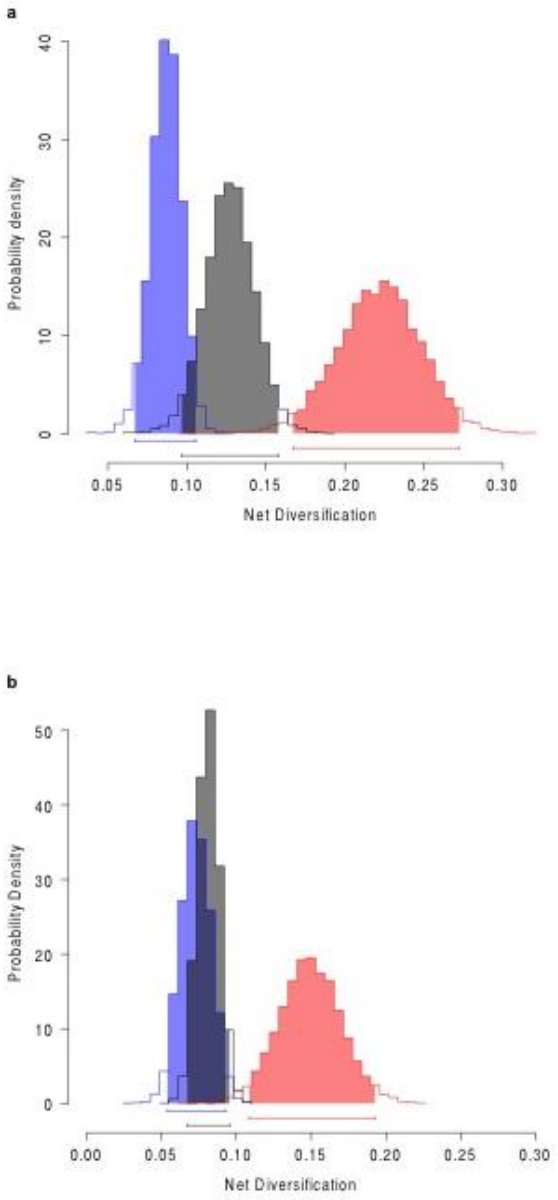

Figure S5.12 Posterior distribution of state-dependent rates for *Fundulopanchax* test. Rates taken from (a) a full 12 parameter MuSSE model and (b) BAMM analyses where the genus *Fundulopanchax* has been changed from annual to non-annual. Graphs show net diversification rate for viviparous (red), annual (blue) and non-annual oviparous (NAO) (grey).

Table S5.1 Table of sampled species, the loci used for each species and the relevant accession numbers.

Accession	Tip label	*Organism*	Gene
GQ119680	Fun_Adinia_xen	*Adinia xenica*	cytB
GQ119858	Fun_Adinia_xen	*Adinia xenica*	RAG1
JN024713	Fun_Adinia_xen	*Adinia xenica*	COI1
KC826901	Fun_Adinia_xen	*Adinia xenica*	MYH6
ACU80048	Poe_Alfaro_cul	*Alfaro cultratus*	16S
EF017429	Poe_Alfaro_cul	*Alfaro cultratus*	RAG1
EF017480	Poe_Alfaro_cul	*Alfaro cultratus*	12S
EF017531	Poe_Alfaro_cul	*Alfaro cultratus*	cytB
EF017580	Poe_Alfaro_cul	*Alfaro cultratus*	NADH1
KJ696868	Poe_Alfaro_cul	*Alfaro cultratus*	ENC1
KJ696977	Poe_Alfaro_cul	*Alfaro cultratus*	GLYT
KJ697087	Poe_Alfaro_cul	*Alfaro cultratus*	MYH6
KJ697460	Poe_Alfaro_cul	*Alfaro cultratus*	SH3PX3
KJ697570	Poe_Alfaro_cul	*Alfaro cultratus*	X-SRC
AF510839	Goo_Allodont_pol	*Allodontichthys polylepis*	cytB
AY356555	Goo_Allodont_pol	*Allodontichthys polylepis*	COI1
AF510813	Goo_Alloopho_rob	*Alloophorus robustus*	cytB
AY356561	Goo_Alloopho_rob	*Alloophorus robustus*	COI1
AF510795	Goo_Allotoca_cat	*Allotoca catarinae*	cytB
AY356562	Goo_Allotoca_cat	*Allotoca catarinae*	COI1
AF510818	Goo_Ameca_spl	*Ameca splendens*	cytB
AY356564	Goo_Ameca_spl	*Ameca splendens*	COI1
KJ696869	Goo_Ameca_spl	*Ameca splendens*	ENC1
KJ696978	Goo_Ameca_spl	*Ameca splendens*	GLYT
KJ697088	Goo_Ameca_spl	*Ameca splendens*	MYH6
KJ697267	Goo_Ameca_spl	*Ameca splendens*	RAG1
KJ697461	Goo_Ameca_spl	*Ameca splendens*	SH3PX3
KJ697571	Goo_Ameca_spl	*Ameca splendens*	X-SRC
AF449341	Ana_Anableps_ana	*Anableps anableps*	NADH2
EF017405	Ana_Anableps_ana	*Anableps anableps*	RAG1
EF017456	Ana_Anableps_ana	*Anableps anableps*	12S
EF017508	Ana_Anableps_ana	*Anableps anableps*	cytB
EF017558	Ana_Anableps_ana	*Anableps anableps*	NADH1
KJ696870	Ana_Anableps_ana	*Anableps anableps*	ENC1
KJ696979	Ana_Anableps_ana	*Anableps anableps*	GLYT
KJ697089	Ana_Anableps_ana	*Anableps anableps*	MYH6
KJ697572	Ana_Anableps_ana	*Anableps anableps*	X-SRC
AF002551	Riv_Anableps_har	*Anablepsoides hartii*	16S

AF002619	Riv_Anableps_har	*Anablepsoides hartii*	COI2
AF092326	Riv_Anableps_har	*Anablepsoides hartii*	12S
AF092393	Riv_Anableps_har	*Anablepsoides hartii*	NADH2
AY619607	Riv_Anableps_har	*Anablepsoides hartii*	cytB
HQ405569	Riv_Anableps_har	*Anablepsoides hartii*	COI1
KC702145	Riv_Anableps_har	*Anablepsoides hartii*	SH3PX3
KJ696966	Riv_Anableps_har	*Anablepsoides hartii*	ENC1
KJ697076	Riv_Anableps_har	*Anablepsoides hartii*	GLYT
KJ697186	Riv_Anableps_har	*Anablepsoides hartii*	MYH6
U02357	Riv_Anableps_har	*Anablepsoides hartii*	X-SRC
AF299273	Cyp_Aphanius_fas	*Aphanius fasciatus*	cytB
AF449310	Cyp_Aphanius_fas	*Aphanius fasciatus*	NADH2
AF449369	Cyp_Aphanius_fas	*Aphanius fasciatus*	12S
AFU05965	Cyp_Aphanius_fas	*Aphanius fasciatus*	16S
DQ923022	Cyp_Aphanius_fas	*Aphanius fasciatus*	NADH1
AF002506	Riv_Aphyoleb_per	*Aphyolebias peruensis*	cytB
AF002569	Riv_Aphyoleb_per	*Aphyolebias peruensis*	16S
AF002638	Riv_Aphyoleb_per	*Aphyolebias peruensis*	COI2
AF092340	Riv_Aphyoleb_per	*Aphyolebias peruensis*	12S
EF455718	Riv_Aphyoleb_per	*Aphyolebias peruensis*	RAG1
AAU73245	Not_Aphyosem_aus	*Aphyosemion australe*	16S
AF002367	Not_Aphyosem_aus	*Aphyosemion australe*	12S
EF417015	Not_Aphyosem_aus	*Aphyosemion australe*	COI1
EU272816	Not_Aphyosem_aus	*Aphyosemion australe*	cytB
KC701966	Not_Aphyosem_aus	*Aphyosemion australe*	ENC1
KC702098	Not_Aphyosem_aus	*Aphyosemion australe*	SH3PX3
KJ696787	Poe_Aplochei_nor	*Aplocheilichthys normani*	cytB
KJ696873	Poe_Aplochei_nor	*Aplocheilichthys normani*	ENC1
KJ696983	Poe_Aplochei_nor	*Aplocheilichthys normani*	GLYT
KJ697093	Poe_Aplochei_nor	*Aplocheilichthys normani*	MYH6
KJ697200	Poe_Aplochei_nor	*Aplocheilichthys normani*	NADH2
KJ697272	Poe_Aplochei_nor	*Aplocheilichthys normani*	RAG1
KJ697466	Poe_Aplochei_nor	*Aplocheilichthys normani*	SH3PX3
KJ697575	Poe_Aplochei_nor	*Aplocheilichthys normani*	X-SRC
AB373005	Apl_Aplochei_pan	*Aplocheilus panchax*	12S
AB373005	Apl_Aplochei_pan	*Aplocheilus panchax*	NADH2
AB373005	Apl_Aplochei_pan	*Aplocheilus panchax*	cytB
AB373005	Apl_Aplochei_pan	*Aplocheilus panchax*	16S
EF455705	Apl_Aplochei_pan	*Aplocheilus panchax*	RAG1
KC701975	Apl_Aplochei_pan	*Aplocheilus panchax*	ENC1
KC702108	Apl_Aplochei_pan	*Aplocheilus panchax*	SH3PX3

AF000688	Not_Archiaph_gui	*Archiaphyosemion guineense*	12S
AF000711	Not_Archiaph_gui	*Archiaphyosemion guineense*	cytB
FJ872031	Not_Archiaph_gui	*Archiaphyosemion guineense*	16S
FJ872058	Not_Archiaph_gui	*Archiaphyosemion guineense*	NADH2
EF095671	Cic_Astronot_oce	*Astronotus ocellatus*	RAG1
AP009127	Cic_Astronot_oce	*Astronotus ocellatus*	12S
AP009127	Cic_Astronot_oce	*Astronotus ocellatus*	NADH2
AP009127	Cic_Astronot_oce	*Astronotus ocellatus*	NADH1
AP009127	Cic_Astronot_oce	*Astronotus ocellatus*	cytB
AP009127	Cic_Astronot_oce	*Astronotus ocellatus*	COI2
AP009127	Cic_Astronot_oce	*Astronotus ocellatus*	COI1
AP009127	Cic_Astronot_oce	*Astronotus ocellatus*	16S
KF556763	Cic_Astronot_oce	*Astronotus sp. YFTC 21011*	ENC1
KF556834	Cic_Astronot_oce	*Astronotus sp. YFTC 21011*	GLYT
KF556911	Cic_Astronot_oce	*Astronotus sp. YFTC 21011*	MYH6
KF557220	Cic_Astronot_oce	*Astronotus sp. YFTC 21011*	SH3PX3
AF510779	Goo_Ataeniob_tow	*Ataeniobius toweri*	cytB
JQ935854	Goo_Ataeniob_tow	*Ataeniobius toweri*	COI1
KJ696876	Goo_Ataeniob_tow	*Ataeniobius toweri*	ENC1
KJ696986	Goo_Ataeniob_tow	*Ataeniobius toweri*	GLYT
KJ697096	Goo_Ataeniob_tow	*Ataeniobius toweri*	MYH6
KJ697203	Goo_Ataeniob_tow	*Ataeniobius toweri*	NADH2
KJ697275	Goo_Ataeniob_tow	*Ataeniobius toweri*	RAG1
KJ697469	Goo_Ataeniob_tow	*Ataeniobius toweri*	SH3PX3
KJ697577	Goo_Ataeniob_tow	*Ataeniobius toweri*	X-SRC
AY655492	Ath_Atherino_lac	*Atherinomorus lacunosus*	16S
AY655522	Ath_Atherino_lac	*Atherinomorus lacunosus*	COI1
GU932753	Ath_Atherino_lac	*Atherinomorus lacunosus*	cytB
JX188684	Ath_Atherino_lac	*Atherinomorus lacunosus*	GLYT
JX188847	Ath_Atherino_lac	*Atherinomorus lacunosus*	ENC1
JX189538	Ath_Atherino_lac	*Atherinomorus lacunosus*	SH3PX3
JX189786	Ath_Atherino_lac	*Atherinomorus lacunosus*	RAG1
KC827019	Ath_Atherino_lac	*Atherinomorus lacunosus*	MYH6
AF002502	Riv_Atlantir_san	*Atlantirivulus santensis*	cytB
AF002565	Riv_Atlantir_san	*Atlantirivulus santensis*	16S
AF002634	Riv_Atlantir_san	*Atlantirivulus santensis*	COI2
AF092313	Riv_Atlantir_san	*Atlantirivulus santensis*	12S
EF455708	Riv_Atlantir_san	*Atlantirivulus santensis*	RAG1
GU701919	Riv_Atlantir_san	*Atlantirivulus santensis*	COI1
KC702023	Riv_Atlantir_san	*Atlantirivulus santensis*	ENC1
KC702152	Riv_Atlantir_san	*Atlantirivulus santensis*	SH3PX3

AF002589	Riv_Austrofu_lim	*Austrofundulus limnaeus*	COI2
ALU73254	Riv_Austrofu_lim	*Austrofundulus limnaeus*	16S
ALU73300	Riv_Austrofu_lim	*Austrofundulus limnaeus*	cytB
AY850644	Riv_Austrofu_lim	*Austrofundulus limnaeus*	NADH1
AY850647	Riv_Austrofu_lim	*Austrofundulus limnaeus*	NADH2
AY850667	Riv_Austrofu_lim	*Austrofundulus limnaeus*	12S
KC701978	Riv_Austrofu_lim	*Austrofundulus limnaeus*	ENC1
KC702112	Riv_Austrofu_lim	*Austrofundulus limnaeus*	SH3PX3
AF244413	Riv_Austrole_adl	*Austrolebias adloffi*	12S
KC701981	Riv_Austrole_adl	*Austrolebias adloffi*	ENC1
KC702114	Riv_Austrole_adl	*Austrolebias adloffi*	SH3PX3
AF244443	Riv_Austrole_adl	*Austrolebias adloffi-1*	16S
AF245009	Riv_Austrole_adl	*Austrolebias adloffi-1*	cytB
EF017416	Poe_Beloneso_bel	*Belonesox belizanus*	RAG1
EF017467	Poe_Beloneso_bel	*Belonesox belizanus*	12S
EF017519	Poe_Beloneso_bel	*Belonesox belizanus*	cytB
HM443919	Poe_Beloneso_bel	*Belonesox belizanus*	NADH2
JQ612957	Poe_Beloneso_bel	*Belonesox belizanus*	16S
JQ840428	Poe_Beloneso_bel	*Belonesox belizanus*	COI1
KJ696877	Poe_Beloneso_bel	*Belonesox belizanus*	ENC1
KJ696987	Poe_Beloneso_bel	*Belonesox belizanus*	GLYT
KJ697097	Poe_Beloneso_bel	*Belonesox belizanus*	MYH6
KJ697470	Poe_Beloneso_bel	*Belonesox belizanus*	SH3PX3
KJ697578	Poe_Beloneso_bel	*Belonesox belizanus*	X-SRC
EF017419	Poe_Brachyrh_rha	*Brachyrhaphis rhabdophora*	RAG1
KJ696878	Poe_Brachyrh_rha	*Brachyrhaphis rhabdophora*	ENC1
KJ696988	Poe_Brachyrh_rha	*Brachyrhaphis rhabdophora*	GLYT
KJ697098	Poe_Brachyrh_rha	*Brachyrhaphis rhabdophora*	MYH6
KJ697471	Poe_Brachyrh_rha	*Brachyrhaphis rhabdophora*	SH3PX3
KJ697579	Poe_Brachyrh_rha	*Brachyrhaphis rhabdophora*	X-SRC
AF000696	Not_Callopan_occ	*Callopanchax occidentalis*	cytB
AF092293	Not_Callopan_occ	*Callopanchax occidentalis*	12S
FJ872034	Not_Callopan_occ	*Callopanchax occidentalis*	16S
KC702027	Not_Callopan_occ	*Callopanchax occidentalis huwaldi*	ENC1
AF002465	Riv_Campello_dor	*Campellolebias dorsimaculatus*	cytB
AF002516	Riv_Campello_dor	*Campellolebias dorsimaculatus*	16S
AF002584	Riv_Campello_dor	*Campellolebias dorsimaculatus*	COI2
AF092295	Riv_Campello_dor	*Campellolebias dorsimaculatus*	12S
EF017430	Poe_Carlhubb_stu	*Carlhubbsia stuarti*	RAG1
EF017481	Poe_Carlhubb_stu	*Carlhubbsia stuarti*	12S
EF017532	Poe_Carlhubb_stu	*Carlhubbsia stuarti*	cytB

EF017581	Poe_Carlhubb_stu	*Carlhubbsia stuarti*	NADH2
EF017581	Poe_Carlhubb_stu	*Carlhubbsia stuarti*	NADH1
KJ696879	Poe_Carlhubb_stu	*Carlhubbsia stuarti*	ENC1
KJ696989	Poe_Carlhubb_stu	*Carlhubbsia stuarti*	GLYT
KJ697099	Poe_Carlhubb_stu	*Carlhubbsia stuarti*	MYH6
KJ697472	Poe_Carlhubb_stu	*Carlhubbsia stuarti*	SH3PX3
KJ697580	Poe_Carlhubb_stu	*Carlhubbsia stuarti*	X-SRC
KJ696880	Goo_Chapalic_enc	*Chapalichthys pardalis*	ENC1
KJ696990	Goo_Chapalic_enc	*Chapalichthys pardalis*	GLYT
KJ697100	Goo_Chapalic_enc	*Chapalichthys pardalis*	MYH6
KJ697204	Goo_Chapalic_enc	*Chapalichthys pardalis*	NADH2
KJ697276	Goo_Chapalic_enc	*Chapalichthys pardalis*	RAG1
KJ697473	Goo_Chapalic_enc	*Chapalichthys pardalis*	SH3PX3
KJ697581	Goo_Chapalic_enc	*Chapalichthys pardalis*	X-SRC
AF510822	Goo_Characod_aud	*Characodon audax*	cytB
AY356568	Goo_Characod_aud	*Characodon audax*	COI1
AB188690	Bel_Cheilopo_pi	*Cheilopogon pinnatibarbatus*	12S
AB444860	Bel_Cheilopo_pi	*Cheilopogon pinnatibarbatus*	16S
GU440273	Bel_Cheilopo_pi	*Cheilopogon pinnatibarbatus*	COI1
HQ325618	Bel_Cheilopo_pi	*Cheilopogon pinnatibarbatus*	cytB
JX189544	Bel_Cheilopo_pi	*Cheilopogon pinnatibarbatus*	SH3PX3
JX189637	Bel_Cheilopo_pi	*Cheilopogon pinnatibarbatus*	MYH6
JX189792	Bel_Cheilopo_pi	*Cheilopogon pinnatibarbatus*	RAG1
EF017427	Poe_Cnestero_dec	*Cnesterodon decemmaculatus*	RAG1
EF017478	Poe_Cnestero_dec	*Cnesterodon decemmaculatus*	12S
EF017529	Poe_Cnestero_dec	*Cnesterodon decemmaculatus*	cytB
EF017579	Poe_Cnestero_dec	*Cnesterodon decemmaculatus*	NADH2
EF017579	Poe_Cnestero_dec	*Cnesterodon decemmaculatus*	NADH1
GU179152	Poe_Cnestero_dec	*Cnesterodon decemmaculatus*	X-SRC
GU179168	Poe_Cnestero_dec	*Cnesterodon decemmaculatus*	ENC1
GU179197	Poe_Cnestero_dec	*Cnesterodon decemmaculatus*	GLYT
GU179214	Poe_Cnestero_dec	*Cnesterodon decemmaculatus*	SH3PX3
GU179243	Poe_Cnestero_dec	*Cnesterodon decemmaculatus*	MYH6
JX111721	Poe_Cnestero_dec	*Cnesterodon decemmaculatus*	COI1
KJ696882	Goo_Crenicht_nev	*Crenichthys nevadae*	ENC1
KJ696992	Goo_Crenicht_nev	*Crenichthys nevadae*	GLYT
KJ697102	Goo_Crenicht_nev	*Crenichthys nevadae*	MYH6
KJ697278	Goo_Crenicht_nev	*Crenichthys nevadae*	RAG1
KJ697583	Goo_Crenicht_nev	*Crenichthys nevadae*	X-SRC
AY902051	Cyp_Cualac_tes	*Cualac tessellatus*	cytB
AY902109	Cyp_Cualac_tes	*Cualac tessellatus*	NADH2

CTU05968	Cyp_Cualac_tes	*Cualac tessellatus*	16S
JQ935856	Cyp_Cualac_tes	*Cualac tessellatus*	COI1
KJ696795	Cyp_Cubanich_cub	*Cubanichthys cubensis*	cytB
KJ696883	Cyp_Cubanich_cub	*Cubanichthys cubensis*	ENC1
KJ696993	Cyp_Cubanich_cub	*Cubanichthys cubensis*	GLYT
KJ697103	Cyp_Cubanich_cub	*Cubanichthys cubensis*	MYH6
KJ697206	Cyp_Cubanich_cub	*Cubanichthys cubensis*	NADH2
KJ697476	Cyp_Cubanich_cub	*Cubanichthys cubensis*	SH3PX3
KJ697584	Cyp_Cubanich_cub	*Cubanichthys cubensis*	X-SRC
AF002499	Riv_Cynodoni_ten	*Cynodonichthys tenuis*	cytB
AF002626	Riv_Cynodoni_ten	*Cynodonichthys tenuis*	COI2
AF092319	Riv_Cynodoni_ten	*Cynodonichthys tenuis*	12S
EU751964	Riv_Cynodoni_ten	*Cynodonichthys tenuis*	COI1
KC702024	Riv_Cynodoni_ten	*Cynodonichthys tenuis*	ENC1
KC702154	Riv_Cynodoni_ten	*Cynodonichthys tenuis*	SH3PX3
RTU73256	Riv_Cynodoni_ten	*Cynodonichthys tenuis*	16S
AF092296	Riv_Cynopoec_mel	*Cynopoecilus melanotaenia*	12S
AF245465	Riv_Cynopoec_mel	*Cynopoecilus melanotaenia*	cytB
AF449344	Cyp_Cyprinod_var	*Cyprinodon variegatus*	NADH2
AF449406	Cyp_Cyprinod_var	*Cyprinodon variegatus*	12S
AY902062	Cyp_Cyprinod_var	*Cyprinodon variegatus*	cytB
CVU05969	Cyp_Cyprinod_var	*Cyprinodon variegatus*	16S
FN545583	Cyp_Cyprinod_var	*Cyprinodon variegatus*	COI1
KF141215	Cyp_Cyprinod_var	*Cyprinodon variegatus*	RAG1
KF141450	Cyp_Cyprinod_var	*Cyprinodon variegatus*	SH3PX3
KJ696885	Cyp_Cyprinod_var	*Cyprinodon variegatus*	ENC1
KJ696995	Cyp_Cyprinod_var	*Cyprinodon variegatus*	GLYT
KJ697105	Cyp_Cyprinod_var	*Cyprinodon variegatus*	MYH6
KJ697585	Cyp_Cyprinod_var	*Cyprinodon variegatus*	X-SRC
AY356573	Goo_Empetric_lat	*Empetrichthys latos*	COI1
ELU09108	Goo_Empetric_lat	*Empetrichthys latos*	cytB
KJ696886	Not_Epiplaty_ann	*Epiplatys annulatus*	ENC1
KJ696996	Not_Epiplaty_ann	*Epiplatys annulatus*	GLYT
KJ697106	Not_Epiplaty_ann	*Epiplatys annulatus*	MYH6
KJ697279	Not_Epiplaty_ann	*Epiplatys annulatus*	RAG1
AF002402	Not_Fenerbah_for	*Fenerbahce formosus*	12S
AF002404	Not_Fenerbah_for	*Fenerbahce formosus*	16S
JF307807	Not_Fenerbah_for	*Fenerbahce formosus*	cytB
KJ696867	Not_Fenerbah_for	*Fenerbahce formosus*	ENC1
KJ696976	Not_Fenerbah_for	*Fenerbahce formosus*	GLYT
KJ697086	Not_Fenerbah_for	*Fenerbahce formosus*	MYH6

KJ697266	Not_Fenerbah_for	*Fenerbahce formosus*	RAG1
KJ697459	Not_Fenerbah_for	*Fenerbahce formosus*	SH3PX3
KJ697569	Not_Fenerbah_for	*Fenerbahce formosus*	X-SRC
AF449345	Cyp_Floridic_car	*Floridichthys carpio*	NADH2
AF449407	Cyp_Floridic_car	*Floridichthys carpio*	12S
FCU05970	Cyp_Floridic_car	*Floridichthys carpio*	16S
FCU06189	Cyp_Floridic_car	*Floridichthys carpio*	cytB
JQ842470	Cyp_Floridic_car	*Floridichthys carpio*	COI1
KJ696887	Cyp_Floridic_car	*Floridichthys carpio*	ENC1
KJ696997	Cyp_Floridic_car	*Floridichthys carpio*	GLYT
KJ697107	Cyp_Floridic_car	*Floridichthys carpio*	MYH6
KJ697586	Cyp_Floridic_car	*Floridichthys carpio*	X-SRC
KJ696800	Poe_Fluviphy_sim	*Fluviphylax simplex*	cytB
KJ696888	Poe_Fluviphy_sim	*Fluviphylax simplex*	ENC1
KJ696998	Poe_Fluviphy_sim	*Fluviphylax simplex*	GLYT
KJ697108	Poe_Fluviphy_sim	*Fluviphylax simplex*	MYH6
KJ697210	Poe_Fluviphy_sim	*Fluviphylax simplex*	NADH2
KJ697280	Poe_Fluviphy_sim	*Fluviphylax simplex*	RAG1
KJ697481	Poe_Fluviphy_sim	*Fluviphylax simplex*	SH3PX3
KJ697587	Poe_Fluviphy_sim	*Fluviphylax simplex*	X-SRC
AF002403	Not_Foerschi_fla	*Foerschichthys flavipinnis*	12S
AF002407	Not_Foerschi_fla	*Foerschichthys flavipinnis*	16S
AF002409	Not_Foerschi_fla	*Foerschichthys flavipinnis*	cytB
AF002297	Not_Fundulop_gar	*Fundulopanchax gardneri*	cytB
AF002344	Not_Fundulop_gar	*Fundulopanchax gardneri*	16S
AF092289	Not_Fundulop_gar	*Fundulopanchax gardneri*	12S
JN021666	Not_Fundulop_gar	*Fundulopanchax gardneri*	COI1
KJ696889	Not_Fundulop_gar	*Fundulopanchax gardneri*	ENC1
KJ696999	Not_Fundulop_gar	*Fundulopanchax gardneri*	GLYT
KJ697109	Not_Fundulop_gar	*Fundulopanchax gardneri*	MYH6
KJ697211	Not_Fundulop_gar	*Fundulopanchax gardneri*	NADH2
KJ697281	Not_Fundulop_gar	*Fundulopanchax gardneri*	RAG1
KJ697482	Not_Fundulop_gar	*Fundulopanchax gardneri*	SH3PX3
KJ697588	Not_Fundulop_gar	*Fundulopanchax gardneri*	X-SRC
EF032926	Fun_Fundulus_het	*Fundulus heteroclitus*	MYH6
EF032978	Fun_Fundulus_het	*Fundulus heteroclitus*	ENC1
EF032991	Fun_Fundulus_het	*Fundulus heteroclitus*	GLYT
EF033004	Fun_Fundulus_het	*Fundulus heteroclitus*	SH3PX3
FJ445399	Fun_Fundulus_het	*Fundulus heteroclitus*	COI1
FJ445400	Fun_Fundulus_het	*Fundulus heteroclitus*	12S
FJ445400	Fun_Fundulus_het	*Fundulus heteroclitus*	cytB

FJ445400	Fun_Fundulus_het	*Fundulus heteroclitus*	16S
GQ119890	Fun_Fundulus_het	*Fundulus heteroclitus*	RAG1
JF895714	Fun_Fundulus_het	*Fundulus heteroclitus*	NADH2
U02351	Fun_Fundulus_het	*Fundulus heteroclitus*	X-SRC
AP004422	Poe_Gambusia_aff	*Gambusia affinis*	12S
AP004422	Poe_Gambusia_aff	*Gambusia affinis*	NADH2
AP004422	Poe_Gambusia_aff	*Gambusia affinis*	cytB
AP004422	Poe_Gambusia_aff	*Gambusia affinis*	COI1
AP004422	Poe_Gambusia_aff	*Gambusia affinis*	16S
EF017411	Poe_Gambusia_aff	*Gambusia affinis*	RAG1
EF017564	Poe_Gambusia_aff	*Gambusia affinis*	NADH1
EU001907	Poe_Gambusia_aff	*Gambusia affinis*	MYH6
JX188691	Poe_Gambusia_aff	*Gambusia affinis*	GLYT
JX188858	Poe_Gambusia_aff	*Gambusia affinis*	ENC1
JX189550	Poe_Gambusia_aff	*Gambusia affinis*	SH3PX3
KJ696894	Goo_Girardin_viv	*Girardinichthys viviparus*	ENC1
KJ697004	Goo_Girardin_viv	*Girardinichthys viviparus*	GLYT
KJ697114	Goo_Girardin_viv	*Girardinichthys viviparus*	MYH6
KJ697286	Goo_Girardin_viv	*Girardinichthys viviparus*	RAG1
KJ697593	Goo_Girardin_viv	*Girardinichthys viviparus*	X-SRC
EF017441	Poe_Girardin_met	*Girardinus metallicus*	RAG1
EF017493	Poe_Girardin_met	*Girardinus metallicus*	12S
EF017544	Poe_Girardin_met	*Girardinus metallicus*	cytB
EF017593	Poe_Girardin_met	*Girardinus metallicus*	NADH2
FN545595	Poe_Girardin_met	*Girardinus metallicus*	COI1
GMU80052	Poe_Girardin_met	*Girardinus metallicus*	16S
KJ696895	Poe_Girardin_met	*Girardinus metallicus*	ENC1
KJ697005	Poe_Girardin_met	*Girardinus metallicus*	GLYT
KJ697115	Poe_Girardin_met	*Girardinus metallicus*	MYH6
KJ697488	Poe_Girardin_met	*Girardinus metallicus*	SH3PX3
KJ697594	Poe_Girardin_met	*Girardinus metallicus*	X-SRC
AF002472	Riv_Gnathole_zon	*Gnatholebias zonatus*	cytB
AF002524	Riv_Gnathole_zon	*Gnatholebias zonatus*	16S
AF002591	Riv_Gnathole_zon	*Gnatholebias zonatus*	COI2
AF092352	Riv_Gnathole_zon	*Gnatholebias zonatus*	12S
EF455711	Riv_Gnathole_zon	*Gnatholebias zonatus*	RAG1
KC702008	Riv_Gnathole_zon	*Gnatholebias zonatus*	ENC1
KJ696896	Goo_Goodea_gra	*Goodea gracilis*	ENC1
KJ697006	Goo_Goodea_gra	*Goodea gracilis*	GLYT
KJ697116	Goo_Goodea_gra	*Goodea gracilis*	MYH6
KJ697287	Goo_Goodea_gra	*Goodea gracilis*	RAG1

KJ697595	Goo_Goodea_gra	*Goodea gracilis*	X-SRC
AF412125	Poe_Heterand_for	*Heterandria formosa*	cytB
EF017422	Poe_Heterand_for	*Heterandria formosa*	RAG1
EF017473	Poe_Heterand_for	*Heterandria formosa*	12S
EF017575	Poe_Heterand_for	*Heterandria formosa*	NADH1
HQ557453	Poe_Heterand_for	*Heterandria formosa*	COI1
JQ612956	Poe_Heterand_for	*Heterandria formosa*	16S
KJ696897	Poe_Heterand_for	*Heterandria formosa*	ENC1
KJ697007	Poe_Heterand_for	*Heterandria formosa*	GLYT
KJ697117	Poe_Heterand_for	*Heterandria formosa*	MYH6
KJ697490	Poe_Heterand_for	*Heterandria formosa*	SH3PX3
KJ697596	Poe_Heterand_for	*Heterandria formosa*	X-SRC
EF017414	Poe_Heteroph_mil	*Heterophallus milleri*	RAG1
EF017465	Poe_Heteroph_mil	*Heterophallus milleri*	12S
EF017517	Poe_Heteroph_mil	*Heterophallus milleri*	cytB
EF017567	Poe_Heteroph_mil	*Heterophallus milleri*	NADH1
AF510841	Goo_Hubbsina_tur	*Hubbsina turneri*	cytB
AY356578	Goo_Hubbsina_tur	*Hubbsina turneri*	COI1
AF002580	Riv_Hypsoleb_ant	*Hypsolebias antenori*	COI2
CAU73252	Riv_Hypsoleb_ant	*Hypsolebias antenori*	16S
CAU73276	Riv_Hypsoleb_ant	*Hypsolebias antenori*	12S
KF311234	Riv_Hypsoleb_ant	*Hypsolebias antenori*	cytB
AF510831	Goo_Ilyodon_fur	*Ilyodon furcidens*	cytB
AY356579	Goo_Ilyodon_fur	*Ilyodon furcidens*	COI1
KJ696898	Goo_Ilyodon_fur	*Ilyodon furcidens*	ENC1
KJ697008	Goo_Ilyodon_fur	*Ilyodon furcidens*	GLYT
KJ697118	Goo_Ilyodon_fur	*Ilyodon furcidens*	MYH6
KJ697288	Goo_Ilyodon_fur	*Ilyodon furcidens*	RAG1
KJ697597	Goo_Ilyodon_fur	*Ilyodon furcidens*	X-SRC
EF017406	Ana_Jenynsia_lin	*Jenynsia lineata*	RAG1
EF017457	Ana_Jenynsia_lin	*Jenynsia lineata*	12S
EF017509	Ana_Jenynsia_lin	*Jenynsia lineata*	cytB
EF017559	Ana_Jenynsia_lin	*Jenynsia lineata*	NADH2
EF017559	Ana_Jenynsia_lin	*Jenynsia lineata*	NADH1
KJ696899	Ana_Jenynsia_lin	*Jenynsia lineata*	ENC1
KJ697009	Ana_Jenynsia_lin	*Jenynsia lineata*	GLYT
KJ697119	Ana_Jenynsia_lin	*Jenynsia lineata*	MYH6
KJ697598	Ana_Jenynsia_lin	*Jenynsia lineata*	X-SRC
AP006778	Cyp_Jordanel_flo	*Jordanella floridae*	12S
AP006778	Cyp_Jordanel_flo	*Jordanella floridae*	NADH2
AP006778	Cyp_Jordanel_flo	*Jordanella floridae*	COI1

AP006778	Cyp_Jordanel_flo	*Jordanella floridae*	16S
KF141266	Cyp_Jordanel_flo	*Jordanella floridae*	RAG1
KF141498	Cyp_Jordanel_flo	*Jordanella floridae*	SH3PX3
KJ696901	Cyp_Jordanel_flo	*Jordanella floridae*	ENC1
KJ697011	Cyp_Jordanel_flo	*Jordanella floridae*	GLYT
KJ697121	Cyp_Jordanel_flo	*Jordanella floridae*	MYH6
KJ697600	Cyp_Jordanel_flo	*Jordanella floridae*	X-SRC
NC_011387	Cyp_Jordanel_flo	*Jordanella floridae*	cytB
AF002598	Riv_Kryptole_mar	*Kryptolebias marmoratus*	COI2
AF283503	Riv_Kryptole_mar	*Kryptolebias marmoratus*	12S
AF283503	Riv_Kryptole_mar	*Kryptolebias marmoratus*	COI1
AF283503	Riv_Kryptole_mar	*Kryptolebias marmoratus*	16S
AY946275	Riv_Kryptole_mar	*Kryptolebias marmoratus*	NADH2
NC_003290	Riv_Kryptole_mar	*Kryptolebias marmoratus*	cytB
AF283503	Riv_Kryptole_mar	*Kryptolebias marmoratus*	NADH1
AF002483	Riv_Laimosem_gea	*Laimosemion geayi*	cytB
AF002537	Riv_Laimosem_gea	*Laimosemion geayi*	16S
AF002604	Riv_Laimosem_gea	*Laimosemion geayi*	COI2
AY946274	Riv_Laimosem_gea	*Laimosemion geayi*	NADH2
AY946279	Riv_Laimosem_gea	*Laimosemion geayi*	12S
AF002463	Riv_Leptoleb_min	*Leptolebias minimus*	cytB
AF002514	Riv_Leptoleb_min	*Leptolebias minimus*	16S
AF002583	Riv_Leptoleb_min	*Leptolebias minimus*	COI2
AF092297	Riv_Leptoleb_min	*Leptolebias minimus*	12S
KC701998	Riv_Leptoleb_min	*Leptolebias minimus*	ENC1
KC702130	Riv_Leptoleb_min	*Leptolebias minimus*	SH3PX3
EF017431	Poe_Limia_dom	*Limia dominicensis*	RAG1
EF017482	Poe_Limia_dom	*Limia dominicensis*	12S
EF017533	Poe_Limia_dom	*Limia dominicensis*	cytB
EF017582	Poe_Limia_dom	*Limia dominicensis*	NADH2
EF017582	Poe_Limia_dom	*Limia dominicensis*	NADH1
GU179154	Poe_Limia_dom	*Limia dominicensis*	X-SRC
GU179170	Poe_Limia_dom	*Limia dominicensis*	ENC1
GU179199	Poe_Limia_dom	*Limia dominicensis*	GLYT
GU179216	Poe_Limia_dom	*Limia dominicensis*	SH3PX3
GU179245	Poe_Limia_dom	*Limia dominicensis*	MYH6
AF092353	Riv_Llanoleb_ste	*Llanolebias stellifer*	12S
EF455713	Riv_Llanoleb_ste	*Llanolebias stellifer*	RAG1
KC702004	Riv_Llanoleb_ste	*Llanolebias stellifer*	ENC1
KC702139	Riv_Llanoleb_ste	*Llanolebias stellifer*	SH3PX3
GQ119768	Fun_Lucania_goo	*Lucania goodei*	cytB

HQ557449	Fun_Lucania_goo	*Lucania goodei*	COI1
JX188690	Fun_Lucania_goo	*Lucania goodei*	GLYT
JX189549	Fun_Lucania_goo	*Lucania goodei*	SH3PX3
KJ696915	Fun_Lucania_goo	*Lucania goodei*	ENC1
KJ697135	Fun_Lucania_goo	*Lucania goodei*	MYH6
KJ697304	Fun_Lucania_goo	*Lucania goodei*	RAG1
KJ697614	Fun_Lucania_goo	*Lucania goodei*	X-SRC
AF002466	Riv_Marateco_lac	*Maratecoara lacortei*	cytB
AF002517	Riv_Marateco_lac	*Maratecoara lacortei*	16S
AF002585	Riv_Marateco_lac	*Maratecoara lacortei*	COI2
AF092343	Riv_Marateco_lac	*Maratecoara lacortei*	12S
AY902052	Cyp_Megupsil_apo	*Megupsilon aporus*	cytB
AY902110	Cyp_Megupsil_apo	*Megupsilon aporus*	NADH2
MAU05978	Cyp_Megupsil_apo	*Megupsilon aporus*	16S
AF002454	Riv_Melanori_pun	*Melanorivulus punctatus*	12S
AF002504	Riv_Melanori_pun	*Melanorivulus punctatus*	cytB
AF002567	Riv_Melanori_pun	*Melanorivulus punctatus*	16S
AF002636	Riv_Melanori_pun	*Melanorivulus punctatus*	COI2
AF092389	Riv_Melanori_pun	*Melanorivulus punctatus*	NADH2
KC702021	Riv_Melanori_pun	*Melanorivulus punctatus*	ENC1
KC702150	Riv_Melanori_pun	*Melanorivulus punctatus*	SH3PX3
AF002473	Riv_Micromoe_xip	*Micromoema xiphophorus*	cytB
AF002525	Riv_Micromoe_xip	*Micromoema xiphophorus*	16S
AF002592	Riv_Micromoe_xip	*Micromoema xiphophorus*	COI2
AF092351	Riv_Micromoe_xip	*Micromoema xiphophorus*	12S
EF455720	Riv_Micromoe_xip	*Micromoema xiphophorus*	RAG1
EF017435	Poe_Micropoe_pic	*Micropoecilia picta*	RAG1
EF017486	Poe_Micropoe_pic	*Micropoecilia picta*	12S
EF017586	Poe_Micropoe_pic	*Micropoecilia picta*	NADH2
EF017586	Poe_Micropoe_pic	*Micropoecilia picta*	NADH1
GU179161	Poe_Micropoe_pic	*Micropoecilia picta*	X-SRC
GU179177	Poe_Micropoe_pic	*Micropoecilia picta*	ENC1
GU179191	Poe_Micropoe_pic	*Micropoecilia picta*	cytB
GU179206	Poe_Micropoe_pic	*Micropoecilia picta*	GLYT
GU179223	Poe_Micropoe_pic	*Micropoecilia picta*	SH3PX3
GU179251	Poe_Micropoe_pic	*Micropoecilia picta*	MYH6
AF002457	Riv_Moema_pir	*Moema piriana*	12S
AF002507	Riv_Moema_pir	*Moema piriana*	cytB
AF002570	Riv_Moema_pir	*Moema piriana*	16S
AF002639	Riv_Moema_pir	*Moema piriana*	COI2
AF002511	Riv_Nematole_whi	*Nematolebias whitei*	16S

AF002577	Riv_Nematole_whi	*Nematolebias whitei*	COI2
AF092298	Riv_Nematole_whi	*Nematolebias whitei*	12S
CWU41784	Riv_Nematole_whi	*Nematolebias whitei*	cytB
KC701991	Riv_Nematole_whi	*Nematolebias whitei*	ENC1
U02348	Riv_Nematole_whi	*Nematolebias whitei*	X-SRC
AF002510	Riv_Neofundu_par	*Neofundulus paraguayensis*	cytB
AF002573	Riv_Neofundu_par	*Neofundulus paraguayensis*	16S
AF002643	Riv_Neofundu_par	*Neofundulus paraguayensis*	COI2
AF092338	Riv_Neofundu_par	*Neofundulus paraguayensis*	12S
EF455722	Riv_Neofundu_par	*Neofundulus paraguayensis*	RAG1
KC702000	Riv_Neofundu_par	*Neofundulus paraguayensis*	ENC1
EF017423	Poe_Neoheter_tri	*Neoheterandria tridentiger*	RAG1
EF017474	Poe_Neoheter_tri	*Neoheterandria tridentiger*	12S
EF017526	Poe_Neoheter_tri	*Neoheterandria tridentiger*	cytB
EF017576	Poe_Neoheter_tri	*Neoheterandria tridentiger*	NADH2
EF017576	Poe_Neoheter_tri	*Neoheterandria tridentiger*	NADH1
KJ696920	Poe_Neoheter_tri	*Neoheterandria tridentiger*	ENC1
KJ697030	Poe_Neoheter_tri	*Neoheterandria tridentiger*	GLYT
KJ697140	Poe_Neoheter_tri	*Neoheterandria tridentiger*	MYH6
KJ697513	Poe_Neoheter_tri	*Neoheterandria tridentiger*	SH3PX3
KJ697619	Poe_Neoheter_tri	*Neoheterandria tridentiger*	X-SRC
AF000691	Not_Nimbapan_vir	*Nimbapanchax viridis*	12S
AF000715	Not_Nimbapan_vir	*Nimbapanchax viridis*	cytB
FJ872027	Not_Nimbapan_vir	*Nimbapanchax viridis*	16S
FJ872055	Not_Nimbapan_vir	*Nimbapanchax viridis*	NADH2
AF002349	Not_Nothobra_kir	*Nothobranchius kirki*	12S
JF444882	Not_Nothobra_kir	*Nothobranchius kirki*	GLYT
JF444896	Not_Nothobra_kir	*Nothobranchius kirki*	MYH6
JF444908	Not_Nothobra_kir	*Nothobranchius kirki*	SH3PX3
JQ310171	Not_Nothobra_kir	*Nothobranchius kirki*	COI2
NKU73250	Not_Nothobra_kir	*Nothobranchius kirki*	16S
NKU73297	Not_Nothobra_kir	*Nothobranchius kirki*	cytB
AF449346	Cyp_Orestias_aga	*Orestias agassizii*	NADH2
AF449408	Cyp_Orestias_aga	*Orestias agassizii*	12S
JX092172	Cyp_Orestias_aga	*Orestias agassizii*	cytB
KJ696921	Cyp_Orestias_aga	*Orestias agassizii*	ENC1
KJ697031	Cyp_Orestias_aga	*Orestias agassizii*	GLYT
KJ697141	Cyp_Orestias_aga	*Orestias agassizii*	MYH6
KJ697620	Cyp_Orestias_aga	*Orestias agassizii*	X-SRC
OAU05966	Cyp_Orestias_aga	*Orestias agassizii*	16S
EF032927	Bel_Oryzias_la	*Oryzias latipes*	MYH6

EF033005	Bel_Oryzias_la	*Oryzias latipes*	SH3PX3
EF095641	Bel_Oryzias_la	*Oryzias latipes*	RAG1
NC_004387	Bel_Oryzias_la	*Oryzias latipes*	12S
NC_004387	Bel_Oryzias_la	*Oryzias latipes*	NADH2
NC_004387	Bel_Oryzias_la	*Oryzias latipes*	NADH1
NC_004387	Bel_Oryzias_la	*Oryzias latipes*	cytB
NC_004387	Bel_Oryzias_la	*Oryzias latipes*	COI1
NC_004387	Bel_Oryzias_la	*Oryzias latipes*	16S
AF449340	Ana_Oxyzygon_dov	*Oxyzygonectes dovii*	NADH2
AY356581	Ana_Oxyzygon_dov	*Oxyzygonectes dovii*	COI1
EF017407	Ana_Oxyzygon_dov	*Oxyzygonectes dovii*	RAG1
EF017458	Ana_Oxyzygon_dov	*Oxyzygonectes dovii*	12S
EF017510	Ana_Oxyzygon_dov	*Oxyzygonectes dovii*	cytB
EF017560	Ana_Oxyzygon_dov	*Oxyzygonectes dovii*	NADH1
KJ696922	Ana_Oxyzygon_dov	*Oxyzygonectes dovii*	ENC1
KJ697032	Ana_Oxyzygon_dov	*Oxyzygonectes dovii*	GLYT
KJ697142	Ana_Oxyzygon_dov	*Oxyzygonectes dovii*	MYH6
KJ697621	Ana_Oxyzygon_dov	*Oxyzygonectes dovii*	X-SRC
DQ532927	Apl_Pachypan_pla	*Pachypanchax playfairii*	16S
JX190385	Apl_Pachypan_pla	*Pachypanchax playfairii*	GLYT
JX190914	Apl_Pachypan_pla	*Pachypanchax playfairii*	RAG1
JX191048	Apl_Pachypan_pla	*Pachypanchax playfairii*	SH3PX3
KF139432	Apl_Pachypan_pla	*Pachypanchax playfairii*	ENC1
PPU73263	Apl_Pachypan_pla	*Pachypanchax playfairii*	12S
PPU73285	Apl_Pachypan_pla	*Pachypanchax playfairii*	cytB
EF017487	Poe_Pamphori_hol	*Pamphorichthys hollandi*	12S
EF017538	Poe_Pamphori_hol	*Pamphorichthys hollandi*	cytB
EF017587	Poe_Pamphori_hol	*Pamphorichthys hollandi*	NADH2
EF017587	Poe_Pamphori_hol	*Pamphorichthys hollandi*	NADH1
GU701605	Poe_Pamphori_hol	*Pamphorichthys hollandi*	COI1
HQ857422	Poe_Pamphori_hol	*Pamphorichthys hollandi*	SH3PX3
HQ857434	Poe_Pamphori_hol	*Pamphorichthys hollandi*	X-SRC
HQ857446	Poe_Pamphori_hol	*Pamphorichthys hollandi*	RAG1
HQ857458	Poe_Pamphori_hol	*Pamphorichthys hollandi*	MYH6
HQ857464	Poe_Pamphori_hol	*Pamphorichthys hollandi*	GLYT
HQ857470	Poe_Pamphori_hol	*Pamphorichthys hollandi*	ENC1
AF002520	Riv_Papiliol_bit	*Papiliolebias bitteri*	16S
AF002588	Riv_Papiliol_bit	*Papiliolebias bitteri*	COI2
AF092341	Riv_Papiliol_bit	*Papiliolebias bitteri*	12S
KC702006	Riv_Papiliol_bit	*Papiliolebias bitteri*	ENC1
DQ386548	Poe_Phallich_ama	*Phallichthys amates*	16S

EF017410	Poe_Phallich_ama	*Phallichthys amates*	RAG1
EF017461	Poe_Phallich_ama	*Phallichthys amates*	12S
EF017513	Poe_Phallich_ama	*Phallichthys amates*	cytB
EF017563	Poe_Phallich_ama	*Phallichthys amates*	NADH2
EF017563	Poe_Phallich_ama	*Phallichthys amates*	NADH1
KJ696923	Poe_Phallich_ama	*Phallichthys amates*	ENC1
KJ697033	Poe_Phallich_ama	*Phallichthys amates*	GLYT
KJ697143	Poe_Phallich_ama	*Phallichthys amates*	MYH6
KJ697516	Poe_Phallich_ama	*Phallichthys amates*	SH3PX3
KJ697622	Poe_Phallich_ama	*Phallichthys amates*	X-SRC
EF017426	Poe_Phalloce_cau	*Phalloceros caudimaculatus*	RAG1
EF017477	Poe_Phalloce_cau	*Phalloceros caudimaculatus*	12S
EF017578	Poe_Phalloce_cau	*Phalloceros caudimaculatus*	NADH2
EF017578	Poe_Phalloce_cau	*Phalloceros caudimaculatus*	NADH1
KJ696926	Poe_Phalloce_cau	*Phalloceros caudimaculatus*	ENC1
KJ697036	Poe_Phalloce_cau	*Phalloceros caudimaculatus*	GLYT
KJ697146	Poe_Phalloce_cau	*Phalloceros caudimaculatus*	MYH6
KJ697519	Poe_Phalloce_cau	*Phalloceros caudimaculatus*	SH3PX3
KJ697625	Poe_Phalloce_cau	*Phalloceros caudimaculatus*	X-SRC
PCU80053	Poe_Phalloce_cau	*Phalloceros caudimaculatus*	16S
EF017428	Poe_Phallopt_jan	*Phalloptychus januarius*	RAG1
EF017479	Poe_Phallopt_jan	*Phalloptychus januarius*	12S
EF017530	Poe_Phallopt_jan	*Phalloptychus januarius*	cytB
KJ696927	Poe_Phallopt_jan	*Phalloptychus januarius*	ENC1
KJ697037	Poe_Phallopt_jan	*Phalloptychus januarius*	GLYT
KJ697147	Poe_Phallopt_jan	*Phalloptychus januarius*	MYH6
KJ697520	Poe_Phallopt_jan	*Phalloptychus januarius*	SH3PX3
KJ697626	Poe_Phallopt_jan	*Phalloptychus januarius*	X-SRC
AF002467	Riv_Pituna_por	*Pituna poranga*	cytB
AF002518	Riv_Pituna_por	*Pituna poranga*	16S
AF002586	Riv_Pituna_por	*Pituna poranga*	COI2
AF092345	Riv_Pituna_por	*Pituna poranga*	12S
KC702003	Riv_Pituna_por	*Pituna poranga*	ENC1
KC702138	Riv_Pituna_por	*Pituna poranga*	SH3PX3
AF243874	Bel_Platybel_ar	*Platybelone argala*	cytB
AF243950	Bel_Platybel_ar	*Platybelone argala*	16S
JQ840640	Bel_Platybel_ar	*Platybelone argala*	COI1
JX189541	Bel_Platybel_ar	*Platybelone argala*	SH3PX3
JX189789	Bel_Platybel_ar	*Platybelone argala*	RAG1
KC827246	Bel_Platybel_ar	*Platybelone argala*	MYH6
AF002468	Riv_Plesiole_aru	*Plesiolebias aruana*	cytB

AF002519	Riv_Plesiole_aru	*Plesiolebias aruana*	16S
AF002587	Riv_Plesiole_aru	*Plesiolebias aruana*	COI2
AF092342	Riv_Plesiole_aru	*Plesiolebias aruana*	12S
KC702005	Riv_Plesiole_aru	*Plesiolebias aruana*	ENC1
EF017434	Poe_Poecilia_ret	*Poecilia reticulata*	RAG1
EF017485	Poe_Poecilia_ret	*Poecilia reticulata*	12S
EF017585	Poe_Poecilia_ret	*Poecilia reticulata*	NADH2
EF017585	Poe_Poecilia_ret	*Poecilia reticulata*	NADH1
GQ855709	Poe_Poecilia_ret	*Poecilia reticulata*	cytB
GU179162	Poe_Poecilia_ret	*Poecilia reticulata*	X-SRC
GU179178	Poe_Poecilia_ret	*Poecilia reticulata*	ENC1
GU179207	Poe_Poecilia_ret	*Poecilia reticulata*	GLYT
GU179224	Poe_Poecilia_ret	*Poecilia reticulata*	SH3PX3
GU179253	Poe_Poecilia_ret	*Poecilia reticulata*	MYH6
JN028265	Poe_Poecilia_ret	*Poecilia reticulata*	COI1
NC_024238	Poe_Poecilia_ret	*Poecilia reticulata*	16S
AF412129	Poe_Poecilio_elo	*Poeciliopsis elongata*	cytB
AF412172	Poe_Poecilio_elo	*Poeciliopsis elongata*	NADH2
KJ696944	Poe_Poecilio_elo	*Poeciliopsis elongata*	ENC1
KJ697054	Poe_Poecilio_elo	*Poeciliopsis elongata*	GLYT
KJ697164	Poe_Poecilio_elo	*Poeciliopsis elongata*	MYH6
KJ697327	Poe_Poecilio_elo	*Poeciliopsis elongata*	RAG1
KJ697537	Poe_Poecilio_elo	*Poeciliopsis elongata*	SH3PX3
KJ697643	Poe_Poecilio_elo	*Poeciliopsis elongata*	X-SRC
EF017451	Poe_Priapell_com	*Priapella compressa*	RAG1
EF017503	Poe_Priapell_com	*Priapella compressa*	12S
EF017603	Poe_Priapell_com	*Priapella compressa*	NADH2
EF017603	Poe_Priapell_com	*Priapella compressa*	NADH1
KJ525791	Poe_Priapell_com	*Priapella compressa*	SH3PX3
KJ525851	Poe_Priapell_com	*Priapella compressa*	MYH6
KJ525871	Poe_Priapell_com	*Priapella compressa*	GLYT
KJ525891	Poe_Priapell_com	*Priapella compressa*	ENC1
KJ525911	Poe_Priapell_com	*Priapella compressa*	X-SRC
DQ386565	Poe_Priapich_ann	*Priapichthys annectens*	16S
EF017439	Poe_Priapich_ann	*Priapichthys annectens*	RAG1
EF017491	Poe_Priapich_ann	*Priapichthys annectens*	12S
EF017542	Poe_Priapich_ann	*Priapichthys annectens*	cytB
EF017591	Poe_Priapich_ann	*Priapichthys annectens*	NADH2
EF017591	Poe_Priapich_ann	*Priapichthys annectens*	NADH1
KJ696961	Poe_Priapich_ann	*Priapichthys annectens*	ENC1
KJ697071	Poe_Priapich_ann	*Priapichthys annectens*	GLYT

KJ697181	Poe_Priapich_ann	*Priapichthys annectens*	MYH6
KJ697554	Poe_Priapich_ann	*Priapichthys annectens*	SH3PX3
KJ697660	Poe_Priapich_ann	*Priapichthys annectens*	X-SRC
AY155568	Pro_Profundu_gua	*Profundulus guatemalensis*	cytB
GQ119857	Pro_Profundu_gua	*Profundulus guatemalensis*	RAG1
JN028283	Pro_Profundu_gua	*Profundulus guatemalensis*	COI1
U02356	Pro_Profundu_gua	*Profundulus guatemalensis*	X-SRC
AF002285	Not_Pronotho_kiy	*Pronothobranchius kiyawensis*	cytB
AF002348	Not_Pronotho_kiy	*Pronothobranchius kiyawensis*	12S
AF002406	Not_Pronotho_kiy	*Pronothobranchius kiyawensis*	16S
EF464705	Not_Pronotho_kiy	*Pronothobranchius kiyawensis*	COI2
EF017440	Poe_Pseudopo_fes	*Pseudopoecilia festae*	RAG1
EF017492	Poe_Pseudopo_fes	*Pseudopoecilia festae*	12S
EF017543	Poe_Pseudopo_fes	*Pseudopoecilia festae*	cytB
EF017592	Poe_Pseudopo_fes	*Pseudopoecilia festae*	NADH2
EF017592	Poe_Pseudopo_fes	*Pseudopoecilia festae*	NADH1
KJ696965	Poe_Pseudopo_fes	*Pseudopoecilia festae*	ENC1
KJ697075	Poe_Pseudopo_fes	*Pseudopoecilia festae*	GLYT
KJ697185	Poe_Pseudopo_fes	*Pseudopoecilia festae*	MYH6
KJ697558	Poe_Pseudopo_fes	*Pseudopoecilia festae*	SH3PX3
KJ697664	Poe_Pseudopo_fes	*Pseudopoecilia festae*	X-SRC
JQ612894	Poe_Pseudoxi_obl	*Pseudoxiphophorus obliquus*	cytB
JQ612950	Poe_Pseudoxi_obl	*Pseudoxiphophorus obliquus*	16S
AF002595	Riv_Pteroleb_lon	*Pterolebias longipinnis*	COI2
AF092348	Riv_Pteroleb_lon	*Pterolebias longipinnis*	12S
AF244446	Riv_Pteroleb_lon	*Pterolebias longipinnis*	16S
AF245462	Riv_Pteroleb_lon	*Pterolebias longipinnis*	cytB
EF455709	Riv_Pteroleb_lon	*Pterolebias longipinnis*	RAG1
KC702007	Riv_Pteroleb_lon	*Pterolebias longipinnis*	ENC1
EF017453	Poe_Quintana_atr	*Quintana atrizona*	RAG1
EF017505	Poe_Quintana_atr	*Quintana atrizona*	12S
EF017605	Poe_Quintana_atr	*Quintana atrizona*	NADH2
EF017605	Poe_Quintana_atr	*Quintana atrizona*	NADH1
FJ178764	Poe_Quintana_atr	*Quintana atrizona*	cytB
FN545618	Poe_Quintana_atr	*Quintana atrizona*	COI1
AF002470	Riv_Rachovia_mac	*Rachovia maculipinnis*	cytB
AF002522	Riv_Rachovia_mac	*Rachovia maculipinnis*	16S
AF002590	Riv_Rachovia_mac	*Rachovia maculipinnis*	COI2
AY850639	Riv_Rachovia_mac	*Rachovia maculipinnis*	NADH2
AY850639	Riv_Rachovia_mac	*Rachovia maculipinnis*	NADH1
AY850664	Riv_Rachovia_mac	*Rachovia maculipinnis*	12S

EF455714	Riv_Rachovia_mac	*Rachovia maculipinnis*	RAG1
AF002475	Riv_Renova_osc	*Renova oscari*	cytB
AF002527	Riv_Renova_osc	*Renova oscari*	16S
AF002594	Riv_Renova_osc	*Renova oscari*	COI2
AF092346	Riv_Renova_osc	*Renova oscari*	12S
EF455721	Riv_Renova_osc	*Renova oscari*	RAG1
KC702140	Riv_Renova_osc	*Renova oscari*	SH3PX3
AF002533	Riv_Rivulus_cyl	*Rivulus cylindraceus*	16S
AF002601	Riv_Rivulus_cyl	*Rivulus cylindraceus*	COI2
AF092304	Riv_Rivulus_cyl	*Rivulus cylindraceus*	12S
FN544245	Riv_Rivulus_cyl	*Rivulus cylindraceus*	COI1
KC702013	Riv_Rivulus_cyl	*Rivulus cylindraceus*	ENC1
KC702143	Riv_Rivulus_cyl	*Rivulus cylindraceus*	SH3PX3
RCU41782	Riv_Rivulus_cyl	*Rivulus cylindraceus*	cytB
KJ696967	Poe_Scolicht_iot	*Scolichthys iota*	ENC1
KJ697077	Poe_Scolicht_iot	*Scolichthys iota*	GLYT
KJ697187	Poe_Scolicht_iot	*Scolichthys iota*	MYH6
KJ697344	Poe_Scolicht_iot	*Scolichthys iota*	RAG1
KJ697560	Poe_Scolicht_iot	*Scolichthys iota*	SH3PX3
KJ697666	Poe_Scolicht_iot	*Scolichthys iota*	X-SRC
AF092292	Not_Scriptap_ger	*Scriptaphyosemion geryi*	12S
EF464684	Not_Scriptap_ger	*Scriptaphyosemion geryi*	COI2
FJ872033	Not_Scriptap_ger	*Scriptaphyosemion geryi*	16S
JX044123	Not_Scriptap_ger	*Scriptaphyosemion geryi*	cytB
JX124267	Not_Scriptap_ger	*Scriptaphyosemion geryi*	NADH2
KJ696968	Goo_Skiffia_mul	*Skiffia multipunctata*	ENC1
KJ697078	Goo_Skiffia_mul	*Skiffia multipunctata*	GLYT
KJ697188	Goo_Skiffia_mul	*Skiffia multipunctata*	MYH6
KJ697345	Goo_Skiffia_mul	*Skiffia multipunctata*	RAG1
KJ697667	Goo_Skiffia_mul	*Skiffia multipunctata*	X-SRC
AF002410	Riv_Spectrol_cos	*Spectrolebias costai*	12S
AF002461	Riv_Spectrol_cos	*Spectrolebias costai*	cytB
AF002512	Riv_Spectrol_cos	*Spectrolebias costai*	16S
AF002578	Riv_Spectrol_cos	*Spectrolebias costai*	COI2
KC701986	Riv_Spectrol_cos	*Spectrolebias costai*	ENC1
KC702119	Riv_Spectrol_cos	*Spectrolebias costai*	SH3PX3
AF231521	Bel_Strongyl_ma	*Strongylura marina*	16S
AF231554	Bel_Strongyl_ma	*Strongylura marina*	12S
AF231642	Bel_Strongyl_ma	*Strongylura marina*	cytB
HQ937019	Bel_Strongyl_ma	*Strongylura marina*	COI1
JQ282086	Bel_Strongyl_ma	*Strongylura marina*	RAG1

JX189542	Bel_Strongyl_ma	*Strongylura marina*	SH3PX3
JX189635	Bel_Strongyl_ma	*Strongylura marina*	MYH6
AF002474	Riv_Terranat_dol	*Terranatos dolichopterus*	cytB
AF002526	Riv_Terranat_dol	*Terranatos dolichopterus*	16S
AF002593	Riv_Terranat_dol	*Terranatos dolichopterus*	COI2
AF092354	Riv_Terranat_dol	*Terranatos dolichopterus*	12S
EF455716	Riv_Terranat_dol	*Terranatos dolichopterus*	RAG1
KC702029	Riv_Terranat_dol	*Terranatos dolichopterus*	ENC1
KC702157	Riv_Terranat_dol	*Terranatos dolichopterus*	SH3PX3
EF017455	Poe_Tomeurus_gra	*Tomeurus gracilis*	RAG1
EF017507	Poe_Tomeurus_gra	*Tomeurus gracilis*	12S
EF017607	Poe_Tomeurus_gra	*Tomeurus gracilis*	NADH2
EF017607	Poe_Tomeurus_gra	*Tomeurus gracilis*	NADH1
KJ696969	Poe_Tomeurus_gra	*Tomeurus gracilis*	ENC1
KJ697079	Poe_Tomeurus_gra	*Tomeurus gracilis*	GLYT
KJ697189	Poe_Tomeurus_gra	*Tomeurus gracilis*	MYH6
KJ697562	Poe_Tomeurus_gra	*Tomeurus gracilis*	SH3PX3
KJ697668	Poe_Tomeurus_gra	*Tomeurus gracilis*	X-SRC
AF002509	Riv_Trigonec_bal	*Trigonectes balzanii*	cytB
AF002641	Riv_Trigonec_bal	*Trigonectes balzanii*	COI2
AF092334	Riv_Trigonec_bal	*Trigonectes balzanii*	12S
AF244447	Riv_Trigonec_bal	*Trigonectes balzanii*	16S
KC702030	Riv_Trigonec_bal	*Trigonectes balzanii*	ENC1
KC702158	Riv_Trigonec_bal	*Trigonectes balzanii*	SH3PX3
AF449339	Val_Valencia_his	*Valencia hispanica*	NADH2
AF449400	Val_Valencia_his	*Valencia hispanica*	12S
KJ696970	Val_Valencia_his	*Valencia hispanica*	ENC1
KJ697080	Val_Valencia_his	*Valencia hispanica*	GLYT
KJ697190	Val_Valencia_his	*Valencia hispanica*	MYH6
KJ697669	Val_Valencia_his	*Valencia hispanica*	X-SRC
AF243890	Bel_Xenentod_ca	*Xenentodon cancila*	cytB
AF243967	Bel_Xenentod_ca	*Xenentodon cancila*	16S
AF508061	Bel_Xenentod_ca	*Xenentodon cancila*	12S
FJ459538	Bel_Xenentod_ca	*Xenentodon cancila*	COI1
JX189543	Bel_Xenentod_ca	*Xenentodon cancila*	SH3PX3
JX189636	Bel_Xenentod_ca	*Xenentodon cancila*	MYH6
JX190869	Bel_Xenentod_ca	*Xenentodon cancila*	RAG1
EF017454	Poe_Xenodexi_cte	*Xenodexia ctenolepis*	RAG1
EF017506	Poe_Xenodexi_cte	*Xenodexia ctenolepis*	12S
EF017557	Poe_Xenodexi_cte	*Xenodexia ctenolepis*	cytB
EF017606	Poe_Xenodexi_cte	*Xenodexia ctenolepis*	NADH2

EF017606	Poe_Xenodexi_cte	*Xenodexia ctenolepis*	NADH1
KJ696971	Poe_Xenodexi_cte	*Xenodexia ctenolepis*	ENC1
KJ697081	Poe_Xenodexi_cte	*Xenodexia ctenolepis*	GLYT
KJ697191	Poe_Xenodexi_cte	*Xenodexia ctenolepis*	MYH6
KJ697564	Poe_Xenodexi_cte	*Xenodexia ctenolepis*	SH3PX3
KJ697670	Poe_Xenodexi_cte	*Xenodexia ctenolepis*	X-SRC
AF510759	Goo_Xenoopho_cap	*Xenoophorus captiva*	cytB
AY356586	Goo_Xenoopho_cap	*Xenoophorus captiva*	COI1
KJ696972	Goo_Xenoopho_cap	*Xenoophorus captivus*	ENC1
KJ697082	Goo_Xenoopho_cap	*Xenoophorus captivus*	GLYT
KJ697192	Goo_Xenoopho_cap	*Xenoophorus captivus*	MYH6
KJ697346	Goo_Xenoopho_cap	*Xenoophorus captivus*	RAG1
KJ697671	Goo_Xenoopho_cap	*Xenoophorus captivus*	X-SRC
EF017424	Poe_Xenophal_umb	*Xenophallus umbratilis*	RAG1
EF017475	Poe_Xenophal_umb	*Xenophallus umbratilis*	12S
EF017527	Poe_Xenophal_umb	*Xenophallus umbratilis*	cytB
EF017577	Poe_Xenophal_umb	*Xenophallus umbratilis*	NADH2
KJ696973	Poe_Xenophal_umb	*Xenophallus umbratilis*	ENC1
KJ697083	Poe_Xenophal_umb	*Xenophallus umbratilis*	GLYT
KJ697193	Poe_Xenophal_umb	*Xenophallus umbratilis*	MYH6
KJ697566	Poe_Xenophal_umb	*Xenophallus umbratilis*	SH3PX3
KJ697672	Poe_Xenophal_umb	*Xenophallus umbratilis*	X-SRC
AF510825	Goo_Xenotaen_res	*Xenotaenia resolanae*	cytB
AY356590	Goo_Xenotaen_res	*Xenotaenia resolanae*	COI1
AP006777	Goo_Xenotoca_eis	*Xenotoca eiseni*	12S
AP006777	Goo_Xenotoca_eis	*Xenotoca eiseni*	NADH2
AP006777	Goo_Xenotoca_eis	*Xenotoca eiseni*	cytB
AP006777	Goo_Xenotoca_eis	*Xenotoca eiseni*	COI1
AP006777	Goo_Xenotoca_eis	*Xenotoca eiseni*	16S
KJ696974	Goo_Xenotoca_eis	*Xenotoca eiseni*	ENC1
KJ697084	Goo_Xenotoca_eis	*Xenotoca eiseni*	GLYT
KJ697194	Goo_Xenotoca_eis	*Xenotoca eiseni*	MYH6
KJ697348	Goo_Xenotoca_eis	*Xenotoca eiseni*	RAG1
KJ697673	Goo_Xenotoca_eis	*Xenotoca eiseni*	X-SRC
EF017445	Poe_Xiphopho_hel	*Xiphophorus hellerii*	RAG1
EF017597	Poe_Xiphopho_hel	*Xiphophorus hellerii*	NADH2
EF017597	Poe_Xiphopho_hel	*Xiphophorus hellerii*	NADH1
FJ234985	Poe_Xiphopho_hel	*Xiphophorus hellerii*	12S
FJ234985	Poe_Xiphopho_hel	*Xiphophorus hellerii*	cytB
FJ234985	Poe_Xiphopho_hel	*Xiphophorus hellerii*	16S
HQ219147	Poe_Xiphopho_hel	*Xiphophorus hellerii*	COI1

KJ525779	Poe_Xiphopho_hel	*Xiphophorus hellerii*	SH3PX3
KJ525839	Poe_Xiphopho_hel	*Xiphophorus hellerii*	MYH6
KJ525859	Poe_Xiphopho_hel	*Xiphophorus hellerii*	GLYT
KJ525879	Poe_Xiphopho_hel	*Xiphophorus hellerii*	ENC1
KJ525899	Poe_Xiphopho_hel	*Xiphophorus hellerii*	X-SRC
AF510752	Goo_Zoogonet_qui	*Zoogoneticus quitzeoensis*	cytB
AY356592	Goo_Zoogonet_qui	*Zoogoneticus quitzeoensis*	COI1
KJ696975	Goo_Zoogonet_qui	*Zoogoneticus quitzeoensis*	ENC1
KJ697085	Goo_Zoogonet_qui	*Zoogoneticus quitzeoensis*	GLYT
KJ697195	Goo_Zoogonet_qui	*Zoogoneticus quitzeoensis*	MYH6
KJ697349	Goo_Zoogonet_qui	*Zoogoneticus quitzeoensis*	RAG1
U02365	Goo_Zoogonet_qui	*Zoogoneticus quitzeoensis*	X-SRC
Accession	Tip label	*Organism*	Gene
GQ119680	Fun_Adinia_xen	*Adinia xenica*	cytB
GQ119858	Fun_Adinia_xen	*Adinia xenica*	RAG1
JN024713	Fun_Adinia_xen	*Adinia xenica*	COI1
KC826901	Fun_Adinia_xen	*Adinia xenica*	MYH6
ACU80048	Poe_Alfaro_cul	*Alfaro cultratus*	16S
EF017429	Poe_Alfaro_cul	*Alfaro cultratus*	RAG1
EF017480	Poe_Alfaro_cul	*Alfaro cultratus*	12S
EF017531	Poe_Alfaro_cul	*Alfaro cultratus*	cytB
EF017580	Poe_Alfaro_cul	*Alfaro cultratus*	NADH1
KJ696868	Poe_Alfaro_cul	*Alfaro cultratus*	ENC1
KJ696977	Poe_Alfaro_cul	*Alfaro cultratus*	GLYT
KJ697087	Poe_Alfaro_cul	*Alfaro cultratus*	MYH6
KJ697460	Poe_Alfaro_cul	*Alfaro cultratus*	SH3PX3
KJ697570	Poe_Alfaro_cul	*Alfaro cultratus*	X-SRC
AF510839	Goo_Allodont_pol	*Allodontichthys polylepis*	cytB
AY356555	Goo_Allodont_pol	*Allodontichthys polylepis*	COI1
AF510813	Goo_Alloopho_rob	*Alloophorus robustus*	cytB
AY356561	Goo_Alloopho_rob	*Alloophorus robustus*	COI1
AF510795	Goo_Allotoca_cat	*Allotoca catarinae*	cytB
AY356562	Goo_Allotoca_cat	*Allotoca catarinae*	COI1
AF510818	Goo_Ameca_spl	*Ameca splendens*	cytB
AY356564	Goo_Ameca_spl	*Ameca splendens*	COI1
KJ696869	Goo_Ameca_spl	*Ameca splendens*	ENC1
KJ696978	Goo_Ameca_spl	*Ameca splendens*	GLYT
KJ697088	Goo_Ameca_spl	*Ameca splendens*	MYH6
KJ697267	Goo_Ameca_spl	*Ameca splendens*	RAG1
KJ697461	Goo_Ameca_spl	*Ameca splendens*	SH3PX3
KJ697571	Goo_Ameca_spl	*Ameca splendens*	X-SRC

AF449341	Ana_Anableps_ana	*Anableps anableps*	NADH2
EF017405	Ana_Anableps_ana	*Anableps anableps*	RAG1
EF017456	Ana_Anableps_ana	*Anableps anableps*	12S
EF017508	Ana_Anableps_ana	*Anableps anableps*	cytB
EF017558	Ana_Anableps_ana	*Anableps anableps*	NADH1
KJ696870	Ana_Anableps_ana	*Anableps anableps*	ENC1
KJ696979	Ana_Anableps_ana	*Anableps anableps*	GLYT
KJ697089	Ana_Anableps_ana	*Anableps anableps*	MYH6
KJ697572	Ana_Anableps_ana	*Anableps anableps*	X-SRC
AF002551	Riv_Anableps_har	*Anablepsoides hartii*	16S
AF002619	Riv_Anableps_har	*Anablepsoides hartii*	COI2
AF092326	Riv_Anableps_har	*Anablepsoides hartii*	12S
AF092393	Riv_Anableps_har	*Anablepsoides hartii*	NADH2
AY619607	Riv_Anableps_har	*Anablepsoides hartii*	cytB
HQ405569	Riv_Anableps_har	*Anablepsoides hartii*	COI1
KC702145	Riv_Anableps_har	*Anablepsoides hartii*	SH3PX3
KJ696966	Riv_Anableps_har	*Anablepsoides hartii*	ENC1
KJ697076	Riv_Anableps_har	*Anablepsoides hartii*	GLYT
KJ697186	Riv_Anableps_har	*Anablepsoides hartii*	MYH6
U02357	Riv_Anableps_har	*Anablepsoides hartii*	X-SRC
AF299273	Cyp_Aphanius_fas	*Aphanius fasciatus*	cytB
AF449310	Cyp_Aphanius_fas	*Aphanius fasciatus*	NADH2
AF449369	Cyp_Aphanius_fas	*Aphanius fasciatus*	12S
AFU05965	Cyp_Aphanius_fas	*Aphanius fasciatus*	16S
DQ923022	Cyp_Aphanius_fas	*Aphanius fasciatus*	NADH1
AF002506	Riv_Aphyoleb_per	*Aphyolebias peruensis*	cytB
AF002569	Riv_Aphyoleb_per	*Aphyolebias peruensis*	16S
AF002638	Riv_Aphyoleb_per	*Aphyolebias peruensis*	COI2
AF092340	Riv_Aphyoleb_per	*Aphyolebias peruensis*	12S
EF455718	Riv_Aphyoleb_per	*Aphyolebias peruensis*	RAG1
AAU73245	Not_Aphyosem_aus	*Aphyosemion australe*	16S
AF002367	Not_Aphyosem_aus	*Aphyosemion australe*	12S
EF417015	Not_Aphyosem_aus	*Aphyosemion australe*	COI1
EU272816	Not_Aphyosem_aus	*Aphyosemion australe*	cytB
KC701966	Not_Aphyosem_aus	*Aphyosemion australe*	ENC1
KC702098	Not_Aphyosem_aus	*Aphyosemion australe*	SH3PX3
KJ696787	Poe_Aplochei_nor	*Aplocheilichthys normani*	cytB
KJ696873	Poe_Aplochei_nor	*Aplocheilichthys normani*	ENC1
KJ696983	Poe_Aplochei_nor	*Aplocheilichthys normani*	GLYT
KJ697093	Poe_Aplochei_nor	*Aplocheilichthys normani*	MYH6
KJ697200	Poe_Aplochei_nor	*Aplocheilichthys normani*	NADH2

KJ697272	Poe_Aplochei_nor	*Aplocheilichthys normani*	RAG1
KJ697466	Poe_Aplochei_nor	*Aplocheilichthys normani*	SH3PX3
KJ697575	Poe_Aplochei_nor	*Aplocheilichthys normani*	X-SRC
AB373005	Apl_Aplochei_pan	*Aplocheilus panchax*	12S
AB373005	Apl_Aplochei_pan	*Aplocheilus panchax*	NADH2
AB373005	Apl_Aplochei_pan	*Aplocheilus panchax*	cytB
AB373005	Apl_Aplochei_pan	*Aplocheilus panchax*	16S
EF455705	Apl_Aplochei_pan	*Aplocheilus panchax*	RAG1
KC701975	Apl_Aplochei_pan	*Aplocheilus panchax*	ENC1
KC702108	Apl_Aplochei_pan	*Aplocheilus panchax*	SH3PX3
AF000688	Not_Archiaph_gui	*Archiaphyosemion guineense*	12S
AF000711	Not_Archiaph_gui	*Archiaphyosemion guineense*	cytB
FJ872031	Not_Archiaph_gui	*Archiaphyosemion guineense*	16S
FJ872058	Not_Archiaph_gui	*Archiaphyosemion guineense*	NADH2
EF095671	Cic_Astronot_oce	*Astronotus ocellatus*	RAG1
AP009127	Cic_Astronot_oce	*Astronotus ocellatus*	12S
AP009127	Cic_Astronot_oce	*Astronotus ocellatus*	NADH2
AP009127	Cic_Astronot_oce	*Astronotus ocellatus*	NADH1
AP009127	Cic_Astronot_oce	*Astronotus ocellatus*	cytB
AP009127	Cic_Astronot_oce	*Astronotus ocellatus*	COI2
AP009127	Cic_Astronot_oce	*Astronotus ocellatus*	COI1
AP009127	Cic_Astronot_oce	*Astronotus ocellatus*	16S
KF556763	Cic_Astronot_oce	*Astronotus sp. YFTC 21011*	ENC1
KF556834	Cic_Astronot_oce	*Astronotus sp. YFTC 21011*	GLYT
KF556911	Cic_Astronot_oce	*Astronotus sp. YFTC 21011*	MYH6
KF557220	Cic_Astronot_oce	*Astronotus sp. YFTC 21011*	SH3PX3
AF510779	Goo_Ataeniob_tow	*Ataeniobius toweri*	cytB
JQ935854	Goo_Ataeniob_tow	*Ataeniobius toweri*	COI1
KJ696876	Goo_Ataeniob_tow	*Ataeniobius toweri*	ENC1
KJ696986	Goo_Ataeniob_tow	*Ataeniobius toweri*	GLYT
KJ697096	Goo_Ataeniob_tow	*Ataeniobius toweri*	MYH6
KJ697203	Goo_Ataeniob_tow	*Ataeniobius toweri*	NADH2
KJ697275	Goo_Ataeniob_tow	*Ataeniobius toweri*	RAG1
KJ697469	Goo_Ataeniob_tow	*Ataeniobius toweri*	SH3PX3
KJ697577	Goo_Ataeniob_tow	*Ataeniobius toweri*	X-SRC
AY655492	Ath_Atherino_lac	*Atherinomorus lacunosus*	16S
AY655522	Ath_Atherino_lac	*Atherinomorus lacunosus*	COI1
GU932753	Ath_Atherino_lac	*Atherinomorus lacunosus*	cytB
JX188684	Ath_Atherino_lac	*Atherinomorus lacunosus*	GLYT
JX188847	Ath_Atherino_lac	*Atherinomorus lacunosus*	ENC1
JX189538	Ath_Atherino_lac	*Atherinomorus lacunosus*	SH3PX3

JX189786	Ath_Atherino_lac	*Atherinomorus lacunosus*	RAG1
KC827019	Ath_Atherino_lac	*Atherinomorus lacunosus*	MYH6
AF002502	Riv_Atlantir_san	*Atlantirivulus santensis*	cytB
AF002565	Riv_Atlantir_san	*Atlantirivulus santensis*	16S
AF002634	Riv_Atlantir_san	*Atlantirivulus santensis*	COI2
AF092313	Riv_Atlantir_san	*Atlantirivulus santensis*	12S
EF455708	Riv_Atlantir_san	*Atlantirivulus santensis*	RAG1
GU701919	Riv_Atlantir_san	*Atlantirivulus santensis*	COI1
KC702023	Riv_Atlantir_san	*Atlantirivulus santensis*	ENC1
KC702152	Riv_Atlantir_san	*Atlantirivulus santensis*	SH3PX3
AF002589	Riv_Austrofu_lim	*Austrofundulus limnaeus*	COI2
ALU73254	Riv_Austrofu_lim	*Austrofundulus limnaeus*	16S
ALU73300	Riv_Austrofu_lim	*Austrofundulus limnaeus*	cytB
AY850644	Riv_Austrofu_lim	*Austrofundulus limnaeus*	NADH1
AY850647	Riv_Austrofu_lim	*Austrofundulus limnaeus*	NADH2
AY850667	Riv_Austrofu_lim	*Austrofundulus limnaeus*	12S
KC701978	Riv_Austrofu_lim	*Austrofundulus limnaeus*	ENC1
KC702112	Riv_Austrofu_lim	*Austrofundulus limnaeus*	SH3PX3
AF244413	Riv_Austrole_adl	*Austrolebias adloffi*	12S
KC701981	Riv_Austrole_adl	*Austrolebias adloffi*	ENC1
KC702114	Riv_Austrole_adl	*Austrolebias adloffi*	SH3PX3
AF244443	Riv_Austrole_adl	*Austrolebias adloffi-1*	16S
AF245009	Riv_Austrole_adl	*Austrolebias adloffi-1*	cytB
EF017416	Poe_Beloneso_bel	*Belonesox belizanus*	RAG1
EF017467	Poe_Beloneso_bel	*Belonesox belizanus*	12S
EF017519	Poe_Beloneso_bel	*Belonesox belizanus*	cytB
HM443919	Poe_Beloneso_bel	*Belonesox belizanus*	NADH2
JQ612957	Poe_Beloneso_bel	*Belonesox belizanus*	16S
JQ840428	Poe_Beloneso_bel	*Belonesox belizanus*	COI1
KJ696877	Poe_Beloneso_bel	*Belonesox belizanus*	ENC1
KJ696987	Poe_Beloneso_bel	*Belonesox belizanus*	GLYT
KJ697097	Poe_Beloneso_bel	*Belonesox belizanus*	MYH6
KJ697470	Poe_Beloneso_bel	*Belonesox belizanus*	SH3PX3
KJ697578	Poe_Beloneso_bel	*Belonesox belizanus*	X-SRC
EF017419	Poe_Brachyrh_rha	*Brachyrhaphis rhabdophora*	RAG1
KJ696878	Poe_Brachyrh_rha	*Brachyrhaphis rhabdophora*	ENC1
KJ696988	Poe_Brachyrh_rha	*Brachyrhaphis rhabdophora*	GLYT
KJ697098	Poe_Brachyrh_rha	*Brachyrhaphis rhabdophora*	MYH6
KJ697471	Poe_Brachyrh_rha	*Brachyrhaphis rhabdophora*	SH3PX3
KJ697579	Poe_Brachyrh_rha	*Brachyrhaphis rhabdophora*	X-SRC
AF000696	Not_Callopan_occ	*Callopanchax occidentalis*	cytB

AF092293	Not_Callopan_occ	*Callopanchax occidentalis*	12S
FJ872034	Not_Callopan_occ	*Callopanchax occidentalis*	16S
KC702027	Not_Callopan_occ	*Callopanchax occidentalis huwaldi*	ENC1
AF002465	Riv_Campello_dor	*Campellolebias dorsimaculatus*	cytB
AF002516	Riv_Campello_dor	*Campellolebias dorsimaculatus*	16S
AF002584	Riv_Campello_dor	*Campellolebias dorsimaculatus*	COI2
AF092295	Riv_Campello_dor	*Campellolebias dorsimaculatus*	12S
EF017430	Poe_Carlhubb_stu	*Carlhubbsia stuarti*	RAG1
EF017481	Poe_Carlhubb_stu	*Carlhubbsia stuarti*	12S
EF017532	Poe_Carlhubb_stu	*Carlhubbsia stuarti*	cytB
EF017581	Poe_Carlhubb_stu	*Carlhubbsia stuarti*	NADH2
EF017581	Poe_Carlhubb_stu	*Carlhubbsia stuarti*	NADH1
KJ696879	Poe_Carlhubb_stu	*Carlhubbsia stuarti*	ENC1
KJ696989	Poe_Carlhubb_stu	*Carlhubbsia stuarti*	GLYT
KJ697099	Poe_Carlhubb_stu	*Carlhubbsia stuarti*	MYH6
KJ697472	Poe_Carlhubb_stu	*Carlhubbsia stuarti*	SH3PX3
KJ697580	Poe_Carlhubb_stu	*Carlhubbsia stuarti*	X-SRC
KJ696880	Goo_Chapalic_enc	*Chapalichthys pardalis*	ENC1
KJ696990	Goo_Chapalic_enc	*Chapalichthys pardalis*	GLYT
KJ697100	Goo_Chapalic_enc	*Chapalichthys pardalis*	MYH6
KJ697204	Goo_Chapalic_enc	*Chapalichthys pardalis*	NADH2
KJ697276	Goo_Chapalic_enc	*Chapalichthys pardalis*	RAG1
KJ697473	Goo_Chapalic_enc	*Chapalichthys pardalis*	SH3PX3
KJ697581	Goo_Chapalic_enc	*Chapalichthys pardalis*	X-SRC
AF510822	Goo_Characod_aud	*Characodon audax*	cytB
AY356568	Goo_Characod_aud	*Characodon audax*	COI1
AB188690	Bel_Cheilopo_pi	*Cheilopogon pinnatibarbatus*	12S
AB444860	Bel_Cheilopo_pi	*Cheilopogon pinnatibarbatus*	16S
GU440273	Bel_Cheilopo_pi	*Cheilopogon pinnatibarbatus*	COI1
HQ325618	Bel_Cheilopo_pi	*Cheilopogon pinnatibarbatus*	cytB
JX189544	Bel_Cheilopo_pi	*Cheilopogon pinnatibarbatus*	SH3PX3
JX189637	Bel_Cheilopo_pi	*Cheilopogon pinnatibarbatus*	MYH6
JX189792	Bel_Cheilopo_pi	*Cheilopogon pinnatibarbatus*	RAG1
EF017427	Poe_Cnestero_dec	*Cnesterodon decemmaculatus*	RAG1
EF017478	Poe_Cnestero_dec	*Cnesterodon decemmaculatus*	12S
EF017529	Poe_Cnestero_dec	*Cnesterodon decemmaculatus*	cytB
EF017579	Poe_Cnestero_dec	*Cnesterodon decemmaculatus*	NADH2
EF017579	Poe_Cnestero_dec	*Cnesterodon decemmaculatus*	NADH1
GU179152	Poe_Cnestero_dec	*Cnesterodon decemmaculatus*	X-SRC
GU179168	Poe_Cnestero_dec	*Cnesterodon decemmaculatus*	ENC1
GU179197	Poe_Cnestero_dec	*Cnesterodon decemmaculatus*	GLYT

GU179214	Poe_Cnestero_dec	*Cnesterodon decemmaculatus*	SH3PX3
GU179243	Poe_Cnestero_dec	*Cnesterodon decemmaculatus*	MYH6
JX111721	Poe_Cnestero_dec	*Cnesterodon decemmaculatus*	COI1
KJ696882	Goo_Crenicht_nev	*Crenichthys nevadae*	ENC1
KJ696992	Goo_Crenicht_nev	*Crenichthys nevadae*	GLYT
KJ697102	Goo_Crenicht_nev	*Crenichthys nevadae*	MYH6
KJ697278	Goo_Crenicht_nev	*Crenichthys nevadae*	RAG1
KJ697583	Goo_Crenicht_nev	*Crenichthys nevadae*	X-SRC
AY902051	Cyp_Cualac_tes	*Cualac tessellatus*	cytB
AY902109	Cyp_Cualac_tes	*Cualac tessellatus*	NADH2
CTU05968	Cyp_Cualac_tes	*Cualac tessellatus*	16S
JQ935856	Cyp_Cualac_tes	*Cualac tessellatus*	COI1
KJ696795	Cyp_Cubanich_cub	*Cubanichthys cubensis*	cytB
KJ696883	Cyp_Cubanich_cub	*Cubanichthys cubensis*	ENC1
KJ696993	Cyp_Cubanich_cub	*Cubanichthys cubensis*	GLYT
KJ697103	Cyp_Cubanich_cub	*Cubanichthys cubensis*	MYH6
KJ697206	Cyp_Cubanich_cub	*Cubanichthys cubensis*	NADH2
KJ697476	Cyp_Cubanich_cub	*Cubanichthys cubensis*	SH3PX3
KJ697584	Cyp_Cubanich_cub	*Cubanichthys cubensis*	X-SRC
AF002499	Riv_Cynodoni_ten	*Cynodonichthys tenuis*	cytB
AF002626	Riv_Cynodoni_ten	*Cynodonichthys tenuis*	COI2
AF092319	Riv_Cynodoni_ten	*Cynodonichthys tenuis*	12S
EU751964	Riv_Cynodoni_ten	*Cynodonichthys tenuis*	COI1
KC702024	Riv_Cynodoni_ten	*Cynodonichthys tenuis*	ENC1
KC702154	Riv_Cynodoni_ten	*Cynodonichthys tenuis*	SH3PX3
RTU73256	Riv_Cynodoni_ten	*Cynodonichthys tenuis*	16S
AF092296	Riv_Cynopoec_mel	*Cynopoecilus melanotaenia*	12S
AF245465	Riv_Cynopoec_mel	*Cynopoecilus melanotaenia*	cytB
AF449344	Cyp_Cyprinod_var	*Cyprinodon variegatus*	NADH2
AF449406	Cyp_Cyprinod_var	*Cyprinodon variegatus*	12S
AY902062	Cyp_Cyprinod_var	*Cyprinodon variegatus*	cytB
CVU05969	Cyp_Cyprinod_var	*Cyprinodon variegatus*	16S
FN545583	Cyp_Cyprinod_var	*Cyprinodon variegatus*	COI1
KF141215	Cyp_Cyprinod_var	*Cyprinodon variegatus*	RAG1
KF141450	Cyp_Cyprinod_var	*Cyprinodon variegatus*	SH3PX3
KJ696885	Cyp_Cyprinod_var	*Cyprinodon variegatus*	ENC1
KJ696995	Cyp_Cyprinod_var	*Cyprinodon variegatus*	GLYT
KJ697105	Cyp_Cyprinod_var	*Cyprinodon variegatus*	MYH6
KJ697585	Cyp_Cyprinod_var	*Cyprinodon variegatus*	X-SRC
AY356573	Goo_Empetric_lat	*Empetrichthys latos*	COI1
ELU09108	Goo_Empetric_lat	*Empetrichthys latos*	cytB

KJ696886	Not_Epiplaty_ann	*Epiplatys annulatus*	ENC1
KJ696996	Not_Epiplaty_ann	*Epiplatys annulatus*	GLYT
KJ697106	Not_Epiplaty_ann	*Epiplatys annulatus*	MYH6
KJ697279	Not_Epiplaty_ann	*Epiplatys annulatus*	RAG1
AF002402	Not_Fenerbah_for	*Fenerbahce formosus*	12S
AF002404	Not_Fenerbah_for	*Fenerbahce formosus*	16S
JF307807	Not_Fenerbah_for	*Fenerbahce formosus*	cytB
KJ696867	Not_Fenerbah_for	*Fenerbahce formosus*	ENC1
KJ696976	Not_Fenerbah_for	*Fenerbahce formosus*	GLYT
KJ697086	Not_Fenerbah_for	*Fenerbahce formosus*	MYH6
KJ697266	Not_Fenerbah_for	*Fenerbahce formosus*	RAG1
KJ697459	Not_Fenerbah_for	*Fenerbahce formosus*	SH3PX3
KJ697569	Not_Fenerbah_for	*Fenerbahce formosus*	X-SRC
AF449345	Cyp_Floridic_car	*Floridichthys carpio*	NADH2
AF449407	Cyp_Floridic_car	*Floridichthys carpio*	12S
FCU05970	Cyp_Floridic_car	*Floridichthys carpio*	16S
FCU06189	Cyp_Floridic_car	*Floridichthys carpio*	cytB
JQ842470	Cyp_Floridic_car	*Floridichthys carpio*	COI1
KJ696887	Cyp_Floridic_car	*Floridichthys carpio*	ENC1
KJ696997	Cyp_Floridic_car	*Floridichthys carpio*	GLYT
KJ697107	Cyp_Floridic_car	*Floridichthys carpio*	MYH6
KJ697586	Cyp_Floridic_car	*Floridichthys carpio*	X-SRC
KJ696800	Poe_Fluviphy_sim	*Fluviphylax simplex*	cytB
KJ696888	Poe_Fluviphy_sim	*Fluviphylax simplex*	ENC1
KJ696998	Poe_Fluviphy_sim	*Fluviphylax simplex*	GLYT
KJ697108	Poe_Fluviphy_sim	*Fluviphylax simplex*	MYH6
KJ697210	Poe_Fluviphy_sim	*Fluviphylax simplex*	NADH2
KJ697280	Poe_Fluviphy_sim	*Fluviphylax simplex*	RAG1
KJ697481	Poe_Fluviphy_sim	*Fluviphylax simplex*	SH3PX3
KJ697587	Poe_Fluviphy_sim	*Fluviphylax simplex*	X-SRC
AF002403	Not_Foerschi_fla	*Foerschichthys flavipinnis*	12S
AF002407	Not_Foerschi_fla	*Foerschichthys flavipinnis*	16S
AF002409	Not_Foerschi_fla	*Foerschichthys flavipinnis*	cytB
AF002297	Not_Fundulop_gar	*Fundulopanchax gardneri*	cytB
AF002344	Not_Fundulop_gar	*Fundulopanchax gardneri*	16S
AF092289	Not_Fundulop_gar	*Fundulopanchax gardneri*	12S
JN021666	Not_Fundulop_gar	*Fundulopanchax gardneri*	COI1
KJ696889	Not_Fundulop_gar	*Fundulopanchax gardneri*	ENC1
KJ696999	Not_Fundulop_gar	*Fundulopanchax gardneri*	GLYT
KJ697109	Not_Fundulop_gar	*Fundulopanchax gardneri*	MYH6
KJ697211	Not_Fundulop_gar	*Fundulopanchax gardneri*	NADH2

KJ697281	Not_Fundulop_gar	*Fundulopanchax gardneri*	RAG1
KJ697482	Not_Fundulop_gar	*Fundulopanchax gardneri*	SH3PX3
KJ697588	Not_Fundulop_gar	*Fundulopanchax gardneri*	X-SRC
EF032926	Fun_Fundulus_het	*Fundulus heteroclitus*	MYH6
EF032978	Fun_Fundulus_het	*Fundulus heteroclitus*	ENC1
EF032991	Fun_Fundulus_het	*Fundulus heteroclitus*	GLYT
EF033004	Fun_Fundulus_het	*Fundulus heteroclitus*	SH3PX3
FJ445399	Fun_Fundulus_het	*Fundulus heteroclitus*	COI1
FJ445400	Fun_Fundulus_het	*Fundulus heteroclitus*	12S
FJ445400	Fun_Fundulus_het	*Fundulus heteroclitus*	cytB
FJ445400	Fun_Fundulus_het	*Fundulus heteroclitus*	16S
GQ119890	Fun_Fundulus_het	*Fundulus heteroclitus*	RAG1
JF895714	Fun_Fundulus_het	*Fundulus heteroclitus*	NADH2
U02351	Fun_Fundulus_het	*Fundulus heteroclitus*	X-SRC
AP004422	Poe_Gambusia_aff	*Gambusia affinis*	12S
AP004422	Poe_Gambusia_aff	*Gambusia affinis*	NADH2
AP004422	Poe_Gambusia_aff	*Gambusia affinis*	cytB
AP004422	Poe_Gambusia_aff	*Gambusia affinis*	COI1
AP004422	Poe_Gambusia_aff	*Gambusia affinis*	16S
EF017411	Poe_Gambusia_aff	*Gambusia affinis*	RAG1
EF017564	Poe_Gambusia_aff	*Gambusia affinis*	NADH1
EU001907	Poe_Gambusia_aff	*Gambusia affinis*	MYH6
JX188691	Poe_Gambusia_aff	*Gambusia affinis*	GLYT
JX188858	Poe_Gambusia_aff	*Gambusia affinis*	ENC1
JX189550	Poe_Gambusia_aff	*Gambusia affinis*	SH3PX3
KJ696894	Goo_Girardin_viv	*Girardinichthys viviparus*	ENC1
KJ697004	Goo_Girardin_viv	*Girardinichthys viviparus*	GLYT
KJ697114	Goo_Girardin_viv	*Girardinichthys viviparus*	MYH6
KJ697286	Goo_Girardin_viv	*Girardinichthys viviparus*	RAG1
KJ697593	Goo_Girardin_viv	*Girardinichthys viviparus*	X-SRC
EF017441	Poe_Girardin_met	*Girardinus metallicus*	RAG1
EF017493	Poe_Girardin_met	*Girardinus metallicus*	12S
EF017544	Poe_Girardin_met	*Girardinus metallicus*	cytB
EF017593	Poe_Girardin_met	*Girardinus metallicus*	NADH2
FN545595	Poe_Girardin_met	*Girardinus metallicus*	COI1
GMU80052	Poe_Girardin_met	*Girardinus metallicus*	16S
KJ696895	Poe_Girardin_met	*Girardinus metallicus*	ENC1
KJ697005	Poe_Girardin_met	*Girardinus metallicus*	GLYT
KJ697115	Poe_Girardin_met	*Girardinus metallicus*	MYH6
KJ697488	Poe_Girardin_met	*Girardinus metallicus*	SH3PX3
KJ697594	Poe_Girardin_met	*Girardinus metallicus*	X-SRC

AF002472	Riv_Gnathole_zon	*Gnatholebias zonatus*	cytB
AF002524	Riv_Gnathole_zon	*Gnatholebias zonatus*	16S
AF002591	Riv_Gnathole_zon	*Gnatholebias zonatus*	COI2
AF092352	Riv_Gnathole_zon	*Gnatholebias zonatus*	12S
EF455711	Riv_Gnathole_zon	*Gnatholebias zonatus*	RAG1
KC702008	Riv_Gnathole_zon	*Gnatholebias zonatus*	ENC1
KJ696896	Goo_Goodea_gra	*Goodea gracilis*	ENC1
KJ697006	Goo_Goodea_gra	*Goodea gracilis*	GLYT
KJ697116	Goo_Goodea_gra	*Goodea gracilis*	MYH6
KJ697287	Goo_Goodea_gra	*Goodea gracilis*	RAG1
KJ697595	Goo_Goodea_gra	*Goodea gracilis*	X-SRC
AF412125	Poe_Heterand_for	*Heterandria formosa*	cytB
EF017422	Poe_Heterand_for	*Heterandria formosa*	RAG1
EF017473	Poe_Heterand_for	*Heterandria formosa*	12S
EF017575	Poe_Heterand_for	*Heterandria formosa*	NADH1
HQ557453	Poe_Heterand_for	*Heterandria formosa*	COI1
JQ612956	Poe_Heterand_for	*Heterandria formosa*	16S
KJ696897	Poe_Heterand_for	*Heterandria formosa*	ENC1
KJ697007	Poe_Heterand_for	*Heterandria formosa*	GLYT
KJ697117	Poe_Heterand_for	*Heterandria formosa*	MYH6
KJ697490	Poe_Heterand_for	*Heterandria formosa*	SH3PX3
KJ697596	Poe_Heterand_for	*Heterandria formosa*	X-SRC
EF017414	Poe_Heteroph_mil	*Heterophallus milleri*	RAG1
EF017465	Poe_Heteroph_mil	*Heterophallus milleri*	12S
EF017517	Poe_Heteroph_mil	*Heterophallus milleri*	cytB
EF017567	Poe_Heteroph_mil	*Heterophallus milleri*	NADH1
AF510841	Goo_Hubbsina_tur	*Hubbsina turneri*	cytB
AY356578	Goo_Hubbsina_tur	*Hubbsina turneri*	COI1
AF002580	Riv_Hypsoleb_ant	*Hypsolebias antenori*	COI2
CAU73252	Riv_Hypsoleb_ant	*Hypsolebias antenori*	16S
CAU73276	Riv_Hypsoleb_ant	*Hypsolebias antenori*	12S
KF311234	Riv_Hypsoleb_ant	*Hypsolebias antenori*	cytB
AF510831	Goo_Ilyodon_fur	*Ilyodon furcidens*	cytB
AY356579	Goo_Ilyodon_fur	*Ilyodon furcidens*	COI1
KJ696898	Goo_Ilyodon_fur	*Ilyodon furcidens*	ENC1
KJ697008	Goo_Ilyodon_fur	*Ilyodon furcidens*	GLYT
KJ697118	Goo_Ilyodon_fur	*Ilyodon furcidens*	MYH6
KJ697288	Goo_Ilyodon_fur	*Ilyodon furcidens*	RAG1
KJ697597	Goo_Ilyodon_fur	*Ilyodon furcidens*	X-SRC
EF017406	Ana_Jenynsia_lin	*Jenynsia lineata*	RAG1
EF017457	Ana_Jenynsia_lin	*Jenynsia lineata*	12S

EF017509	Ana_Jenynsia_lin	*Jenynsia lineata*	cytB
EF017559	Ana_Jenynsia_lin	*Jenynsia lineata*	NADH2
EF017559	Ana_Jenynsia_lin	*Jenynsia lineata*	NADH1
KJ696899	Ana_Jenynsia_lin	*Jenynsia lineata*	ENC1
KJ697009	Ana_Jenynsia_lin	*Jenynsia lineata*	GLYT
KJ697119	Ana_Jenynsia_lin	*Jenynsia lineata*	MYH6
KJ697598	Ana_Jenynsia_lin	*Jenynsia lineata*	X-SRC
AP006778	Cyp_Jordanel_flo	*Jordanella floridae*	12S
AP006778	Cyp_Jordanel_flo	*Jordanella floridae*	NADH2
AP006778	Cyp_Jordanel_flo	*Jordanella floridae*	COI1
AP006778	Cyp_Jordanel_flo	*Jordanella floridae*	16S
KF141266	Cyp_Jordanel_flo	*Jordanella floridae*	RAG1
KF141498	Cyp_Jordanel_flo	*Jordanella floridae*	SH3PX3
KJ696901	Cyp_Jordanel_flo	*Jordanella floridae*	ENC1
KJ697011	Cyp_Jordanel_flo	*Jordanella floridae*	GLYT
KJ697121	Cyp_Jordanel_flo	*Jordanella floridae*	MYH6
KJ697600	Cyp_Jordanel_flo	*Jordanella floridae*	X-SRC
NC_011387	Cyp_Jordanel_flo	*Jordanella floridae*	cytB
AF002598	Riv_Kryptole_mar	*Kryptolebias marmoratus*	COI2
AF283503	Riv_Kryptole_mar	*Kryptolebias marmoratus*	12S
AF283503	Riv_Kryptole_mar	*Kryptolebias marmoratus*	COI1
AF283503	Riv_Kryptole_mar	*Kryptolebias marmoratus*	16S
AY946275	Riv_Kryptole_mar	*Kryptolebias marmoratus*	NADH2
NC_003290	Riv_Kryptole_mar	*Kryptolebias marmoratus*	cytB
AF283503	Riv_Kryptole_mar	*Kryptolebias marmoratus*	NADH1
AF002483	Riv_Laimosem_gea	*Laimosemion geayi*	cytB
AF002537	Riv_Laimosem_gea	*Laimosemion geayi*	16S
AF002604	Riv_Laimosem_gea	*Laimosemion geayi*	COI2
AY946274	Riv_Laimosem_gea	*Laimosemion geayi*	NADH2
AY946279	Riv_Laimosem_gea	*Laimosemion geayi*	12S
AF002463	Riv_Leptoleb_min	*Leptolebias minimus*	cytB
AF002514	Riv_Leptoleb_min	*Leptolebias minimus*	16S
AF002583	Riv_Leptoleb_min	*Leptolebias minimus*	COI2
AF092297	Riv_Leptoleb_min	*Leptolebias minimus*	12S
KC701998	Riv_Leptoleb_min	*Leptolebias minimus*	ENC1
KC702130	Riv_Leptoleb_min	*Leptolebias minimus*	SH3PX3
EF017431	Poe_Limia_dom	*Limia dominicensis*	RAG1
EF017482	Poe_Limia_dom	*Limia dominicensis*	12S
EF017533	Poe_Limia_dom	*Limia dominicensis*	cytB
EF017582	Poe_Limia_dom	*Limia dominicensis*	NADH2
EF017582	Poe_Limia_dom	*Limia dominicensis*	NADH1

GU179154	Poe_Limia_dom	*Limia dominicensis*	X-SRC
GU179170	Poe_Limia_dom	*Limia dominicensis*	ENC1
GU179199	Poe_Limia_dom	*Limia dominicensis*	GLYT
GU179216	Poe_Limia_dom	*Limia dominicensis*	SH3PX3
GU179245	Poe_Limia_dom	*Limia dominicensis*	MYH6
AF092353	Riv_Llanoleb_ste	*Llanolebias stellifer*	12S
EF455713	Riv_Llanoleb_ste	*Llanolebias stellifer*	RAG1
KC702004	Riv_Llanoleb_ste	*Llanolebias stellifer*	ENC1
KC702139	Riv_Llanoleb_ste	*Llanolebias stellifer*	SH3PX3
GQ119768	Fun_Lucania_goo	*Lucania goodei*	cytB
HQ557449	Fun_Lucania_goo	*Lucania goodei*	COI1
JX188690	Fun_Lucania_goo	*Lucania goodei*	GLYT
JX189549	Fun_Lucania_goo	*Lucania goodei*	SH3PX3
KJ696915	Fun_Lucania_goo	*Lucania goodei*	ENC1
KJ697135	Fun_Lucania_goo	*Lucania goodei*	MYH6
KJ697304	Fun_Lucania_goo	*Lucania goodei*	RAG1
KJ697614	Fun_Lucania_goo	*Lucania goodei*	X-SRC
AF002466	Riv_Marateco_lac	*Maratecoara lacortei*	cytB
AF002517	Riv_Marateco_lac	*Maratecoara lacortei*	16S
AF002585	Riv_Marateco_lac	*Maratecoara lacortei*	COI2
AF092343	Riv_Marateco_lac	*Maratecoara lacortei*	12S
AY902052	Cyp_Megupsil_apo	*Megupsilon aporus*	cytB
AY902110	Cyp_Megupsil_apo	*Megupsilon aporus*	NADH2
MAU05978	Cyp_Megupsil_apo	*Megupsilon aporus*	16S
AF002454	Riv_Melanori_pun	*Melanorivulus punctatus*	12S
AF002504	Riv_Melanori_pun	*Melanorivulus punctatus*	cytB
AF002567	Riv_Melanori_pun	*Melanorivulus punctatus*	16S
AF002636	Riv_Melanori_pun	*Melanorivulus punctatus*	COI2
AF092389	Riv_Melanori_pun	*Melanorivulus punctatus*	NADH2
KC702021	Riv_Melanori_pun	*Melanorivulus punctatus*	ENC1
KC702150	Riv_Melanori_pun	*Melanorivulus punctatus*	SH3PX3
AF002473	Riv_Micromoe_xip	*Micromoema xiphophorus*	cytB
AF002525	Riv_Micromoe_xip	*Micromoema xiphophorus*	16S
AF002592	Riv_Micromoe_xip	*Micromoema xiphophorus*	COI2
AF092351	Riv_Micromoe_xip	*Micromoema xiphophorus*	12S
EF455720	Riv_Micromoe_xip	*Micromoema xiphophorus*	RAG1
EF017435	Poe_Micropoe_pic	*Micropoecilia picta*	RAG1
EF017486	Poe_Micropoe_pic	*Micropoecilia picta*	12S
EF017586	Poe_Micropoe_pic	*Micropoecilia picta*	NADH2
EF017586	Poe_Micropoe_pic	*Micropoecilia picta*	NADH1
GU179161	Poe_Micropoe_pic	*Micropoecilia picta*	X-SRC

GU179177	Poe_Micropoe_pic	*Micropoecilia picta*	ENC1
GU179191	Poe_Micropoe_pic	*Micropoecilia picta*	cytB
GU179206	Poe_Micropoe_pic	*Micropoecilia picta*	GLYT
GU179223	Poe_Micropoe_pic	*Micropoecilia picta*	SH3PX3
GU179251	Poe_Micropoe_pic	*Micropoecilia picta*	MYH6
AF002457	Riv_Moema_pir	*Moema piriana*	12S
AF002507	Riv_Moema_pir	*Moema piriana*	cytB
AF002570	Riv_Moema_pir	*Moema piriana*	16S
AF002639	Riv_Moema_pir	*Moema piriana*	COI2
AF002511	Riv_Nematole_whi	*Nematolebias whitei*	16S
AF002577	Riv_Nematole_whi	*Nematolebias whitei*	COI2
AF092298	Riv_Nematole_whi	*Nematolebias whitei*	12S
CWU41784	Riv_Nematole_whi	*Nematolebias whitei*	cytB
KC701991	Riv_Nematole_whi	*Nematolebias whitei*	ENC1
U02348	Riv_Nematole_whi	*Nematolebias whitei*	X-SRC
AF002510	Riv_Neofundu_par	*Neofundulus paraguayensis*	cytB
AF002573	Riv_Neofundu_par	*Neofundulus paraguayensis*	16S
AF002643	Riv_Neofundu_par	*Neofundulus paraguayensis*	COI2
AF092338	Riv_Neofundu_par	*Neofundulus paraguayensis*	12S
EF455722	Riv_Neofundu_par	*Neofundulus paraguayensis*	RAG1
KC702000	Riv_Neofundu_par	*Neofundulus paraguayensis*	ENC1
EF017423	Poe_Neoheter_tri	*Neoheterandria tridentiger*	RAG1
EF017474	Poe_Neoheter_tri	*Neoheterandria tridentiger*	12S
EF017526	Poe_Neoheter_tri	*Neoheterandria tridentiger*	cytB
EF017576	Poe_Neoheter_tri	*Neoheterandria tridentiger*	NADH2
EF017576	Poe_Neoheter_tri	*Neoheterandria tridentiger*	NADH1
KJ696920	Poe_Neoheter_tri	*Neoheterandria tridentiger*	ENC1
KJ697030	Poe_Neoheter_tri	*Neoheterandria tridentiger*	GLYT
KJ697140	Poe_Neoheter_tri	*Neoheterandria tridentiger*	MYH6
KJ697513	Poe_Neoheter_tri	*Neoheterandria tridentiger*	SH3PX3
KJ697619	Poe_Neoheter_tri	*Neoheterandria tridentiger*	X-SRC
AF000691	Not_Nimbapan_vir	*Nimbapanchax viridis*	12S
AF000715	Not_Nimbapan_vir	*Nimbapanchax viridis*	cytB
FJ872027	Not_Nimbapan_vir	*Nimbapanchax viridis*	16S
FJ872055	Not_Nimbapan_vir	*Nimbapanchax viridis*	NADH2
AF002349	Not_Nothobra_kir	*Nothobranchius kirki*	12S
JF444882	Not_Nothobra_kir	*Nothobranchius kirki*	GLYT
JF444896	Not_Nothobra_kir	*Nothobranchius kirki*	MYH6
JF444908	Not_Nothobra_kir	*Nothobranchius kirki*	SH3PX3
JQ310171	Not_Nothobra_kir	*Nothobranchius kirki*	COI2
NKU73250	Not_Nothobra_kir	*Nothobranchius kirki*	16S

NKU73297	Not_Nothobra_kir	*Nothobranchius kirki*	cytB
AF449346	Cyp_Orestias_aga	*Orestias agassizii*	NADH2
AF449408	Cyp_Orestias_aga	*Orestias agassizii*	12S
JX092172	Cyp_Orestias_aga	*Orestias agassizii*	cytB
KJ696921	Cyp_Orestias_aga	*Orestias agassizii*	ENC1
KJ697031	Cyp_Orestias_aga	*Orestias agassizii*	GLYT
KJ697141	Cyp_Orestias_aga	*Orestias agassizii*	MYH6
KJ697620	Cyp_Orestias_aga	*Orestias agassizii*	X-SRC
OAU05966	Cyp_Orestias_aga	*Orestias agassizii*	16S
EF032927	Bel_Oryzias_la	*Oryzias latipes*	MYH6
EF033005	Bel_Oryzias_la	*Oryzias latipes*	SH3PX3
EF095641	Bel_Oryzias_la	*Oryzias latipes*	RAG1
NC_004387	Bel_Oryzias_la	*Oryzias latipes*	12S
NC_004387	Bel_Oryzias_la	*Oryzias latipes*	NADH2
NC_004387	Bel_Oryzias_la	*Oryzias latipes*	NADH1
NC_004387	Bel_Oryzias_la	*Oryzias latipes*	cytB
NC_004387	Bel_Oryzias_la	*Oryzias latipes*	COI1
NC_004387	Bel_Oryzias_la	*Oryzias latipes*	16S
AF449340	Ana_Oxyzygon_dov	*Oxyzygonectes dovii*	NADH2
AY356581	Ana_Oxyzygon_dov	*Oxyzygonectes dovii*	COI1
EF017407	Ana_Oxyzygon_dov	*Oxyzygonectes dovii*	RAG1
EF017458	Ana_Oxyzygon_dov	*Oxyzygonectes dovii*	12S
EF017510	Ana_Oxyzygon_dov	*Oxyzygonectes dovii*	cytB
EF017560	Ana_Oxyzygon_dov	*Oxyzygonectes dovii*	NADH1
KJ696922	Ana_Oxyzygon_dov	*Oxyzygonectes dovii*	ENC1
KJ697032	Ana_Oxyzygon_dov	*Oxyzygonectes dovii*	GLYT
KJ697142	Ana_Oxyzygon_dov	*Oxyzygonectes dovii*	MYH6
KJ697621	Ana_Oxyzygon_dov	*Oxyzygonectes dovii*	X-SRC
DQ532927	Apl_Pachypan_pla	*Pachypanchax playfairii*	16S
JX190385	Apl_Pachypan_pla	*Pachypanchax playfairii*	GLYT
JX190914	Apl_Pachypan_pla	*Pachypanchax playfairii*	RAG1
JX191048	Apl_Pachypan_pla	*Pachypanchax playfairii*	SH3PX3
KF139432	Apl_Pachypan_pla	*Pachypanchax playfairii*	ENC1
PPU73263	Apl_Pachypan_pla	*Pachypanchax playfairii*	12S
PPU73285	Apl_Pachypan_pla	*Pachypanchax playfairii*	cytB
EF017487	Poe_Pamphori_hol	*Pamphorichthys hollandi*	12S
EF017538	Poe_Pamphori_hol	*Pamphorichthys hollandi*	cytB
EF017587	Poe_Pamphori_hol	*Pamphorichthys hollandi*	NADH2
EF017587	Poe_Pamphori_hol	*Pamphorichthys hollandi*	NADH1
GU701605	Poe_Pamphori_hol	*Pamphorichthys hollandi*	COI1
HQ857422	Poe_Pamphori_hol	*Pamphorichthys hollandi*	SH3PX3

HQ857434	Poe_Pamphori_hol	*Pamphorichthys hollandi*	X-SRC
HQ857446	Poe_Pamphori_hol	*Pamphorichthys hollandi*	RAG1
HQ857458	Poe_Pamphori_hol	*Pamphorichthys hollandi*	MYH6
HQ857464	Poe_Pamphori_hol	*Pamphorichthys hollandi*	GLYT
HQ857470	Poe_Pamphori_hol	*Pamphorichthys hollandi*	ENC1
AF002520	Riv_Papiliol_bit	*Papiliolebias bitteri*	16S
AF002588	Riv_Papiliol_bit	*Papiliolebias bitteri*	COI2
AF092341	Riv_Papiliol_bit	*Papiliolebias bitteri*	12S
KC702006	Riv_Papiliol_bit	*Papiliolebias bitteri*	ENC1
DQ386548	Poe_Phallich_ama	*Phallichthys amates*	16S
EF017410	Poe_Phallich_ama	*Phallichthys amates*	RAG1
EF017461	Poe_Phallich_ama	*Phallichthys amates*	12S
EF017513	Poe_Phallich_ama	*Phallichthys amates*	cytB
EF017563	Poe_Phallich_ama	*Phallichthys amates*	NADH2
EF017563	Poe_Phallich_ama	*Phallichthys amates*	NADH1
KJ696923	Poe_Phallich_ama	*Phallichthys amates*	ENC1
KJ697033	Poe_Phallich_ama	*Phallichthys amates*	GLYT
KJ697143	Poe_Phallich_ama	*Phallichthys amates*	MYH6
KJ697516	Poe_Phallich_ama	*Phallichthys amates*	SH3PX3
KJ697622	Poe_Phallich_ama	*Phallichthys amates*	X-SRC
EF017426	Poe_Phalloce_cau	*Phalloceros caudimaculatus*	RAG1
EF017477	Poe_Phalloce_cau	*Phalloceros caudimaculatus*	12S
EF017578	Poe_Phalloce_cau	*Phalloceros caudimaculatus*	NADH2
EF017578	Poe_Phalloce_cau	*Phalloceros caudimaculatus*	NADH1
KJ696926	Poe_Phalloce_cau	*Phalloceros caudimaculatus*	ENC1
KJ697036	Poe_Phalloce_cau	*Phalloceros caudimaculatus*	GLYT
KJ697146	Poe_Phalloce_cau	*Phalloceros caudimaculatus*	MYH6
KJ697519	Poe_Phalloce_cau	*Phalloceros caudimaculatus*	SH3PX3
KJ697625	Poe_Phalloce_cau	*Phalloceros caudimaculatus*	X-SRC
PCU80053	Poe_Phalloce_cau	*Phalloceros caudimaculatus*	16S
EF017428	Poe_Phallopt_jan	*Phalloptychus januarius*	RAG1
EF017479	Poe_Phallopt_jan	*Phalloptychus januarius*	12S
EF017530	Poe_Phallopt_jan	*Phalloptychus januarius*	cytB
KJ696927	Poe_Phallopt_jan	*Phalloptychus januarius*	ENC1
KJ697037	Poe_Phallopt_jan	*Phalloptychus januarius*	GLYT
KJ697147	Poe_Phallopt_jan	*Phalloptychus januarius*	MYH6
KJ697520	Poe_Phallopt_jan	*Phalloptychus januarius*	SH3PX3
KJ697626	Poe_Phallopt_jan	*Phalloptychus januarius*	X-SRC
AF002467	Riv_Pituna_por	*Pituna poranga*	cytB
AF002518	Riv_Pituna_por	*Pituna poranga*	16S
AF002586	Riv_Pituna_por	*Pituna poranga*	COI2

AF092345	Riv_Pituna_por	*Pituna poranga*	12S
KC702003	Riv_Pituna_por	*Pituna poranga*	ENC1
KC702138	Riv_Pituna_por	*Pituna poranga*	SH3PX3
AF243874	Bel_Platybel_ar	*Platybelone argala*	cytB
AF243950	Bel_Platybel_ar	*Platybelone argala*	16S
JQ840640	Bel_Platybel_ar	*Platybelone argala*	COI1
JX189541	Bel_Platybel_ar	*Platybelone argala*	SH3PX3
JX189789	Bel_Platybel_ar	*Platybelone argala*	RAG1
KC827246	Bel_Platybel_ar	*Platybelone argala*	MYH6
AF002468	Riv_Plesiole_aru	*Plesiolebias aruana*	cytB
AF002519	Riv_Plesiole_aru	*Plesiolebias aruana*	16S
AF002587	Riv_Plesiole_aru	*Plesiolebias aruana*	COI2
AF092342	Riv_Plesiole_aru	*Plesiolebias aruana*	12S
KC702005	Riv_Plesiole_aru	*Plesiolebias aruana*	ENC1
EF017434	Poe_Poecilia_ret	*Poecilia reticulata*	RAG1
EF017485	Poe_Poecilia_ret	*Poecilia reticulata*	12S
EF017585	Poe_Poecilia_ret	*Poecilia reticulata*	NADH2
EF017585	Poe_Poecilia_ret	*Poecilia reticulata*	NADH1
GQ855709	Poe_Poecilia_ret	*Poecilia reticulata*	cytB
GU179162	Poe_Poecilia_ret	*Poecilia reticulata*	X-SRC
GU179178	Poe_Poecilia_ret	*Poecilia reticulata*	ENC1
GU179207	Poe_Poecilia_ret	*Poecilia reticulata*	GLYT
GU179224	Poe_Poecilia_ret	*Poecilia reticulata*	SH3PX3
GU179253	Poe_Poecilia_ret	*Poecilia reticulata*	MYH6
JN028265	Poe_Poecilia_ret	*Poecilia reticulata*	COI1
NC_024238	Poe_Poecilia_ret	*Poecilia reticulata*	16S
AF412129	Poe_Poecilio_elo	*Poeciliopsis elongata*	cytB
AF412172	Poe_Poecilio_elo	*Poeciliopsis elongata*	NADH2
KJ696944	Poe_Poecilio_elo	*Poeciliopsis elongata*	ENC1
KJ697054	Poe_Poecilio_elo	*Poeciliopsis elongata*	GLYT
KJ697164	Poe_Poecilio_elo	*Poeciliopsis elongata*	MYH6
KJ697327	Poe_Poecilio_elo	*Poeciliopsis elongata*	RAG1
KJ697537	Poe_Poecilio_elo	*Poeciliopsis elongata*	SH3PX3
KJ697643	Poe_Poecilio_elo	*Poeciliopsis elongata*	X-SRC
EF017451	Poe_Priapell_com	*Priapella compressa*	RAG1
EF017503	Poe_Priapell_com	*Priapella compressa*	12S
EF017603	Poe_Priapell_com	*Priapella compressa*	NADH2
EF017603	Poe_Priapell_com	*Priapella compressa*	NADH1
KJ525791	Poe_Priapell_com	*Priapella compressa*	SH3PX3
KJ525851	Poe_Priapell_com	*Priapella compressa*	MYH6
KJ525871	Poe_Priapell_com	*Priapella compressa*	GLYT

KJ525891	Poe_Priapell_com	*Priapella compressa*	ENC1
KJ525911	Poe_Priapell_com	*Priapella compressa*	X-SRC
DQ386565	Poe_Priapich_ann	*Priapichthys annectens*	16S
EF017439	Poe_Priapich_ann	*Priapichthys annectens*	RAG1
EF017491	Poe_Priapich_ann	*Priapichthys annectens*	12S
EF017542	Poe_Priapich_ann	*Priapichthys annectens*	cytB
EF017591	Poe_Priapich_ann	*Priapichthys annectens*	NADH2
EF017591	Poe_Priapich_ann	*Priapichthys annectens*	NADH1
KJ696961	Poe_Priapich_ann	*Priapichthys annectens*	ENC1
KJ697071	Poe_Priapich_ann	*Priapichthys annectens*	GLYT
KJ697181	Poe_Priapich_ann	*Priapichthys annectens*	MYH6
KJ697554	Poe_Priapich_ann	*Priapichthys annectens*	SH3PX3
KJ697660	Poe_Priapich_ann	*Priapichthys annectens*	X-SRC
AY155568	Pro_Profundu_gua	*Profundulus guatemalensis*	cytB
GQ119857	Pro_Profundu_gua	*Profundulus guatemalensis*	RAG1
JN028283	Pro_Profundu_gua	*Profundulus guatemalensis*	COI1
U02356	Pro_Profundu_gua	*Profundulus guatemalensis*	X-SRC
AF002285	Not_Pronotho_kiy	*Pronothobranchius kiyawensis*	cytB
AF002348	Not_Pronotho_kiy	*Pronothobranchius kiyawensis*	12S
AF002406	Not_Pronotho_kiy	*Pronothobranchius kiyawensis*	16S
EF464705	Not_Pronotho_kiy	*Pronothobranchius kiyawensis*	COI2
EF017440	Poe_Pseudopo_fes	*Pseudopoecilia festae*	RAG1
EF017492	Poe_Pseudopo_fes	*Pseudopoecilia festae*	12S
EF017543	Poe_Pseudopo_fes	*Pseudopoecilia festae*	cytB
EF017592	Poe_Pseudopo_fes	*Pseudopoecilia festae*	NADH2
EF017592	Poe_Pseudopo_fes	*Pseudopoecilia festae*	NADH1
KJ696965	Poe_Pseudopo_fes	*Pseudopoecilia festae*	ENC1
KJ697075	Poe_Pseudopo_fes	*Pseudopoecilia festae*	GLYT
KJ697185	Poe_Pseudopo_fes	*Pseudopoecilia festae*	MYH6
KJ697558	Poe_Pseudopo_fes	*Pseudopoecilia festae*	SH3PX3
KJ697664	Poe_Pseudopo_fes	*Pseudopoecilia festae*	X-SRC
JQ612894	Poe_Pseudoxi_obl	*Pseudoxiphophorus obliquus*	cytB
JQ612950	Poe_Pseudoxi_obl	*Pseudoxiphophorus obliquus*	16S
AF002595	Riv_Pteroleb_lon	*Pterolebias longipinnis*	COI2
AF092348	Riv_Pteroleb_lon	*Pterolebias longipinnis*	12S
AF244446	Riv_Pteroleb_lon	*Pterolebias longipinnis*	16S
AF245462	Riv_Pteroleb_lon	*Pterolebias longipinnis*	cytB
EF455709	Riv_Pteroleb_lon	*Pterolebias longipinnis*	RAG1
KC702007	Riv_Pteroleb_lon	*Pterolebias longipinnis*	ENC1
EF017453	Poe_Quintana_atr	*Quintana atrizona*	RAG1
EF017505	Poe_Quintana_atr	*Quintana atrizona*	12S

EF017605	Poe_Quintana_atr	*Quintana atrizona*	NADH2
EF017605	Poe_Quintana_atr	*Quintana atrizona*	NADH1
FJ178764	Poe_Quintana_atr	*Quintana atrizona*	cytB
FN545618	Poe_Quintana_atr	*Quintana atrizona*	COI1
AF002470	Riv_Rachovia_mac	*Rachovia maculipinnis*	cytB
AF002522	Riv_Rachovia_mac	*Rachovia maculipinnis*	16S
AF002590	Riv_Rachovia_mac	*Rachovia maculipinnis*	COI2
AY850639	Riv_Rachovia_mac	*Rachovia maculipinnis*	NADH2
AY850639	Riv_Rachovia_mac	*Rachovia maculipinnis*	NADH1
AY850664	Riv_Rachovia_mac	*Rachovia maculipinnis*	12S
EF455714	Riv_Rachovia_mac	*Rachovia maculipinnis*	RAG1
AF002475	Riv_Renova_osc	*Renova oscari*	cytB
AF002527	Riv_Renova_osc	*Renova oscari*	16S
AF002594	Riv_Renova_osc	*Renova oscari*	COI2
AF092346	Riv_Renova_osc	*Renova oscari*	12S
EF455721	Riv_Renova_osc	*Renova oscari*	RAG1
KC702140	Riv_Renova_osc	*Renova oscari*	SH3PX3
AF002533	Riv_Rivulus_cyl	*Rivulus cylindraceus*	16S
AF002601	Riv_Rivulus_cyl	*Rivulus cylindraceus*	COI2
AF092304	Riv_Rivulus_cyl	*Rivulus cylindraceus*	12S
FN544245	Riv_Rivulus_cyl	*Rivulus cylindraceus*	COI1
KC702013	Riv_Rivulus_cyl	*Rivulus cylindraceus*	ENC1
KC702143	Riv_Rivulus_cyl	*Rivulus cylindraceus*	SH3PX3
RCU41782	Riv_Rivulus_cyl	*Rivulus cylindraceus*	cytB
KJ696967	Poe_Scolicht_iot	*Scolichthys iota*	ENC1
KJ697077	Poe_Scolicht_iot	*Scolichthys iota*	GLYT
KJ697187	Poe_Scolicht_iot	*Scolichthys iota*	MYH6
KJ697344	Poe_Scolicht_iot	*Scolichthys iota*	RAG1
KJ697560	Poe_Scolicht_iot	*Scolichthys iota*	SH3PX3
KJ697666	Poe_Scolicht_iot	*Scolichthys iota*	X-SRC
AF092292	Not_Scriptap_ger	*Scriptaphyosemion geryi*	12S
EF464684	Not_Scriptap_ger	*Scriptaphyosemion geryi*	COI2
FJ872033	Not_Scriptap_ger	*Scriptaphyosemion geryi*	16S
JX044123	Not_Scriptap_ger	*Scriptaphyosemion geryi*	cytB
JX124267	Not_Scriptap_ger	*Scriptaphyosemion geryi*	NADH2
KJ696968	Goo_Skiffia_mul	*Skiffia multipunctata*	ENC1
KJ697078	Goo_Skiffia_mul	*Skiffia multipunctata*	GLYT
KJ697188	Goo_Skiffia_mul	*Skiffia multipunctata*	MYH6
KJ697345	Goo_Skiffia_mul	*Skiffia multipunctata*	RAG1
KJ697667	Goo_Skiffia_mul	*Skiffia multipunctata*	X-SRC
AF002410	Riv_Spectrol_cos	*Spectrolebias costai*	12S

AF002461	Riv_Spectrol_cos	*Spectrolebias costai*	cytB
AF002512	Riv_Spectrol_cos	*Spectrolebias costai*	16S
AF002578	Riv_Spectrol_cos	*Spectrolebias costai*	COI2
KC701986	Riv_Spectrol_cos	*Spectrolebias costai*	ENC1
KC702119	Riv_Spectrol_cos	*Spectrolebias costai*	SH3PX3
AF231521	Bel_Strongyl_ma	*Strongylura marina*	16S
AF231554	Bel_Strongyl_ma	*Strongylura marina*	12S
AF231642	Bel_Strongyl_ma	*Strongylura marina*	cytB
HQ937019	Bel_Strongyl_ma	*Strongylura marina*	COI1
JQ282086	Bel_Strongyl_ma	*Strongylura marina*	RAG1
JX189542	Bel_Strongyl_ma	*Strongylura marina*	SH3PX3
JX189635	Bel_Strongyl_ma	*Strongylura marina*	MYH6
AF002474	Riv_Terranat_dol	*Terranatos dolichopterus*	cytB
AF002526	Riv_Terranat_dol	*Terranatos dolichopterus*	16S
AF002593	Riv_Terranat_dol	*Terranatos dolichopterus*	COI2
AF092354	Riv_Terranat_dol	*Terranatos dolichopterus*	12S
EF455716	Riv_Terranat_dol	*Terranatos dolichopterus*	RAG1
KC702029	Riv_Terranat_dol	*Terranatos dolichopterus*	ENC1
KC702157	Riv_Terranat_dol	*Terranatos dolichopterus*	SH3PX3
EF017455	Poe_Tomeurus_gra	*Tomeurus gracilis*	RAG1
EF017507	Poe_Tomeurus_gra	*Tomeurus gracilis*	12S
EF017607	Poe_Tomeurus_gra	*Tomeurus gracilis*	NADH2
EF017607	Poe_Tomeurus_gra	*Tomeurus gracilis*	NADH1
KJ696969	Poe_Tomeurus_gra	*Tomeurus gracilis*	ENC1
KJ697079	Poe_Tomeurus_gra	*Tomeurus gracilis*	GLYT
KJ697189	Poe_Tomeurus_gra	*Tomeurus gracilis*	MYH6
KJ697562	Poe_Tomeurus_gra	*Tomeurus gracilis*	SH3PX3
KJ697668	Poe_Tomeurus_gra	*Tomeurus gracilis*	X-SRC
AF002509	Riv_Trigonec_bal	*Trigonectes balzanii*	cytB
AF002641	Riv_Trigonec_bal	*Trigonectes balzanii*	COI2
AF092334	Riv_Trigonec_bal	*Trigonectes balzanii*	12S
AF244447	Riv_Trigonec_bal	*Trigonectes balzanii*	16S
KC702030	Riv_Trigonec_bal	*Trigonectes balzanii*	ENC1
KC702158	Riv_Trigonec_bal	*Trigonectes balzanii*	SH3PX3
AF449339	Val_Valencia_his	*Valencia hispanica*	NADH2
AF449400	Val_Valencia_his	*Valencia hispanica*	12S
KJ696970	Val_Valencia_his	*Valencia hispanica*	ENC1
KJ697080	Val_Valencia_his	*Valencia hispanica*	GLYT
KJ697190	Val_Valencia_his	*Valencia hispanica*	MYH6
KJ697669	Val_Valencia_his	*Valencia hispanica*	X-SRC
AF243890	Bel_Xenentod_ca	*Xenentodon cancila*	cytB

AF243967	Bel_Xenentod_ca	*Xenentodon cancila*	16S
AF508061	Bel_Xenentod_ca	*Xenentodon cancila*	12S
FJ459538	Bel_Xenentod_ca	*Xenentodon cancila*	COI1
JX189543	Bel_Xenentod_ca	*Xenentodon cancila*	SH3PX3
JX189636	Bel_Xenentod_ca	*Xenentodon cancila*	MYH6
JX190869	Bel_Xenentod_ca	*Xenentodon cancila*	RAG1
EF017454	Poe_Xenodexi_cte	*Xenodexia ctenolepis*	RAG1
EF017506	Poe_Xenodexi_cte	*Xenodexia ctenolepis*	12S
EF017557	Poe_Xenodexi_cte	*Xenodexia ctenolepis*	cytB
EF017606	Poe_Xenodexi_cte	*Xenodexia ctenolepis*	NADH2
EF017606	Poe_Xenodexi_cte	*Xenodexia ctenolepis*	NADH1
KJ696971	Poe_Xenodexi_cte	*Xenodexia ctenolepis*	ENC1
KJ697081	Poe_Xenodexi_cte	*Xenodexia ctenolepis*	GLYT
KJ697191	Poe_Xenodexi_cte	*Xenodexia ctenolepis*	MYH6
KJ697564	Poe_Xenodexi_cte	*Xenodexia ctenolepis*	SH3PX3
KJ697670	Poe_Xenodexi_cte	*Xenodexia ctenolepis*	X-SRC
AF510759	Goo_Xenoopho_cap	*Xenoophorus captiva*	cytB
AY356586	Goo_Xenoopho_cap	*Xenoophorus captiva*	COI1
KJ696972	Goo_Xenoopho_cap	*Xenoophorus captivus*	ENC1
KJ697082	Goo_Xenoopho_cap	*Xenoophorus captivus*	GLYT
KJ697192	Goo_Xenoopho_cap	*Xenoophorus captivus*	MYH6
KJ697346	Goo_Xenoopho_cap	*Xenoophorus captivus*	RAG1
KJ697671	Goo_Xenoopho_cap	*Xenoophorus captivus*	X-SRC
EF017424	Poe_Xenophal_umb	*Xenophallus umbratilis*	RAG1
EF017475	Poe_Xenophal_umb	*Xenophallus umbratilis*	12S
EF017527	Poe_Xenophal_umb	*Xenophallus umbratilis*	cytB
EF017577	Poe_Xenophal_umb	*Xenophallus umbratilis*	NADH2
KJ696973	Poe_Xenophal_umb	*Xenophallus umbratilis*	ENC1
KJ697083	Poe_Xenophal_umb	*Xenophallus umbratilis*	GLYT
KJ697193	Poe_Xenophal_umb	*Xenophallus umbratilis*	MYH6
KJ697566	Poe_Xenophal_umb	*Xenophallus umbratilis*	SH3PX3
KJ697672	Poe_Xenophal_umb	*Xenophallus umbratilis*	X-SRC
AF510825	Goo_Xenotaen_res	*Xenotaenia resolanae*	cytB
AY356590	Goo_Xenotaen_res	*Xenotaenia resolanae*	COI1
AP006777	Goo_Xenotoca_eis	*Xenotoca eiseni*	12S
AP006777	Goo_Xenotoca_eis	*Xenotoca eiseni*	NADH2
AP006777	Goo_Xenotoca_eis	*Xenotoca eiseni*	cytB
AP006777	Goo_Xenotoca_eis	*Xenotoca eiseni*	COI1
AP006777	Goo_Xenotoca_eis	*Xenotoca eiseni*	16S
KJ696974	Goo_Xenotoca_eis	*Xenotoca eiseni*	ENC1
KJ697084	Goo_Xenotoca_eis	*Xenotoca eiseni*	GLYT

KJ697194	Goo_Xenotoca_eis	*Xenotoca eiseni*	MYH6
KJ697348	Goo_Xenotoca_eis	*Xenotoca eiseni*	RAG1
KJ697673	Goo_Xenotoca_eis	*Xenotoca eiseni*	X-SRC
EF017445	Poe_Xiphopho_hel	*Xiphophorus hellerii*	RAG1
EF017597	Poe_Xiphopho_hel	*Xiphophorus hellerii*	NADH2
EF017597	Poe_Xiphopho_hel	*Xiphophorus hellerii*	NADH1
FJ234985	Poe_Xiphopho_hel	*Xiphophorus hellerii*	12S
FJ234985	Poe_Xiphopho_hel	*Xiphophorus hellerii*	cytB
FJ234985	Poe_Xiphopho_hel	*Xiphophorus hellerii*	16S
HQ219147	Poe_Xiphopho_hel	*Xiphophorus hellerii*	COI1
KJ525779	Poe_Xiphopho_hel	*Xiphophorus hellerii*	SH3PX3
KJ525839	Poe_Xiphopho_hel	*Xiphophorus hellerii*	MYH6
KJ525859	Poe_Xiphopho_hel	*Xiphophorus hellerii*	GLYT
KJ525879	Poe_Xiphopho_hel	*Xiphophorus hellerii*	ENC1
KJ525899	Poe_Xiphopho_hel	*Xiphophorus hellerii*	X-SRC
AF510752	Goo_Zoogonet_qui	*Zoogoneticus quitzeoensis*	cytB
AY356592	Goo_Zoogonet_qui	*Zoogoneticus quitzeoensis*	COI1
KJ696975	Goo_Zoogonet_qui	*Zoogoneticus quitzeoensis*	ENC1
KJ697085	Goo_Zoogonet_qui	*Zoogoneticus quitzeoensis*	GLYT
KJ697195	Goo_Zoogonet_qui	*Zoogoneticus quitzeoensis*	MYH6
KJ697349	Goo_Zoogonet_qui	*Zoogoneticus quitzeoensis*	RAG1
U02365	Goo_Zoogonet_qui	*Zoogoneticus quitzeoensis*	X-SRC

Table S5.2 Character states and sampling fractions per genera as well as data sources.

Tree name	Genus	Family	No species	Sampling fraction	No. species source	Annual	Annual source	Viviparous	Viviparous source
Ana_Anableps_ana	*Anableps*	Anablepidae	3	0.33	FishBase	0	FishBase	1	[1]
Ana_Jenynsia_lin	*Jenynsia*	Anablepidae	14	0.07	FishBase	0	FishBase	1	[1]
Ana_Oxyzygon_dov	*Oxyzygonectes*	Anablepidae	1	1	FishBase	0	FishBase	0	[1]
Apl_Aplochei_pan	*Aplocheilus*	Aplocheilidae	7	0.14	FishBase	0	FishBase	0	FishBase
Apl_Pachypan_pla	*Pachypanchax*	Aplocheilidae	7	0.14	FishBase	0	FishBase	0	FishBase
Cyp_Aphanius_fas	*Aphanius*	Cyprinodontidae	33	0.03	FishBase	0	FishBase	0	[2]
Cyp_Cualac_tes	*Cualac*	Cyprinodontidae	1	1	FishBase	0	FishBase	0	[2]
Cyp_Cubanich_cub	*Cubanichthys*	Cyprinodontidae	2	0.5	FishBase	0	FishBase	0	[2]
Cyp_Cyprinod_var	*Cyprinodon*	Cyprinodontidae	49	0.02	FishBase	0	FishBase	0	[2]
Cyp_Floridic_car	*Floridichthys*	Cyprinodontidae	2	0.5	FishBase	0	FishBase	0	[2]
Cyp_Jordanel_flo	*Jordanella*	Cyprinodontidae	1	1	FishBase	0	FishBase	0	[2]
Cyp_Megupsil_apo	*Megupsilon*	Cyprinodontidae	1	1	FishBase	0	FishBase	0	[2]
Cyp_Orestias_aga	*Orestias*	Cyprinodontidae	44	0.02	FishBase	0	FishBase	0	[2]
Fun_Adinia_xen	*Adinia*	Fundulidae	1	1	FishBase	0	FishBase	0	FishBase
Fun_Fundulus_het	*Fundulus*	Fundulidae	39	0.03	FishBase	0	FishBase	0	FishBase
Fun_Lucania_goo	*Lucania*	Fundulidae	3	0.33	FishBase	0	FishBase	0	FishBase
Goo_Allodont_pol	*Allodontichthys*	Goodeidae	4	0.25	FishBase	0	FishBase	1	FishBase
Goo_Alloopho_rob	*Alloophorus*	Goodeidae	1	1	FishBase	0	FishBase	1	FishBase
Goo_Allotoca_cat	*Allotoca*	Goodeidae	8	0.13	FishBase	0	FishBase	1	FishBase
Goo_Ameca_spl	*Ameca*	Goodeidae	1	1	FishBase	0	FishBase	1	FishBase
Goo_Ataeniob_tow	*Ataeniobius*	Goodeidae	1	1	FishBase	0	FishBase	1	FishBase
Goo_Chapalic_enc	*Chapalichthys*	Goodeidae	3	0.33	FishBase	0	FishBase	1	FishBase
Goo_Characod_aud	*Characodon*	Goodeidae	3	0.33	FishBase	0	FishBase	1	FishBase

Goo_Crenicht_nev	*Crenichthys*	Goodeidae	2	0.5	FishBase	0	FishBase	0	[3]
Goo_Empetric_lat	*Empetrichthys*	Goodeidae	2	0.5	FishBase	0	FishBase	0	[3]
Goo_Girardin_viv	*Girardinichthys*	Goodeidae	3	0.33	FishBase	0	FishBase	1	FishBase
Goo_Goodea_gra	*Goodea*	Goodeidae	3	0.33	FishBase	0	FishBase	1	[3]
Goo_Hubbsina_tur	*Hubbsina*	Goodeidae	1	1	FishBase	0	FishBase	1	FishBase
Goo_Ilyodon_fur	*Ilyodon*	Goodeidae	5	0.2	FishBase	0	FishBase	1	[3]
Goo_Skiffia_mul	*Skiffia*	Goodeidae	4	0.25	FishBase	0	FishBase	1	FishBase
Goo_Xenoopho_cap	*Xenoophorus*	Goodeidae	1	1	FishBase	0	FishBase	1	FishBase
Goo_Xenotaen_res	*Xenotaenia*	Goodeidae	1	1	FishBase	0	FishBase	1	FishBase
Goo_Xenotoca_eis	*Xenotoca*	Goodeidae	3	0.33	FishBase	0	FishBase	1	FishBase
Goo_Zoogonet_qui	*Zoogoneticus*	Goodeidae	3	0.33	FishBase	0	FishBase	1	FishBase
Not_Aphyosem_aus	*Aphyosemion*	Nothobranchiidae	97	0.01	FishBase	0	FishBase	0	FishBase
Not_Archiaph_gui	*Aphyosemion*	Nothobranchiidae	1	1	FishBase	0	FishBase	0	FishBase
Not_Callopan_occ	*Callopanchax*	Nothobranchiidae	5	0.2	FishBase	1	[4]	0	FishBase
Not_Epiplaty_ann	*Epiplatys*	Nothobranchiidae	36	0.03	FishBase	0	FishBase	0	FishBase
Not_Fenerbah_for	*Fenerbahce*	Nothobranchiidae	2	0.5	FishBase	0	FishBase	0	FishBase
Not_Foerschi_fla	*Foerschichthys*	Nothobranchiidae	1	1	FishBase	0	FishBase	0	FishBase
Not_Fundulop_gar	*Fundulopanchax*	Nothobranchiidae	29	0.03	FishBase	1	FishBase	0	FishBase
Not_Nimbapan_vir	*Nimbapanchax*	Nothobranchiidae	5	0.2	FishBase	0	FishBase	0	FishBase
Not_Nothobra_kir	*Nothobranchius*	Nothobranchiidae	62	0.02	FishBase	1	FishBase	0	FishBase
Not_Pronotho_kiy	*Pronothobranchius*	Nothobranchiidae	1	1	FishBase	1	FishBase	0	FishBase
Not_Scriptap_ger	*Scriptaphyosemion*	Nothobranchiidae	13	0.08	FishBase	0	FishBase	0	FishBase
Poe_Alfaro_cul	*Alfaro*	Poeciliidae	2	0.5	FishBase	0	FishBase	1	FishBase
Poe_Aplochei_nor	*Aplocheilichthys*	Poeciliidae	24	0.04	FishBase	0	FishBase	0	FishBase
Poe_Beloneso_bel	*Belonesox*	Poeciliidae	1	1	FishBase	0	FishBase	1	FishBase
Poe_Brachyrh_rha	*Brachyrhaphis*	Poeciliidae	12	0.08	FishBase	0	FishBase	1	FishBase

Poe_Carlhubb_stu	*Carlhubbsia*	Poeciliidae	2	0.5	FishBase	0	FishBase	1	FishBase
Poe_Cnestero_dec	*Cnesterodon*	Poeciliidae	10	0.1	FishBase	0	FishBase	1	FishBase
Poe_Fluviphy_sim	*Fluviphylax*	Poeciliidae	5	0.2	FishBase	0	[2]	0	[2]
Poe_Gambusia_aff	*Gambusia*	Poeciliidae	45	0.02	FishBase	0	FishBase	1	FishBase
Poe_Girardin_met	*Girardinus*	Poeciliidae	7	0.14	FishBase	0	FishBase	1	[5]
Poe_Heterand_for	*Heterandria*	Poeciliidae	9	0.11	FishBase	0	FishBase	1	FishBase
Poe_Heteroph_mil	*Heterophallus*	Poeciliidae	2	0.5	FishBase	0	FishBase	1	FishBase
Poe_Limia_dom	*Limia*	Poeciliidae	21	0.05	FishBase	0	FishBase	1	FishBase
Poe_Micropoe_pic	*Micropoecilia*	Poeciliidae	4	0.25	FishBase	0	FishBase	1	FishBase
Poe_Neoheter_tri	*Neoheterandria*	Poeciliidae	3	0.33	FishBase	0	FishBase	1	FishBase
Poe_Pamphori_hol	*Pamphorichthys*	Poeciliidae	6	0.17	FishBase	0	FishBase	1	FishBase
Poe_Phallich_ama	*Phallichthys*	Poeciliidae	4	0.25	FishBase	0	FishBase	1	FishBase
Poe_Phalloce_cau	*Phalloceros*	Poeciliidae	22	0.05	FishBase	0	FishBase	1	FishBase
Poe_Phallopt_jan	*Phalloptychus*	Poeciliidae	2	0.5	FishBase	0	FishBase	1	FishBase
Poe_Poecilia_ret	*Poecilia*	Poeciliidae	40	0.03	FishBase	0	FishBase	1	FishBase
Poe_Poecilio_elo	*Poeciliopsis*	Poeciliidae	24	0.04	FishBase	0	FishBase	1	FishBase
Poe_Priapell_com	*Priapella*	Poeciliidae	6	0.17	FishBase	0	FishBase	1	FishBase
Poe_Priapich_ann	*Priapichthys*	Poeciliidae	7	0.14	FishBase	0	FishBase	1	FishBase
Poe_Pseudopo_fes	*Pseudopoecilia*	Poeciliidae	3	0.33	FishBase	0	FishBase	1	FishBase
Poe_Pseudoxi_obl	*Pseudoxiphophorus*	Poeciliidae	1	1	FishBase	0	FishBase	1	FishBase
Poe_Quintana_atr	*Quintana*	Poeciliidae	1	1	FishBase	0	FishBase	1	FishBase
Poe_Scolicht_iot	*Scolichthys*	Poeciliidae	2	0.5	FishBase	0	FishBase	1	FishBase
Poe_Tomeurus_gra	*Tomeurus*	Poeciliidae	1	1	FishBase	0	FishBase	0	[6]
Poe_Xenodexi_cte	*Xenodexia*	Poeciliidae	1	1	FishBase	0	FishBase	1	[7]
Poe_Xenophal_umb	*Xenophallus*	Poeciliidae	1	1	FishBase	0	FishBase	1	FishBase
Poe_Xiphopho_hel	*Xiphophorus*	Poeciliidae	28	0.04	FishBase	0	FishBase	1	FishBase

Pro_Profundu_gua	*Profundulus*	Profundulidae	8	0.13	FishBase	0	FishBase	0	FishBase
Riv_Anableps_har	*Anablepsoides*	Rivulidae	49	0.02	FishBase	0	FishBase	0	FishBase
Riv_Aphyoleb_per	*Aphyolebias*	Rivulidae	8	0.13	FishBase	1	FishBase	0	FishBase
Riv_Atlantir_san	*Atlantirivulus*	Rivulidae	11	0.09	FishBase	0	FishBase	0	FishBase
Riv_Austrofu_lim	*Austrofundulus*	Rivulidae	7	0.14	FishBase	1	FishBase	0	FishBase
Riv_Austrole_adl	*Austrolebias*	Rivulidae	42	0.02	FishBase	1	FishBase	0	FishBase
Riv_Campello_dor	*Campellolebias*	Rivulidae	4	0.25	FishBase	1	FishBase	0	FishBase
Riv_Cynodoni_ten	*Cynodonichthys*	Rivulidae	27	0.04	FishBase	0	FishBase	0	FishBase
Riv_Cynopoec_mel	*Cynopoecilus*	Rivulidae	5	0.2	FishBase	1	FishBase	0	FishBase
Riv_Gnathole_zon	*Gnatholebias*	Rivulidae	1	1	FishBase	1	FishBase	0	FishBase
Riv_Hypsoleb_ant	*Hypsolebias*	Rivulidae	22	0.05	FishBase	1	FishBase	0	FishBase
Riv_Kryptole_mar	*Kryptolebias*	Rivulidae	8	0.13	FishBase	0	FishBase	0	FishBase
Riv_Laimosem_gea	*Laimosemion*	Rivulidae	25	0.04	FishBase	0	FishBase	0	FishBase
Riv_Leptoleb_min	*Leptolebias*	Rivulidae	7	0.14	FishBase	1	FishBase	0	FishBase
Riv_Llanoleb_ste	*Llanolebias*	Rivulidae	1	1	FishBase	1	FishBase	0	FishBase
Riv_Marateco_lac	*Maratecoara*	Rivulidae	3	0.33	FishBase	1	FishBase	0	FishBase
Riv_Melanori_pun	*Melanorivulus*	Rivulidae	38	0.03	FishBase	0	FishBase	0	FishBase
Riv_Micromoe_xip	*Micromoema*	Rivulidae	1	1	FishBase	1	FishBase	0	FishBase
Riv_Moema_pir	*Moema*	Rivulidae	9	0.11	FishBase	1	FishBase	0	FishBase
Riv_Nematole_whi	*Nematolebias*	Rivulidae	2	0.5	FishBase	1	FishBase	0	FishBase
Riv_Neofundu_par	*Neofundulus*	Rivulidae	5	0.2	FishBase	1	FishBase	0	FishBase
Riv_Papiliol_bit	*Papiliolebias*	Rivulidae	2	0.5	FishBase	1	FishBase	0	FishBase
Riv_Pituna_por	*Pituna*	Rivulidae	6	0.17	FishBase	1	FishBase	0	FishBase
Riv_Plesiole_aru	*Plesiolebias*	Rivulidae	8	0.13	FishBase	1	FishBase	0	FishBase
Riv_Pteroleb_lon	*Pterolebias*	Rivulidae	3	0.33	FishBase	1	FishBase	0	FishBase
Riv_Rachovia_mac	*Rachovia*	Rivulidae	4	0.25	FishBase	1	FishBase	0	FishBase

Riv_Renova_osc	*Renova*	Rivulidae	1	1	FishBase	1	FishBase	0	FishBase
Riv_Rivulus_cyl	*Rivulus*	Rivulidae	5	0.2	FishBase	0	FishBase	0	FishBase
Riv_Spectrol_cos	*Simpsonichthys*	Rivulidae	43	0.02	FishBase	1	FishBase	0	FishBase
Riv_Terranat_dol	*Terranatos*	Rivulidae	1	1	FishBase	1	FishBase	0	FishBase
Riv_Trigonec_bal	*Trigonectes*	Rivulidae	6	0.17	FishBase	1	FishBase	0	FishBase
Val_Valencia_his	*Valencia*	Valenciidae	2	0.5	FishBase	0	FishBase	0	FishBase

Table S5.2 References

1. Meyer, A. & Lydeard, C. The evolution of copulatory organs, internal fertilization, placentae and viviparity in killifishes (Cyprinodontiformes) inferred from a DNA phylogeny of the tyrosine kinase gene X-src. *Proceedings of the Royal Society B: Biological Sciences* **254,** 153–162 (1993).

2. Parenti, L. R. A phylogenetic and biogeographic analysis of cyprinodontiform fishes (Teleostei, Atherinomorpha). Bulletin of the AMNH; v. 168, article 4. (1981).

3. Webb, S. A. *et al.* Molecular phylogeny of the livebearing Goodeidae (Cyprinodontiformes). *Molecular Phylogenetics and Evolution* **30,** 527–544 (2004).

4. Sonnenberg, R. & Busch, E. Description of Callopanchax sidibei (Nothobranchiidae: Epiplateinae), a new species of killifish from southwestern Guinea, West Africa. *Bonn zoological Bulletin* (2010).

5. Hrbek, T., Seckinger, J. & Meyer, A. A phylogenetic and biogeographic perspective on the evolution of poeciliid fishes. *Molecular Phylogenetics and Evolution* **43,** 986–998 (2007).

6. Parenti, L. R., LoNostro, F. L. & Grier, H. J. Reproductive histology of Tomeurus gracilis Eigenmann, 1909 (Teleostei: Atherinomorpha: Poeciliidae) with comments on evolution of viviparity in atherinomorph fishes. *J. Morphol.* **271,** 1399–1406 (2010).

7. Reznick, D., Hrbek, T., Caura S., De Greef, J. & Roff, D. Life history of Xenodexia ctenolepis: implications for life history evolution in the family Poeciliidae. *Biological Journal of the Linnean Society* **92,** 77–85 (2007).

Figure 5.1 Photo Attribution

Fish images used in Figure 5.1, barring *Austrolebias charrua* (taken by TVD), were modified from images attributed (from top to bottom) to Cisamarc, Cardet co6cs, Wiki-Harfus at the German language Wikipedia, Per Harald Olsen and The Xiphophorus Genetic Stock Center, respectively.

Appendix V Supplementary material for chapter 6

Table S6.1 Genbank accessions, species and descriptions of Rhodopsin sequences used in this study.

Accession	Tip label	Organism	Description
AY296738	*Lucania*	*Lucania goodei*	Lucania goodei RH1 opsin mRNA, complete cds
GU179271	*Cnesterodon*	*Cnesterodon decemmaculatus*	Cnesterodon decemmaculatus from Uruguay rhodopsin (RH) gene, partial cds
GU179273	*Limia*	*Limia dominicensis*	Limia dominicensis from Haiti rhodopsin (RH) gene, partial cds
GU179280	*Micropoecilia*	*Micropoecilia picta*	Micropoecilia picta from Trinidad and Tobago rhodopsin (RH) gene, partial cds
GU179281	*Poecilia*	*Poecilia reticulata*	Poecilia reticulata from Trinidad and Tobago rhodopsin (RH) gene, partial cds
HQ857440	*Pamphorichthys*	*Pamphorichthys hollandi*	Pamphorichthys hollandi rhodopsin (RH) gene, partial cds
KC702035	*Aphyosemion*	*Aphyosemion australe*	Aphyosemion australe rhodopsin gene, partial cds
KC702042	*Aplocheilus*	*Aplocheilus lineatus*	Aplocheilus lineatus rhodopsin gene, partial cds
KC702045	*Austrofundulus*	*Austrofundulus limnaeus*	Austrofundulus limnaeus rhodopsin gene, partial cds
KC702047	*Campellolebias*	*Campellolebias brucei*	Campellolebias brucei rhodopsin gene, partial cds
KC702048	*Austrolebias*	*Austrolebias adloffi*	Austrolebias adloffi rhodopsin gene, partial cds
KC702051	*Simpsonichthys*	*Simpsonichthys boitonei*	Simpsonichthys boitonei rhodopsin gene, partial cds
KC702056	*Hypsolebias*	*Hypsolebias magnificus*	Hypsolebias magnificus rhodopsin gene, partial cds
KC702057	*Nematolebias*	*Nematolebias whitei*	Nematolebias whitei rhodopsin gene, partial cds
KC702061	*Fundulopanchax*	*Fundulopanchax gardneri*	Fundulopanchax gardneri rhodopsin gene, partial cds
KC702064	*Maratecoara*	*Maratecoara formosa*	Maratecoara formosa rhodopsin gene, partial cds
KC702065	*Neofundulus*	*Neofundulus paraguayensis*	Neofundulus paraguayensis rhodopsin gene, partial cds
KC702066	*Nothobranchius*	*Nothobranchius orthonotus*	Nothobranchius orthonotus rhodopsin gene, partial cds
KC702068	*Pachypanchax*	*Pachypanchax playfairii*	Pachypanchax playfairii rhodopsin gene, partial cds
KC702070	*Pituna*	*Pituna poranga*	Pituna poranga rhodopsin gene, partial cds
KC702071	*Llanolebias*	*Llanolebias stellifer*	Llanolebias stellifer rhodopsin gene, partial cds
KC702072	*Pterolebias*	*Pterolebias longipinnis*	Pterolebias longipinnis rhodopsin gene, partial cds

KC702073	*Gnatholebias*	*Gnatholebias zonatus*	Gnatholebias zonatus rhodopsin gene, partial cds
KC702074	*Renova*	*Renova oscari*	Renova oscari rhodopsin gene, partial cds
KC702077	*Rivulus*	*Rivulus cylindraceus*	Rivulus cylindraceus rhodopsin gene, partial cds
KC702079	*Anablepsoides*	*Anablepsoides hartii*	Anablepsoides hartii rhodopsin gene, partial cds
KC702082	*Laimosemion*	*Laimosemion mahdiaensis*	Laimosemion mahdiaensis rhodopsin gene, partial cds
KC702083	*Kryptolebias*	*Kryptolebias marmoratus*	Kryptolebias marmoratus rhodopsin gene, partial cds
KC702087	*Melanorivulus*	*Melanorivulus punctatus*	Melanorivulus punctatus rhodopsin gene, partial cds
KC702088	*Atlantirivulus*	*Atlantirivulus santensis*	Atlantirivulus santensis rhodopsin gene, partial cds
KC702089	*Cynodonichthys*	*Cynodonichthys tenuis*	Cynodonichthys tenuis rhodopsin gene, partial cds
KC702092	*Callopanchax*	*Callopanchax occidentalis huwaldi*	Callopanchax occidentalis huwaldi rhodopsin gene, partial cds
KC702093	*Scriptaphyosemion*	*Scriptaphyosemion banforense*	Scriptaphyosemion banforense rhodopsin gene, partial cds
KC702094	*Terranatos*	*Terranatos dolichopterus*	Terranatos dolichopterus rhodopsin gene, partial cds
KC702095	*Trigonectes*	*Trigonectes balzanii*	Trigonectes balzanii rhodopsin gene, partial cds
KJ525799	*Xiphophorus*	*Xiphophorus hellerii*	Xiphophorus hellerii rhodopsin (RH) gene, partial cds
KJ525811	*Priapella*	*Priapella compressa*	Priapella compressa rhodopsin (RH) gene, partial cds
KJ697350	*Fenerbahce*	*Fenerbahce formosus*	Fenerbahce formosus rhodopsin (RH) gene, partial cds
KJ697351	*Alfaro*	*Alfaro cultratus*	Alfaro cultratus rhodopsin (RH) gene, partial cds
KJ697352	*Ameca*	*Ameca splendens*	Ameca splendens rhodopsin (RH) gene, partial cds
KJ697353	*Anableps*	*Anableps anableps*	Anableps anableps rhodopsin (RH) gene, partial cds
KJ697357	*Aplocheilichthys*	*Aplocheilichthys spilauchen*	Aplocheilichthys spilauchen rhodopsin (RH) gene, partial cds
KJ697359	*Ataeniobius*	*Ataeniobius toweri*	Ataeniobius toweri rhodopsin (RH) gene, partial cds
KJ697360	*Belonesox*	*Belonesox belizanus*	Belonesox belizanus rhodopsin (RH) gene, partial cds
KJ697361	*Brachyrhaphis*	*Brachyrhaphis rhabdophora*	Brachyrhaphis rhabdophora rhodopsin (RH) gene, partial cds
KJ697362	*Carlhubbsia*	*Carlhubbsia stuarti*	Carlhubbsia stuarti rhodopsin (RH) gene, partial cds
KJ697363	*Chapalichthys*	*Chapalichthys pardalis*	Chapalichthys pardalis rhodopsin (RH) gene, partial cds
KJ697365	*Crenichthys*	*Crenichthys nevadae*	Crenichthys nevadae rhodopsin (RH) gene, partial cds

KJ697367	*Cubanichthys*	*Cubanichthys pengelleyi*	Cubanichthys pengelleyi rhodopsin (RH) gene, partial cds
KJ697368	*Cyprinodon*	*Cyprinodon variegatus*	Cyprinodon variegatus rhodopsin (RH) gene, partial cds
KJ697369	*Epiplatys*	*Epiplatys annulatus*	Epiplatys annulatus rhodopsin (RH) gene, partial cds
KJ697370	*Floridichthys*	*Floridichthys carpio*	Floridichthys carpio rhodopsin (RH) gene, partial cds
KJ697371	*Fluviphylax*	*Fluviphylax simplex*	Fluviphylax simplex rhodopsin (RH) gene, partial cds
KJ697373	*Fundulus*	*Fundulus cingulatus*	Fundulus cingulatus rhodopsin (RH) gene, partial cds
KJ697375	*Gambusia*	*Gambusia holbrooki*	Gambusia holbrooki rhodopsin (RH) gene, partial cds
KJ697377	*Girardinichthys*	*Girardinichthys viviparus*	Girardinichthys viviparus rhodopsin (RH) gene, partial cds
KJ697378	*Girardinus*	*Girardinus metallicus*	Girardinus metallicus rhodopsin (RH) gene, partial cds
KJ697379	*Goodea*	*Goodea gracilis*	Goodea gracilis rhodopsin (RH) gene, partial cds
KJ697380	*Heterandria*	*Heterandria formosa*	Heterandria formosa rhodopsin (RH) gene, partial cds
KJ697381	*Ilyodon*	*Ilyodon furcidens*	Ilyodon furcidens rhodopsin (RH) gene, partial cds
KJ697382	*Jenynsia*	*Jenynsia lineata*	Jenynsia lineata rhodopsin (RH) gene, partial cds
KJ697384	*Jordanella*	*Jordanella floridae*	Jordanella floridae rhodopsin (RH) gene, partial cds
KJ697403	*Neoheterandria*	*Neoheterandria tridentiger*	Neoheterandria tridentiger rhodopsin (RH) gene, partial cds
KJ697404	*Orestias*	*Orestias agassizii*	Orestias agassizii rhodopsin (RH) gene, partial cds
KJ697405	*Oxyzygonectes*	*Oxyzygonectes dovii*	Oxyzygonectes dovii rhodopsin (RH) gene, partial cds
KJ697406	*Phallichthys*	*Phallichthys amates*	Phallichthys amates rhodopsin (RH) gene, partial cds
KJ697409	*Phalloceros*	*Phalloceros caudimaculatus*	Phalloceros caudimaculatus rhodopsin (RH) gene, partial cds
KJ697410	*Phalloptychus*	*Phalloptychus januarius*	Phalloptychus januarius rhodopsin (RH) gene, partial cds
KJ697427	*Poeciliopsis*	*Poeciliopsis elongata*	Poeciliopsis elongata rhodopsin (RH) gene, partial cds
KJ697444	*Priapichthys*	*Priapichthys annectens*	Priapichthys annectens rhodopsin (RH) gene, partial cds
KJ697447	*Profundulus*	*Profundulus labialis*	Profundulus labialis rhodopsin (RH) gene, partial cds
KJ697448	*Pseudopoecilia*	*Pseudopoecilia festae*	Pseudopoecilia festae rhodopsin (RH) gene, partial cds
KJ697450	*Scolichthys*	*Scolichthys iota*	Scolichthys iota rhodopsin (RH) gene, partial cds
KJ697451	*Skiffia*	*Skiffia multipunctata*	Skiffia multipunctata rhodopsin (RH) gene, partial cds

KJ697452	*Tomeurus*	*Tomeurus gracilis*	Tomeurus gracilis rhodopsin (RH) gene, partial cds
KJ697453	*Valencia*	*Valencia hispanica*	Valencia hispanica rhodopsin (RH) gene, partial cds
KJ697454	*Xenodexia*	*Xenodexia ctenolepis*	Xenodexia ctenolepis rhodopsin (RH) gene, partial cds
KJ697455	*Xenoophorus*	*Xenoophorus captivus*	Xenoophorus captivus rhodopsin (RH) gene, partial cds
KJ697456	*Xenophallus*	*Xenophallus umbratilis*	Xenophallus umbratilis rhodopsin (RH) gene, partial cds
KJ697457	*Xenotoca*	*Xenotoca eiseni*	Xenotoca eiseni rhodopsin (RH) gene, partial cds
KJ697458	*Zoogoneticus*	*Zoogoneticus quitzeoensis*	Zoogoneticus quitzeoensis rhodopsin (RH) gene, partial cds

Table S6.2 Amino acid substitutions at site under selection that have an unknown effect on Rhodopsin λ_{max} according to S. Yokoyama et al. 2008.

Site	AA with unknown effect on λ_{max}
8	F
112	V
162	M
165	N,G
213	C,V
217	A
266	C,T
304	A